PREPARATION OF SIC-BASED FIBERS FROM ORGANOSILICON POLYMERS: (I) EFFECTS OF POLYVINYLSILAZANE ON THE CHARACTERISTICS AND PROCESSING BEHAVIOR OF POLYCARBOSILANE-BASED SOLUTIONS AND (II) SYNTHESIS, CHARACTERIZATION, AND PROCESSING OF POLYMETHYLSILANES

By

MOHAMED SALEEM

A DISSERTATION PRESENTED TO THE GRADUATE SCHOOL
OF THE UNIVERSITY OF FLORIDA IN PARTIAL FULFILLMENT
OF THE REQUIREMENTS FOR THE DEGREE OF
DOCTOR OF PHILOSOPHY

UNIVERSITY OF FLORIDA

1998

ACKNOWLEDGMENTS

I am grateful to Dr. M.D. Sacks for his invaluable guidance and support. I am thankful to Drs. C.D. Batich, J.H. Simmons, E.D. Whitney, R. Drago, and D. Talham for serving on my committee. I would like to thank Dr. S. Bates, Dr. A. Morrone, R. Crockett, W. Acree, and E. Lambers for their help in use of various analytical instruments.

I would also like to thank G.W. Schieffele, J.H. Dow, Y.J. Lin, K. Wang, R. Raghunathan, T.J. Williams, and G. Staab for their assistance in carrying out various experiments in this study. I am grateful to Drs. Rajiv Bendale and Priya Bendale for many useful technical discussions throughout the course of this study. Thanks are also due to U. Mahajan, S. Lathi, M. Lakshmipathy, and J. DePuy for their help in compiling this dissertation. I would aiso like to thank P. Raghunathan, R. Raghunathan, J. Sethuraman, J.H. Dow, V. Shenoy, U. Shenoy, N. Srinivasa, A. Srinivasa, H. Kannan, D. Kuruvilla, E. Naveen, R. Parikh, C. Parikh, and V. Srinivas for their friendship throughout the course of my stay in Gainesville.

Finally, my special gratitude goes to Anuradha and Prakash Krishnans, for their friendship, support, and encouragement, and for providing an atmosphere of home away from home.

TABLE OF CONTENTS

ACKNOWLEDGMENTS ii

LIST OF TABLES vii

LIST OF FIGURES xi

ABSTRACT xxi

1. INTRODUCTION 1

2. LITERATURE REVIEW 5
2.1. Background 5
2.2. Polysilane synthesis 7
2.2.1. Wurtz-coupling of dichlorosilanes with alkali metal 7
2.2.1.1. Mechanism 7
2.2.1.2. Mode of addition of reagents 10
2.2.1.3. Effect of alkali metal 12
2.2.1.4. Solvent effects 14
2.2.1.5. Temperature effects 23
2.2.2. Ultrasonically activated Wurtz-coupling reactions 25
2.2.3. Polymerization of monoalkylchlorosilanes 26
2.2.4. Polysilane copolymers 28
2.2.5. Dehydrocoupling 28
2.2.6. Redistribution/substitution reactions 37
2.3. Pyrolysis behavior 42
2.4. Cross-linking of polysilane polymers 60
2.4.1. Oxidative cross-linking 60
2.4.2. Room temperature vulcanization 60
2.4.3. Photo-cross linking 62
2.5. Applications of Polysilane Polymers 63
2.5.1. Precursor for β-SiC 63
2.5.2. Photoinitiators for radical polymerization 68
2.5.3. Photoresists in microelectronics 69

3. EXPERIMENTAL PROCEDURE 72
3.1. Role of polyvinylsilazane as a spinning aid for polycarbosilane 72
3.1.1. Polymer synthesis 72
3.1.2. Spin dope preparation, fiber spinning, and fiber heat treatment 74
3.1.3. Characterization of PCS polymer solutions 77
3.1.4. Characterization of fibers 82
3.2. Synthesis and characterization of polymethylsilane (PMS) polymers 84

3.2.1. Starting materials 84
3.2.2. Procedure for polymerization 84
3.2.3 Determination of polymer yield 89
3.2.4. General procedure for heat treatment of PMS-based polymer solutions 90
3.2.5. Procedure for fractional precipitation of PMS polymers 91
3.2.6. Characterization of polymers and samples prepared by heat treatment of the polymers 92
3.3. Spinning and characterization of fibers prepared from PMS-based polymers 95
3.3.1. Spin dope preparation, fiber spinning, and fiber heat treatment 95
3.3.2. Fiber characterization 98

4. RESULTS AND DISCUSSION 100
4.1. Effect of PSZ as a cross-linking/processing aid for spinning of fibers from PCS solution 100
4.1.1. Fiber spinning characteristics 100
4.1.2. Polymer solution characteristics 107
4.1.2.1. Molecular weight and intrinsic viscosity measurements 107
4.1.2.2. Studies on rate of evaporation of solvents from PCS and PCS+PSZ solutions 111
4.1.2.3. Contact angle measurements 114
4.1.2.4. Surface tension measurements 126
4.1.3. Characterization of fibers 137
4.1.3.1. Characterization of fibers by FTIR 137
4.1.3.1.1. FTIR spectra of PCS fibers during heat treatment in nitrogen 143
4.1 3.1.2. FTIR spectra of PCS fibers heat-treated in air 151
4.1.3.1.3. FTIR spectra of air-heat treated PCS fibers during heat treatment in nitrogen 155
4.1.3.1.4. FTIR spectra of PSZ during heat treatment in nitrogen 162
4.1.3.1.5. FTIR spectra of PCS+PSZ fibers during heat treatment in nitrogen 172
4.1.3.1.6. FTIR spectra of air-heat treated PCS+PSZ fibers during heat treatment in nitrogen 184
4.1.3.2. Mechanical properties of fibers 195
4.2. Synthesis and characterization of polymethylsilane polymers 216
4.2.1. Effect of synthesis conditions on molecular weight 220
4.2.2. Effect of synthesis conditions on polymer yield 229
4.2.3. Characterization of PMS polymers and ceramic residues resulting from pyrolysis 225
4.2.3.1. Weight loss behavior 233
4.2.3.2. FTIR spectroscopy studies on PMS polymers 236
4.2.3.3. XRD characteristics 252
4.2.3.4. EMA analysis 256
4.2.4. Sensitivity of PMS polymers to oxygen contamination 260
4.3. Preparation of silicon carbide fibers from polymethylsilane polymers 265
4.3.1. Methods to increase molecular weight of PMS polymers 268

4.3.1.1. Heat treatment of PMS polymers 268
4.3.1.2. Fractional precipitation 289
4.3.2. Spinning of fibers from PMS-based polymers 299
4.3.2.1. Spinning of fibers from as-prepared blends of PMS:PCS polymers 299
4.3.2.2. Spinning of heat-treated PMS polymers and PMS:PCS polymer blends 306
4.3.2.3. Spinning of fibers from fractionally-precipitated PMS polymers 331
4.3.3. Fiber extension experiments on PMS polymer spin dopes containing PSZ 339

5. SUMMARY AND CONCLUSIONS 346

APPENDIX A RHEOLOGICAL CHARACTERIZATION OF PCS AND PCS+PSZ POLYMER SPIN DOPES..... 351

APPENDIX B FIBER SPINNING CHARACTERISTICS FOR PCS AND PCS+PSZ SPIN BATCHES 357

APPENDIX C FIBER EXTENSION DISTANCES FOR PCS AND PCS+PSZ SPIN DOPES 362

APPENDIX D INTRINSIC VISCOSITY CALCULATIONS FOR PCS, PCS+PSZ AND PMS POLYMERS 365

APPENDIX E RESULTS OF SURFACE TENSION MEASUREMENTS 371

APPENDIX F TEMPERATURE AND WEIGHT GAINS FOR HEAT TREATMENT OF PCS, PCS+PSZ FIBERS IN AIR 376

APPENDIX G WEIGHT LOSS DATA FOR PCS, PCS+PSZ FIBERS (AIR-HEAT TREATED AND NON-AIR HEAT TREATED) AFTER PYROLYSIS AT 1150°C IN NITROGEN 378

APPENDIX H TENSILE STRENGTH DATA FOR PYROLYZED PCS AND PCS+PSZ FIBERS 380

APPENDIX I GPC MOLECULAR WEIGHT DISTRIBUTIONS FOR PMS POLYMERS FRACTIONALLY-PRECIPITATED BY ADDITION OF ALCOHOLS 400

APPENDIX J GPC MOLECULAR WEIGHT DISTRIBUTIONS FOR PMS POLYMERS FRACTIONALLY-PRECIPITATED BY ADDITION OF ACETONE 403

APPENDIX K CALCULATIONS FOR EXCESS SILICON AND CARBON IN SIC FIBERS 413

APPENDIX L CHARACTERISTICS OF PMS POLYMERS SYNTHESIZED FROM MDCS MONOMER 415

APPENDIX M CHARACTERISTICS OF PMS POLYMERS SYNTHESIZED FROM MDCS AND MTCS MONOMER MIXTURE 417

APPENDIX N CHEMICAL FORMULAS FOR MONOMERS USED IN WURTZ-COUPLING POLYMERIZATION 424

REFERENCES 426

LIST OF TABLES

Table		Page
2.1.	Effect of diglyme and heptane additions on polymerization of some dichlorosilane monomers	17
2.2.	Effect of temperature on polymerization of methylphenyldichlorosilane	24
2.3.	Effect of sonication time on molecular weights and polydispersities of polymethylphenylsilane	26
2.4.	Summary of methylsilane polymerization by catalytic dehydrogenation reactions	30
2.5.	Effect of time and temperature on polymerization of phenylsilane in the presence of a lanthanoid complex	35
2.6.	Ceramic yield and chemical compositions upon pyrolysis of polysilane homopolymers, copolymers, and terpolymers	43
2.7.	Synthesis conditions and characteristics of PMS polymers prepared by Wood	48
2.8.	Pyrolysis results for catalytically cross-linked polysilane polymers	50
2.9.	Peak assignments for IR absorption spectra of vinylic polysilanes	56
2.10.	Ceramic yield characteristics and decomposition temperatures for polysilane polymers synthesized by Abu-Eid et al.	59
2.11.	List of polysilanes that can be used in radical polymerization	69
3.1.	Properties of reagents used in synthesis of polymethylsilane polymers	85
4.1.	Fiber spinning characteristics for PCS and PCS+PSZ spin dopes spun under identical conditions	104
4.2.	Average fiber extension distances for PCS and PCS+PSZ spin dopes at the same viscosities used in the fiber spinning experiments	108
4.3.	Surface tension values for PCS and PCS+PSZ solutions in toluene at different solids-loadings	128

4.4. FTIR peak assignments for polycarbosilane (PCS) fibers 139

4.5. FTIR peak assignments for polydimethylsilane (PDMS) polymer 141

4.6. FTIR peak assignments for PCS fibers (batch 65s) heat-treated in air at 187°C 153

4.7. FTIR peak assignments for polyvinylsilazane (PSZ) polymer 166

4.8. FTIR peak assignments for PCS+PSZ fibers (batch 70s)..... 174

4.9. FTIR peak assignments for PCS+PSZ fibers (batch 70s) heat-treated in air at 177°C 186

4.10. Average tensile strengths and rupture strains for PCS and PCS+PSZ fibers (green, heat treatment in air at 180 ±10°C, heat treatment in nitrogen at 400°C, and heat treatment in air at 180 ±10°C followed by heat treatment in nitrogen at 400°C) 196

4.11. Tensile properties of as-spun and air-heat treated (187°C) PCS fibers, heat-treated to various temperatures between 200 and 1150°C in nitrogen . 203

4.12. Tensile properties of as-spun and air-heat treated (177°C) PCS+PSZ fibers, heat-treated to various temperatures between 200 and 1150°C in nitrogen 204

4.13. Properties of SiC fibers spun from PCS 211

4.14. Properties of SiC fibers spun from PCS+PSZ 211

4.15. Synthesis conditions and characteristics for PMS polymers 219

4.16. FTIR peak assignments for polymethylsilane polymer PMS-F (batch PMS-256) 239

4.17. FTIR peak assignments for polymethylsilane polymer PMS-C (batch PMS-263) 240

4.18. d-spacings and 2θ Bragg angles for Si and β-SiC 257

4.19. Crystallite sizes for Si and SiC calculated by Scherrer's formula for various polymers pyrolyzed at 1350°C in nitrogen at 10°C/min with no hold 258

4.20. Results of Electron Microprobe Analysis (EMA) on pyrolyzed ceramic fibers from PMS polymers 259

4.21. Conditions for heat treatment for PMS polymers containing PSZ, DCP, and DB 270

4.22. Nomenclature of PMS polymers used in the heat treatment experiments ... 271

4.23. Conditions and results of heat treatment for PMS/PCS polymer blends 282

4.24. Molecular weight distributions for PCS polymers used in the heat treatment of PMS/PCS blends 283

4.25. Conditions for fractional precipitation of PMS polymers 290

4.26. Results of EMA analysis on fractionally precipitated 1150°C-pyrolyzed (nitrogen) polymers 295

4.27. Conditions for fiber spinning experiments from as-prepared PMS/PCS polymer blends (non-heat treated) 300

4.28. Tensile strengths of SiC fibers spun from as-prepared PMS:PCS polymer blends 305

4.29. Conditions and qualitative results for fiber spinning experiments from heat-treated PMS and PMS/PCS polymer blends 307

4.30. Tensile strengths of SiC fibers spun from heat-treated PMS polymers and PMS/PCS polymer blends 323

4.31. Elemental analysis by EMA for SiC fibers prepared from heat-treated PMS/PCS polymer blends 332

4.32. Conditions and qualitative results of fiber spinning experiments for fractionally-precipitated PMS polymers..... 333

4.33. Tensile strengths of SiC fibers spun from fractionally-precipitated PMS polymers 336

4.34. Elemental analysis by electron microprobe for SiC fibers prepared from fractionally-precipitated PMS polymers 336

4.35. Results of fiber extension experiments for PMS polymers containing PSZ . 341

D-1. Intrinsic viscosity calculations for PCS and PCS+PSZ solutions in toluene . 365

D-2. Intrinsic viscosity calculations for PMS polymer in toluene 368

D-3. Intrinsic viscosity calculations for PMS polymer in toluene-1,4 dioxane mixture (50:50 by volume) 369

E-1. Results of surface tension measurements 371

F-1. Air-heat treatment temperatures and weight gains for PCS and PCS+PSZ fibers 376

G-1. Weight loss data for PCS, PCS+PSZ fibers (air-heat treated and non-air heat treated) after pyrolysis at 1150°C in nitrogen 378

H-1. Tensile strength data for pyrolyzed PCS fibers (batch 63s). 380

H-2. Tensile strength data for pyrolyzed PCS fibers (batch 64s) 381

H-3. Tensile strength data for pyrolyzed PCS fibers (batch 65s) 384

H-4. Tensile strength data for pyrolyzed PCS fibers (batch 69s) 387

H-5. Tensile strength data for pyrolyzed PCS+PSZ fibers (batch 67s)..... 390

H-6. Tensile strength data for pyrolyzed PCS+PSZ fibers (batch 68s) 394

H-7. Tensile strength data for pyrolyzed PCS+PSZ fibers (batch 70s) 397

L-1. Results of characterization of PMS polymers synthesized from MDCS 415

M-1. Results of characterization of PMS polymers synthesized from MDCS and MTCS (70:30 wt%) 417

LIST OF FIGURES

Figure		Page
2.1.	Schematic showing mechanism of Wurtz coupling polymerization	8
2.2.	Effect of reactant addition rate on molecular weight distribution of phenyl methylsilane	11
2.3.	Effect of sodium surface area on the rate of consumption of hexylmethyl-dichlorosilane	13
2.4.	UV-Vis Diffuse reflectance spectrum of purple solid isolated during Wurtz polymerization	15
2.5.	Chemical formulas of polar solvents used in Wurtz polymerization	16
2.6.	Schematic illustration of the influence of solvent on the polymer/sodium particle interaction during Wurtz polymerization	20
2.7.	Rate of disappearance of monomer n-hexylmethyldichlorosilane as a function of time and weight percent of 15-Crown-5 ether	22
2.8.	GPC of polymethylsilanes synthesized by Mu and Harrod	32
2.9.	Scheme for redistribution/substitution reactions of chlorodisilanes	39
2.10.	Structure of methylchloropolysilane polymer	40
2.11.	IR spectral changes during pyrolysis of a polysilane polymer	45
2.12.	Changes in intensities of pendant groups based on IR spectra for polysilane polymer	46
2.13.	TGA plots for polymethylsilane polymers, prepared by Zhang et al.	51
2.14.	FTIR spectra of PMS polymer, prepared by Zhang et al.	53
2.15.	TGA and DTA plots for a VPS polymer heated in nitrogen at 20°C/min to 1200°C	55
2.16.	IR spectra of VPS polymer:(a) 25°C (b) 250°C (c) 400°C (d) 650°C (e) 1000°C	57

2.17. FTIR spectrum of polymethylsilane polymer, prepared by Abu-Eid et al. ... 61

2.18. Scheme for photo cross-linking reactions of polysilane polymers 64

2.19. Comparison of single layer photoresist process vs. multilayer photoresist process 71

3.1. Structure of 1,3,5-trimethyl-1,3,5-trivinylcyclotrisilazane 72

3.2. Schematic of reaction assembly for PSZ synthesis 73

3.3. Definition of terms in Young's equation and schematic illustration of the geometry for determination of the contact angle by the sessile drop method..... 79

3.4. Schematic of reaction assembly for synthesis of polymethylsilane 87

4.1. Plots of (A) shear stress vs. shear rate (B) viscosity vs. shear rate for a PCS spin dope (solids concentration ~68 wt%) 101

4.2. Plots of (A) shear stress vs. shear rate (B) viscosity vs. shear rate for a PCS+PSZ spin dope (solids concentration ~70 wt%) 102

4.3. Schematic illustration of globule formation during spinning of fibers from PCS spin dope 106

4.4. GPC molecular weight distributions: (A) PCS (B) PSZ 109

4.5 Plots of η_{sp}/c vs. c for (A) PCS (B) PCS+PSZ (C) PSZ 110

4.6. (a) Percentage change in weight of PCS and PCS+PSZ spin dope as a function of time due to evaporation of toluene, and (b) Absolute weight change of PCS and PCS+PSZ spin dopes as a function of time due to evaporation of toluene 112

4.7. Advancing and receding contact angles for water on: (A) teflon substrate (B) stainless steel substrate as a function of cumulative drop volume 115

4.8. Advancing and receding contact angles for toluene on teflon substrate as a function of cumulative drop volume 117

4.9. Advancing and receding contact angles for toluene on stainless steel substrate as a function of cumulative drop volume..... 118

4.10. Advancing and receding contact angles for PCS (33 wt%)/toluene solution on stainless steel substrate as a function of cumulative drop volume 119

4.11. Advancing and receding contact angles for PCS+PSZ (33 wt%)/toluene solution on stainless steel substrate as a function of cumulative drop volume 120

4.12. Advancing and receding contact angles of PCS (33 wt%)/toluene solution on teflon substrate as a function of cumulative drop volume 121

4.13. Advancing and receding contact angles of PCS+PSZ (33 wt%)/toluene solution on teflon substrate as a function of cumulative drop volume 122

4.14. Advancing and receding contact angles for PCS (33 wt%)/toluene solution on a stainless steel substrate coated with PCS as a function of cumulative drop volume 124

4.15. Advancing and receding contact angles for PCS+PSZ (33 wt%)/toluene solution on a stainless steel substrate coated with PCS+PSZ as a function of cumulative drop volume 125

4.16. Plots of: (A) shear stress vs. shear rate (B) viscosity vs. shear rate for a 33 wt% PCS solution used in surface tension measurement 129

4.17. Plots of: (A) shear stress vs. shear rate (B) viscosity vs. shear rate for a 50 wt% PCS solution used in surface tension measurement 130

4.18 Plots of: (A) shear stress vs. shear rate (B) viscosity vs. shear rate for a 66 wt% PCS solution used in surface tension measurement 131

4.19. Plots of: (A) shear stress vs. shear rate (B) viscosity vs. shear rate for a 33 wt% PCS+PSZ solution used in surface tension measurement 132

4.20. Plots of: (A) shear stress vs. shear rate (B) viscosity vs. shear rate for a 50 wt% PCS+PSZ solution used in surface tension measurement 133

4.21. Plots of: (A) shear stress vs. shear rate (B) viscosity vs. shear rate for a 66 wt% PCS+PSZ solution used in surface tension measurement 134

4.22. Surface tension as a function of concentration for PCS and PCS+PSZ solutions 135

4.23. Surface tension as a function of viscosity for PCS and PCS+PSZ solutions 136

4.24. Room temperature FTIR spectra of green PCS fibers 138

4.25. Room temperature FTIR spectra of polydimethylsilane (PDMS) 140

4.26. FTIR spectra of PCS fibers during heat treatment to 600°C at 1°C/min in nitrogen atmosphere 144

4.27. Intensity vs. temperature from FTIR spectra for PCS (green) fibers 145

4.28. Subtraction spectra for PCS fibers (69s) heat-treated in nitrogen, 600-40°C 149

4.29. Comparison of FTIR spectra of PCS fibers before and after heat treatment at 600°C in nitrogen 150

4.30. Room temperature FTIR spectra for PCS fibers heat-treated in air at 187°C 152

4.31. Subtraction spectra for PCS fibers heat-treated in air at 187°C (65s) and PCS green fibers (69s) 154

4.32. Comparison of FTIR spectra of PCS fibers at 40°C before and after heat treatment in air 156

4.33. FTIR spectra for air-heat treated (187°C) PCS fibers during heat treatment to 600°C at 1°C/min in nitrogen 157

4.34. Intensity vs. temperature from FTIR spectra for PCS (air-heat treated at 187°C) fibers during heat treatment in nitrogen to 600°C 158

4.35. FTIR spectra of air-heat treated Nippon PCS fibers during heat treatment in nitrogen to 500°C (from Ichikawa et al.) 160

4.36. Comparison of FTIR spectra of air-heat treated (187°C) PCS fibers before and after heat treatment at 600°C in nitrogen 163

4.37. Subtraction spectra for air-heat treated (187°C) PCS fibers heat treated in nitrogen (600-40°C) 164

4.38. Room temperature FTIR spectra for PSZ polymer (batch 0831A)..... 165

4.39. FTIR spectra for PSZ polymer during heat treatment to 600°C at 1°C/min in nitrogen 167

4.40. Intensity vs. temperature from FTIR spectra of PSZ 169

4.41. Room temperature FTIR spectra of PCS+PSZ green fibers (batch 70s).. 173

4.42. FTIR spectra of PCS+PSZ green fibers during heat treatment to 600°C in nitrogen 175

4.43. Intensity vs. temperature from FTIR spectra of PCS+PSZ fibers 176

4.44. Comparison of FTIR spectra of PCS+PSZ fibers (70s) before and after heat treatment at 600°C in nitrogen 179

4.45. Subtraction spectra for PCS+PSZ fibers (70s), 600-40°C 180

4.46. Subtraction spectra for PCS+PSZ and PCS fibers at 40°C 181

4.47. Subtraction spectra for PCS+PSZ and PCS fibers at 600°C 182

4.48. Room temperature FTIR spectra of PCS+PSZ fibers heat-treated in air at 177°C 185

4.49. FTIR spectra of air-heat treated PCS+PSZ fibers during heat treatment to 600°C in nitrogen 188

4.50. Intensity vs. temperature from FTIR spectra of air-heat treated PCS+PSZ fibers 189

4.51. Comparison of spectra for air-heat treated PCS+PSZ fibers before and after heat treatment at 600°C in nitrogen 191

4.52. Subtraction spectra for air-heat treated PCS+PSZ fibers, 600-40°C 192

4.53. Comparison of spectra for air-heat treated PCS fibers (batch 65s) and PCS+PSZ fibers (batch 70s) at 40°C 193

4.54. Comparison of spectra for air-heat treated PCS fibers (batch 65s) and PCS+PSZ fibers (batch 70s) after heat treatment in nitrogen 194

4.55. Average tensile strength for PCS, PCS+PSZ fibers, as-spun and after heat treatment in (i) nitrogen at 400°C (ii) air at 180 ±10°C (iii) air at 180 ±10°C, followed by nitrogen at 400°C 197

4.56. Average rupture strain for PCS, PCS+PSZ fibers, as-spun and after heat treatment in (i) nitrogen at 400°C (ii) air at 180 ±10°C (iii) air at 180 ±10°C, followed by nitrogen at 400°C 198

4.57. Plots of (a) tensile strength vs. heat treatment temperature (b) % elongation vs. temperature for polyacrylonitrile (PAN) fibers 200

4.58. Schematic of structural changes taking place in PCS during heat treatment in air at 180 ±10°C 202

4.59. Average rupture strain vs. temperature for: (A) PCS (batch 69s) and (B) PCS+PSZ fibers (batch 70s) 206

4.60. Average rupture strain vs. temperature for fibers heat-treated in air: (A) PCS (batch 65s/ 187°C air heat treatment), and (B) PCS+PSZ (batch 70s/ 177°C air heat treatment) 207

4.61. Average tensile strength vs. temperature for (A) PCS (batch 69s), and (B) PCS+PSZ fibers (batch 70s) 208

4.62. Distribution of tensile strengths for fibers after pyrolysis at 1150°C in nitrogen (A) PCS (B) PCS+PSZ 212

4.63. Distribution of diameters for fibers after pyrolysis at 1150°C in nitrogen (A) PCS (B) PCS+PSZ 213

4.64. Average tensile strength vs. temperature for fibers heat-treated in air: (A) PCS (batch 65s/ 187°C air heat treatment), and (B) PCS+PSZ (batch 70s/ 177°C air heat treatment) 214

4.65. Schematic for Wurtz polymerization of (a) MDCS (b) MDCS and MTCS (70:30 wt%) 217

4.66. (a) Gel permeation chromatograms for polymers prepared from MDCS (A) toluene (B) Toluene:THF (95:5 vol%) (C) Toluene, dioxane (50:50 vol%) (b) Gel permeation chromatograms for polymers prepared from MDCS:MTCS(70:30 wt%) (A) toluene (B) Toluene:THF (95:5 vol%) (C) Toluene, dioxane (50:50 vol%) 221

4.67. Effect of cosolvents on molecular weight of PMS polymers A,B, and C (prepared using 100% MDCS) 223

4.68. Effect of cosolvents on molecular weight of PMS polymers D,E, and F (prepared using MDCS/MTCS (70/30 wt%)) 224

4.69. Plot of η_{sp}/c vs. C for polymer F (batch PMS-256) (MDCS/MTCS (70/30 wt%); toluene/1,4-dioxane (50/50)) in toluene 226

4.70. Plot of η_{sp}/c vs. C for polymer F (batch PMS-256) (MDCS/MTCS (70/30 wt%); toluene/1,4-dioxane (50/50)) in a mixture of toluene and 1,4-dioxane (50:50 vol%) 227

4.71. Schematic illustration for solvent effects in polymerization of MDCS (a) in toluene (b) in a 50:50 mixture of toluene:1,4-dioxane 228

4.72. Effect of cosolvents on yield for PMS polymers D,E, and F (prepared from MDCS/MTCS (70/30 wt%)) 230

4.73. Effect of cosolvents on yield for PMS polymers A,B, and C (prepared from 100% MDCS) 232

4.74. TGA plots (% weight vs. temperature) for polymers prepared with 100% MDCS 234

4.75. TGA plots (% weight vs. temperature) for polymers prepared with 70:30 wt% MDCS:MTCS 235

4.76. Room temperature FTIR spectra of PMS polymer C (batch PMS-263) (prepared from 100% MDCS in toluene/dioxane solvent) 237

4.77. Room temperature FTIR spectra of PMS polymer F (batch PMS-256) (prepared from 70:30 wt% MDCS:MTCS in toluene/dioxane solvent)..... 238

4.78. FTIR spectra of PMS polymer C (100% MDCS; toluene, dioxane (50:50 vol%)), 40 to 600°C at 5°C/min in nitrogen 242

4.79. Intensity vs. temperature from FTIR spectra for PMS polymer C 244

4.80. FTIR spectra of PMS polymer C, 750 to 1150°C at 5°C/min in nitrogen 247

4.81. FTIR spectra of PMS polymer F (MDCS, MTCS (70:30 wt%)), toluene, dioxane (50:50 vol%)), 40 to 600°C at 5°C/min in nitrogen 248

4.82. Intensity vs. temperature from FTIR spectra for PMS polymer F 250

4.83. FTIR spectra of PMS polymer F, 750 to 1150°C at 5°C/min in nitrogen ... 253

4.84. XRD patterns for PMS polymers prepared from monomer MDCS: (A) 100% toluene, (B) toluene:THF (95:5 Vol%), and (C) toluene:dioxane (50:50 vol%) 254

4.85. XRD patterns for PMS polymers prepared from monomers MDCS:MTCS (70:30 wt%): (A) 100% toluene, (B) toluene:THF (95:5 Vol%), and (C) toluene:dioxane (50:50 vol%) 255

4.86. FTIR spectra of PMS polymer C (100% MDCS; toluene/dioxane (50:50 vol%)) exposed to air, shown as a function of time 261

4.87. Intensity vs. time of exposure to air from FTIR spectra for PMS polymer C. 262

4.88. Gel permeation chromatograms for PMS-231 polymer: (A) after 3 days of storage, (B) after 260 days of storage, and (C) after heat treatment (PMS-231-H) 273

4.89. Polydispersity index vs. molecular weight for PMS polymers containing 5-14.5 wt% PSZ (and 0.5-1.5 wt% DCP) as additives 274

4.90. GPC molecular weight distributions for: (A) PMS-214-A (B) PMS-214-A-H . 275

4.91. GPC molecular weight distributions for: (A) PMS-216-A (B) PMS-216-A-H... 277

4.92. GPC molecular weight distribution for PMS-216-A2-H 278

4.93. GPC molecular weight distributions for: (A) PMS-219-A (B) PMS-219-A-H.. 280

4.94. GPC molecular weight distributions for: (A) PMS-223-AD2-A (B) PMS-223-AD2-H 281

4.95. GPC molecular weight distribution for PMS-216-AP-H 285

4.96. GPC molecular weight distribution for PMS-217-AP-H 285

4.97. GPC molecular weight distribution for PMS-217-AP2-H 286

4.98. GPC molecular weight distribution for PMS-218-AP-H 286

4.99. GPC molecular weight distribution for PMS-220-AP2-H 288

4.100. GPC molecular weight distribution for PMS-221-AP2-H 288

4.101. GPC molecular weight distribution for PMS-240 polymer (A) before and (B) after fractional precipitation with alcohol mixture..... 293

4.102. Plot of non-solvent to polymer ratio vs. final M_w for polymers precipitated using acetone as non-solvent 296

4.103. GPC molecular weight distribution for PMS-250 polymer (A) before and (B) after fractional precipitation with acetone 298

4.104. SEM micrographs of as-spun fibers (batch 24s) prepared from PMS/PCS blends (non-heat treated) showing necking..... 303

4.105. SEM micrographs of pyrolyzed fibers (batch 26s) prepared from PMS/PCS blends (non-heat treated) showing necking 304

4.106. Plots of (A) shear stress vs. shear rate and (B) viscosity vs. shear rate for UF-33s spin dope 311

4.107. Plots of (A) shear stress vs. shear rate and (B) viscosity vs. shear rate for UF-35s spin dope 312

4.108. Plots of (A) shear stress vs. shear rate and (B) viscosity vs. shear rate for UF-36s spin dope 313

4.109. Plots of (A) shear stress vs. shear rate and (B) viscosity vs. shear rate for UF-45s spin dope 316

4.110. Plots of (A) shear stress vs. shear rate and (B) viscosity vs. shear rate for UF-42s spin dope 318

4.111. Plots of (A) shear stress vs. shear rate and (B) viscosity vs. shear rate for UF-56s spin dope 319

4.112. Plots of (A) shear stress vs. shear rate and (B) viscosity vs. shear rate for UF-54s spin dope 321

4.113. Plots of (A) shear stress vs. shear rate and (B) viscosity vs. shear rate for UF-52s spin dope 322

4.114. SEM micrographs of pyrolyzed fibers (batch 42s) prepared from heat-treated PMS/PCS polymer blends showing necking between fibers ... 324

4.115. SEM micrographs of UF-35s fibers after heat treatment at 1700°C in argon: (A) and (B) surfaces, (C) fiber cross section 326

4.116. SEM micrographs of fracture surfaces of UF-35s fibers after heat treatment at 1700°C in argon 328

4.117. GPC molecular weight distribution for PMS-242 polymer: (A) before and (B) after fractional precipitation 342

4.118. Average extension for fibers drawn from PMS-based polymers as a function of amount of PSZ 0908A added 344

A-1. Plots of (A) shear stress vs. shear rate and (B) viscosity vs. shear rate for 64s spin dope (PCS) (solids concentration ~67 wt%) 351

A-2. Plots of (A) shear stress vs. shear rate and (B) viscosity vs. shear rate for 65s spin dope (PCS) (solids concentration ~66 wt%) 352

A-3. Plots of (A) shear stress vs. shear rate and (B) viscosity vs. shear rate for 69s spin dope (PCS) (solids concentration ~66 wt%) 353

A-4. Plots of (A) shear stress vs. shear rate and (B) viscosity vs. shear rate for 67s spin dope (PCS+PSZ) (solids concentration ~69 wt%) 354

A-5. Plots of (A) shear stress vs. shear rate and (B) viscosity vs. shear rate for 68s spin dope (PCS+PSZ) (solids concentration ~70 wt%) 355

C-1. Fiber extension distances for PCS spin dope 362

C-2. Fiber extension distances for PCS+PSZ spin dope 363

I-1. GPC molecular weight distributions for PMS-241 (A) before and (B) after fractional precipitation with alcohols 400

I-2. GPC molecular weight distributions for PMS-243 (A) before and (B) after fractional precipitation with alcohols 401

J-1. GPC molecular weight distributions for PMS-245 (A) before (B) and (C) after two fractional precipitations with acetone 403

J-2. GPC molecular weight distributions for PMS-246 (A) before and (B) after fractional precipitation with acetone 404

J-3. GPC molecular weight distributions for PMS-247 (A) before and (B) after fractional precipitation with acetone 405

J-4. GPC molecular weight distributions for PMS-248 (A) before and (B) after fractional precipitation with acetone 406

J-5. GPC molecular weight distributions for PMS-249 (A) before and (B) after fractional precipitation with acetone 407

J-6. GPC molecular weight distributions for PMS-251 (A) before and (B) after fractional precipitation with acetone 408

J-7. GPC molecular weight distributions for PMS-252 (A) before and (B) after fractional precipitation with acetone 409

J-8. GPC molecular weight distributions for PMS-253 (A) before and (B) after fractional precipitation with acetone 410

J-9. GPC molecular weight distributions for PMS-254 (A) before and (B) after fractional precipitation with acetone 411

Abstract of Dissertation Presented to the Graduate School
of the University of Florida in Partial Fulfillment of the
Requirements for the Degree of Doctor of Philosophy

PREPARATION OF SIC-BASED FIBERS FROM ORGANOSILICON POLYMERS:
(I) EFFECTS OF POLYVINYLSILAZANE ON THE CHARACTERISTICS AND
PROCESSING BEHAVIOR OF POLYCARBOSILANE-BASED SOLUTIONS AND
(II) SYNTHESIS, CHARACTERIZATION, AND PROCESSING OF
POLYMETHYLSILANES

By

Mohamed Saleem

August 1998

Chairman: Dr. Michael D. Sacks
Major Department: Materials Science and Engineering

The effect of the addition of polyvinylsilazane (PSZ) on the characteristics (i.e., spinnability, rheological behavior, wetting behavior, evaporation behavior, etc.) of polycarbosilane (PCS) solutions was investigated. Spinnability of PCS solution was characterized by number of breaks occurring during spinning and amount of fibers formed after spinning. PCS and PCS+PSZ solutions were characterized by measuring surface tension, contact angles and rate of solvent evaporation. Effect of PSZ on mechanical properties of SiC fibers prepared from PCS and PCS+PSZ solutions was also investigated. Chemical changes taking place in PCS and PCS+PSZ fibers during heat treatment from 40-600°C in nitrogen were studied by Fourier transform infrared spectroscopy (FTIR).

Addition of PSZ to PCS greatly improved spinnability of PCS solutions. Significant differences in wetting characteristics were observed for PCS solutions and

PCS+PSZ solutions deposited on stainless steel and teflon substrates, as well as on PCS-coated and PCS+PSZ-coated stainless steel substrates. The rate of evaporation of solvent was higher for PCS solution than for PCS+PSZ solution at identical polymer concentrations. As-spun PCS and PCS+PSZ fibers developed similar tensile strengths and rupture strains. After heat treatment at 400°C in nitrogen, PCS+PSZ fibers showed higher tensile strength and rupture strain compared to PCS fibers. Based on FTIR spectra of PCS and PCS+PSZ fibers during heat treatment from 40-600°C, it is suggested that PSZ acts as a cross-linking aid for PCS. PCS+PSZ fibers developed higher tensile strengths than PCS fibers at all heat treatment temperatures between 200-1150°C.

SiC fibers were fabricated from polymethylsilane (PMS) and PMS/PCS polymer blends. PMS polymers were synthesized by a Wurtz-coupling polymerization of methyldichlorosilane (MDCS) and methyltrichlorosilane (MTCS) in 70:30 wt% proportion with sodium in refluxing toluene. The addition of polar solvents (i.e., THF and 1,4-dioxane) to toluene improved yields and increased the molecular weight of PMS polymers. As-prepared PMS polymers with additives were heat-treated to increase molecular weight to permit fiber spinning. As-prepared PMS polymers were also fractionally-precipitated to isolate higher molecular weight fractions suitable for fiber spinning. The heat treatment approach was ineffective in obtaining molecular weight increases reproducibly. Fractionally- precipitated PMS polymers were useful in preparation of high strength pyrolyzed SiC fibers. These fibers, however, exhibited poor thermal stability at high temperatures. More investigations will be needed to address this problem.

CHAPTER 1
INTRODUCTION

There has been much interest in the preparation of ceramic materials from organosilicon-based preceramic polymers. Polycarbosilane (PCS) polymers, in particular, have been shown to be useful for producing SiC-based ceramic materials, particularly fibers. Continuous SiC fibers with fine diameter and high strength are of considerable interest for the development of ceramic-matrix composites for high temperature applications. Commercially available fibers (e.g., Nicalon™, Nippon Carbon Company, Tokyo, Japan and Tyranno™, Ube Industries, Tokyo, Japan) are not pure stoichiometric SiC, i.e., the fibers contain relatively high concentrations of excess carbon and oxygen. (In addition, Tyranno™ fibers are actually Si-Ti-C-O fibers.) As a consequence, these fibers degrade extensively at high temperatures. This degradation is associated with the presence of oxygen (~8-15 wt%) and excess carbon (~15 wt%) in the fibers. At high temperatures, carbothermal reduction reactions occur between carbon and siliceous material in the fibers, leading to large weight losses and degradation in mechanical properties. The fibers contain excess carbon as a result of the high C:Si ratios in the starting materials. (PCS has a high C:Si ratio, as it is formed by pressure pyrolysis of polydimethylsilane (PDMS) which has a C:Si ratio of ~2. (PDMS is produced from dimethyldichlorosilane, $(CH_3)_2SiCl_2$, which, in turn, also has a C:Si ratio of 2.) The high C:Si ratio in the preceramic polymer, PCS, leads to excess C in the SiC-based fibers after pyrolysis.) The oxygen in SiC-based fibers, such as Nicalon™ and

Tyranno™, is a result of an oxidative curing step that is used to render the fibers infusible during pyrolytic conversion to SiC.

There has been considerable interest in recent years in producing SiC-based fibers with improved thermomechanical properties. Much of the effort in this area has been directed toward fabrication of fine-diameter, high-strength, polymer-derived fibers which have low oxygen content [Lip91A; Lip91B; Lip94A; Lip94B; Lip95; Tak94; Tak95; Tor92A; Tor92B; Tor94]. The development of such fibers with both carbon-rich and near-stoichiometric compositions have been reported by several research groups, including those at Nippon Carbon Co. (Hi-Nicalon™ and Hi-Nicalon™ Type S fibers [Tak94; Tak95], Dow Corning Co. (Sylramic™ fibers) [Lip95], and the University of Florida (UF and UF-HM fibers) [Tor94; Sac95A; Sac95B]. All of these fibers show improved thermochemical stability and thermomechanical properties compared to fibers which contain large amounts of oxygen, such as Nicalon™ and Tyranno™ fibers.

The approach developed at the University of Florida is based on using a high-molecular-weight PCS polymer which is infusible. Hence, an oxidative curing step is unnecessary during pyrolysis. In producing SiC-based fibers from the high-molecular-weight PCS polymers, Toreki et al. [Tor90] reported that the addition of a polyvinylsilazane (PSZ) polymer to a PCS-based spinning solution (in amounts up to 14.5 wt%) improved fiber spinnability and produced fibers with improved mechanical properties. The reasons for these improvements were not investigated.

There are two major areas of investigation described in this dissertation. The first area of investigation concerned the effects of PSZ on both spinnability and mechanical properties of the SiC-based fibers prepared using the University of Florida method. Fibers were spun from PCS solutions by dry spinning with and without PSZ. Mechanical properties of these fibers were evaluated after heat treatment at various temperatures

up to 1150°C. Fourier transform infrared spectroscopy (FTIR) was used to study the chemical changes occurring in these fibers during pyrolysis. In an effort to understand the effect of PSZ on spinnability of PCS solutions, polymer solutions were characterized using several methods, including measurements of surface tension, contact angles, rheological characteristics (e.g., intrinsic viscosity), and the rate of evaporation of solvent from the solutions.

The second major area of investigation was the synthesis and processing of PMS (polymethylsilane) polymers for the fabrication of SiC-based fibers. There has been limited work on the preparation of SiC fibers from organosilicon polymer blends. SiC fibers may be fabricated by using PMS polymers and PMS/PCS polymer blends. PMS polymers generally produce an excess of elemental Si (in addition to SiC) upon pyrolysis. As indicated earlier, PCS polymers form an excess of elemental C upon pyrolysis. Therefore, a combination of these two polymers might potentially be used to form SiC fibers with controlled stoichiometry.

PMS polymers were synthesized in this study by Wurtz-coupling polymerization of methyldichlorosilanes (MDCS) and methyltrichlorosilanes (MTCS) with sodium (Na) in refluxing solvent/solvent mixtures. One of the major disadvantage of this method is poor polymer yields. Polymer yields and molecular weight distributions are quite sensitive to substituents (pendant groups) in the monomers, order of reagent addition, solvent additives, reaction temperatures, etc. It has been reported that addition of polar solvents promote anionic polymerization (such as Wurtz-coupling polymerization) and increase polymer yields [Mil93; Gau89]. In this study, effects of addition of polar solvents THF and 1,4-Dioxane on polymer yield and molecular weight were investigated.

One of the main drawbacks of PMS polymers for use in fiber fabrication is that they are liquids at room temperature and generally have low molecular weight ($M_n \leq$

1,000 and $M_w \leq 2,500$). In order to form fibers from these polymers, an increased molecular weight and an increased extent of cross-linking are needed so that the polymers are solids at room temperature (and remain solids during pyrolysis). Investigations were carried out to increase the molecular weight/cross-linking of these polymers as well as produce a solid polymer with sufficiently high molecular weight to permit fiber spinning. Two approaches were utilized to raise the molecular weight/cross-linking of the polymer: (1) polymerization and cross-linking by heat treatment with additives and (2) fractional precipitation of higher molecular weight fractions by addition of nonsolvents. The additives used consisted of polyvinylsilazane (PSZ), dicumyl peroxide (DCP), and decaborane (DB). The nonsolvents used were a mixture of methanol and 2-propanol, and acetone. Fibers were spun from heat-treated PMS, PMS/PCS polymer blends, and fractionally-precipitated PMS polymers, and converted to SiC fibers by pyrolysis at 1000-1150°C in a nitrogen atmosphere.

CHAPTER 2
LITERATURE REVIEW

2.1 Background

There has been much interest in recent years in the preparation of ceramic materials by pyrolysis of organometallic polymers. A wide range of ceramic materials can be produced by this method, such as SiC, Si_3N_4, B_4C, BN, SiO_2, Al_2O_3 and AlN. In this review, only silicon-based preceramic polymers, viz., polysilanes are discussed. Polysilanes are a class of polymers with Si-Si backbone in their main chain. The interest in polysilanes stems from a number of commercially attractive applications such as precursors to β-SiC fibers, photoresists in multilayer microlithography and photoinitiators in radical polymerization. Despite the commercial significance of these polymers, polysilane technology suffers from the lack of well-controlled and reproducible methods for synthesis of polysilanes with high yields, high molecular weight, and narrow polydispersity.

A number of factors need to be considered when selecting a polysilane polymer for a specific application: (1) nature of the ceramic material (chemical composition and crystal structure) produced after further processing (e.g., heat treatment), (2) elemental composition of the starting polymer (which influences the final stoichiometry of the ceramic produced), (3) molecular architecture of the polymer (linear vs. cross-linked polymer, which strongly influences the ceramic yield), (4) sensitivity to air (i.e., oxygen and water vapor) of the polymer, (5) starting molecular weight, (6) capacity of the

polymer to be cross-linked at some stage in processing, and (7) solubility in common organic solvents. As indicated in (1) above, pyrolysis conditions (temperature, atmosphere, and heating rate) play a very important role in determining the characteristics (yield, elemental composition, and crystal structure) of the ceramic produced. The ceramic yield (i.e., weight percentage retained after polymer-to-ceramic conversion) is an important consideration when discussing the suitability of a polysilane polymer as a precursor for silicon carbide. As indicated in (3) above, molecular architecture also has great impact on the ceramic yield of the polymer synthesized. Cross-linked or branched polymers give much higher ceramic yield than their linear counterparts. However, excessive cross-linking is generally not desirable, as it would make the processing of the polymer difficult (i.e., the polymer will be less likely to melt or to be soluble in common solvents). It is sometimes desirable that the final composition of the ceramic produced be that of near-stoichiometric silicon carbide. A convenient method of achieving this is to start with a polymer which has a 1:1 Si:C ratio, such as polymethylsilanes. This can be contrasted to polyphenylsilanes, for example, which have Si:C ratios of 1:6, and, therefore, result in SiC/C mixtures upon pyrolysis.

Polysilane polymers were first synthesized by Kipping [Kip21] in the early 1920's by condensation reaction of diphenyldichlorosilane with sodium. This polymer was not useful in practical applications since it was intractable (i.e., not processable into useful articles because of poor solubility and infusibility). Subsequently, in 1949, Burkhard [Bur49] reacted dimethyldichlorosilane with sodium to produce poly(dimethylsilane), which also was insoluble in common organic solvents and infusible. In 1975, Yajima and coworkers [Yaj75; Yaj78A; Yaj78B] were able to convert poly(dimethylsilane) to a tractable form of polycarbosilane (PCS) by pressure pyrolysis in an autoclave at 450°C. The polycarbosilanes were then melt spun into fibers which were subsequently heat

treated to form SiC-based ceramic fibers. The conversion process of polydimethylsilane to polycarbosilane takes place by Kumada rearrangement reactions and is described in detail elsewhere [Shi58].

2.2 Polysilane Synthesis

The prominent methods of synthesis of polysilanes are:

(i) Wurtz-coupling (dehalocoupling) reactions of chlorosilanes with alkali metals.

(ii) Dehydrocoupling of primary organosilanes in the presence of a catalyst.

(iii) Redistribution/substitution reactions of chlorosilanes.

2.2.1 Wurtz-coupling of dichlorosilanes with alkali metal

2.2.1.1 Mechanism

Wurtz-coupling of dichlorosilanes with an alkali metal is a strongly exothermic and heterogeneous reaction. The reaction can be represented as follows:

$$R^1 R^2 SiCl_2 + 2Na \xrightarrow{\text{Solvent, Reflux}} (R^1 R^2 Si)_n + 2NaCl \qquad (2.1)$$

where R^1, R^2 can be H, CH_3, C_6H_5, C_6H_{13}, etc.

The detailed reaction chemistry is shown in Figure 2.1 [Ben91]. Although many polymers are produced by this route, it suffers from the disadvantages of poor reproducibility, polymodal molecular weight distributions, and low polymer yields. Poor reproducibility arises because it is difficult to control the exothermic and heterogeneous reaction (i.e., the reaction is heterogeneous in that it involves liquid and solid reagents [Zei86A]). In addition, some reaction variables, such as the purity of the chlorosilanes, and the state of dispersion of sodium, are difficult to control [Mar92].

Initiation

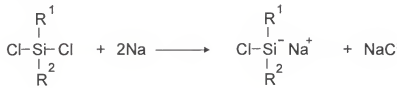

(2.2)

Propagation

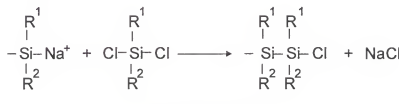

(Rate determining)

(2.3)

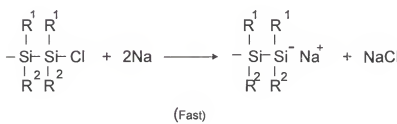

(Fast)

(2.4)

Figure 2.1. Reaction scheme for Wurtz-coupling polymerization reaction

Polymer yields and molecular weight distributions are quite sensitive to substituents (pendant groups) in the monomers, order of reagent addition, solvent composition, reaction temperatures, etc. The reaction is usually carried out at elevated temperatures (~100°C) using a suitable alkali metal dispersion. Sodium, potassium or lithium could be chosen as alkali metals but sodium is usually preferred because potassium and lithium are relatively more flammable and hazardous. In the Wurtz-coupling reaction, sodium is normally employed as a dispersion in an appropriate solvent such as toluene, xylene, THF, etc. As discussed in section 2.2.1.4, the choice of solvents plays an important role in determining the polymer molecular weight distribution and polymer yields.

Equation (2.1) is indicative of the fact the polymerization reaction proceeds by condensation type mechanism. However, Worsfold [Wor88] and Miller et al. [Mil91] reported, based on the characteristics of the polymers produced during the reaction, that it proceeds by an addition type mechanism. In an addition type polymerization reaction, high molecular weight polymer fractions form very early in the reaction and the formation of high molecular weight polymer is not affected by the stoichiometry of the reagents (i.e., high molecular weight polymer forms even when one of the reagents is in excess). Worsfold demonstrated these characteristics for Wurtz-coupling polymerization of hexylmethyldichlorosilane (carried out in the "normal mode" (see section 2.2.1.2) in which monomers are added to molten sodium) by isolating high molecular weight polymer (~10^5) in the early stages of reaction. The rate determining step in Wurtz-coupling polymerization is the reaction between silyl radical and monomer, as shown by equation (2.3) in Figure 2.1. The reaction between chlorine-ended chain and sodium takes place rapidly (equation (2.4) in Figure 2.1). Weyenberg [Wey69] et al. have

demonstrated by gas chromatography that molecules containing sequences of Si atoms react faster than molecules containing single atoms.

2.2.1.2 Mode of addition of reagents

At the beginning of the reaction, molten sodium (melting point of sodium = 98.5°C) can be added to dichlorosilanes dissolved in a suitable solvent at the reflux temperature of the solvent ('inverse' mode of addition) or dichlorosilanes dissolved in a small amount of solvent could be added to the molten sodium dispersed in the inert solvent ('normal' mode of addition). The inverse mode of addition usually leads to higher molecular weight polymers with lower polymer yields compared to the normal mode of addition. The former method is also more hazardous (i.e., due to handling of sodium) and difficult to control.

Zeigler [Zei86A; Zei87] investigated the effect of rate of monomer addition (in the normal mode) and sodium addition (in the inverse mode) on the polymodality of the molecular weight distribution in the synthesis of polymethylphenylsilane. Zeigler concluded that the rate of reagent addition (monomer or sodium) and the mode of addition had an important role in determining the molecular weight distribution because of its influence in controlling the rate of diffusion of reactive species to and from the sodium surface. When the rates of addition of Na or monomer were kept constant (for a range of addition rates 80-640 meq/min (i.e., moles equivalent per min)), the molecular weight distributions were nearly monomodal and the average molecular weights remained approximately constant at 600,000 for inverse mode of addition and 4000 for normal mode of addition. However, when the addition rate was varied, there was a tendency to form a bimodal molecular weight distribution. Figure 2.2 shows the effect of the rate of Na addition (inverse mode) on the $(PhMeSi)_n$ molecular weight distribution.

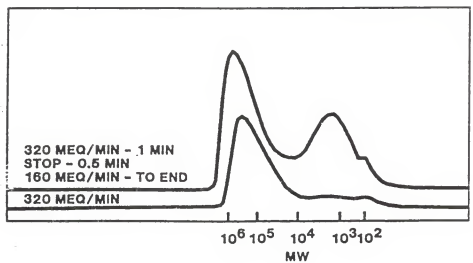

Figure 2.2. Effect of reactant addition rate on $(PhMeSi)_n$ molecular weight distribution [Zei86].

(Zeigler et al. did not provide plots of the molecular weight distributions obtained by using different monomer addition rates (normal mode)).

2.2.1.3 Effect of alkali metal

As indicated earlier, sodium, potassium or lithium could be chosen as the alkali metal for the polymerization reaction. Based on ease of handling (for example, sodium is available as 3-5 mm pellets where as potassium and lithium are available as blocks of materials and need to be cut into smaller sizes for accurately weighing) and flammability considerations, sodium is normally preferred over the other two. Alternatively, alloys of sodium and potassium of varying composition could be used but these alloys often cause degradation of polymer molecular weight and form cyclic oligomers at elevated temperatures (~100°C) (Na/K alloy promotes hydrogen abstraction from solvent and causes chain transfer) [Mil93].

The polymerization reactions take place very close to the alkali metal surface and, hence, the surface area of the alkali metal plays a very important role in determining the molecular weight distribution of the polymer formed. Worsfold [Wor88] studied the effect of sodium surface area on the molecular weight of polymers formed during the polymerization of hexylymethyldichlorosilane and found that rate of consumption of monomers increased as the sodium surface area increased (Figure 2.3) (The monomer consumption was monitored by removing small amounts of the reaction contents periodically during the course of reaction and analyzing the samples by gas chromatography (GC).) Therefore, to obtain good polymer yield in a reasonable time, it is important to use a fine dispersion of sodium in the reaction solvent.

The plots in Figure 2.3 show a sigmoidal behavior. The incubation period is interpreted as the time during which initiation occurs, i.e., according to equation (2.2) in

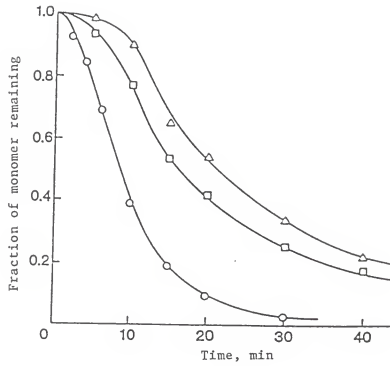

Figure 2.3. Effect of sodium surface area on the rate of consumption of hexylmethyldichlorosilane [Wor88]; Δ: 0.20 m^2 , □ : 0.67 m^2, o: 4.64 m^2 per mole of dichlorosilane

Figure 2.1. It might be expected, based on equation (2.2), that the rate of initiation would be dependent upon the available sodium surface area. The results in Figure 2.3 are consistent with this interpretation in that the incubation period decreases with increasing sodium surface area.

The Wurtz polymerization reaction is strongly exothermic and the initially clear reaction mixture changes to purple or dark blue color quickly. Miller et al. [Mil91] attributed this blue color to 'defects' in sodium chloride, i.e., color centers produced by incorporation of sodium ions in the interstitials of precipitating sodium chloride. Benfield et al. [Ben91] suggested, based on spectroscopic studies, that the blue color is due to colloidal Na particles (submicron) formed during the reaction. They collected diffuse reflectance ultraviolet-visible (UV Vis) spectra of the products formed during the reaction and found that there were two absorption bands for polysilanes, a sharper band below 400 nm and a broader band centered around 560 nm (Figure 2.4). Comparing this spectra with published results of sodium colloids and defect centers of sodium chloride, the authors concluded that the absorptions in the UV-Vis spectra were due to colloidal sodium formed during the reaction.

2.2.1.4 Solvent effects

The influence of types of solvents on Wurtz-coupling reactions of dichlorosilanes with sodium was first noted by Miller et al.[Mil93] in the preparation of polycyclohexylmethylsilane (normal mode). They reported that when diglyme (diethyleneglycol dimethylether, see Figure 2.5) was added to the reaction mixture of sodium and monomers, overall polymer yield and molecular weight distribution are affected (see Table 2.1). When diglyme was added in low concentrations (~10 vol%) in the polymerization of cyclohexylmethylsilane, there was a significant increase in polymer

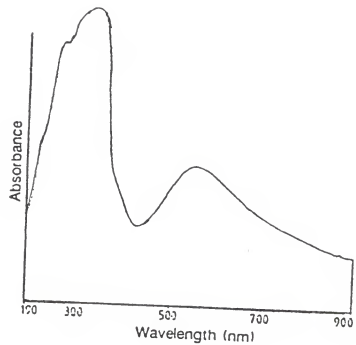

Figure 2.4. UV-Vis Diffuse Reflectance spectrum of purple solid isolated during Wurtz polymerization [Ben91].

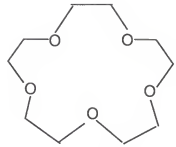

15-Crown-5 Ether $(CH_2)_{10}O_5$
(1,4,7,10,13-Pentaoxacyclopentadecane)

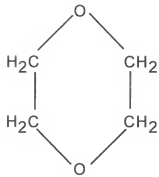

1,4-Dioxane

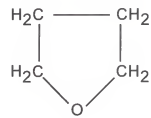

Tetrahydrofuran (THF)

$(CH_3OCH_2CH_2)_2O$
Diethyleneglycol dimethylether (Diglyme)

Figure 2.5. Chemical formulas of polar solvents used in Wurtz-coupling polymerization

Table 2.1: Effect of diglyme and heptane additions on polymerization of some dichlorosilane monomers [Mil91].

Polymer	toluene:diglyme (vol%)	Yield, %	$M_w \times 10^{-3}$	R [c]
$(c\text{-HexSiMe})_n$	100:0	20	804, 4.5 [b]	8.7
$(c\text{-HexSiMe})_n$	90:10	35	1477, 24.8 [b]	0.12
$(c\text{-HexSiMe})_n$	75:25	32	23.1 [a]	...
$(c\text{-HexSiMe})_n$	25:75	33	16.5 [a]	...
$(n\text{-dodecylSiMe})_n$	100:0	8	1345, 8.4 [b]	2.73
$(n\text{-dodecylSiMe})_n$	70:30	33	476, 40.7 [b]	0.74
$(n\text{-Hex}_2\text{Si})_n$	100:0	5.9	1982, 1.2 [b]	3.12
$(n\text{-Hex}_2\text{Si})_n$	95:5	34	1008, 22.3 [b]	3.4
$(n\text{-Hex}_2\text{Si})_n$	90:10	36	1358, 26.6 [b]	2.6
$(n\text{-Hex}_2\text{Si})_n$	70:30	37	1073, 31.7 [b]	1.42
$(n\text{-dodecyl}_2\text{Si})_n$	100:0	3	521, 14.1 [b]	5.2
$(n\text{-dodecyl}_2\text{Si})_n$	70:30	34	570, 27.4 [b]	2.3
$(PhMeSi)_n$	100:0	25	383, 16 [b]	...
Polymer	toluene:heptane (vol%)	Yield, %	$M_w \times 10^{-3}$	R [c]
$(n\text{-Hex}_2\text{Si})_n$	84:16	27	1386, 1.1 [b]	...
$(PhMeSi)_n$	85:15	9	1390, 10.5 [b]	...

[a] monomodal; [b] bimodal; [c] ratio of amounts of high molecular weight to low molecular weight fractions

yield and average molecular weight. At higher concentration of diglyme (~25 vol%), polymer molecular weight distribution became monomodal and overall molecular weight of the polymer decreased drastically. The polymer yield remained relatively high (32%). The effect on polymer yield of diglyme additions was particularly significant in the case of polysilane polymers derived from symmetric dialkylsilane monomers (e.g., dicholoro-di-n-hexylsilane, dichloro-di-n-dodecylsilane) (see Table 2.1). In the case of poly(di-n-hexylsilane), a typical dialkyldichlorosilane derived polymer, the yield of the polymer was only 5.9% when synthesized in toluene alone as a solvent . The polymer yield increased approximately six fold (~34-37%) when diglyme was added in amounts of 5, 10, and 30% by volume of toluene. The addition of diglyme also resulted in lower average molecular weight of the polymer. In the case of dichloro-di-n-dodecylsilane, the addition of 30% diglyme resulted in large increase in the polymer yield (from 3 to 34%), while the average molecular weight increased slightly for each mode in the distribution. Also, the high molecular weight proportion of the polymer decreased significantly.

Table 2.1 also shows the effect of addition of a non-polar solvent (i.e., heptane) on polymerization of diakyldichlorosilane monomers (dicholoro-di-n-hexylsilane) and arylakyldichlorosilane monomers (phenylmethyldichlorosilane). Addition of heptane caused an increase in polymer yield for the case of polymerization of dicholoro-di-n-hexylsilane and a decrease in polymer yield for the case of polymerization of phenylmethyldichlorosilane. The heptane addition resulted in lower average molecular weight in the former case and higher average molecular weight in the latter case. Miller et al. explain that polymerization of arylalkyldichlorosilanes is highly exothermic and takes place rapidly because arylalkyldichlorosilanes are not sterically hindered unlike dialkyldichlorosilanes. Solvent effects on polymerization of arylalkyldichlorosilanes are

not well understood because of the difficulty in obtaining controlled kinetic data (due to the rapid polymerization rates).

Miller et al. attempted to explain the observation of increased polymer yield for dialkyldichlorosilanes in the presence of polar cosolvents such as diglyme, crown ethers etc., by suggesting the presence of silyl anion radical intermediates (such as shown in equation (2.2) in Figure 2.1) as the main propagating species in the polymerization. It is well known that polar solvents aid in the transfer of electrons from metal to monomer, promoting formation of silyl anion radicals [Gau90; Mil93; Bil83]. A large number of radicals formed would mean a large number of initiation sites and this would favor an increased polymer yield. However, Miller et al. [Mil91] reported the same beneficial effect (i.e., improved yield) when 16 vol% of non-polar solvent (i.e., heptane) was added to toluene in the polymerization of dialkyldichlorosilane (such as dichloro-di-n-hexylsilane).

Zeigler et al. [Zei87] have developed a model concerning the bulk solvent effects in the polymerization of dialkyldichlorosilanes when monomer is present in excess compared to sodium (inverse mode of addition). According to their model, yield and molecular weight are determined by effective monomer concentration at the sodium surface. This depends on the rate of diffusion of monomer to the sodium surface, which, in turn, depends on degree of coverage of the sodium by growing polymer chains (see Figure 2.6). In a "good" solvent (i.e., in which the difference in polymer and solvent solubility parameters, $\Delta\delta = \delta_p - \delta_s$, approaches zero), polymer-solvent contacts are highly favored and the polymer coils are relatively extended in the solvent. Thus, polymers tend to remain in the solvent phase and tend not to adsorb on the sodium particle surfaces. The monomer continues to have easy access to sodium surface and

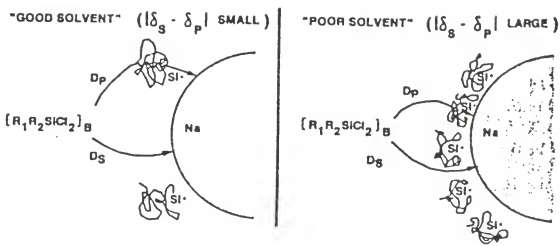

Figure 2.6. Schematic illustration of the influence of solvent on the polymer/sodium particle interaction during Wurtz polymerization [Zei87].

new initiation reactions can occur readily. This tends to result in high polymer yield (because monomer is "consumed" readily) and low average molecular weight. (Because there are a large number of chains, the amount of chain extension is limited since the supply of monomer is fixed.) In a poor solvent on the other hand, polymer coils are contracted and there is a much greater tendency for the polymer chains to absorb on the sodium particle surfaces. Since the direct path of monomer to the sodium surface (through the solvents) is impeded now, the monomer is forced to diffuse through polymer chains. This tends to promote propagation reactions (at the reactive chain ends) (i.e., causes formation of longer chain polymers) and leads to lower polymer yield and higher overall polymer molecular weight. In the extreme case when the solvent is 'too poor', the polymer would tend to precipitate out of solution, which is not desirable. Thus, Zeigler et al. model suggests that there is an optimum $\Delta\delta$ for a given polysilane polymer-solvent system which would dictate the yield and overall molecular weight of the polymer.

Gauthier and Worsfold [Gau89] investigated the influence of cosolvent 15-crown-5 ether ('phase-transfer catalyst') on the Wurtz-coupling polymerization of n-hexylmethyldichlorosilane (Figure 2.5 shows structure of 15-crown-5 ether). The primary solvent used was toluene and the amount of 15-crown-5 ether used was in the range of 0.25-4 mol% (of hexylmethyldichlorosilane). They also found that in the presence of the cosolvent, the polymer yield becomes high, the overall molecular weight of the polymer decreases, and the molecular weight distribution changes from bimodal to monomodal.

Figure 2.7 shows the amount of monomer consumed as a function of time in the study by Gauthier and Worsfold. They suggested that silyl anionic intermediates (shown

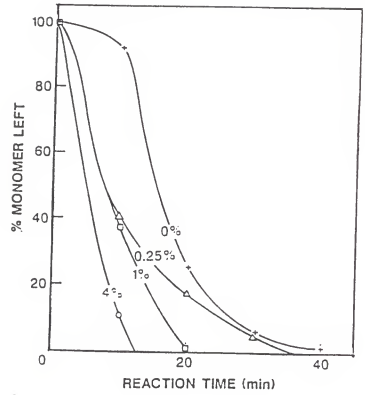

Figure 2.7. Rate of disappearance of monomer n-hexylmethyldichlorosilane as a function of time and weight percent of 15-crown-5 ether [Gau89].

by equation (2.2) in Figure 2.1) are involved in the polymerization of n-hexylmethyldichlorosilane and claimed that 15-crown-5 ether accelerated the occurrence of initiation reactions. Although data is limited, it is evident that the rate of monomer consumption is increased with small additions of 15-crown-5 ether.

2.2.1.5 Temperature effects

Miller et al. [Mil93] investigated the effect of temperature on the molecular weight distribution and yield for polymers produced from diaryl and dialkyl substituted chlorosilanes. They found in the case of polymerization of methylphenyldichlorosilane in toluene that lowering the reaction temperature to 65°C (from the refluxing temperature of 110°C) decreased the total yield from 25% to 10%, while causing an increase in molecular weight of the polymer. In addition, the molecular weight distribution changed from bimodal to monomodal (Table 2.2). However, in the presence of a polar solvent (i.e., 15% diglyme), lowering the reaction temperature to 65°C (instead of the reflux temperature) resulted in the opposite trends from what is noted above, i.e., the polymer yield increased slightly and the polymer molecular weight decreased. (The latter changes may have been within the limits of experimental error.)

When polymerization was carried out in a blend of toluene/15% heptane, lowering the reaction temperature to 65°C had no effect on polymer yield or overall polymer molecular weight. Miller et al. also reported that low temperature (65°C) polymerization of alkyl substituted chlorosilanes (such as dichloro-di-n-hexylsilane) took place sluggishly. The typical change in color to purple or dark blue was conspicuously absent. In addition, the yield for such a polymerization was less than a percent (i.e., essentially no polymerization occurred).

Jones et al. [Jon94] investigated polymerization of methylphenylsilane in THF at low temperatures (-79°C) using a sodium/electron acceptor complex. The electron

Table 2.2. Effect of temperature on polymerization of methylphenyldichlorosilane [Mil93].

($PhMeSiCl_2$ + Na ⟶ $(PhMeSi)_n$)

Solvent	Temperature,°C	Additive	Yield, %	$M_w \times 10^{-3}$	$M_n \times 10^{-3}$
Toluene	Reflux	—	25	383, 16 [a]	267, 8.1 [a]
Toluene	65	—	10	1073 [b]	377 [b]
Toluene/15% Heptane	Reflux	—	9	1390,10.5 [a]	375, 6 [a]
Toluene/15% Heptane	65	—	9	1367 [b]	580 [b]
Toluene/15% Heptane	Reflux	Diglyme (15%)	25	23.8 [b]	9.7 [b]
Toluene/15% Heptane	65	Diglyme (15%)	28	14.2 [b]	6.7 [b]

[a] bimodal; [b] monomodal

acceptors used in the polymerization were naphthalene, anthracene and tetraphenyl ethene, and were used in stoichiometric excess to disperse sodium. The disadvantages of typical Wurtz-type polymerization (e.g., low polymer yields, poor reproducibility) persisted, but polydispersities of the polymer produced were much lower (1.5-3) than that of typical Wurtz-type polymerization (> 5).

2.2.2 Ultrasonically-activated Wurtz-coupling reactions

Matyjaszewski et al. [Mat88; Mat91; Kim88] pioneered the use of ultrasonic energy in the Wurtz-coupling synthesis of polysilanes (derived from aryl-substituted monomers) having high molecular weight and monomodal distributions. Use of ultrasonic energy enabled reactions to be performed at low or ambient temperatures. The principle of ultrasonic polymerization is based on the implosive collapse of cavities with very high pressures and temperatures existing locally for short duration of times [Pri94]. The ultrasonic energy is generated using an immersion-type probe or ultrasonic bath. The reasons for obtaining monomodal and high-molecular-weight distributions for the polymers synthesized by ultrasonic method is attributed to the formation of high quality sodium dispersions which are continuously regenerated during the coupling process with continuous removal of sodium chloride byproduct from the sodium surfaces.

Matyjaszewski et al. report that polymer molecular weight distribution becomes broader and the average molecular weight decreases as the reaction temperature increases. It was also observed that prolonged sonication (both during and after the addition of monomer) results in degradation of high-molecular-weight components, as shown in Table 2.3. (This results in polymers with lower average molecular weight and lower polydispersity.)

Table 2.3: Effect of sonication time on molecular weights and polydispersities of polymethylphenylsilane [Kim88].

Molecular Weight	Sonication time (min) During addition of monomers			Sonication time (min) After addition of monomers			
	5	10	15	30	60	80	120
$M_n \cdot 10^{-5}$	3.8	2.24	2.30	1.82	1.48	1.06	0.40
$M_w \cdot 10^{-5}$	17.3	6.68	6.35	3.73	2.57	1.57	0.47
M_w/M_n	4.5	2.98	2.71	2.05	1.73	1.48	1.17

Matyjaszewski et al. also observed that ultrasonic polymerization of dialkyl-substituted chlorosilanes occur sluggishly when compared with that of diaryl-substituted dichlorosilanes and that cosolvent additions (e.g., diglyme) and higher temperatures were required to obtain any meaningful yield of polymer. In general, polymer yields for ultrasonic synthesis of polysilanes are low when compared to those of classic Wurtz-coupling reactions performed at high temperatures (i.e., the reflux temperatures of the solvents). Furthermore, the ultrasonic synthesis method is amenable only for aryl-substituted dichlorosilanes. However, it has better potential for control of polymer molecular weight and is less hazardous to perform, since the reactions are carried out at or near ambient temperatures.

2.2.3 Polymerization of monoalkylchlorosilanes

Although a lot of information is available on the Wurtz-coupling reactions of aryl-substituted and dialkyl-substituted chlorosilanes, information is scarce on the polymerization of monoalkylchlorosilanes. Seyferth et al. [Sey92] have synthesized polymethylsilanes by condensation of methyldichlorosilanes with sodium (normal mode) in a solvent mixture of hexane and THF (7:1 by volume) at reflux for 16 h. The polymer was a liquid with a composition of $((CH_3SiH)_{0.8}(CH_3Si)_{0.2})_n$ (elucidated by NMR

spectroscopy) and was produced in high yields (i.e., 60 to 70%). Average molecular weights for these polymers were reported to be low (620-690). When the polymerization was carried out in THF instead of a mixture of THF and hexane, the resulting polymer apparently had higher molecular weight (absolute numbers were not reported) and more cross-linked structure. The latter conclusions were based on NMR sudies (showing a lower concentration of Si-H bonds) and thermogravimetric analysis (TGA) (showing higher ceramic yield). When the reaction was carried out in xylene (under refluxing conditions), the yellow-colored polymer was produced with a yield of 40%, molecular weight in the range of 520-600 (M_w), and structure of $((CH_3SiH)_{0.4}(CH_3Si)_{0.36})_n$ (determined from NMR).

Qiu and Du [Qiu89A; Qiu89B] prepared polymethylsilane polymers by condensation of methyldichlorosilane with sodium (normal addition mode) in a blend of toluene and dioxane (33:67 vol% ratio). It is expected that dioxane, a dipolar solvent, will promote polymerization of $MeHSiCl_2$ (i.e., higher reaction rate). (The effect of polar solvents on Wurtz-coupling reaction of dichlorosilanes with sodium was discussed in section 2.2.1.4) The polymerization was carried out at the reflux temperatures of the toluene-dioxane solvent mixture. The end point of polymerization was determined by testing for the acidic nature of the reaction contents. The reaction was stopped when the reactions contents did not test acidic (pH=6-7). The reaction contents were separated from the NaCl precipitates by filtering and the polymer was isolated by evaporation of the polymer solution under vacuum. The polymer was fractionated by adding, drop by drop, a mixture of methanol and 2-propanol with vigorous stirring. The precipitate was collected and dried in a vacuum oven at room temperature for 2 h. The polymers synthesized by this method were used in studies involving oxidative cross-linking, photo

cross-linking, and room temperature vulcanization. The polymer was produced in ~45% yield and had an appearance of pale yellow waxy solid with M_w ~1,800.

2.2.4 Polysilane copolymers

As discussed in section 2.1, when dialkyldichlorosilane is reacted with sodium in a refluxing solvent, polydimethylsilane polymer is formed which is infusible and insoluble in common organic solvents (e.g., toluene, benzene, xylene, etc.). West et al. [Wes81; Wes86A] discovered that when phenylmethyldichlorosilane was added to dialkyldichlorosilane in a 1:1 proportion by volume, and the reaction was carried out under same conditions, the resultant polysilane copolymer was highly soluble in common organic solvents (e.g., toluene, xylene, etc.). West et al. referred to this copolymer as "poly(silastyrene)" (PSS). The copolymerization reaction can be represented as:

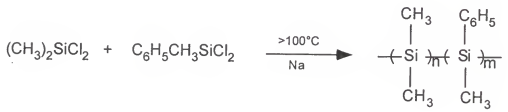

(2.5)

The PSS copolymer had a bimodal molecular weight distribution with modal values of ~15,000 and ~300,000.

2.2.5 Dehydrocoupling

Harrod et al. [Har88; Mu91A; Mu91B; Ait89; Ait87; Ait85] were the first to report a catalyst-based synthetic route for polysilanes prepared from primary organosilanes

(e.g., $RSiH_3$, where R is an alkyl or aryl group) with the evolution of hydrogen. The reaction can be represented as

$$nRSiH_3 \xrightarrow[20\text{-}65°C]{\text{Catalyst}} -\left(-\underset{\displaystyle H}{\overset{\displaystyle R}{\overset{|}{\underset{|}{Si}}}}-\right)_n- + H_2 \qquad (2.6)$$

The catalysts used were early transition metal complexes of titanium and zirconium, namely, bis(η^5-cyclopentadienyl) dimethyltitanium (Cp_2TiMe_2)(Dimethyl Titanocene, DMT) and bis (η^5-cyclopentadienyl) dimethylzirconium (Cp_2ZrMe_2) (Dimethyl Zirconocene, DMZ). Mu and Harrod [Mu91A] have investigated polymerization of methylsilane by dehydrocoupling in the presence of DMT catalyst and reported significantly higher yield of polymer in the form of a glassy solid in comparison to that produced by classic Wurtz-coupling reactions. Table 2.4 shows polymerization conditions (temperature, catalysts, solvents, time, amount of monomer used) and characteristics of the polymers produced (yield, molecular weight, etc.). Their method, however, suffers from the following disadvantages: (i) the reaction must be performed at 9-10 atm at 50°C because methylsilane is a gas at room temperatures; enhancing reaction rate would require working at higher pressures, which in turn requires sophisticated instrumentation in order to perform the experiments safely and (ii) handling methylsilane is dangerous since it is spontaneously flammable in air.

The monomer, methylsilane, was synthesized from methyltrichlorosilane. Methyltrichlorosilane was reacted with a suspension of lithium aluminum hydride in THF at 50°C for 3 h and then reaction products were cooled under liquid N_2 temperature to

Table 2.4. Summary of methylsilane polymerization by catalytic dehydrogenation reactions [Mu91A].

Run #	Solvent	Catalyst	$MeSiH_3$ (psi x L[b])	T, °C	Time, days	Amount of PMS, g	Yield, %	M_w [c]	M_n [c]	M_w/M_n	% Cyclics[c]
1	cyclohexene +toluene[a]	DMT (50 mg)	120 x 0.12	20	6	1.52	90	1590	790	2.01	0.4
2	cyclohexene +toluene[a]	DMT (50 mg)	130 x 0.12	20	9	1.82	~100	6350	1200	5.30	1.6
3	cyclohexene +toluene[a]	DMT (50 mg)	140 x 0.12	20	12	1.96	~100	10100	1250	8.10	3.4
4	cyclohexene +toluene[a]	DMT (50 mg)	120 x0.12	45	4	1.68	~100	7890	1240	6.36	0.5
5	cyclohexene +toluene[a]	DMT (50 mg)	110 x0.12	65	1	1.53	~100	12990	1260	10.30	0.5
6	Toluene	DMT (50 mg)	100 x0.12	20	9	0.37	26	830	560	1.48	4.6
7	cyclohexene +toluene[a]	DMZ (60 mg)	110 x0.12	20	5	1.43	~92	1730	800	2.16	...
8	cyclohexene +toluene[a]	DMZ (60 mg)	130 x0.12	20	7	1.81	~100	6010	1080	5.56	0.8
9	cyclohexene +toluene[a]	DMZ (60 mg)	125 x0.12	20	9	1.75	~100	9990	1350	7.40	2.5
10	cyclohexene +toluene[a]	DMZ (60 mg)	100 x0.12	65	1	1.40	~100	Insoluble			
11	Toluene	DMZ (60 mg)	110 x0.12	20	7	0.99	64	1020	620	1.65	3.8

[a] Cyclohexene:toluene proportion 70:30 (Vol %); [b] Volume of silane gas used

[c] Based on the assumption that the low molecular weight species in the gel permeation chromatograms are cyclic oligomers.

trap methylsilane. The subsequent polymerization of polymethylsilane was carried out in cyclohexene solvent which helps to avoid build up of hydrogen produced during reaction by promoting hydrogenation of cyclohexene to cyclohexane.

Molecular weight characteristics of some of the polymers synthesized by Mu and Harrod are illustrated by the GPC profiles in Figure 2.8. (The chromatograms are for samples associated with the entries in Table 2.4. The "A" chromatograms, from top-to-bottom, correspond to run #s 3,2,1, and 6, respectively, and the "B" chromatograms, from top-to-bottom, correspond to run #s 9,8,7, and 11, respectively.) The bimodal distributions that develop with longer reaction times are reported to be typical of dehydrocoupling of primary organosilanes. The lower molecular weight peak (appearing as a shoulder in most chromatograms in Figure 2.8) is attributed due to cyclic oligomers. The high polydispersity of these polymers can be attributed to branching/cross-linking that occurs at residual SiH_3, SiH_2 and SiH groups during prolonged reaction.

Mu and Harrod also studied polymerization of phenylsilane by dehydrocoupling using the aforementioned catalysts The polyphenylsilane polymer synthesized with DMT and DMZ had average degrees of polymerization of 1,000 and 2,000, respectively (corresponding to molecular weights of 46,000 and 92,000, respectively). In both cases, gel permeation chromatograms did not suggest the presence of cyclic oligomers (i.e., low molecular weight oligomers were not observed). Harrod et al. also report that secondary organosilanes (e.g., phenylmethylsilane) do not polymerize easily under similar reaction conditions and form only dimers and trimers. Brown-Wensley [Bro85; Bro87] has shown that a good catalyst for conversion of secondary silanes (R_2SiH_2) to dimeric silanes ($HR_2Si\text{-}SiR_2H$) is a $(Ph_3P)_3RhCl$ complex.

While Harrod's work on the synthesis of poly(arylsilanes) (e.g., poly(phenylsilane)) indicated that cyclic oligomers do not form, Campbell and Hilty

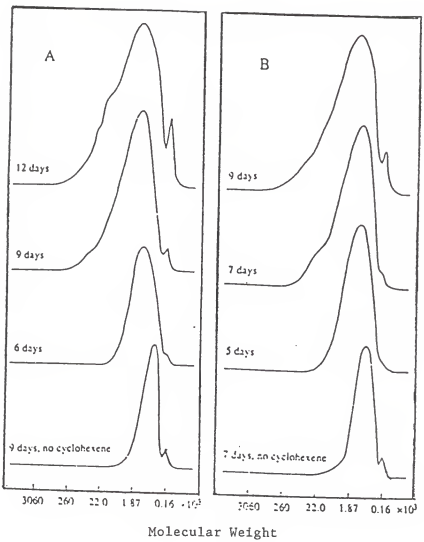

Figure 2.8. GPC of polymethylsilanes synthesized by Mu and Harrod [Mu91A]. A: DMT catalyst B: DMZ catalyst

[Cam89] have shown by gas chromatography that they are the main products in the polymerization of alkylsilanes (e.g., n-butylsilanes) catalyzed by DMZ. This is attributed to the ability of DMZ to promote reversible reactions for both primary and secondary silanes. In the case of polymerization of methylsilane, Campbell et al. reported the presence of a small amount of cyclic oligomers (n=5 to 10), in agreement with the results of Mu and Harrod. Thus, it can be concluded that formation of cyclic oligomers is inevitable in the polymerization of alkylsilanes by dehydrocoupling.

In general, DMZ and DMT catalysts are effective for polymerization of primary organosilanes. However, as shown by Mu and Harrod [Mu91A], polymerization rates for primary silanes are about ten times faster using DMZ compared to using DMT. Nevertheless, molecular weight characteristics of the polymers synthesized with the two catalysts are essentially identical. The DMT-catalyzed polymerization exhibited a pronounced induction period and a complete reduction of titanium to Ti (III). In contrast, an induction period was absent for DMZ catalyzed reactions and a slight auto-acceleration in the reaction rates was observed in the reactions at low catalyst or monomer concentrations.

The mechanism of catalytically activated dehydrocoupling of organosilanes is complex. Harrod [Har88] suggested (based on NMR studies) that the mechanism involved formation of titanium (IV) silylhydride ($Cp_2Ti(H)(SiH_2R)$) which decomposed by elimination of α-hydride from the SiH_2R group, followed by release of H_2 from the complex to give $Cp_2Ti{=}SiHR$ (silylene) complex. A number of metallocene (catalyst) derivatives are formed during polymerization that can be isolated and these compounds are presumed inactive in the polymerization cycle. Propagation then occurred by repetitive insertion of the silylene into a Ti-Si bond (a rapid addition mechanism) in which the intermediates are not observable because they are short-lived or because they are

spectroscopically 'silent' (i.e., absent in NMR because of paramagnetic nature). At present, a mechanism for chain termination is not elucidated, although catalyst-induced chain scission has been observed in the polymerization of cyclohexasilanes.

Since early transition metal complexes are not effective for dehydrocoupling of secondary silanes, other catalysts have been investigated. Corey et al. [Cor91] synthesized disilanes through pentasilanes by using a Cp_2ZrCl_2-nBuLi mixture as a catalyst for dehydrocoupling of phenylmethylsilanes in toluene at 90°C. (This temperature is higher than that used for dehydrocoupling of primary silanes.) This condensation reaction of secondary silanes is sensitive to steric effects (i.e., steric hindrance) of the substituents, as observed by the sluggish reaction of Ph_2SiH_2 compared to $PhMeSiH_2$ [Cor91].

Sakakura et al., [Sak91; Sak93] have developed a method for producing polysilanes by dehydrocoupling of primary organosilanes using a lanthanoid complex (1.5 wt%) as a catalyst. They reported that lanthanoid complexes have higher activity and selectivity than early transition metal complexes used by Harrod et al. In this case, the dehydrogenative reactions of phenylsilanes were performed at temperatures ranging from 20°C to 160°C and in the presence of a solvent such as toluene or benzene, with reaction times extending from several hours to several days. The authors reported that higher polymerization temperatures and longer reaction times lead to higher polymer molecular weight. The effect of the above variables in the polymerization of phenylsilane in the presence of hydrobis(pentamethylcyclopentadienyl)-neodymium catalysts (lanthanoid complex) is illustrated in Table 2.5.

Table 2.5: Effect of time and temperature on polymerization of phenylsilane in the presence of a lanthanoid complex [Sak93].

Temperature, °C	Time, days	Product Appearance	M_w	M_n
25	15	oil	520	1.26
80	2	gum	780	1.37
100	2	gum	990	1.54
130	2	solid	1600	1.91
130, 160 [a]	2, 7 [a]	solid	4380	3.09

[a] 2 days at 130°C followed by 7 days at 160°C.

Berris [Ber92] has also developed a process for synthesizing polysilane polymers with a M_w of ~1000-1500 by dehydrogenative coupling of primary organosilanes in the presence of (1-1.7 wt%) dimethyldialkylphosphine nickelhalide (e.g., 1,2-bis(dimethylphosphine) ethanenickel(II)chloride, dmpe $NiCl_2$) at temperatures of 20°C to 50°C in the presence of an inert solvent. The reaction time varied from 1 h to 10 days, depending on the temperature used (i.e., lower reaction times were used at higher temperatures). The dmpe $NiCl_2$ catalyst was reported to have a much higher activity than the early transition metal complexes used by Harrod et al.[Har88].

Seyferth et al. [Sey88; Sey90; Sey92; Sey93] have used dehydrogenative coupling to cross-link low molecular weight polymethylsilanes (containing multiple secondary or tertiary Si-H bonds) which had been synthesized by the Wurtz-coupling reaction of methyldichlorosilane with sodium in hexane/THF. This resulted in polymers that could be pyrolyzed to produce near-stoichiometric SiC with high yield (in the range of 95-98%). The low molecular weight polymethylsilanes were reacted with ~3 wt% cyclopentadienyl zirconium hydride catalyst in an inert solvent (such as hexane) at reflux temperatures. (Hexane was chosen because it readily dissolves the catalyst and it has a low reflux temperature.) Seyferth et al. [Sey93] observed that the products of the dehydrogenative coupling reaction of low-molecular-weight polysilanes with cyclopentadienyl zirconium hydride catalyst ranged from oil to solid (both orange in color) depending upon time-temperature conditions of the reaction. In order to impart infusibility to articles prepared from these cross-linked polymers (e.g., fibers), photolysis is required which can be accomplished by UV irradiation in hexane for 2 hours.

Tilley [Til91; Til93] developed a method of producing cross-linked, high-molecular-weight, silicon-rich polymers by dehydrogenative coupling reactions of organosilanes. The reaction of more than one Si-H group per silicon center caused

cross-linking of chains and increased molecular weights. A wide range of homopolymers with different structures were prepared by modifying the reaction conditions to vary the degree of branching (cross-linking) or chain extension. For example, when 1,3-disilylbenzene(1,3-$(H_3Si)_2C_6H_4$) or 1,3-dimethylsilyl benzene (1,3-$(CH_3H_2Si)_2C_6H_4$) was reacted in the presence of cyclopentadienyl zirconium hydride catalyst ($Cp_2(ZrH_2)_2$), the resulting polymer was highly cross-linked and high in molecular weight. The disilyl monomers (1,3-disilyl benzene or 1,3-dimethylsilylbenezene) developed by Tilley were prepared by reacting tetraethoxysilanes ($Si(OEt)_4$) or methyl triethoxysilanes ($CH_3Si(OEt)_3$) with dibromobenzene and magnesium in an inert solvent, followed by reduction of the intermediate compound (1,3-di(triethoxylsilyl)-benzene or di-(trimethoxysiloxy)-benzene) with lithium aluminum hydride. The dehydrogenative polymerization was then carried out by adding organosilanes (containing multiple Si-H groups per silicon center) drop by drop to a benzene solution containing the catalyst and stirring for 24 hours at 20-65°C under nitrogen. Many of the polymers prepared by Tilley's method were highly cross-linked and were insoluble in common solvents (e.g., toluene), indicating difficulty in controlling cross-linking reactions. The soluble polymers exhibited M_w ranging from 5,500 to 90,000 and M_n ranging from 1,300 to 2,200.

2.2.6 Redistribution/substitution reactions:-

Baney et al. [Ban82; Ban83; Ban85] prepared another class of polysilane polymers, methylpolysilanes (MPS polymers) by catalytic redistribution reactions involving Si-Si/Si-Cl bonds of methylchlorodisilane mixtures[¶] . The methylchlorodisilane mixtures, comprising 55 wt% $[MeCl_2Si]_2$, 35 wt% $Me_2ClSiSiMeCl_2$, and 10 wt%

[¶] Methylpolysilane (MPS) polymers, as described by Baney et al. have a structure of $[((CH_3)_2Si)_x(CH_3Si)_y]_n$. They are different from polymethylsilane (PMS) polymers discussed earlier, which have a structure of $[(CH_3SiH)_x(CH_2Si)_y]_n$.

($Me_3Cl_3Si_2$), were obtained as fractions from an industrial process for manufacture of methylchlorosilanes. The catalyst used for the redistribution/substitution reactions of methylchlorodisilane mixtures was tetrabutylphosphonium chloride. The proposed reaction scheme for these reactions is shown in Figure 2.9.

The rearrangement of disilanes into a monomer/polymer mixture occurred when the disilane mixture was heated to 250°C. Additional monomeric methylchlorosilanes formed even after the starting disilanes reacted completely. This occurred by the reaction of any Si-Cl bond with a terminal Si-Si bond in the polysilane backbone. The amount of monomers formed and the extent of polymerization were controlled by manipulating the heating schedule and final reaction temperature. The resulting yellow-colored methylchloropolysilane polymers (MCPS) were soluble in toluene and had polycyclic structures with seven rings per molecule ($(Me_2Si)_3(MeSi)_{17}Cl_5$)) as determined by gas chromatography (see Figure 2.10). The Si-Cl bonds in the methylchloropolysilane polymers were highly reactive and permitted easy chemical modification (such as reaction with Grignard reagents (alkyl-magnesium halide or phenyl-magnesium halide) to form methylpolysilane polymer (MPS). According to Baney et al., MCPS polymer reacts readily with Grignard reagents to replace the reactive Si-Cl groups with more stable Si-R groups. The modified polymers can be melt spun to form fibers which can be subsequently pyrolyzed to SiC as discussed in section 2.4.

The chemical modification of methylchloropolysilanes (MCPS) can also be accomplished by reducing MCPS over a slurry of lithium aluminum hydride under an inert blanket in a refluxing solvent such as toluene [Ban83]. The excess reducing agent is neutralized by adding water and aqueous NaOH and the solution is subsequently filtered to give a yellow-colored polymer of composition ($((CH_3)_2Si)_{0.6}(CH_3Si)_{0.4})_n$).

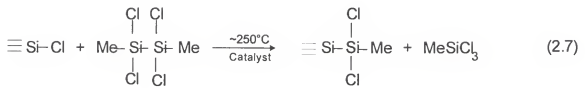

(2.7)

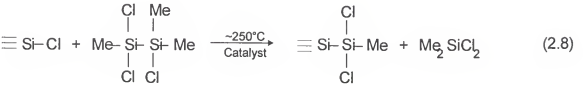

(2.8)

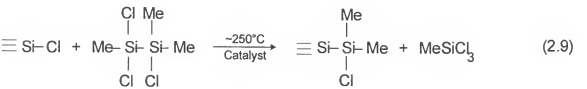

(2.9)

Figure 2.9. Scheme for redistribution/substitution reactions of chlorodisilanes.

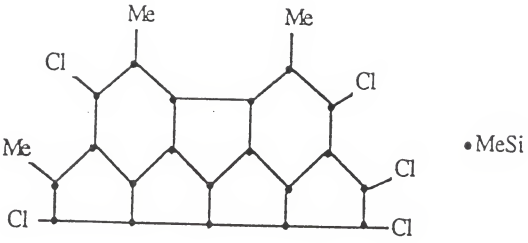

Figure 2.10. Structure of methylchloropolysilane polymer [Ban83].

(Information on oxygen incorporation into the polymer due to the addition of water and NaOH was not reported.)

The main disadvantage of Baney et al. MPS polymers from the point of view of subsequent processing for ceramic articles (e.g., fibers) is their poor oxidative stability (MPS polymers are pyrophoric). Burns [Bur90] attributed this tendency for spontaneous oxidation to a large number of Si-H groups in the polymer structure. The polymer develops a cross-linked structure upon oxidation due to the formation of Si-O-Si networks. Burns developed a remedy to the problem of oxidative instability in these MPS polymers by inserting multiple unsaturated bonds (such as acetylene or phenyl acetylene or diene compounds). According to Burns, by selectively inserting multiple unsaturated bonds in the Si-Si backbone, the final Si:C stoichiometry can also be controlled (unmodified MPS polymers typically yield silicon-rich ceramic residue). The insertion reaction can be carried out by reacting MPS polymers with ~8 wt% unsaturated compounds (e.g., phenyl acetylene) in the presence of a transition metal catalyst (e.g., tetrakis (triphenylphosphine) palladium or tris(tri-phenylphosphine) rhodium chloride) in an inert solvent such as toluene at reflux temperatures for ~20 hours. In addition to better oxidative stability and control of stoichiometry, Burns' method presents opportunities to synthesize polycarbosilanes by introducing unsaturated moieties between Si-Si bonds. An example of such a synthesis is reported as the reaction between 1,3-butadiene with a linear polysilane polymer [Bur90].

Bujalski et al. [Buj90] developed an alternate method of synthesis of chlorine-containing polysilanes. These polymers were prepared by reacting a mixture of 70-99 wt% of one or more of chlorine-containing disilanes (e.g., $((CH_3)_2ClSi)_2$, $(CH_3Si)_2ClSiSiCl_2CH_3$, $(CH_3Cl_2Si)_2$ etc.) with one or more of monoorganosilanes (e.g., $C_6H_5SiCl_3$). The reaction required 0.1 to 2 wt% rearrangement catalyst (e.g., quaternary

ammonium halide, quaternary phosphonium halide, etc.) at temperatures ranging from 100°C to 340°C. The polysilanes (solid at room temperature) were easily converted to silicon carbide by pyrolysis at elevated temperatures (at >1000°C). According to Bujalski et al., the use of a monoorganosilane (of structure R'SiX where R' is methyl, phenyl or octyl groups and X is chlorine) (or a mixture of monoorganosilanes) permits control of the glass transition temperature T_g of the polysilanes as well as the stoichiometry of the silicon carbide produced. Their work suggests using monoorganosilanes with silyl groups R'Si (where R'=n-octyl) allows a greater reduction in T_g of the polymer compared to using monoorganosilanes R'SiX (where R'=phenyl). Bujalski et al. reported that all the n-octyl groups are lost as olefins upon pyrolysis and this results in a carbon-deficient ceramic. In contrast, polymers with phenyl groups produce a carbon-rich ceramic after pyrolysis. However, the final Si:C stoichiometry also depends significantly on the presence of methyl radicals in the polysilane (CH_3Si or $(CH_3Si)_2Si$), which are generally not lost upon pyrolysis. Bujalski et al. indicated that presence of the n-octyl or phenyl-Si units enabled "fine tuning" of the silicon and carbon contents in the ceramic.

2.3. Pyrolysis Behavior

Carlsson et al. [Car90] have studied the pyrolysis behavior of various silicon backbone polymers such as polyphenylsilanes, poly-n-2-hexylsilanes, and polydimethylsilanes by means of thermogravimetric analysis (TGA) and Fourier transform infrared spectroscopy (FTIR). Polymers for the TGA study were heated at 10°C/min with 10 min isothermal holds at 200°C, 400°C, 600°C and 1000°C. Polymers for FTIR study were heated at 360°C, 454°C, 650°C, and 1200°C, with a 90 min hold at each temperature. Their results are summarized in Table 2.6. The effect of pendant groups (such as phenyl) on pyrolysis yield is particularly noticeable. For example,

Table 2.6. Ceramic yields and chemical compositions of polysilane homopolymers, copolymers and terpolymers [Car90].

Batch	Polymer[a]	Yield (wt%)		Inorganic Residue Analysis (wt%)			
		Theor.[b]	Observed[c]	C[d]	Si[d]	Calculated SiC Yield[e]	SiC Yield (%Theor)[f]
	Homopolymers						
I	$(CH_3\text{-}Si\text{-}CH_3)_n$	69	1.0	42	58	0.8	1.2
II	$(C_6H_5\text{-}Si\text{-}CH_3)_n$	33	24.6	55	39	13.7	41.5
III	$(C_6H_{13}\text{-}Si\text{-}CH_3)_n$	31	5.8	32	67	5.6	17.5
	Copolymers						
IV	$(C_6H_5\text{-}Si\text{-}CH_3)_{1.0}$ $(CH_3\text{-}Si\text{-}CH_3)_{1.0}$	51	13	62	51	7.1	15.4
V	$(C_6H_5\text{-}Si\text{-}CH_3)_{1.0}$ $(C_6H_{13}\text{-}Si\text{-}CH_3)_{1.0}$	32	8	49	49	5.9	17.9
VI	$(CH_2{=}CH\text{-}Si\text{-}CH_3)_{1.0}$ $(C_6H_5\text{-}Si\text{-}CH_3)_{9.0}$	36	39.1	65	38	19.5	54.5
	Terpolymers (5:5:1)						
VIIa	$(C_6H_5\text{-}Si\text{-}CH_3)$ $(C_6H_{13}\text{-}Si\text{-}CH_3)$ $(CH_2{=}CH\text{-}Si\text{-}CH_3)$[g]	36	7	47	54	5.3	15.6
VIIb	$(C_6H_5\text{-}Si\text{-}CH_3)$ $(C_6H_{13}\text{-}Si\text{-}CH_3)$ $(CH_2{=}CH\text{-}Si\text{-}CH_3)$[h]	36	22	53	42	14.8	41.2
VIII	$(C_6H_5\text{-}Si\text{-}CH_3)$ $(CH_3\text{-}Si\text{-}CH_3)$ $(CH_2{=}CH\text{-}Si\text{-}CH_3)$	52	27	61	45	15.1	29.1
IX	$(C_6H_5\text{-}Si\text{-}CH_3)$ $(C_6H_{13}\text{-}Si\text{-}CH_3)$ $(CH_2{=}CH\text{-}CH_2\text{-}Si\text{-}CH_3)$	51	21	61	47	11.6	22.8

[a] The functional groups shown are attached to Si as side groups.
[b] Theoretical conversion to SiC (for e.g., $(CH_3\text{-}Si\text{-}CH_3)_n \longrightarrow$ SiC is 69% conversion).
[c] Observed ceramic yield.
[d] C+Si total in some cases exceed 100%. The totals appeared as such in the paper and presumably reflect experimental error in the measuring technique.
[e] The ceramic residue consists of SiC and C. The percentage of SiC is calculated by multiplying the experimentally observed yield by the factor (100-C)/70 wt% where C is the carbon content of the residue. (Note that the theoretical composition of SiC is 70 wt% Si/ 30 wt% C.)
[f] [Calculated SiC yield[d]/theoretical SiC yield[b]]x100.
[g] low MW viscous oil.
[h] high MW fraction.

polydimethylsilane with methyl groups as substituents gives high theoretical yield (69%) but low pyrolysis yield (~1%). (Experiments by Wood [Woo84] and West et al. [Wes81] also confirm this observation.) Replacement of a methyl substituent by a bulky phenyl group (as in polyphenylmethylsilane) results in improved pyrolysis yield, ~25% (presumably due to the retention of some phenyl groups during pyrolysis). (It is also possible that high yield depends on the ability to develop a Si-C-Si-C backbone with sufficient cross-linking.)

Figure 2.11 shows the FTIR spectra of a polysilane terpolymer (polymer VIIb shown in Table 2.6) during pyrolysis to 1200°C. The polymer was cast as a thin film on a silicon wafer and heated under argon atmosphere and spectra were collected at different temperatures. The typical absorptions for the as-prepared polysilane occurred at 3050 cm^{-1} (due to the C-H stretching vibration of $Si-CH=CH_2$), 1428 cm^{-1} (due to the CH_2 bending vibration of $Si-C_6H_5$), 1468 cm^{-1} (due to the CH bending vibration of $Si-C_6H_{13}$) and 2100 cm^{-1} (due to stretching vibration of Si-H), and 1247 cm^{-1} (due to the rocking vibration of $Si-CH_3$). Figure 2.12 shows the changes in concentrations in residual pendant organic groups calculated based on the IR spectra, allowing for reduction in thickness of the film which occurred during pyrolysis. The slight increase in the Si-H group intensity is attributed to methylene insertion reactions taking place between 200°C and 450°C. (This observation was also confirmed by Schilling [Sch84; Sch88] and Schmidt [Sch91] by NMR studies and resembled reactions occuring during the conversion of polydimethylsilane to polycarbosilane [Has83].) Carlsson et al. indicated that no significant changes occurred during the pyrolysis up to 300°C but rapid elimination of $-CH_3$, $-C_6H_5$ and $-C_6H_{13}$ groups occurred between 300°C and 450°C. The increase in the absorption intensity at 1030 cm^{-1} corresponded to formation of $Si-(CH_2)_n-Si$ linkages and network.

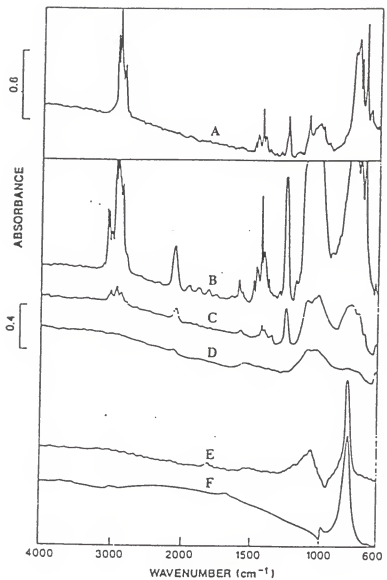

Figure 2.11. IR spectral changes during pyrolysis of a polysilane polymer (VIIb in Table 2.6) [Car90]; A: initial film; B: 360°C (1.5 h hold); C: 454°C (1.5 h); D: 650°C (1.5 h); E:1200°C (1.5 h); F: dispersion of single crystal SiC whiskers in KBr for comparison.

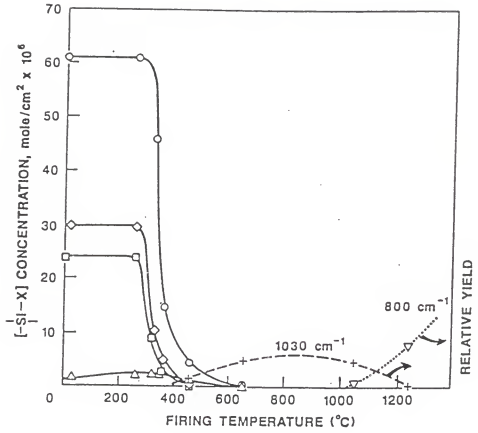

Figure 2.12. Change in intensities of pendant groups based on IR spectra for polysilane polymer (VIIb in Table 2.6) [Car90] : o: $\rho(CH_3)$ from Si-CH_3; ◊: δ (CH_2) of Si-C_6H_5 ; □: δ (CH) of Si-C_6H_{13} ; +: δ (CH_2) of Si-$(CH_2)_n$-Si ; Δ:ν (Si-H) ; ∇: ν (Si-C)

Wood [Woo84] studied the pyrolysis behavior of three different polymethylsilanes (designated as PMS-I, PMS-II and PMS-III) prepared by Wurtz-coupling reactions of dichlorosilane with sodium in the presence of hexane, hexane/THF (7:1 volume) mixture and THF, respectively. Table 2.7 gives a summary of the synthesis conditions and characteristics for the three polymers. PMS-I showed very low ceramic yield (~25%) upon pyrolysis to 1000°C. The low ceramic yield was attributed to the loss of Si by volatilization of low molecular weight components (which was confirmed by mass spectral analysis of the pyrolysis species). X-ray Diffraction (XRD) analysis of the ceramic residue obtained from pyrolysis of PMS-I showed peaks due to excess Si as well as SiC peaks. The pyrolyzed ceramic had an overall composition of 67% SiC and 33 wt% Si (calculated based on the Si/C ratio determined by elemental analysis). Polymer PMS-II showed a ceramic yield of ~27% . The XRD analysis of the pyrolyzed ceramic residue showed no Si peaks (for unknown reasons) although elemental analysis revealed silicon-rich composition (77 wt% SiC and 23 wt% Si). PMS-III showed a much higher ceramic yield of 60% compared to the other two PMS polymers and had an elemental composition of 75 wt% SiC and 25 wt% Si. (XRD analysis showed both Si and SiC peaks.) The differences in the pyrolysis yields were attributed to differences in cross-linking in the three polymers. Based on NMR data, both PMS-I and PMS-II contained higher number of Si-H functionalities (which are potential cross-linking sites) compared to PMS-III. (This suggested that cross-linking was more extensive in PMS-III due to consumption of Si-H moieties by condensation reactions. Recall that a polar solvent such as THF aids in the anionic polymerization of methylchlorosilanes with sodium and leads to formation of polymers which are rich in Si-H groups; these Si-H groups undergo condensation causing extensive cross-linking in the polymer).

Table 2.7. Synthesis conditions and characteristics for PMS polymers prepared by Wood [Woo84].

Polymer Designation	Synthesis Conditions	Molecular Weight	Ceramic Yield ,% [c]	Composition
PMS-I	Reflux, Hexane	520	25	67 wt% SiC, 33 wt% Si
PMS-II	Reflux, Hexane:THF[a]	620-690	27	77 wt% SiC, 23 wt% Si
PMS-III	Reflux, THF	--- [b]	60	75 wt% SiC, 25 wt% Si

[a] 7:1 Volume proportion
[b] Insoluble in benzene, hence cryoscopic determination of molecular weight could not be carried out.
[c] Pyrolyzed to 1000°C in nitrogen atmosphere at 10°C/min

Seyferth at al. [Sey93] have significantly enhanced pyrolysis yields of PMS polymers prepared by Wood's method by dehydrogenatively cross-linking the polymers in the presence of early transition metal complex catalysts (zirconocene and titanocene) (see section 2.3). The ceramic yield of PMS polymers increased from ~25% (for unmodified polymer) to 74% (for cross-linked polymer). The ceramic residue after pyrolysis for a typical cross-linked polysilane polymer had an elemental composition of 98% SiC, 1.6% ZrC and traces of elemental Si (as opposed to 74% SiC and 26% Si for an unmodified polymer). Table 2.8 shows pyrolysis results for a number of *cross-linked* polymethylsilane polymers prepared under different processing conditions (i.e., varying catalyst concentration, solvent, and reflux time). It is evident from the table that the type of solvent used for the catalytic cross-linking plays an important role in determining the ceramic yield of the polymer produced. For example, it appears that hexane and benzene are good solvents for cross-linking in comparison with polar solvents ether and THF. (This is not to be confused with the effect of polar solvents on Wurtz-coupling of dichlorosilanes. For example, Wood reported higher ceramic yield using THF and lower yield using hexane. Seyferth et al.'s results indicated that non-polar solvents are useful in dehydrogenative cross-linking of low molecular weight polysilanes prepared by the Wurtz-coupling method.) Furthermore, there appears to be a level of catalyst concentration above which the pyrolysis yield does not change significantly, but below which the pyrolysis yield decreases.

Zhang et al. [Zha91; Zha94A; Zha94B] studied the pyrolysis behavior of polymethylsilane polymers prepared by dehydrocoupling of methylsilane in the presence of a DMZ (Dimethyl Zirconocene) catalyst. Ceramic yields were ~60% when the polymer did not contain any processing additives and ~75% when 5-20% processing additives were added (Figure 2.13). (The chemistry of the processing additives was not specified.)

Table 2.8. Pyrolysis results for catalytically cross-linked polysilane polymers [Sey93][a].

% Catalyst (DMZ) mol%	Solvent	Reaction condition	Polymer appearance	Pyrolysis yield, %
1.0	Hexane[b]	30 min/reflux	Orange solid	62
0.57	Hexane[b]	30 min/reflux	Orange solid	74
0.54	Hexane[b]	30 min/reflux	Orange solid	81
0.14	Hexane[b]	30 min/reflux	Yellow wax	40
0.56	Benzene[c]	30 min/reflux	Orange solid	72
0.37	Ether[d]	30 min/reflux	Yellow Oil	23
0.38	THF[e]	30 min/reflux	Yellow Oil	31
0.48	Hexane	16 h/ 25° C	Yellow solid	67
0.47	Hexane[b]	2 h/reflux	Orange solid	62

Reflux temperatures: [b] 68.7°C; [c] 80.1°C; [d] 34.9°C; [e] 66°C

[a] The polymethylsilane polymer used for these experiments was PMS-I, prepared by Wood by Wurtz-coupling reaction of methyldichlorosilane with sodium in hexane. The ceramic yield for this polymer was ~25 wt%.

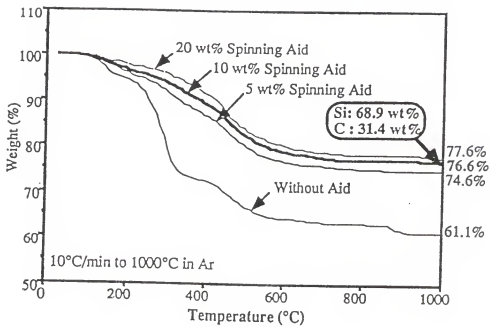

Figure 2.13. TGA plots for polymethylsilane polymer prepared by Zhang et al. [Zha94]

The pyrolyzed ceramic residue had an elemental composition of 69 wt% Si/ 31wt% C (i.e., close to stoichiometric composition). The bulk of the weight loss is shown to occur between 200°C and 600°C in a gradual manner. This weight loss behavior is different from that of Wood's polymethylsilane polymers (prepared by Wurtz coupling reaction), where weight loss is reported to occur between 130°C and 410°C. (The heating rates were comparable, i.e., 10°C/min to 1000°C.) Zhang et al. also studied the chemical evolution of the polymethyslilane polymer during pyrolysis to 1100°C using diffuse reflectance infrared Fourier transform spectroscopy (DRIFTS). Figure 2.14 shows DRIFT spectra of polymethylsilane polymer heated to selected temperatures at 1°C/min in nitrogen and held at temperature for 0.5 h. The 400°C spectra shows the appearance of a strong peak at ~1350 cm^{-1} attributed to the bending vibration of Si-CH_2-Si group. (This is analogous to the thermal rearrangement taking place during the conversion of polydimethylsilane to polycarbosilane.) Schmidt et al. [Sch91] have reported similar observations. At 600°C, the polymer is shown to lose well-defined molecular structure with the only peaks remaining attributed to ν (C-H) of CH_3 (2896 cm^{-1}), ν (Si-H) (~2068 cm^{-1}), and δ (CH_2) of Si-CH_2-Si (at 1354 cm^{-1}). These peaks disappeared at temperatures >800°C, and the spectra showed absorptions in the region of 400 cm^{-1} to 1000 cm^{-1} corresponding to β-SiC.

Recall that linear polysilanes prepared by the Wurtz-coupling reaction of dialkyl or monoalkyl chlorosilanes have ceramic yields of only up to $\leq$ 25% [Bur49; Qiu89; Woo84]. Schilling and Kanner [Sch88] reported that when olefinic halosilanes are used as monomers in the Wurtz-coupling reaction with sodium, the resultant polysilanes contain olefinic groups which act as backbone branching sites and cause in-situ cross-linking. This resulted in relatively higher ceramic yields (38-50%) for these polymers.

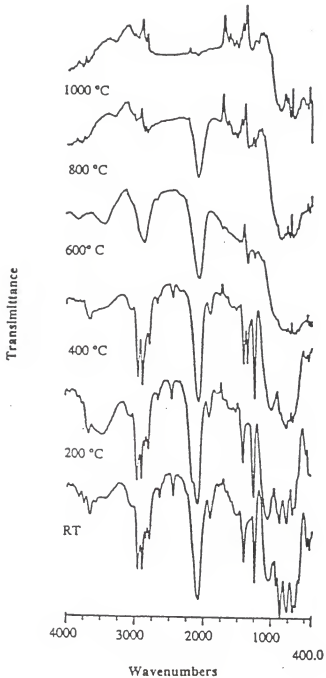

Figure 2.14. DRIFT Spectra of PMS polymer, prepared by Zhang et al. [Zha94].

The olefin groups in olefinic halosilanes do not react with sodium and, therefore, are retained in large amounts in the polymer.

Schmidt et al. [Sch91] have studied the pyrolysis characteristics of vinylic polysilane (VPS) (manufactured by Union Carbide Corporation, Tarrytown, NY based on Schilling and Kanner's patent [Sch88]). The polymer was prepared using Me_3SiCl, Me_2SiCl_2, CH_2=$CHSiMeCl_2$ monomers in 0.85 :0.3: 1 proportion under refluxing conditions in a xylene/THF mixture (7:1 wt ratio). The TGA profile of the VPS polymer is shown in Figure 2.15. The pyrolysis process can be divided into three distinct regions based on the TGA of profile: (i) ~ 50-300°C, where thermal cross-linking occurred without much loss of weight, (ii) ~300-750°C, where major weight loss occurred due to polymer degradation, and (iii) above 750°C, where small weight losses were observed. The ceramic yield was ~58%, which is slightly higher than that reported by Schilling and Kanner. The DTA showed a strong exotherm at around 250°C, corresponding to cross-linking reactions, and a weaker exotherm (at about 450°C) during regime of large weight loss. Schmidt et al. suggested that the exotherm at about ~1100°C may be indicative of partial crystallization of silicon carbide. Elemental analysis of the ceramic formed after pyrolysis at 1000°C showed a composition of 55% Si, 40% C, 2.7% O, and less than a percent each of H and N. The presence of excess carbon (~17 wt%) in the ceramic is not surprising, considering the fact that vinylic groups are retained in the polymer backbone due to early cross-linking reactions at temperatures less than 300°C. The transmission IR spectra of as-received VPS and VPS heat-treated at temperatures of 250°C, 400°C, 650°C and 1000°C in nitrogen atmosphere are shown in Figure 2.16. Table 2.9 [Qiu89B; Col64] lists the IR peak assignments for the VPS polymer. The VPS polymer undergoes following changes upon heating to 250°C: (i) decrease in

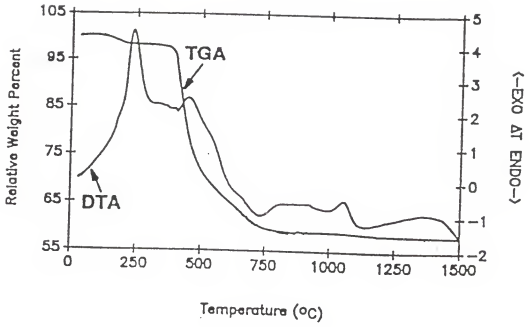

Figure 2.15. TGA and DTA plots for a VPS polymer heated in N_2 at 20°C/min to 1200°C [Sch91].

Table 2.9. Peak assignments for IR absorption spectra of vinylic polysilanes [Qiu89B; Col64]

Peak (cm^{-1})	Assignment
3048 (m)	ν ($CH=CH_2$) of $Si-CH=CH_2$
2952 (s)	ν_{as} (C-H) of CH_3
2894 (s)	ν_s (C-H) of CH_3
2078 (s)	ν (Si-H)
1732 (w)	ν (C=O)
1582 (w)	ν (C=C) of $Si-CH=CH_2$
1397 (s)	δ ($Si-CH=CH_2$)
1246 (vs)	δ_s (CH_3) from $Si-CH_3$
1000-1100 (s)	ω (CH_2) from $Si - CH_2 - Si$,ν (Si-O-Si)
937 (m)	δ (Si-H)
750-850	ν_{as} (Si-C)

ν = stretching ; δ = bending ; ω = bending ; ρ = rocking; vs = very strong; s = strong; m =medium; w = weak

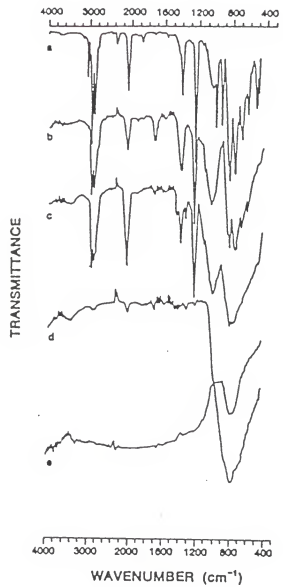

Figure 2.16. IR spectra of VPS polymer; (a) room temperature (b) 250°C (c) 400°C (d) 650°C (e) 1000°C [Sch91].

asymmetric stretching of CH_2 band (3048 cm^{-1}) (ii) decrease in intensity and broadening of $Si-CH=CH_2$ deformation band (1397 cm^{-1}), (iii) slight decrease in both the intensity and area, and broadening of the Si-H stretching band (2078 cm^{-1}), and (iv) appearance of bending vibration at 1640 cm^{-1}, due to C-H bending vibration of $Si-CH=CH_2$. The decrease in intensity and broadening of $Si-CH=CH_2$ band is attributed to loss of vinyl groups due to cross-linking reactions. The increase in Si-H absorption band at 400°C could be attributed to methylene insertion reactions, similar to the reactions occurring in the conversion of polydimethylsilane to polycarbosilane [Yaj78B]. The absorption band at 1642 cm^{-1} due to the C-H bending vibration of $Si-CH=CH_2$ disappears beyond 250°C due to the loss of vinylic groups.

Abu-Eid et al. [Abu92] have also studied the pyrolysis behavior of polysilane polymers prepared by Wurtz-coupling of monoorganosilanes (R^1R^2SiCl where R^1 = CH_3 and R^2=H, C_2H_5, C_3H_7, C_4H_9, C_6H_{11}, C_8H_{17} or C_6H_5) with sodium in an inert solvent. Table 2.10 shows information regarding the polymer characteristics and the pyrolysis behavior. According to Abu-Eid et al., the high ceramic yield for polymethylsilane ($(CH_3SiH)_n$) is due to an early onset of intermediate carbosilane formation and cross-linking of Si-H functionalities (e.g., reaction with moisture to form Si-OH, and subsequent condensation to form Si-O-Si networks). The relatively high ceramic yield for polydimethylsilane (~25%) is not consistent with values (~1%) reported by Wood [Woo84] and Carlsson et al. [Car90]. For other dialkyl or alkylaryl polysilanes listed in the table, the low ceramic yields are consistent with previously reported values.

Table 2.10. Ceramic yield characteristics and decomposition temperatures for polysilane polymers synthesized by Abu-Eid et al. [Abu92].

Polymer Type	Theor. SiC yield,%	Actual ceramic yield,%	% of Theor. yield	Onset of decomp. temp, °C	End of decomp. temp, °C
$[(CH_3)_2Si]_n$	69.0	25.0	36.0	240	610
$[(C_2H_5)_2Si]_n$	46.5	7.0	15.0	170	600
$[(CH_3SiC_3H_7)]_n$	46.5	7.8	17.0	330	650
$[(CH_3Si\text{-}n\text{-}C_4H_9)]_n$	40.0	2.5	6.3	280	500
$[(CH_3Si\text{-}n\text{-}C_8H_{17})]_n$	25.6	11.2	43.8	260	540
$[(CH_3SiH)]_n$	91.0	60.0	66.0	240	750
$[(CH_3SiC_6H_5)]_n$	33.3	21.5	64.6	270	520

2.4. Cross-linking of Polysilane Polymers

Polysilane polymers exhibit a wide range of properties based on the pendant substituent groups in the polymer chain and the degree of cross-linking. The physical appearance of the polymer could range from that of a viscous liquid (e.g., polymethylsilane) to a solid (e.g., polymethylphenylsilane) depending on the molecular architecture of the polymer (cross-linking, molecular weight, side groups etc.). The polymers can be cross-linked by oxidation, room temperature vulcanization, and photolysis.

2.4.1 Oxidative cross-linking

Oxidative cross-linking of polysilane polymers can be accomplished by converting Si-H groups in the polymer to Si-O-C or Si-O-Si groups by reacting with air or moisture. These oxidatively cross-linked polymers are insoluble in organic solvents and do not melt (i.e., infusible) during pyrolysis to silicon carbide. The degree and rate of cross-linking depends on the amount of Si-H groups present in the polymer. Figure 2.17 shows an FTIR spectrum of a polymethylsilane polymer which clearly demonstrates the air sensitivity of these polymers as indicated by the broad absorption band around 3450 cm^{-1}. (This absorption is due to Si-OH stretching which arises from conversion of Si-H.) The oxygen sensitivity of the polysilane polymers is attractive for some applications (e.g., multilayer lithography), but the incorporation of oxygen is sometimes not desirable if the polymer is used as a SiC precursor.

2.4.2 Room temperature vulcanization

The Si-H groups present in the polysilane polymers have been exploited in the preparation of highly cross-linked polymers by catalytic dehydrogenation (see section 2.3).

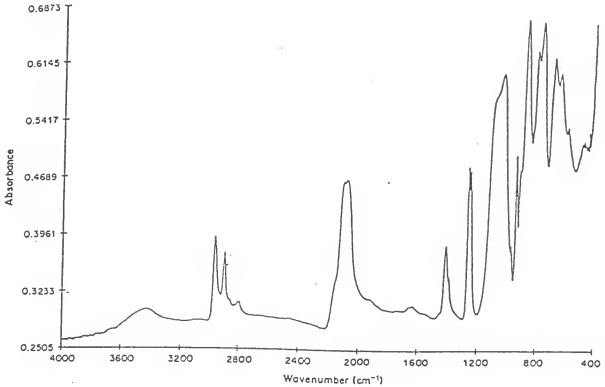

Figure 2.17. FTIR spectrum of polymethylsilane polymer prepared by Abu-Eid et al. [Abu92]

West et al. [Wes86B] have cross-linked Si-H containing polyphenylsilane polymers by using a vinylic silane monomer (e.g., trivinylphenylsilane, trivinylmethylsilane) as the cross-linking agent in the presence of traces of chloroplatinic acid as a catalyst. During the reaction, the initially viscous reaction mixture transforms to a solid polymer, which is insoluble and infusible (a process analogous to room temperature vulcanization of silicone elastomers). The cross-linking reaction can be represented as:

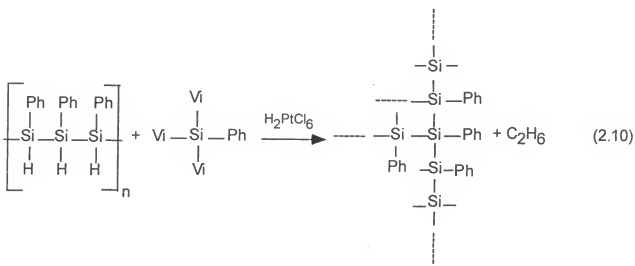

(2.10)

Vi → $CH=CH_2$

Ph → C_6H_5

2.4.3 Photo-cross linking

Qiu and Du [Qiu89B] have shown that when polysilane polymers such as polymethylsilane and polyphenylsilane were irradiated with UV light of wavelength 254

nm in nitrogen or vacuum, cross-linking of the polymer occurred with the formation of insoluble material. One of the disadvantages of photo-cross linking is that some degradation of polymer molecular weight (due to photo-scission) always accompanies photo-cross linking (as shown by equations (2.11), (2.12), and (2.13)). However, West et al. [Wes86B] observed that when a cross-linking agent containing C=C double bonds (e.g., tetravinylsilane) was mixed with the polymer and then irradiated with UV light, no degradation in molecular weight occurred and all of the polymer converted to an insoluble material. The photo cross-linking takes place by cleavage of polysilane chains to form radicals and addition of these radicals to C=C double bonds of vinylic silanes (polyunsaturated additives), causing formation of cross-links and generation of new carbon radicals. These new carbon radicals sustain further cross-linking reactions (equation (2.14)). The reactions can be represented as given in Figure 2.18.

2.5. Applications of Polysilane Polymers

There are three main technological applications of polysilane polymers: (i) precursors for β-SiC, (ii) photoinitiators for radical polymerization reactions, and (iii) photoresists in microelectronics.

2.5.1 Precursor for β-SiC

Yajima and Hasegawa [Yaj78A; Yaj78B; Has83A; Has83B; Has86; Ich86; Has89] pioneered research in the preparation of β-SiC from polysilane-based preceramic polymers. They first synthesized polydimethylsilane (PDMS) by Wurtz-coupling of dimethyldichlorosilane with sodium in xylene at 135°C and then converted the insoluble PDMS to a soluble polycarbosilane by pressure pyrolysis at ~450°C. The

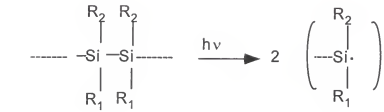

(2.11)

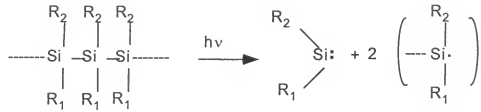

(2.12)

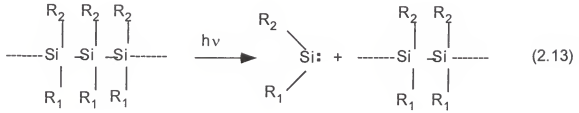

(2.13)

where R_1= n-C_4H_{11}, n-C_6H_{13}, or c-C_6H_{11};
R_2= c-C_4H_{11} or CH_3

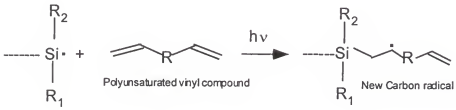

(2.14)

Figure 2.18. Scheme for photo cross-linking reactions of polysilane polymers

conversion of PDMS to PCS takes place by Kumada rearrangement [Shi58], in which insertion of CH_2 groups into the main chain Si-Si takes place, leaving a hydrogen bound to silicon, as shown below:

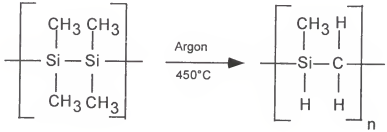

(2.15)

PDMS PCS

Yajima et al. melt spun the polycarbosilane polymers ($M_w \approx 3{,}000$) into fibers and subsequently converted them to SiC by pyrolysis. The fibers required an air-curing step (~200°C, 2-4 h) to render them infusible during pyrolysis to silicon carbide. These fibers, commercially produced as Nicalon™ fibers (by Nippon carbon company, Tokyo, Japan), degrade rapidly at temperatures in excess of 1400°C due to carbothermal reduction reactions between siliceous material and carbon. This leads to evolution of volatile species (primarily CO and SiO) which results in large weight losses, formation of porosity, and growth of SiC grains and other strength degrading flaws in the fiber structure. In recent years, a lot of attention has been directed toward improving the thermomechanical stability of fibers derived via organosilicon polymer route. A method developed at University of Florida involves preparation of fibers ("UF Fibers") by dry spinning of high-molecular-weight polycarbosilanes. SiC fibers were produced with low oxygen content and either carbon-rich (non-stoichiometric) or near-stoichiometric composition [Tor92A; Tor92B; Tor94; Sac95A; Sac95B]. Non-stoichiometric UF fibers

have room temperature mechanical properties similar to that of Nicalon™ fibers, with average tensile strengths ~3 GPa. In addition, UF fibers showed significantly improved thermomechanical stability compared to Nicalon, as indicated by lower weight losses, lower specific surface areas, and improved strength retention after heat treatment to 1700°C. Near-stoichiometric UF fibers ("UF-HM Fibers") have high tensile strengths (2.1-3.4 GPa), fine grain sizes (mostly ~0.1-0.2 μm), high bulk densities (~3.1-3.2 g/cm^3) and small residual pore sizes (mostly 0.1 μm). These fibers retained ~93% of their initial strength after heat treatment in argon at 1800°C.

It is also possible to convert polysilane polymers to silicon carbide fibers directly without resorting to the preparation of intermediate polycarbosilane polymers. As discussed in section 2.1.6, West et al. [Wes81; Wes86A] have prepared phenylmethylsilane-dimethylsilane copolymers, (Polysilastyrene (PSS)), which afford improved processability over PDMS. However, the fibers prepared from these polymers require a cross-linking (curing) step to make them infusible in order to survive pyrolysis. Since the polymers lack Si-H groups (eliminating the possibility of air-curing), the only operative cross-linking mechanism is by UV irradiation. Thermomechanical data on the fibers prepared by this method have not been reported.

Lipowitz et al. [Lip89] have prepared SiC fibers from methylpolysilane (MPS) polymers, synthesized based on Baney et al.'s redistribution/substitution reactions of methylchlorodisilanes (as discussed in section 2.2.6). Fibers were melt spun, cross-linked (cured) and converted to SiC by pyrolysis. By varying the ratio of alkyl to phenyl Grignard reagents (used to react the intermediate methylchloropolysilane polymer), fibers with composition ranging from silicon-rich through stoichiometric to carbon-rich were produced. The method of cross-linking was not specified but the relatively low

oxygen content in the fibers (0.6-6.0 wt%) compared to Nicalon ™ suggests that air-curing step was not used. The low oxygen content in the fibers contributed to improved thermomechanical stability of these fibers over that of Nicalon™ fibers.

More recently, Lipowitz et al. [Lip91A; Lip91B; Lip94A; Lip94B; Lip95] developed near-stoichiometric, polycrystalline SiC fibers using polycarbosilane and methylpolydisilylazane polymers. Fibers were melt spun, oxidatively cross-linked, and heat treated at temperatures above 1600°C in argon in order to react excess carbon and oxygen in the fibers. As noted earlier, PC-derived fibers normally become very weak and develop a porous, large-grained microstructure during this type of heat treatment. However, Lipowitz et al. incorporated a boron-based sintering additive in the polymer which allowed fibers to be densified after the carbothermal reduction reactions discussed earlier. The resulting fibers had fine diameter (8-10 μm), high relative density, small average grain sizes (in the range ~0.03-0.5 μm, depending on the Si:C ratio), low oxygen content (<0.1%), high tensile strength (2.6 GPa), high elastic modulus (up to 420 GPa), and good strength retention after high temperature (1800°C) heat treatment in argon. The key limitation in this process was apparently a difficulty in producing continuous fibers.

Takeda et al. [Tak94] have reported the development of low-oxygen-content (0.4 wt%), fine-diameter (~15 μm) SiC fibers. These fibers ('Hi-Nicalon') were prepared in a similar manner as Nicalon (i..e., by melt spinning of polycarbosilane) except that cross-linking was accomplished by electron beam irradiation instead of oxidation. The high temperature stability of the fibers increased dramatically as the oxygen content of the fibers decreased. Fibers with 0.5 wt% oxygen retained high strength (~2.4 GPa) and high modulus (~250 GPa) after heat treatment at 1500°C in argon. These fibers had a chemical composition of 62% Si, 37.5% C, and 0.5 wt% O. The main drawback of this

method is that cross-linking of the polymer by electron beam irradiation is a slower and expensive processing step. More recently, Takeda et al. [Tak95] produced near-stoichiometric SiC fibers ('Hi-Nicalon Type S') by a modified Hi-Nicalon process. These fibers had a chemical composition of 69% Si and 31% C, and exhibited better thermomechanical than Hi-Nicalon fibers.

Zhang et al. [Zha91; Zha94A; Zha94B] have solution-spun fibers from polymethylsilane polymers (see section 3) and converted them to SiC fibers by pyrolysis. Since the precursor polymer was low in molecular weight, it required addition of a cross-linking agent (unspecified chemistry) to render the fibers infusible. The additive also acted as a spinning aid for the polymer, in addition to providing extra carbon to adjust the stoichiometry of the ceramic produced to that of pure SiC. The SiC fibers produced by Zhang et al. had near-stoichiometric composition. Dense fibers were produced by adding a boron-based sintering additive. DRIFT spectra of the 1000°C pyrolyzed fibers showed the presence of a small amount of oxygen (exact amount not determined). This was attributed to contamination during to handling, as PMS polymers are very sensitive towards air. Thermomechanical stability data on these fibers indicate that they are superior to commercially available Nicalon™ fibers, although no directly comparable data was reported.

Seyferth et al. [Sey92] have demonstrated the potential for production of near-stoichiometric SiC fibers from polymethylsilane polymers which are catalytically cross-linked (see section 2.2.2). However, the fibers need an additional curing step, which can be brought about by UV irradiation. Information on thermomechanical properties on these fibers is not available.

2.5.2 Photoinitiators for Radical Polymerization

The ability of polysilane polymers to form silyl radicals on photo-irradiation has been exploited in the free radical polymerization of styrene, methyl methacrylate etc. Table 2.11 lists a variety of monomers that can be polymerized by using polysilanes as photoinitiators. One disadvantage with the use of polysilanes as photoinitiators is that rate of polymerization is low when compared with conventional photoinitiators such as benzoin methylether.

Table 2.11. List of polysilanes that can be used in radical polymerization [Wes88].

Polysilanes used	Monomers polymerized
$(PhC_2H_4SiMe)_n$	Styrene
$[(PhC_2H_4SiMe)_{0.8}(Me_2Si)_{1.0}]_n$	Ethyl acrylate
$[(PhC_2H_4SiMe)_{1.0}(PhMeSi)_{0.6}]_n$	Methyl methacrylate
$(PhMeSi)_n$	Isooctyl acrylate
$[(PhMeSi)(Me_2Si)]_n$	Acrylic acid
$[(CyHexSiMe)_n]$	Phenoxyethyl acrylate
$[(CyHexSiMe)_{0.7}(Me_2Si)_{1.0}]_n$	1,6-hexanediol diacrylate

However, this disadvantage is more than compensated by the fact that the silyl radicals are insensitive to termination of polymerization by oxygen. This is beneficial because less rigorous control over atmosphere is needed. Although, speculative in nature, this oxygen insensitivity is attributed to scavenging of oxygen by secondary species formed during photolysis [Wol88].

2.5.3 Photoresists in Microelectronics

The current technology in microelectronics is geared towards use of sub-micron features in the integrated circuit chips, leading to an increase in aspect ratio

(height/width) of features in IC chips [Mil88; Mil90A; Mil90B]. The classical single layer resist process used in microlithography has been found to be inadequate when dealing with current trends and lithographers have resorted to multilayer resist processes to meet the current requirements. Figure 2.19 shows a comparison of single layer process vs multilayer process [Mil88]. The classical single layer resist process (wet development) involves exposure of the resist and development of a pattern using a suitable solvent. There is a loss in line width control for small features since wet development processes are isotropic. In the case of multilayer photoresist process, the wafer is covered with a thick, inert planarizing polymer layer followed by a thin layer of photoresist. High resolution in line width can be achieved since the resist layer can be thinner than what is acceptable in single layer resist process (0.05- 0.2 μm compared to ~1 μm for single layer resists). Subsequently, the pattern can be wet developed (without loss in resolution) or dry developed during imaging (ablative exposure) down to the planarizing layer and the image can be transferred through the planarizing layer by O_2-RIE (oxygen resistant ion etching). A necessary requirement for the multilayer resist process is that the photoresist remaining after developing must be resistant to O_2-RIE, in order to mask the underlying polymer effectively. Polysilanes have been found to be ideally suited for use as photoresists since they are stable to O_2-RIE by forming a thin layer of inert SiO_2. In addition, polysilanes possess excellent processing properties such as good thermal stability, solubility for coatings, and imageability to light and ionizing radiation.

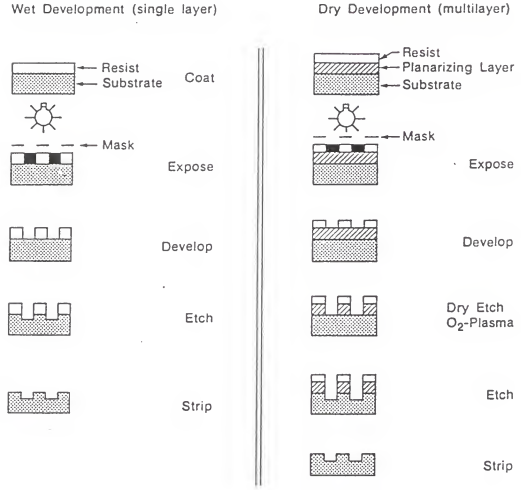

Figure 2.19: Comparison of single layer photoresist process vs. multilayer photoresist process [Mil88].

CHAPTER 3
EXPERIMENTAL PROCEDURES

3.1 Role of Polyvinylsilazane as a Spinning Aid for Polycarbosilane

3.1.1 Polymer synthesis

PSZ was synthesized according to the procedures developed by Toreki et al. [Tor90]. This involved polymerization of a cyclic vinylsilazane (1,3,5-trimethyl-1,3,5-trivinylcyclotrisilazane†) (see Figure 3.1) in the presence of a radical initiator, dicumyl peroxide (DCP). The reaction assembly used for PSZ synthesis is shown in Figure 3.2. In a typical PSZ synthesis, 20 g of cyclic vinylsilazane monomer was mixed with 0.090 g of DCP and 7.5 g of toluene in a 50 ml double-necked flask. Polymerization was typically carried out under nitrogen at a temperature of 125°C for 18 h.

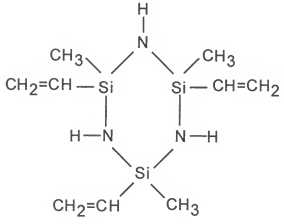

Figure 3.1. Structure of 1,3,5-trimethyl-1,3,5-trivinylcyclotrisilazane

† Petrarch Systems, Bristol, PA.

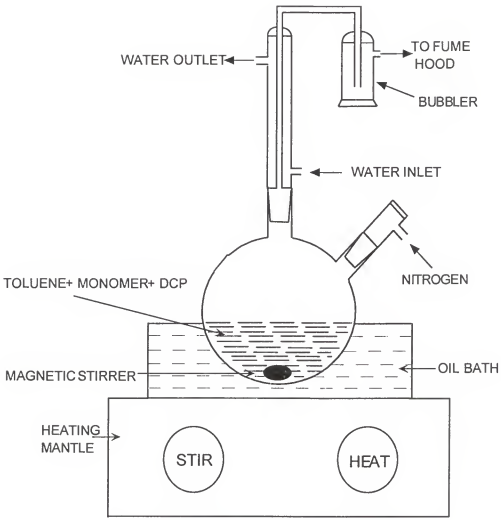

Figure 3.2. Schematic of reaction assembly for PSZ synthesis

The molecular weight of PSZ was controlled by selectively removing low molecular weight fractions ('oils') by fractional distillation using an oil bath at temperatures ranging from 125 to 150°C.

Polycarbosilane (PCS) was synthesized according to the methods reported by Toreki et al. [Tor92] and procedures developed at University of Florida. PCS was synthesized by pressure pyrolysis of polydimethylsilane† in a stainless steel autoclave‡ under a nitrogen atmosphere at ~450°C. PCS polymers were prepared and supplied for this study by coworkers at University of Florida. PCS lots 268, 269, and 262 (combined in 3:2:1 proportion) were used in this study. The average molecular weight was ~11,000. (The GPC molecular weight distribution for the combined PCS polymer is discussed in section 4.1.1.) This relatively high molecular weight PCS not only enabled preparation of highly concentrated solutions (e.g., typically ~70 wt%), but also allowed fibers to be pyrolyzed without melting.

3.1.2 Spin dope preparation, fiber spinning, and fiber heat treatment

The Influence of polyvinylsilazane (PSZ) as a spinning aid and a cross-linking agent in the low temperature heat treatment of PCS fibers was investigated in this study. Two types of polymer solutions were prepared for fiber spinning: one containing 14.5 wt% PSZ and the other without any PSZ. The PCS polymers used in this study were dried in a vacuum furnace for 12 h to remove any adsorbed moisture, traces of solvent, etc. prior to solution preparation. The dried PCS polymers were then dissolved in toluene at 33 wt% solids loading. For use in fiber spin batches, PSZ was dissolved in toluene at 25 wt% solids loading, filtered through a 0.1 μm filter, and mixed with the PCS solution.

---

† Nisso Company, Tokyo, Japan

‡ Model 4651, Parr Instrument Company, Moline, IL.

The polymer solutions were filtered through 0.1 μm filter and concentrated in a rotary evaporator at ~50°C until ~25-30 wt% solvent remained. A 'flow test' was used as a rough indication that an appropriate viscosity for fiber spinning was attained. The flow test was carried out by tilting the glass vial containing the concentrated polymer solution at a 45° angle and measuring the time taken for the solution to travel 2.5 cm. (A fixed size of glass vial was used for concentrating the polymer solution and carrying out the flow test.) Use of the flow test minimized the number of iterations needed to reach the optimum viscosity for fiber spinning and enabled conservation of spin dope material (i.e., by not making any rheological measurements until just before the concentrated polymer solution was ready for fiber spinning). The rheological characteristics of the final polymer solution were determined by using a cone-plate viscometer[¶]. Approximately 0.5 ml of the concentrated polymer solution was used for the measurement. The measurements were made first by increasing the shear rate from 1 to 40 s^{-1} and then decreasing the shear rate back to 1 s^{-1}. A toluene-soaked paper tissue was wrapped around the inside periphery of the cylinder containing the concentrated polymer solution in order saturate the local atmosphere with toluene and thereby to minimize evaporation of toluene from the polymer solution during the measurement. Care was taken to make sure that toluene-soaked paper tissue did not come in contact with polymer solution or interfere in the measurement in any other way.

Fiber spinning was carried out inside a glove box[§] . The glove box was purged with nitrogen three times prior to each spinning experiment. The spin dope was transferred to a spinneret assembly inside the glove box. Four-hole spinnerets of ~70 μm hole sizes were used for fiber spinning. Care was taken to clean the spinnerets

[¶] Model HBT, Brookfield Engineering Laboratories,Inc., Stoughton, MA.
[§] Model 50001, Labconco Corporation, Kansas City, MO.

thoroughly before spinning to ensure that there were no particulates blocking the spinneret holes. The face of spinneret was wiped clean with a toluene-soaked paper tissue prior to commencement of spinning. Continuous 'green' fibers were formed by winding on a wheel which was placed approximately 30 cm from the spinneret face. The spinning conditions (winding speed, nitrogen pressure, and solution viscosity) were kept constant to enable comparison of fibers produced with and without PSZ. The solution viscosity was ~35-40 Pa·s, the applied gas pressure during spinning was 400 psi, and the speed of the fiber collection wheel was ~210 rpm (~440 linear ft/min). The spinning behavior was documented by noting the number of fiber breaks occurring at regular intervals of time. After fiber spinning, batches (typically < 0.5-1 g) were cut from the wheel. These bundles were wrapped in aluminum foil as an ~ 24 cm bundle, then cut into four ~ 12 cm long bundles, labeled, and stored in a vacuum desiccator for at least 12 h (to remove some of the residual solvent from fibers) prior to pyrolysis. Some fibers were pyrolyzed by heating in a tube furnace in nitrogen at 13°C/min to 1150°C (1 h hold at temperature). The flow rate of nitrogen used for pyrolysis was 30 std. atm cc/min.

In order to study the effect of oxidative cross-linking on fiber mechanical properties, several batches of PCS and PCS+PSZ fibers were heat-treated in flowing air to temperatures of 180 ±10°C in a tube furnace. The flow rate of air was 50 std. atm cc/min. The heating schedule used was: 1°C/min to 50°C, 18 min hold at 50°C, 1°C/min to 65°C, 18 min hold at 65°C, 1°C/min to 80°C, 12 min hold at 80°C, 1°C/min to 95°C, 18 min hold at 95°C, 1°C/min to final temperature (180 ±10°C), 1 h hold at temperature. PCS and PCS+PSZ (green and air-heat treated) fibers were also heat-treated in flowing nitrogen (30 std.atm cc/min) in a tube furnace for 1 h at temperatures in the range of

200-1000°C. The heat treatment rate was 1°C/min to 150°C and 4°C/min from 150°C to the final temperature.

3.1.3 Characterization of PCS polymer solutions

The molecular weight distributions of PCS polymers were determined by Gel Permeation Chromatography (GPC)[¶] using polystyrene columns and standards[†] , and THF (tetrahydrofuran) as the solvent. PCS solutions for GPC were prepared by mixing 0.5 wt% of polymer in THF and filtering the solution through a 0.1 μm filter. Polymer solutions were passed through 1000 Å and 500 Å columns connected in series. The mobile phase for the columns was THF. GPC for PSZ polymers were analyzed using 10,000 Å and 1,000 Å columns connected in series. THF could not be used as the mobile phase for PSZ since the chromatogram showed no clear elution peaks corresponding to the different molecular weight species in the polymer (i.e., the chromatogram showed a broad peak and a valley). For this reason, toluene was used as the mobile phase and the PSZ polymers were dissolved in toluene (0.5 wt%) instead of THF. The columns were conditioned by purging toluene through them for 24 h prior to analysis.

The intrinsic viscosities of polymer solutions were determined according to ASTM D-446 procedure by employing a Ubellohde Viscometer (type 0C)[¶¶] . The measurements were carried out in a water bath maintained at 30°C and the concentrations of polymer solutions used ranged from 2 to 6 wt%. The efflux time t required for the solution to pass through the capillary of the viscometer between marked

---

[¶] Waters600E Systems Controller, Waters410 Differential Refractometer and Waters707 Autosampler, Millipore Corporation, Waters Chromatography Division, Milford, MA.

[†] Phenomenex Corporation, Torrance, CA.

[¶¶] Industrial Research Glasswares Ltd, Union, NJ.

lines was measured. The corresponding efflux time t_0 for the pure solvent (toluene) was also measured. The specific viscosity η_{sp} was determined according to formula:

$$\eta_{sp} = (t-t_0)/t_0 \qquad (3.1)$$

The intrinsic viscosity $[\eta]$ was calculated according Huggins equation:

$$\eta_{sp}/c = [\eta] + k'[\eta]^2 c \qquad (3.2)$$

where c is the concentration of the polymer solution used in the measurement, in g/dl. $[\eta]$ was determined by plotting η_{sp}/c vs. c, and extrapolating the straight line to c=0.

Contact angle measurements of polymer solutions were carried out using the sessile drop method and a Contact Angle Goniometer[§]. In the sessile drop method, a liquid droplet is deposited on a solid substrate, as illustrated in Figure 3.3. Measurements were made of the angle formed by the intersection of a line along the solid-liquid interface and a line tangent to the droplet surface, both of which pass through the three-phase (solid-liquid-vapor) intersection point. The substrates used for measurement were stainless steel, teflon, and stainless steel which were first coated with PCS or PCS+PSZ. The concentrations of polymer solutions (PCS and PCS+PSZ) were 33 wt%. The stainless steel (2 cm x 2 cm) and teflon substrates (3 cm x 3 cm) were cleaned in an ultrasonicator bath[‡‡], followed by rinsing in acetone and drying in an oven at 70°C for 30 min. (The teflon substrate was polished on 1 μm diamond wheel for 20 min to obtain a smooth surface prior to measurement.)

Initially, contact angles of water and toluene were measured on teflon and stainless steel substrates to enable comparison with reported values in literature. Both advancing and receding contact angles were measured using the drop-buildup and drop-withdrawal methods. A Hamilton syringe, calibrated up to 0.5 ml was used for

---

[§] Rame-Hart, Inc., Mountain Lakes, NJ.
[‡‡] Model FS 28, Fisher Scientific, Pittsburgh, PA.

adding and withdrawing drops. Efforts were made to use larger drop sizes in order to minimize liquid evaporation effects. (For toluene/stainless steel combination, the total drop size possible was 0.05 ml before the drop boundary exceeded the boundary of the substrate.) In experiments with pure toluene and toluene-based polymer solutions, the immediate environment was saturated with toluene-soaked paper tissues to minimize the effects of liquid evaporation. The duration of measurement for advancing and receding contact angles was ~3 min each. The measurements were carried out in a room where air drafts were minimal.

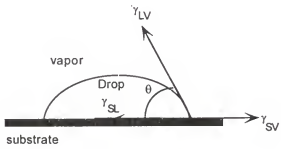

$$\gamma_{SV} = \gamma_{SL} + \gamma_{LV} \cos\theta$$

(Young's equation)

where γ_{SV} = solid-vapor specific interfacial energy

γ_{SL} = solid-liquid specific interfacial energy

γ_{LV} = liquid-vapor specific interfacial energy

θ = contact angle

$\theta = 180°$ for a completely non-wetting liquid

$\theta = 0°$ for a completely wetting liquid

Figure 3.3. Definition of terms in Young's equation and schematic illustration of the geometry for determination of the contact angle by the sessile drop method.

PCS and PCS+PSZ polymer solutions (33 wt%) were used to prepare coated stainless steel substrates. The coatings were deposited using a spin coater[‡], operated for 30 sec at 2000 rpm. 0.15 g polymer solutions were used for spin coating. Both PCS and PCS+PSZ solutions formed smooth films on stainless steel substrates. (The coated substrates were observed in an optical microscope at 20X magnification and no roughness or defects could be detected.) The polymeric coatings were cross-linked by heating the substrates at 1°C/min to 200°C (1 h hold) in nitrogen. (Without this cross-linking step, the polymer films would be dissolved when toluene or toluene-based polymer solution drops were deposited on the substrates for contact angle measurements.)

The surface tension of polymer solutions was measured using a Rosano Surface Tensiometer[§]. This instrument operates using the Wilhemy Plate method. A wettable platinum blade was immersed in the liquid and then the vertical force necessary to pull the blade out of the liquid was measured. The surface tension in dynes/cm was calculated using the formula:

$$\gamma = (F/W) * 0.98 \qquad (3.3)$$

where

γ = Surface Tension in dynes/cm

F= Force in mg ($1\ mg_f = 0.98$ dyne)

W=Perimeter of blade (5 cm)

Five independent measurements were made for each solvent and polymer solution investigated and the results of these measurements were averaged. The platinum blade was cleaned using a non-carbon producing flame (i.e., blue-colored flame tip in a

‡ Model EC101D-R485, Headway Research Inc, Garland,TX.
§ Biolar Corporation, North Grafton, MA.

Bunsen burner) prior to each measurement. When PCS solutions were used, the platinum blade was first soaked in toluene for 5 min and then rinsed in acetone before flame cleaning. Initially, surface tensions of standard liquids such as water and acetone were measured to test the accuracy of the instrument. The measured surface tension values were compared with the values reported in a technical handbook [CRC92].

Two toluene-based 33 wt% polymer solutions, one with PCS and the other with PCS+14.5 wt% PSZ, were prepared and the solutions were filtered through 0.1 μm filter prior to measurement. Viscosities of the solutions were measured using a cone-plate viscometer by the method described in Section 3.1.2. After completing the measurement, the 33 wt% polymer solutions were concentrated successively to 50 and 66 wt% polymer. Surface tension and viscosity measurements were made for each concentrated solution. Surface tension measurements could not be made with more concentrated solutions. (An attempt was made to measure the surface tension of a PCS solution with 68 wt% solids loading (which had a viscosity of 32-35 Pa·s). In this case, the platinum blade did not penetrate the polymer solution and the thread attached to the blade began to coil up.) Glycerol (viscosity: 0.6-0.57 Pa·s) and polydimethylsiloxane (viscosity: 12 Pa·s) (which have viscosities in a similar range as the PCS and PCS+PSZ solutions concentrated to 50 wt% and 66 wt% solids, respectively) were used to assess the validity of surface tension measuring technique when applied to more viscous liquids. (The surface tensions of these liquids are reported in technical handbooks [CRC92].) The rate of solvent evaporation was minimized during the measurements by covering the container used to hold the liquids with aluminum foil and by placing two small beakers filled with toluene next to the container. Care was taken to ensure that the aluminum foil did not interfere with the thread used to pull out the platinum blade from the solution.

Experiments with PCS and PCS+PSZ solutions were carried out to assess the differences in solvent evaporation rates from the two solutions. Identical amounts of PCS and PCS+PSZ solutions with identical solids loading (68 wt%) were prepared. Vials containing the polymer solutions were placed in an analytical balance (with an accuracy up to 5 decimals) and the change in weight was monitored as a function of time (up to 30 min). The change in weight was noted every 10 sec up to 5 min, every 30 sec for the next 5 min, and every 60 sec for the remaining 20 min. The percentage weight change for the polymer solutions was plotted as a function of time.

Fiber extension experiments were carried out inside a glove box. Polymer solutions (PCS and PCS+PSZ(14.5 wt%)) were concentrated to the same viscosities used in fiber spinning experiments. Fiber extension distances were determined by dipping a glass rod (~0.5 cm diameter) in ~4 g of bulk polymer solution (in a glass vial) and drawing fibers by hand until they became separated from the bulk solution. The drawing process was carried out in approximately 1-2 seconds or less for each fiber. Approximately 25 filaments were drawn and average fiber extension distances and standard deviations were calculated.

3.1.4 Characterization of fibers

Fiber tensile strengths were measured at room temperature according to ASTM procedure D3379-75 [AST88]. Fibers were tested in the green state as well as after heat treatments to various temperatures in the range of 200-1150°C. Fibers were also tested after oxidation at temperatures of 180 ±10°C. For mechanical testing, individual fibers were attached to paper tabs using wood glue[§] and loaded in tension (0.5 mm/min

[§] Titebond II, Franklin International, Columbus, OH.

cross-head speed) until failure using a mechanical testing apparatus[‡]. The gage length was 25 mm and at least eight fibers (but usually 15-20) were tested for each batch. To calculate tensile strengths, fiber diameters were determined using an optical microscope equipped with a micrometer in the eyepiece. Two measurements of fiber diameter were made per fiber, and an average fiber diameter was used for calculation of tensile strengths.

FTIR spectra of fibers (as-spun and air-heat treated) were collected in the range 600-4000 cm^{-1} in diffuse reflectance mode[¶]. FTIR spectra were obtained by mixing ground fibers with diamond powder[§] (0.01 g fibers in 0.3 g diamond powder). The fibers were heat-treated from 30 to 600°C in nitrogen at 1°C/min and spectra were collected at intervals of 80°C. Background spectra for diamond were also collected separately, at room temperature and during heat treatment from 30 to 600°C at 1°C/min in nitrogen. Fibers were also separately heat-treated at 5°C/min to temperatures of 750°C, 900°C, and 1050°C (1 h hold) in nitrogen. The pyrolyzed fibers were then ground and mixed with diamond powder (0.01 g fibers in 0.3 g diamond powder) and spectra were collected in the diffuse reflectance mode at room temperature. All intensities in the spectra were converted to Kubelka-Munk units using the conversion:

$$f(R) = (1-R)^2/2R \qquad (3.4)$$

where R = reflectance in absolute units

f(R) = reflectance in Kubelka-Munk units

[‡] Model 1122, Instron Corporation, Canton, MA.
[¶] Nicolet 60SX Spectrometer, Nicolet Instruments Company, Madison, WI.
[§] Size 30 (22-36), Engis Corporation, Wheeling, IL.

3.2 Synthesis and Characterization of Polymethylsilane (PMS) Polymers

3.2.1 Starting materials

Polymethylsilane polymer was prepared by Wurtz-coupling reactions of methyldichlorosilane (MDCS) and methyltrichlorosilane (MTCS) (usually 70:30 wt% proportion[§]) with sodium in the presence of toluene, toluene: THF (95:5 % by volume), or toluene: 1,4-dioxane (50:50 % by volume). The properties of various reagents used are listed in Table 3.1.

Reactant Charges (Typical):

Methyldichlorosilane (MDCS) (70 wt%)	... 36.85 g (33.5 ml)
Methyltrichlorosilane (MTCS) (30 wt%)	.... 15.94 g (12.5 ml)
Sodium (15 wt% excess of equivalent chlorine in monomers)	.... 25.4 g
Toluene	.... 380 ml
THF	.... 20 ml
When 1,4-Dioxane is used:	
Toluene	.... 200 ml
1,4-Dioxane	.... 200 ml

(The toluene:1,4-dioxane ratios were 60:40, and 40:60 (by volume) for polymers PMS-240 and PMS-241).

3.2.2 Procedure for polymerization

All polymerization reactions were carried out in a blanket of nitrogen. The monomer handling operations were carried out in a glove bag under argon. All glasswares were oven dried at 75°C for 12 h after initial cleaning and the reaction

---

[§] One experiment was also carried out with 30:70 MDCS:MTCS ratio.

Table 3.1. Properties of reagents in synthesis of polymethylsilane polymers [Dea88].

Chemicals	MW	State (25°C)	Density(g/cc)	Boiling Point,°C
Methyldichlorosilane	115.00	liquid	1.100	41.0
Methyltrichlorosilane	149.50	liquid	1.275	66.0
Sodium	22.99 [a]	solid	0.968	97.8 [b]
Toluene	92.14	liquid	0.866	110.6
Tetrahydrofuran (THF)	72.11	liquid	0.889	66.0
1,4-Dioxane	88.10	liquid	1.033	101.2

[a] atomic weight; [b] melting point

assembly was thoroughly purged with nitrogen for 30 min prior to use. The reaction assembly (see Figure 3.4) consisted of a 1000 ml three-necked flask equipped with a reflux condenser, pressure-equalizing addition funnel, inert gas inlet port, a magnetic stirrer, oil bath and a heating mantle. In a typical polymerization, 25.4 g of sodium (1.27 gmoles, 15 wt% excess)[¶] and 400 ml of toluene[‡] were heated to reflux (~110°C for toluene-THF mixture at 760 mm Hg and ~105°C for toluene-1,4 dioxane mixture at 760 mm Hg). When THF[†] and 1,4-Dioxane[§] were used as additives, the total volume of the solvent mixture was kept constant at 400 ml in the desired proportions. After the sodium melted completely (~30 min; melting point: 98°C) and formed a fine dispersion, 33.5 ml methyldichlorosilane[¥] and 12.5 ml of methyltrichlorosilane[§§] monomers in 70:30 wt% proportion was added drop by drop through the addition funnel. The total time for the addition of monomer(s) was one hour, during which time the heating mantle was turned off to prevent the reaction from becoming violently exothermic. The reaction contents were tested for acidity periodically. This was done as follows: the reaction contents were allowed to settle for 2-3 min (i.e., stirring of the reaction contents was stopped) and about 0.5 cc of the clear polymer solution was pipetted out and added to a water-soaked pH paper. If chlorosilane monomer remains in the solution, it will react with water on the pH paper to form HCl. This will, in turn, cause the pH paper to change color to pink. The polymerization was carried out at reflux until the solution no longer tested acidic (i.e., pH of 6-7; wet pH paper remained colorless after the clear polymer

---

[¶] 3 to 8 mm spheres, Aldrich Chemical Company, Milwaukee, WI.
[‡] Grade Optima, Fisher Scientific Company, Fair Lawn, NJ.
[†] Grade HPLC, Fisher Scientific Company, Fair Lawn, NJ.
[§] Grade ACS, Fisher Scientific Company, Fair Lawn, NJ.
[¥] 99% purity, Aldrich Chemical Company, Milwaukee, WI.
[§§] 97% purity, Aldrich Chemical Company, Milwaukee, WI.

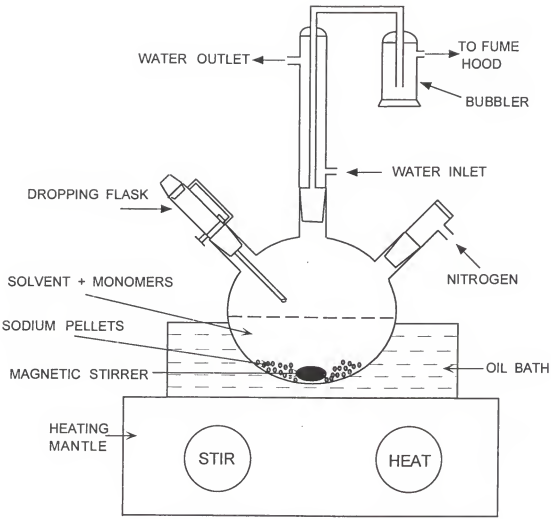

Figure 3.4. Reaction assembly for synthesis of polymethylsilane polymers

solution was reacted with it[¶]). The reaction vessel was allowed to cool to room temperature and the reaction contents (i.e., Na/NaCl precipitate) were centrifuged at 1500 rpm for 10 min in 50 ml centrifuge tubes. During centrifuging, the black-colored Na/NaCl precipitate was separated out from the clear (i.e., transparent), yellow-colored polymer solution. The polymer solution was decanted and filtered through 20 μm Whatman filter paper and concentrated in a rotary evaporator[▲] under vacuum to yield a viscous, clear yellow/ dull-colored polymer. The rotary evaporation was carried out 15 min beyond the point at which the solvent stopped condensing into the collection flask of the distillation apparatus. After rotary evaporation, the flask containing the polymer was vented to N_2 to minimize contamination from air. The polymer was then dissolved in toluene (~33 wt%) in a refrigerator for further processing/characterization.

In view of the hazards associated with handling Na, several saftey precautions should be taken: (1) Na should be weighed in a dry beaker containing toluene (~20 ml). (2) The polymer solutions/Na-NaCl suspensions should not be exposed to atmospheric air during synthesis. (3) The Na-NaCl suspension (dark colored 'sludge' collected in centrifuge tubes) must be neutralized by carefully adding 2-propanol and water (50 ml each) sequentially. This was done to remove excess Na present in the sludge so that the sludge would not create waste disposal hazards. The OH group in 2-propanol reacts with Na forming NaOH. Addition of water enables removal of traces of Na left behind in the sludge.

[¶] Color range for pH test: 3-6: pink (acidic); 6-7: no color change (neutral); 7-10 : blue-green (basic).
[▲] Buichi R-114, Brinkman Instruments, Westbury, NY

3.2.3 Determination of polymer yield

The actual polymer yield was determined by carrying out a solids loading test. This was done as follows: two clean aluminum weighing pans were weighed before and after adding 10 drops of polymer solution. The weighing pans were then quickly transferred to a vacuum oven maintained at 65°C and dried under vacuum for 2 h. The weighing dishes were weighed after drying. Knowing the differences in weights of the aluminum pans before and after drying, the solids loadings were calculated. The polymer yield was calculated from the knowledge of total polymer solution in hand (after rotary evaporation and dissolution in toluene). (Since this method doesn't take into consideration the polymer trapped in the void space between Na/NaCl precipitates, the actual yield is an underestimate.)

For polymers prepared from methyldichlorosilane (MDCS), the reaction is:

$$CH_3SiHCl_2 + 2Na \rightarrow -- [CH_3SiH]_x -- + 2NaCl$$

The molecular weight of MDCS is 115 g/gmol and the molecular weight of the repeating unit (R.U), -- $[CH_3SiH]_x$--, is 44.08. Therefore, starting with 0.3204 gmoles of MDCS (corresponding to 36.85 g) produces 0.3204 gmole of R.U or 14.10 g (theoretical yield). The polymer yield is calculated as a percentage by dividing the actual polymer yield by the theoretical yield determined above (and then multiplying by 100).

For polymers prepared from a mixture of methyldichlorosilane (MDCS) and methyltrichlorosilane (MTCS) (70:30 proportion by weight), the reaction is:

$$CH_3SiHCl_2 + CH_3SiCl_3 + 5Na \rightarrow -- [CH_3SiH]_x --- [CH_3Si]_y -- + 5NaCl$$

The molecular weight of MTCS is 149.50 g/gmol and that of the R.U --$[CH_3Si]_y$-- is 43.08. Therefore, 0.3204 gmole of MDCS (corresponding to 36.85 g) produces 0.3204 gmole of R.U -- $[CH_3SiH]_x$-- or 14.10 g and 0.107 gmole of MTCS (corresponding to 15.94 g) produces 0.107 gmole of R.U --$[CH_3Si]_y$-- or 4.58 g. Thus, the total yield is

18.70 g. The polymer yield is calculated as a percentage of theoretical yield by dividing the actual polymer yield by the theoretical yield (and then multiplying by 100).

3.2.4 General procedure for heat treatment of PMS-based polymer solutions

PMS polymer solution (33 wt% in toluene) was mixed with PCS (where applicable in ratios of 90:10, 70:30, etc.) and the solution was filtered through a 0.1 μm filter. (The concentration of polymer solution was kept at 33 wt% after mixing with PCS by adding the necessary amount of toluene.) The additives polyvinylsilazane (PSZ) (amounts in the range of 0.25-14.5 wt%), dicumyl peroxide (DCP) (amounts in the range of 0.5-1.5 wt%), and decaborane (DB) (amounts in the range of 1-6 wt%) were dissolved in toluene at 25 wt% solids loading, and separately added (where applicable) to the polymer solutions after filtering through 0.1 μm filter. The polymer solution was then transferred to a teflon container (20 ml size) and encased in a stainless steel pressure bomb[§] . The teflon container was backfilled with N_2 before encasing in the pressure bomb. The polymer solution (approximately 10-15 g) was heat-treated at temperatures in the range of 50-150°C in a convection oven and were sometimes given multiple treatments at successively increasing temperatures in this range. The effects of these heat treatments on the polymer solution viscosity and/or the polymer molecular weight (determined by GPC) were determined in some cases. Polymer solutions showed increases in viscosity after heat treatments and this was taken as a measure of increase in branching/molecular weight of the polymer. The viscosity of the polymer solution was measured using a cone-plate viscometer[‡]. Heat treatments of polymer solutions were usually stopped when increases in viscosity of at least ~250% were obtained (e.g., increases from 2 mPa·s to 7 mPa·s). After heat treatments, polymer

[§] Model 243AC, Parr Instrument Company, Moline, IL.
[‡] Model LVT, Brookfield Engineering Labortaories, Stoughton, MA.

solutions were transferred to glass vials and filtered through 1.0 μm, 0.45 μm, and 0.1 μm filters[§] (where applicable) and stored in a refrigerator for use in fiber spinning experiments.

Some variations in the solution preparation/heat treatment procedures are noted as follows: (1) The original stock solutions PMS-220-A and PMS-221-A were divided into two parts. Type B PCS was added to one part (PMS-220-AP and PMS-221-AP) and type C PCS was added to the other part (PMS-220-AP2 and PMS-221-AP2). The heat treatment was then carried out separately for these polymer solutions, (2) In the case of PMS-216-A, PMS-217-AP, and PMS-218-AP, the original stock solutions were divided into two parts each, and heat treatments were carried out separately, (3) PMS-218-AP stock solution was divided into two portions (PMS-218-AP and PMS-218-AP2). After the first heat treatment (PMS-218-AP-H), the total amount of PSZ in the polymer solution was raised to 14.5 wt% in the second portion and heat treatment was carried out separately (PMS-218-AP2-H).

3.2.5 Procedure for fractional precipitation of PMS polymers

The as-synthesized PMS polymers (stored in toluene) were subjected to rotary evaporation under vacuum in order to remove the toluene and 1,4-dioxane solvents After rotary evaporation, the flask containing the polymer was vented to N_2 to minimize contamination from air. Then, THF was added to the polymer in suitable proportions. THF, being a polar solvent, promotes fractional precipitation. Typically, 25 ml of THF was added for 8 g of polymer. The polymer solution was then transferred to a conical flask containing a magnetic stirrer. Polymers PMS-240 through PMS-243 were fractionally precipitated by adding a mixture of 150 ml of 2-propanol and 150 ml of

---

[§] Puradisk 25TF, Whatman International Ltd., Maidstone, England.

methanol dropwise and with vigorous stirring. The precipitated polymer solution was transferred to teflon centrifuge tubes and centrifuged at 2000 rpm for 10 min. The clear supernatant was decanted out. The 'wet' cake collected at the end of centrifugation was placed in a glass vial and dried in a vacuum oven at room temperature. To prevent splashing of the polymer from vial during vacuum drying, the vial was covered with an aluminum foil which had been perforated with tiny holes. After drying, the glass vial containing the polymer was removed from the vacuum oven (by venting to N_2) and backfilled with N_2. The dried polymer was dissolved in toluene (33 wt%) and stored in a refrigerator for further processing (fiber spinning). Polymers PMS-245 through PMS-255 were fractionally precipitated by addition of acetone. The acetone to polymer ratios (ml of acetone per g of polymer) used ranged from 20 to 27. The procedure for fractional precipitation with acetone was identical to that of precipitation with alcohols.

3.2.6 Characterization of polymers and samples prepared by heat treatment of the polymers

Molecular weight distributions of polymers were determined by GPC according to the methods described in section 3.1.3. Polymer solutions were passed through 1000 Å and 500 Å columns connected in series. The mobile phase for the columns was THF.

Weight loss behavior was monitored by Thermal Gravimetric Analysis (TGA)[§]. Samples were heat-treated in argon at 10°C/min to 1200°C (no hold time). Sample preparation for TGA involved using rotary evaporation to concentrate the original polymer solutions (33 wt% in toluene) to 70-80 wt% and then drying the concentrated polymers solution in a vacuum oven at 75°C for 5 min to drive off any residual solvent completely. (The vacuum oven was vented to nitrogen to prevent oxygen contamination

[§] Model STA-409, Netzch Company, Exton, PA.

in the sample.) The dried polymer solution was quickly (<1 min) transferred to a TGA sample holder to minimize exposure to air. In some cases, the ceramic yield was determined by pyrolyzing polymers in a tube furnace to 1000°C in nitrogen at 10°C/min. (The ceramic yield was determined by measuring the weights before and after pyrolysis.)

In the case of polymers fractionally-precipitated by nonsolvents, a portion of the dried polymer was subjected to pyrolysis to determine if the polymer melted during pyrolysis ('melt' test) as well as to evaluate ceramic yield. The dried polymer was crushed into coarse powder, weighed and transferred into a tube furnace quickly (<2 min). The pyrolysis schedule used for the melt test was: 5°C/min to 1000°C in nitrogen with no hold at temperature. The polymer was considered to have undergone no melting if the pyrolyzed polymer retained sharp corners and edges. It was considered partially melted if some rounding of edges and corners occurred and if the pyrolyzed chunks were stuck to the alumina boat used for pyrolysis.

Phase analyses of the pyrolyzed samples was carried out by X-ray diffraction (XRD)[55]. All the samples for XRD were heat-treated in argon at 10°C/min to 1350°C (no hold time). The pyrolyzed residues were slightly ground with a mortar and pestle and subsequently mixed with collodian/amyl acetate (1:7 volume ratio). The mixture was deposited on a glass slide and dried at room temperature prior to analysis.

The crystallite sizes for the Si and SiC phases were determined by the XRD line broadening method using Scherrer's formula:

$$t = 0.9\,\lambda / (B \cos\theta) \qquad (3.5)$$

where t = crystallite size in Å

---

[55] Model APD 3720, Phillips Instruments Company, Mt. Vernon, NY.

λ= wavelength in Å

B= full width half maximum (FWHM) in radians

θ= Bragg angle in degrees

Elemental analyses for Si, C, and O on pyrolyzed samples (1000°C or 1150°C in nitrogen) were obtained using an Electron Microprobe Analyzer[¥] (EMA) equipped with X-ray wavelength dispersion spectrometers. The accelerating voltage used was 12 kV. High purity CVD SiC, SiO_2 and single crystal Si were used as measurement standards for C, O, and Si analyses, respectively. The analyses were carried out using polished samples. For the purpose of polishing, chunks of pyrolyzed sample were mounted in an alumina matrix. The samples were prepared by slip casting an aqueous suspension of submicrometer alumina powder around the chunks of pyrolyzed sample. The samples were held within a cylindrical tube that was placed upon a plaster of Paris block. Water from the casting suspension was drawn into the porous plaster block and the alumina powder was consolidated around individual chunks of the pyrolyzed sample. The dried alumina powder matrix was partially densified by heat treating the composite sample for 3 h at 1100°C in a nitrogen atmosphere. The porous sample was then mounted in a thermosetting resin[††] . The mounted samples were ground with SiC powder slurries on a glass plate. The following grit sizes of powders were used in succession: 120, 180, 240, 320, 400, 600, and 1000. After fine grinding, samples were polished using an automatic polisher[‡‡] containing a Fe_2O_3/SiO_2 suspension[§§] on a polishing grade cloth[¶¶].

[¥] JEOL Superprobe 733, Japan Electro-Optics Ltd (JEOL)., Tokyo, Japan.
[††] Quickmount, Fulton Metallurgical Products Corp., Saxonburg, PA.
[‡‡] Vibromet Polishing Wheel, Buehler, Ltd., Lake Bluff, IL.
[§§] MasterPolish II, Buehler, Ltd., Lake Bluff, IL.
[¶¶] Polymet, Buehler, Ltd., Lake Bluff, IL.

This polishing step was typically carried out for 1-3 days. After polishing, samples were cleaned in an ultrasonic cleaner with de-ionized water.

FTIR* spectra of polymer samples were collected in the region 600-4000 cm^{-1}. The spectra were collected in the diffuse reflectance mode. Sample preparation for obtaining FTIR spectra for the polymers involved mixing 0.15 g of 10-15 wt% polymer solution with diamond powder, heating the mixture on a hot-stage¥ to 45°C for 3 h in nitrogen (to remove toluene), and then cooling back to room temperature. Pyrolysis behavior of the polymers in the FTIR mode was studied by using the hot stage to heat treat the samples from 30°C to 600°C in N_2 at 1°C/min and collecting spectra *in-situ* at regular intervals of temperature (i.e., every 80°C). FTIR spectra of samples pyrolyzed to 750, 900, 1050 and 1150°C (5°C/min to temperature in nitrogen with no hold time) were collected separately.

The intrinsic viscosities of polymer solutions were determined according to ASTM D-446 procedure by employing a Ubellohde Viscometer (type 0B), as described in section 3.1.2. The concentrations of polymer solutions used were in the range of 1 to 8 wt%.

3.3 Spinning and Characterization of Fibers Prepared from PMS-based Polymers

3.3.1 Spin dope preparation, fiber spinning, and fiber heat treatment

The as-prepared or fractionally-precipitated PMS polymer solutions were generally filtered through 0.1 μm PTFE filter. (However, some polymer solutions were filterable only through 0.45 μm or 1.0 μm filters.) It is important to filter the polymer

* Nicolet 60SX Spectrometer, Nicolet Instruments Company, Madison, WI.
¥ Harrick Corporation, Ossining, NY.

solutions through the smallest-sized filter possible in order to eliminate strength-limiting defects in fiber batches spun from these solutions.

The additives for fiber spinning, PSZ and DB, were filtered separately through 0.1 μm filters and added to the PMS solution. The amount of PSZ added ranged from 0.25 to 14.5 wt% and the amount of DB added ranged from 0.25 to 6 wt%. PSZ is a highly viscous liquid at room temperature. For use in fiber spin batches, PSZ was dissolved in toluene at 25 wt% solids loading and filtered through a 0.1 μm filter. Decaborane (DB) ($B_{10}H_{14}$) was purchased commercially[‡] . DB was dissolved in toluene at 25 wt% solids loading and filtered through a 0.1 μm filter prior to use in fiber spin batches.

The polymer solution containing additives was concentrated in a rotary evaporator at ~50°C until ~15-30 wt% solvent remained. A 'flow test' was used as a rough indication that an appropriate viscosity for fiber spinning was attained (see section 3.1.1). The rheological characteristics of the final polymer solution were determined by using a cone-plate viscometer[¶] (described in section 3.1.1).

Fiber spinning was carried out inside a glove box. The glove box was purged with nitrogen three times prior to each spinning experiment. The spin dope was transferred to spinneret assembly inside the glove box. Three-hole spinnerets of ~40 μm or four-hole spinnerets of ~70 μm hole sizes were used for fiber spinning. Care was taken to clean the spinnerets thoroughly before spinning to ensure that there were no particulates blocking the spinneret holes. The face of spinneret was wiped clean with a toluene-soaked paper tissue prior to commencement of spinning. Fibers were formed at room temperature by extruding the polymer solutions through the spinneret under

[‡] Consumer Health Research, Los Angeles, CA.
[¶] Model HBT, Brookfield Engineering Laboratories,Inc., Stoughton, MA.

nitrogen pressure. Nitrogen pressures used in spinning of PMS-based fibers ranged from 300 to 550 psi. Three filaments were extruded simultaneously in most experiments. Continuous 'green' fibers were collected by winding (at speeds of 30-200 rpm) on a wheel (diameter ~8 in) which was placed approximately 30 cm below the spinneret. In some cases, the spinning behavior was documented by noting the number of fiber breaks occurring during spinning. After fiber spinning, batches (typically < 0.1-0.2 g) were cut from the wheel. These bundles were wrapped in aluminum foil as an ~24 cm bundle, then cut into four ~12 cm long bundles, labeled, and stored in a vacuum desiccator for at least 12 h (to remove solvent traces from fibers) prior to pyrolysis.

The preparation of fibers from PMS-PCS polymer blends involved mixing PMS (solution) with PCS (solid) in desired proportions (90:10, 70:30, 60:40, 40:60, 25:75) and filtering the polymer solutions through smallest-sized filter possible (i.e., 0.1 μm, 0.45 μm or 1.0 μm). When PCS was mixed with PMS, the overall solids loading was kept at 33 wt% by adding the required amount of toluene to the PMS-PCS blend. Additives were mixed with the PMS-PCS blend as in the case described above for PMS polymers. The spin dope preparation and fiber spinning procedures were identical to the procedures used for spinning of fibers from PMS polymers. In the case of heat-treated PMS polymer and heat-treated PMS-PCS polymer blends (containing additives), the solutions were filtered and concentrated directly by rotary evaporation. The fiber spinning procedures were identical to that of PMS polymers described above.

The fibers were pyrolyzed in a tube furnace[¥] in a flowing nitrogen atmosphere (30 std. atm/cc min). Fibers were transferred from the vacuum desiccator to the furnace quickly (<2 min) in order to minimize oxygen contamination from exposure to air. The

[¥] Model 59344, Lindberg Furnaces, Watertown, WI.

fibers were placed in a graphite foil[†] boat upon removal from the vacuum desiccator. The furnace was purged with nitrogen for ~15 min prior to heat treatment. Fibers were heated to either 1000°C or 1150°C with 1 h hold at maximum temperature. The heating rate was 1°C/min to 200°C and 10°C/min to maximum temperature. Heat treatment of the 1000°C or 1150°C-pyrolyzed fibers to 1500°C was carried out in a tube furnace at 10°C/min in a flowing argon atmosphere (30 std. atm/cc min) with 1 h hold. Heat treatment to 1700°C was carried out at 10°C/min in a box furnace[§] in argon at 10°C/min with 1 h hold.

3.3.2 Fiber characterization

Fiber tensile strengths were measured at room temperature according to ASTM procedure D3379-75 [AST88], described in section 3.1.3. Pyrolyzed fibers (1000°C or 1150°C heat treatment) and, in some cases, fibers which were heat-treated to 1500°C and 1700°C, were tested.

Fibers were examined by scanning electron microscopy[¶] (SEM). The accelerating voltages used were 5 kV and 15 kV for green and heat-treated fibers, respectively. An aluminum mount, 0.75" diameter, and 0.5" thickness, was used to hold fibers. In order to observe the fiber cross-section, a narrow slit (1 mm wide) was created in the center of the mount for placing the fibers vertically. The fibers were attached to a small piece of aluminum foil and held in place with a double-sided adhesive tape. The foil, with fibers placed upright, was inserted into the narrow slit. To observe the fiber surfaces, the fibers were laid flat on the aluminum foil and held in place with a double

---

[†] Grafoil ™, UCar, Pittsburgh, PA.
[§] Model M-60, Centorr Vacuum Industries, Nashua, NH.
[¶] Model JSM-6400, JEOL, Tokyo, Japan.

sided tape. Prior to examination by SEM, fibers were coated with a layer of Au-Pd for 20 sec using a sputter coater[‡].

Elemental analyses of pyrolyzed fibers were carried out using an Electron Microprobe Analyzer according to the methods described in section 3.2.4, with the exception that fibers were cast upright in the sub-micrometer alumina suspension so that fibers could be cross-sectioned perpendicular to the long dimension of the fibers.

Fractography was carried out on selected batches of fibers. The fibers were mounted onto paper tabs. Each paper tab was given a number and labeled at the top and the bottom, so that fiber fragments could be identified after tensile testing. The diameters of fibers were determined using an optical microscope, as per the methods described earlier in the section. The fibers were then coated with glycerin. Tensile strength data on 21 fibers were collected. Except in a few cases, only one fragment (i.e., the top or the bottom portion) of the fractured fiber remained attached to the paper tab after testing. The fiber fragments were taped to stiff aluminum foil pieces (cut from aluminum weighing dishes). The fragments were subsequently sonicated for 5 sec in 1N HNO_3 solution, then 5 sec in 1N NH_4OH, and finally 2 min in methanol. This process enabled removal of debris and dust adhered to the fracture surfaces. The fibers were then mounted on an aluminum stub as described earlier in the section for observing the cross-sectional features by SEM.

[‡] Denton Vacuum Division, Moorestown, NJ.

CHAPTER 4
RESULTS AND DISCUSSION

4.1 Effect of PSZ as a Cross-linking/Processing Aid for Spinning of Fibers from PCS Solution

This section gives detailed results and analyses for investigations involving use of Polyvinylsilazane (PSZ) as a spinning aid/cross-linking agent in the preparation of fibers from PCS spin dopes. Results of fiber spinning experiments, and characterization of polymer solutions and fibers are discussed.

4.1.1 Fiber spinning characteristics

PCS and PCS+PSZ spin dopes were prepared with similar characteristics (see section 3.1.2). Solutions were initially filtered under the same conditions (0.1 μm at 20 psi) and spin dopes were prepared with essentially the same viscosity (~35-40 Pa·s). The spin dopes were spun using the same applied pressure (~400 psi nitrogen) and spinning speed (i.e., ~440 linear ft/min).

Figure 4.1 and 4.2 show typical plots of shear stress vs. shear rate and viscosity vs. shear rate, respectively, for polymer spin dopes (PCS and PCS+PSZ) used in fiber spinning. (The rheological flow behavior for various PCS and PCS+PSZ spin dopes used in this study are shown in Appendix A.) The spinning solutions showed essentially Newtonian rheological flow behavior. The typical viscosities of the solutions used in fiber spinning were ~35-40 Pa·s. PCS solution had a lower solids loading (~65-68%) than PCS+PSZ (~69-70%) at comparable viscosities. Both PCS and PCS+PSZ spin dopes have similar rheological flow behavior. The solutions showed essentially no

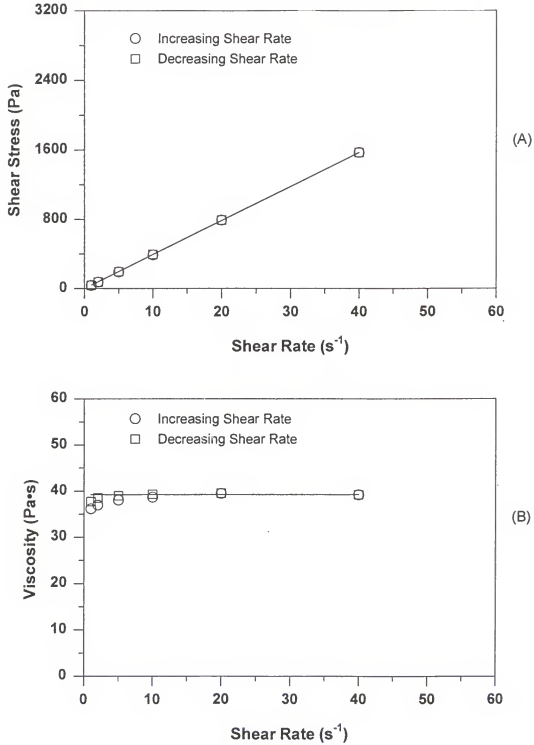

Figure 4.1. Plots of (A) shear stress vs. shear rate (B) viscosity vs. shear rate for a PCS spin dope (solids concentration ~68 wt%, batch 63s).

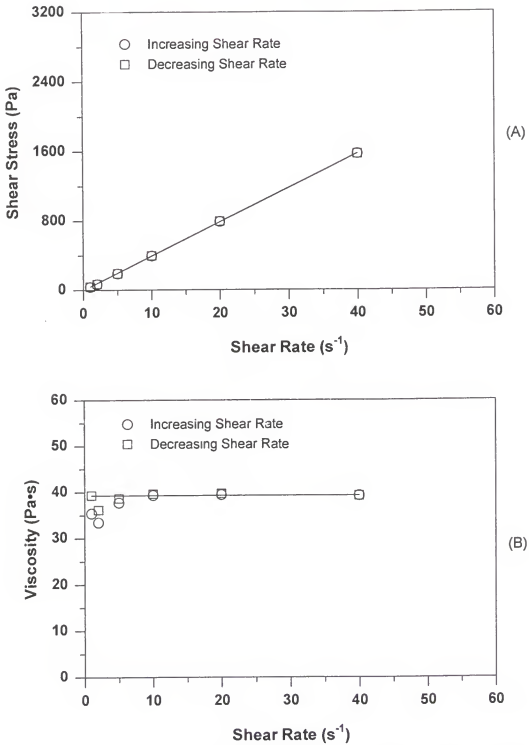

Figure 4.2. Plots of (A) shear stress vs. shear rate (B) viscosity vs. shear rate for a PCS+PSZ spin dope (solids concentration ~70 wt%, batch 70s).

thixotropy under the measuring conditions. The PCS and PCS+PSZ solutions showed a slight decrease in viscosity at low shear rates. This is presumably because stress measurement is inaccurate at low shear rates[‡] . Also, viscosity values were slightly higher for "down curves" (i.e., decreasing shear rates) than for "up curves" (i.e., increasing shear rates) at low shear rates. This is probably due to some slight solvent evaporation from spin dope during rheology measurements. (Solvent evaporation would increase the polymer concentration and result in higher solution viscosity.)

The increase in solids loading for the PCS+PSZ solution in comparison with PCS solution at similar viscosities may be explained as follows: The PSZ polymer (pure, not containing any solvent) is a liquid and has a viscosity of ~18 Pa·s. Figure 4.1 shows that a PCS solution with 68 wt% polymer has a viscosity of ~39 Pa·s. If some PSZ (with no solvent) were added to the latter PCS solution, the overall viscosity of the new solution would be lower. In order to raise the viscosity back to ~39 Pa·s, it would be necessary to remove some solvent. Hence, it is obvious that the mixed PSZ/PCS solution will have a higher polymer concentration, compared to a pure PCS solution, at a fixed viscosity.

Table 4.1 shows the results obtained from spinning the PCS and PCS+PSZ spin dopes. The detailed fiber spinning characteristics (i.e., number of breaks vs. time) for individual fiber batches is presented in Appendix B. It is evident from the table that addition of PSZ to PCS greatly improved the spinning of fibers. For example, PCS spin dopes showed spin line breakage rates (i.e., number of breaks per minute per spinneret hole) of ~ 0.4-3.1. In contrast, the rates were only ~0.1-0.3 for the PCS+PSZ spin dopes. With less breaks (and, therefore, less interruptions of the fiber collection

---

[‡] The shear stress vs. shear rate data is usually curve-fitted through the origin (linear fit) and the viscosity vs. shear rate data is obtained from the curve-fitted data.

Table 4.1. Fiber spinning characteristics for PCS and PCS+PSZ spin dopes spun under identical conditions.

(1) PCS Fiber batches:

Batch	Amount of spin dope[a] (g)	Amount of polymer (g)	Amount of fibers collected (g)	% of fibers yielded[b]	Duration of spinning (min)	Total number of breaks	Number of breaks[c]
63s	4.41	2.99	0.30	10	17	46	3.07
64s	4.62	3.06	0.26	8.5	23	62	1.51
65s	3.78	2.49	0.45	18.1	17	22	0.81
69s	4.48	2.97	0.53	17.8	17	14	0.44

(2) PCS+PSZ fiber batches

Batch	Amount of spin dope (g)	Amount of polymer (g)	Amount of fibers collected (g)	% of fibers yielded[a]	Duration of spinning (min)	Total number of breaks	Number of breaks[b]
67s	4.58	3.16	1.07	33.9	24	20	0.29
68s	4.51	3.16	1.05	33.3	14	6	0.11
70s	4.56	3.19	1.03	32.3	12	5	0.11

[a] Amount of spin dope = amount of polymer + amount of solvent
[b] Percentage yield = 100 x (Amount of fibers collected/Amount of polymer in the spin dope)
[c] Number of breaks during spinning per minute per spinneret hole. Fibers were spun using a four-hole, 70-μm hole diameter spinneret

process), it was also possible to obtain more fibers using the PCS+PSZ spin dopes (see Table 4.1).

It was observed in the course of spinning fibers from PCS spin dopes that globules of polymer formed periodically (approximately every 1-2 min) on the exit face of the spinneret. This phenomenon was absent during spinning of PCS+PSZ spin dopes. Formation of globules was apparently responsible for spin line breaks in the case of PCS spin dopes, as it necessitated cleaning the spinneret face with a toluene-soaked paper tissue and restarting the spinning process. This also contributed to lower fiber output for PCS spin dopes, as polymer was wasted when the globules were wiped off the spinneret exit face as part of the efforts to restart fiber spinning after breaks occurred. Formation of globules on spinneret face is shown schematically in Figure 4.3. Globules usually formed at the holes on the spinneret face. They often detached from the spinneret face by gravity after reaching a maximum size of ~ 2 mm.

It should be noted that there was a "learning curve" involved in spinning of these fibers. Improved spinning occurred (i.e., lower breakage rates and higher yield of fibers were observed) as the fiber spinning operator gained more experience in handling of the spin dope. It is evident, for example, that improved spinning occurred with successive batches for the four PCS spin dopes (Table 4.1). Nevertheless, the best batch prepared with PCS spin dope (i.e., batch 69s) still had higher breakage rates during spinning compared to even the first batch prepared with PCS+PSZ spin dopes.

It was also observed, qualitatively, during the course of spinning experiments that fibers prepared from PCS+PSZ solutions could be stretched more easily compared to fibers from PCS solutions. Fiber extension experiments carried out separately confirmed this observation. Fiber extension distances were determined by dipping a glass rod in the bulk solution (at the same viscosities as used in fiber spinning

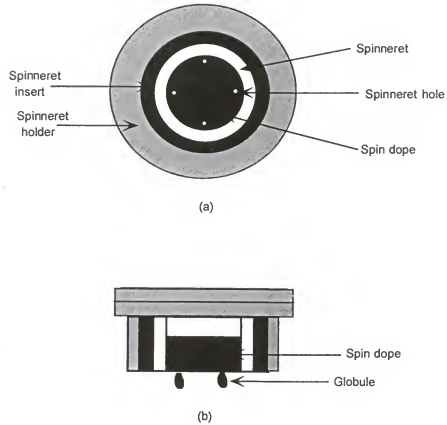

Figure 4.3. Schematic illustration of globule formation during spinning of fibers from PCS spin dope: (a) top view (b) front view of the spinneret assembly.

experiments, viz., ~35-40 Pa·s) and drawing fibers until they became separated from the bulk solution. Average fiber extensions are shown in Table 4.2, while the results for individual fibers are shown in Appendix C. Table 4.2 shows that the average fiber extension for the PCS+PSZ solution was 27% greater than the average extension for the PCS solution. The differences in fiber extension may be related to a difference in drying behavior of the polymer solutions (see section 4.1.2.2). (The rate of evaporation of solvent (toluene) is greater for PCS solutions than for PCS+PSZ solutions.)

4.1.2 Polymer solution characteristics

To understand the differences in spinning characteristics of PCS and PCS+PSZ spin dopes, the polymer solutions were characterized by measuring molecular weight and intrinsic viscosity, wettability on different substrates, surface tension, and rate of evaporation of solvent from spin dopes.

4.1.2.1 Molecular weight and intrinsic viscosity measurements

Figure 4.4 shows GPC molecular weight distributions for the PCS† and PSZ‡ polymers. It can be seen that molecular weights (M_n and M_w) and polydispersity indices (PDI's) for the two polymers are similar. However, PSZ has a bimodal molecular weight distribution. Figure 4.5 shows plots of η_{sp}/c vs. c (where η_{sp} is the specific viscosity and c is concentration in g/dl) for PCS, PSZ, and PCS+PSZ solutions. Also shown are the intrinsic viscosity [η] values which are the y-axis intercepts obtained by extrapolation (to c=0) of the least- squares fit of the data. Details of calculations of intrinsic viscosities for these solutions are shown in Appendix D. The intrinsic viscosities of PCS, PSZ, and

† PCS used in this study was-prepared by G. Staab at University of Florida.
‡ PSZ used in this study was-prepared by G. Schieffele at University of Florida.

Table 4.2. Average fiber extension distances for PCS and PCS+PSZ spin dopes at the same viscosities used in the fiber spinning experiments.

Polymer batch	# of fibers drawn	Average fiber extension, cm[a]
PCS	50	11.08 ± 5.3
PCS+PSZ	49	14.07 ± 7.4

[a] Fiber extension distance was determined by dipping a glass rod in the bulk polymer solution and drawing fibers until they became separated from the bulk solution.

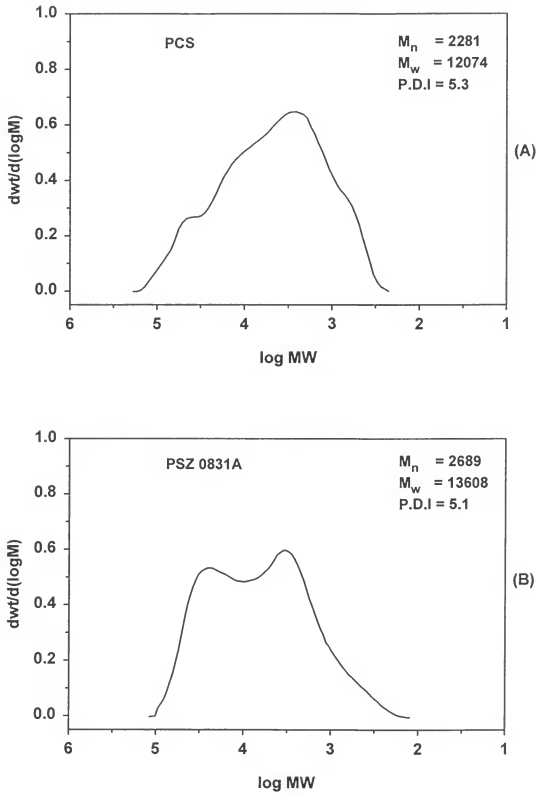

Figure 4.4. GPC molecular weight distributions for: (A) PCS and (B) PSZ.

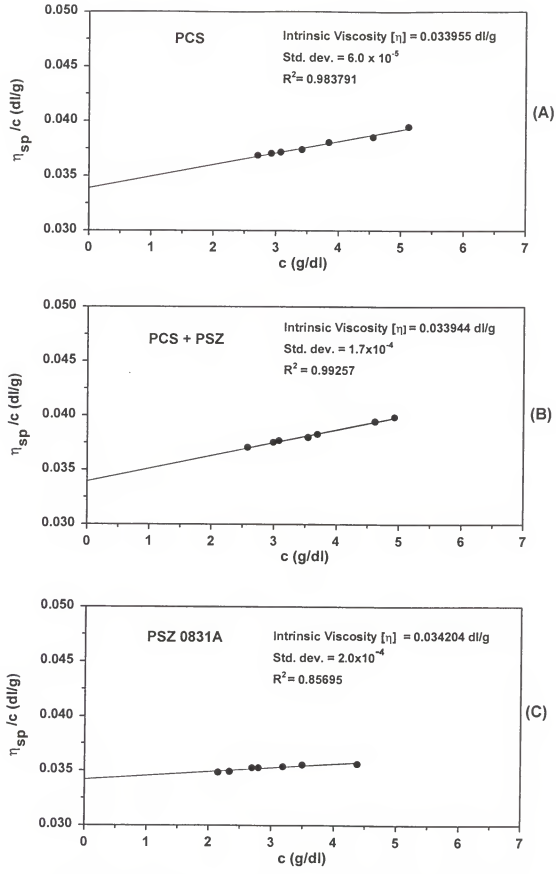

Figure 4.5. Plots of η_{sp}/c vs. concentration for (A) PCS, (B) PCS+PSZ, and (C) PSZ solutions.

PCS+PSZ solutions are similar[§]. This is somewhat surprising because PSZ has a larger fraction of higher molecular weight molecules compared to PCS. If other factors were constant, this should result in a higher intrinsic viscosity. However, the intrinsic viscosity also depends on the polymer/solvent interactions, the polymer molecular shape (e.g., linear vs. equiaxed), and the polymer chain flexibility.

4.1.2.2 Studies on rates of evaporation of solvents from PCS and PCS+PSZ solutions

Experiments were carried out on PCS and PCS+PSZ solutions to assess changes in rate of solvent evaporation as a result of addition of PSZ to PCS. Changes in solvent evaporation rate would have an influence on the drying characteristics of the polymer spin dope near the spinneret surface and extension of fibers from spin dope and consequently, could influence the process of fiber spinning. The rate of solvent evaporation was monitored for PCS/toluene and PCS+PSZ/toluene solutions prepared with 68 wt% polymer. Figures 4.6a and 4.6b show the percentage weight change vs. time and absolute weight change vs. time, respectively, for both polymer solutions. It is evident that the toluene evaporation rate was much slower for the PCS+PSZ solution. This suggests that rate of evaporation of solvent near the spinneret face will be lower for PCS+PSZ spin dope compared to PCS (and, hence, drying effects at the spinneret face will be minimized also). When the polymer spin dope dries rapidly on the spinneret face, it may form drier material which could obstruct the spinneret holes and interfere with fiber formation and spinning. In addition, a faster drying rate may have an adverse effect on filament extension and winding. It was shown in section 4.1.1 that fiber extensions were lower for PCS polymer solution compared to PCS+PSZ solution (see Table 4.2). This might be caused by a faster drying rate of the filament pulled from the polymer

[§] The regression coefficient in the intrinsic viscosity calculations for PSZ was considerably lower than the values obtained for the PCS and PCS+PSZ solutions.

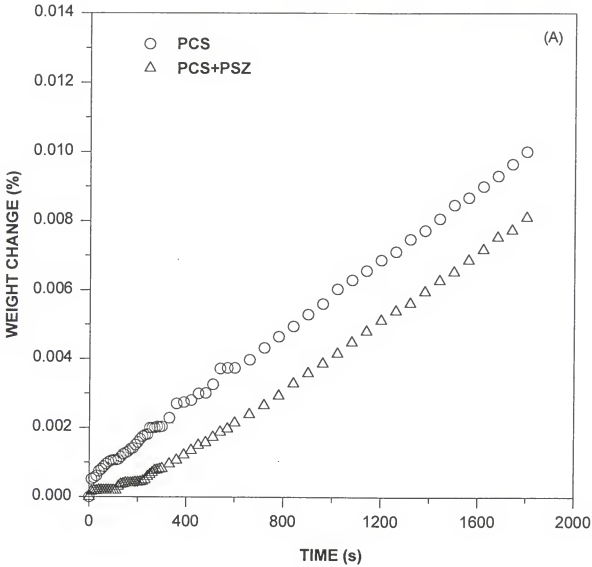

Figure 4.6. (A) Percent change in weight of PCS and PCS+PSZ spin dope as a function of time due to evaporation of toluene, and (B) absolute weight change as a function for PCS and PCS+PSZ solutions.

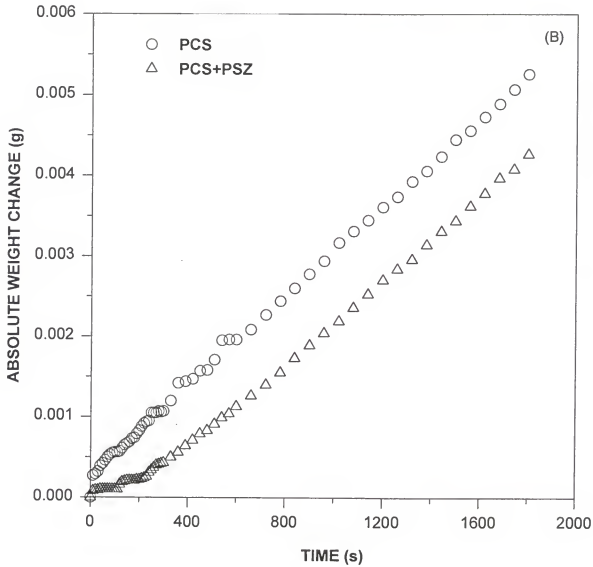

Figure 4.6. (Cont'd.)

solution (i.e., faster drying of the filament would cause it to become solid-like and brittle more quickly and cause it to separate from the bulk solution at a shorter distance). The lower rate of evaporation for PCS+PSZ solution is presumably caused by higher binding energy of toluene to PSZ. (Therefore, it requires higher thermal energy in order to release toluene molecules from PSZ.)

4.1.2.3 Contact angle measurements

Contact angles of water on teflon and stainless substrates were measured first for the purpose establishing a protocol for the measurements. Teflon and stainless steel substrates were chosen to have low and high surface energies, respectively. In addition, the material of construction for the spinneret used in fiber spinning is stainless steel. Both advancing and receding contact angles were measured using the drop-buildup (i.e., adding droplets of fixed size to the existing droplet) and drop-withdrawal method (removing droplets of fixed size from an existing droplet). Due to the higher evaporation rate during measurement of receding contact angle, the error involved in the measurement is likely to be large and, for this reason, only advancing contact angles were taken into consideration in the analysis of results. (Although efforts were made to saturate the local atmosphere with the solvent for which the contact angle was measured, it was not possible to completely avoid solvent evaporation from the sessile drop during the course of the measurement.)

Eight drop sizes were used for the measurement of the contact angle of water on teflon, from a minimum cumulative drop size of 0.3 ml to a maximum cumulative drop size of 1.0 ml. The advancing contact contact angles remained constant at 105° when drop size was increased from 0.3 ml to 1.0 ml whereas the receding contact angles decreased from 105° to 92°. The detailed results are shown in Figure 4.7. The measured contact angles were in reasonable agreement with the reported values in

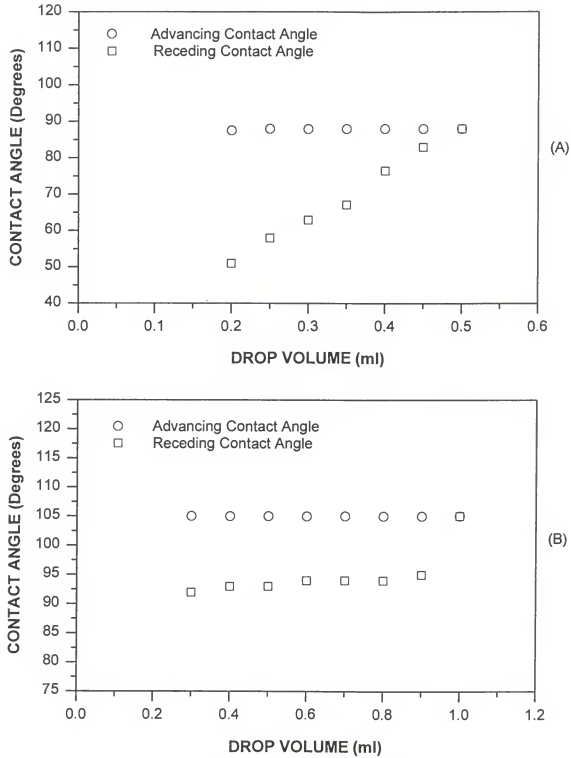

Figure 4.7. Advancing and receding contact angles for water on (A) teflon substrate (B) stainless steel substrate as a function of cumulative drop volume.

literature [Wu82]. (Wu obtained an advancing contact angle of 108° and receding contact angle of 105°. No information was available on drop sizes or how the measurements were carried out). For water on stainless steel, the advancing contact angle varied from 82 to 85° when the drop size was increased from 0.006 ml to 0.042 ml. The receding contact angles decreased from 85 to 45° for the same range of drop sizes.

Contact angles of toluene were measured on teflon and stainless steel substrates. For toluene on teflon, the advancing contact angles ranged from 22 to 33° for drop sizes of 0.20 to 0.50 ml (see Figure 4.8). (0.5 ml was the largest drop size possible for this particular measurement because of the small substrate size.) Toluene was considerably more wetting on stainless steel, with advancing contact angles in the range of only 4.7 to 5° for a drop sizes of 0.006 to 0.042 ml (see Figure 4.9). For toluene on stainless steel, the maximum drop size possible was <0.05 ml, due to its rapid spreading on stainless steel.

Contact angles for PCS and PCS+PSZ solutions (polymer concentrations of 33 wt% in toluene) were measured on stainless steel and teflon substrates. The largest possible drop sizes were used in the measurement to minimize the effects of solvent evaporation from the droplets of polymer solutions. Figures 4.10, 4.11, 4.12, and 4.13 show the variations in contact angles as a function of drop sizes for PCS on stainless steel, PCS+PSZ on stainless steel, PCS on teflon and PCS+PSZ on teflon, respectively. It can be seen that contact angles for PCS+PSZ solution are lower than those for PCS solution, on both stainless steel and teflon substrates. In addition, contact angles for PCS and PCS+PSZ solutions are lower on stainless steel substrates than on teflon substrates.

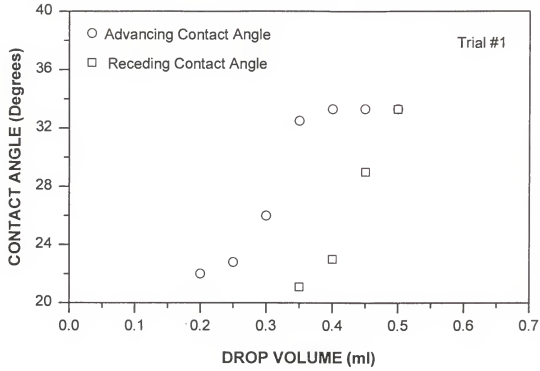

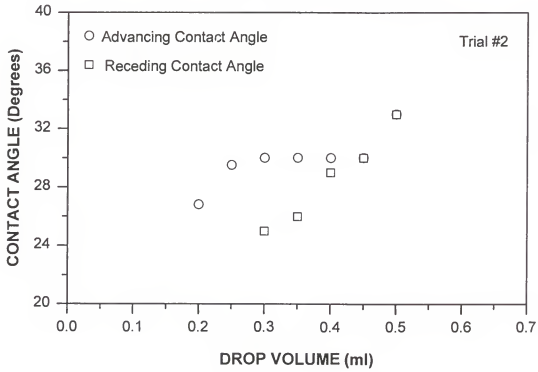

Figure 4.8. Advancing and receding contact angles for toluene on teflon substrate as a function of cumulative drop volume.

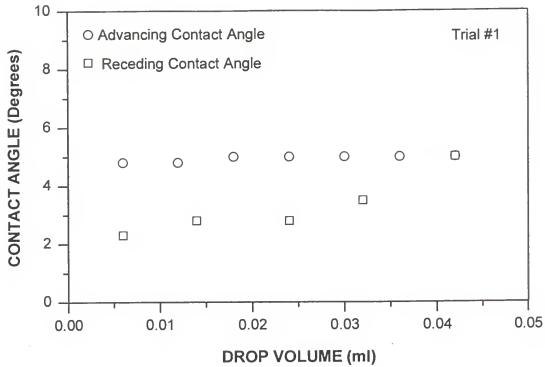

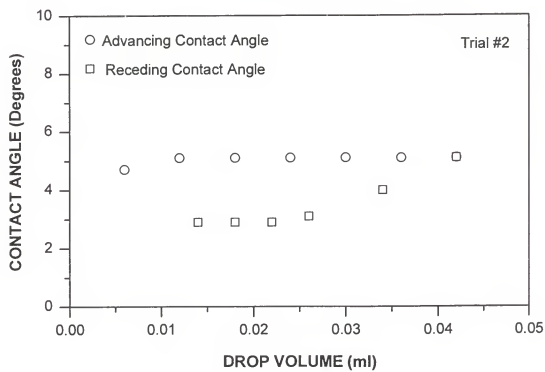

Figure 4.9. Advancing and receding contact angles for toluene on stainless steel substrate as a function of cumulative drop volume.

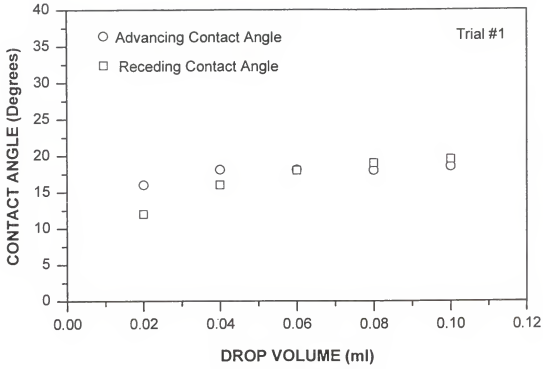

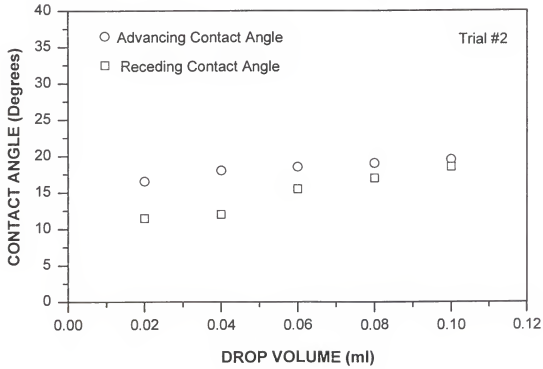

Figure 4.10. Advancing and receding contact angles for PCS (33 wt%)/toluene solution on stainless steel substrate as a function of cumulative drop volume.

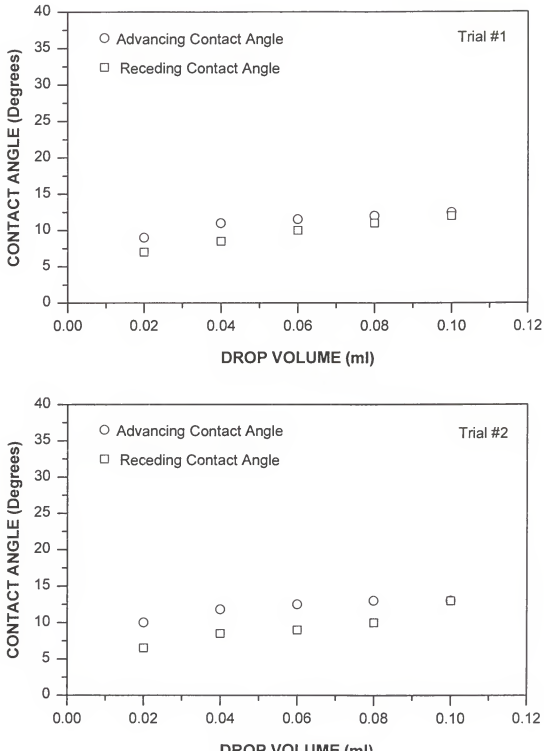

Figure 4.11. Advancing and receding contact angles for PCS+PSZ (33 wt%)/toluene solution on stainless steel substrate as a function of cumulative drop volume.

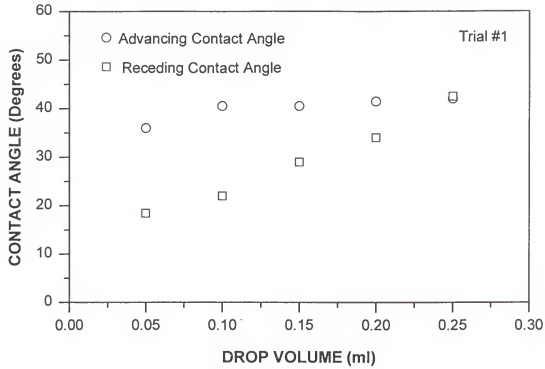

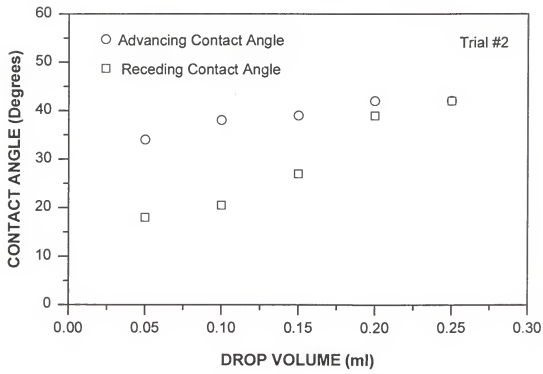

Figure 4.12. Advancing and receding contact angles for PCS (33 wt%)/toluene solution on teflon substrate as a function of cumulative drop volume.

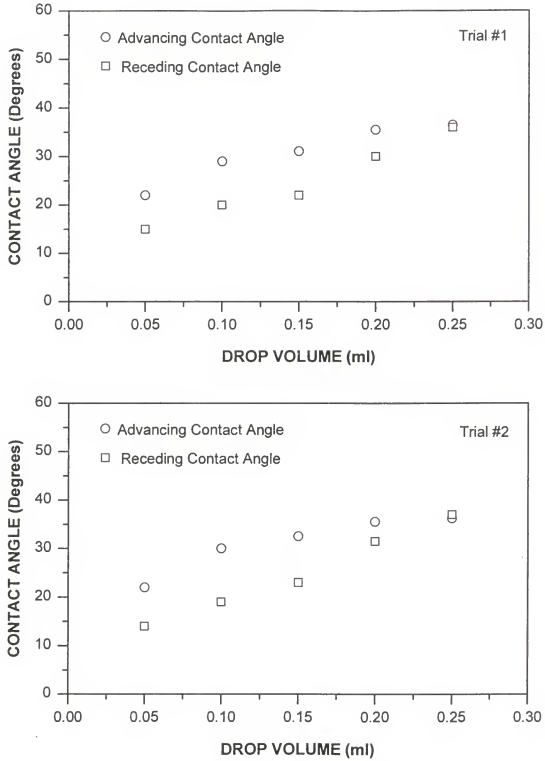

Figure 4.13. Advancing and receding contact angles for PCS+PSZ(33 wt%)/toluene solution on teflon substrate as a function of cumulative drop volume.

It is possible that spinneret holes become coated with a thin film of the polymer solution during the process of fiber spinning. For this reason, contact angles of PCS (~33 wt%)/toluene solution and PCS/PSZ (~33 wt%)/toluene solution were measured on stainless steel substrates which had been previously coated with thin films of PCS and PCS/PSZ, respectively. (As described in Chapter 3.1.3, thin films were prepared by spin coating the same solutions that were used to form the sessile drops for the contact angle measurements.) Figure 4.14 shows the contact angles for PCS solution on PCS-coated stainless steel. The contact angles are considerably higher (especially the advancing angles) compared to the contact angles for PCS solution on uncoated stainless steel (Figure 4.10). (The advancing contact angles in Figure 4.14 range from 38.0 to 41.5°, while the advancing angles in Figure 4.10 range from 16.0 to 18.5°.) In contrast to these results, the contact angles of PCS+PSZ solution on (PCS+PSZ)-coated stainless steel (Figure 4.15) remain low and have similar values to the contact angles for PCS+PSZ solution on uncoated stainless steel (Figure 4.11). (The advancing angles range from 15.0 to 22.0° and 9.0 to 12.5° in Figures 4.15 and 4.11, respectively.) The poorer wetting behavior (i.e., higher contact angles) for PCS solutions on PCS-coated stainless steel may be a factor related to the problems (e.g., globule formation) in spinning fibers from PCS solutions (with no PSZ).

Contact angle hysteresis (i.e., differences in advancing and receding angles for a fixed drop size) was observed in all the measurements made in this study. Contact angle hysteresis has been observed in many other studies also. For example, Herzberg and Marian [Her70] have reported contact angle hysteresis for water on polymethylmethacrylate and polyethylene substrates. Reasons for contact angle hysteresis include (1) differences in evaporation of solvent from the substrate surface encountered during measurement of advancing contact angles and receding contact

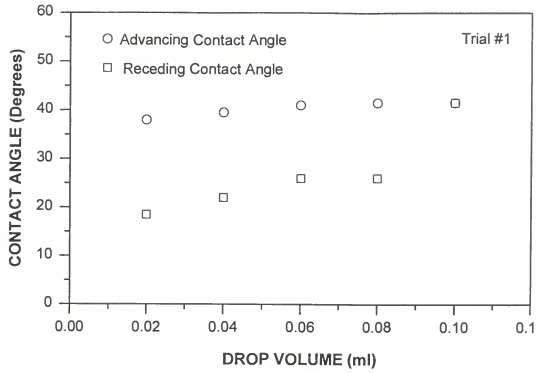

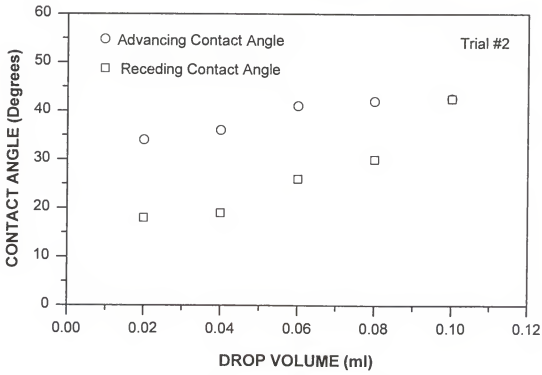

Figure 4.14. Advancing and receding contact angles for PCS (33 wt%)/toluene solution on a stainless steel substrate coated with PCS as a function of cumulative drop volume.

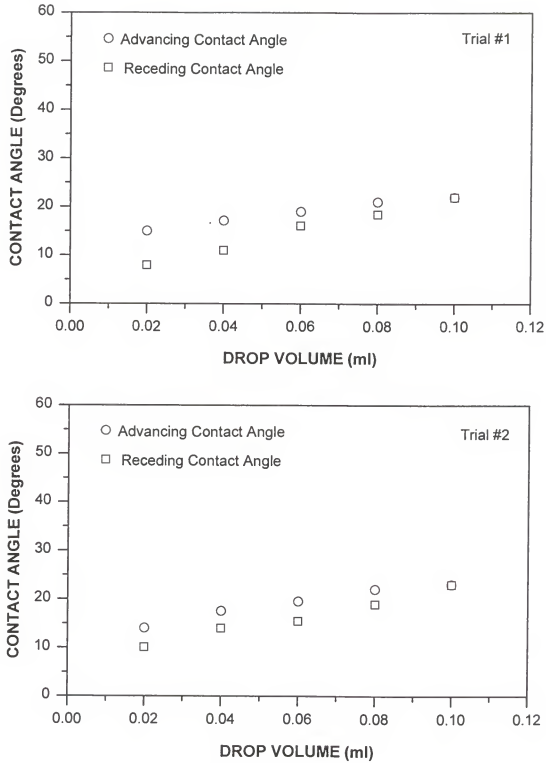

Figure 4.15. Advancing and receding contact angles for PCS+PSZ (33 wt%)/toluene solution on a stainless steel substrate coated with PCS+PSZ as a function of drop volume.

angles and (2) surface roughness of the substrates [Wu84; Her70]. Wu et al. [Wu84] have observed that hysteresis increases with increase in surface roughness. In the present study, larger hysteresis was observed for measurements of water and toluene on teflon compared to that observed for measurements on stainless steel (Figures 4.7a and 4.8). This may be due to the greater roughness of the teflon substrates. (The teflon substrates were polished on a 1 μm diamond wheel, but they still had rougher surfaces than stainless steel.) It was also observed that PCS and PCS+PSZ solutions showed greater contact angle hysteresis on teflon (Figures 4.12 and 4.13, respectively) compared to the same solutions on stainless steel (Figures 4.10 and 4.11, respectively).

A large contact angle hysteresis was observed for the PCS solution on PCS-coated stainless steel (Figure 4.14), i.e., compared to the hysteresis observed for the PCS solution on uncoated stainless steel (Figure 4.10). The reason for this difference is unclear. There was also a tendency for contact angle hysteresis to be greater with PCS solutions compared to PCS+PSZ solutions. (This was most pronounced when coated stainless steel substrates were used (Figures 4.14 and 4.15). In contrast, there was no significant difference in contact angle hysteresis for the experiments with uncoated stainless steel (Figures 4.10 and 4.11).) This effect may be related to the differences in solvent evaporation rates from the solutions. As indicated in Figures 4.6a and 4.6b, toluene evaporated at a higher rate in the early stages from a PCS solution (compared to a PCS+PSZ solution).

4.1.2.4 Surface tension measurements

Experiments were carried out to determine if there were changes in surface tension characteristics of the PCS polymer solution as a result of addition of PSZ to PCS. In order to establish measurement protocols, surface tension experiments were carried out for water, acetone, and toluene, and compared with published results

[CRC92]. The detailed results are presented in Appendix E. The measured values were within 5% of published surface tension values for each liquid.

Table 4.3 shows surface tension values for PCS and PCS+PSZ solutions at three different solids loading (33 wt%, 50 wt%, and 66 wt%). The rheological behavior of the polymer solutions at these concentrations are shown in Figures 4.16-4.21. The solutions exhibited essentially near-Newtonian rheological behavior. (However, the most concentrated PCS solution (66 wt%) in Figure 4.18 showed slight shear thinning behavior.)

Figures 4.22 and 4.23 show plots of surface tension vs. concentration and surface tension vs. viscosity for these solutions. At the lowest concentration (33 wt% polymer), the surface tension of the PCS solution was only slightly higher than PCS+PSZ solution. The differences in surface tension values increased slightly with increasing polymer concentrations. It should be noted that the error involved in surface tension measurement probably becomes larger at higher concentrations (and higher viscosities) and the absolute values reported may not be reliable. For example, the margin of error involved in measurement of surface tension for glycerol (which has a viscosity of ~0.6 Pa·s) was ~9% (measured value: 0.068 N/m (Appendix E), reported value: 0.063 N/m [CRC92]). Similarly, the margin of error involved in the measurement of surface tension for polydimethylsiloxane (which had a viscosity of 12.1 Pa·s) was ~11% (measured value: 0.024 N/m (Appendix E), reported value: 0.022 N/m [And91][§§] . In the case of polymer solutions, possible sources of error also may result from: (i) evaporation of solvent, and (ii) residual polymer remaining on the platinum blade used

[§§] The polydimethylsiloxane used in the present study (PDMS 12500) was manufactured by GE Silicones, Cincinnati, OH. The surface tension values published by Anderson et al. [And91] was obtained on an identical polymer. Anderson et al. did not report the technique used for surface tension measurement.

Table 4.3. Surface tension values for PCS and PCS+PSZ solutions in toluene at different solids-loadings[§].

Solids-loading, %	Surface tension (N/m)	
	PCS	PCS+PSZ
33	0.0284 ± 0.0001	0.0275 ± 0.0001
50	0.0340 ± 0.0001	0.0321 ± 0.0001
66	0.0377 ± 0.0003	0.0350 ± 0.0001

[§] Number of measurements =5

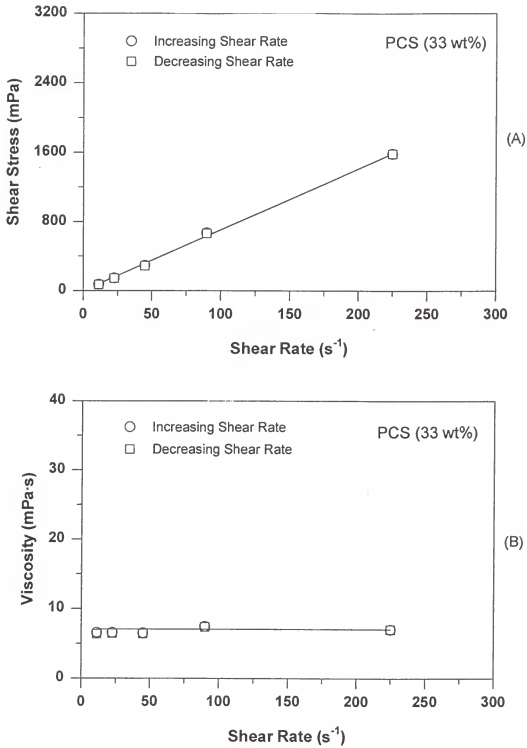

Figure 4.16. Plots of: (A) shear stress vs. shear rate and (B) viscosity vs. shear rate for a 33 wt% PCS solution used in surface tension measurement.

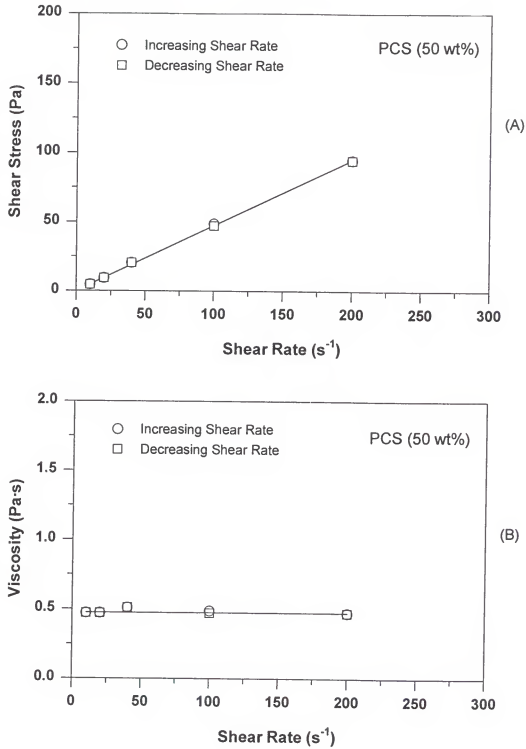

Figure 4.17. Plots of: (A) shear stress vs. shear rate and (B) viscosity vs. shear rate for a 50 wt% PCS solution used in surface tension measurement.

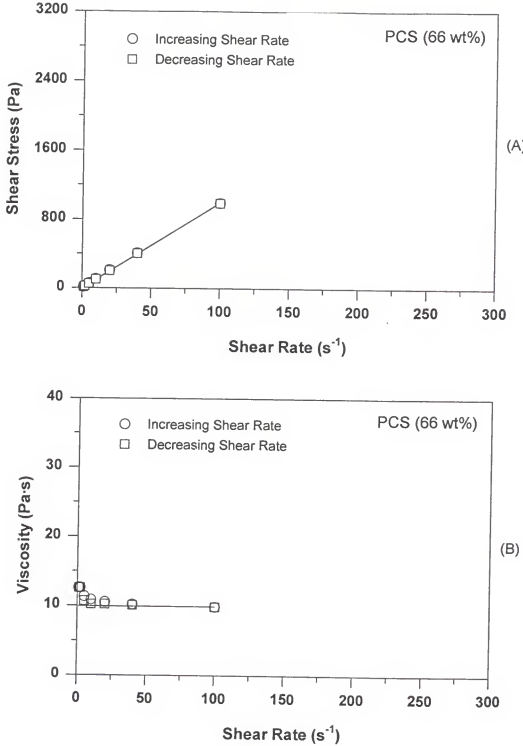

Figure 4.18. Plots of: (A) shear stress vs. shear rate and (B) viscosity vs. shear rate for a 66 wt% PCS solution used in surface tension measurement.

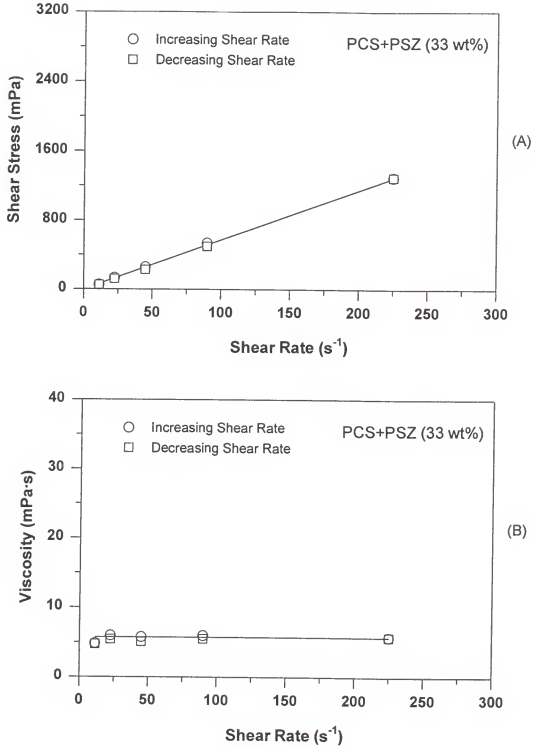

Figure 4.19. Plots of: (A) shear stress vs. shear rate and (B) viscosity vs. shear rate for a 33 wt% PCS+PSZ solution used in surface tension measurement.

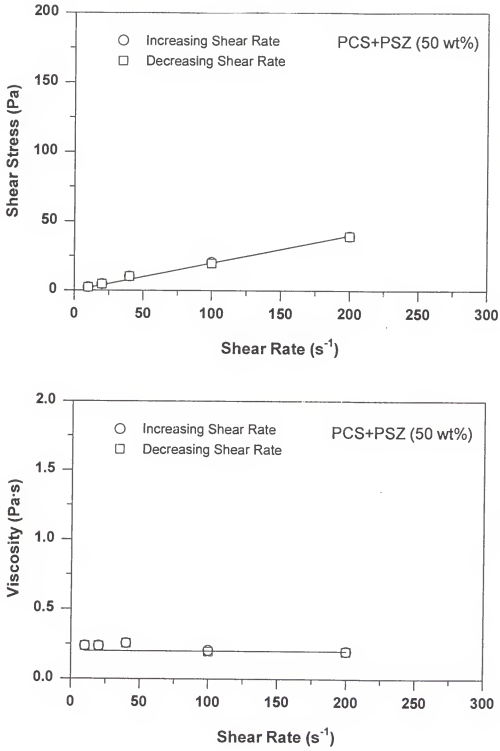

Figure 4.20. Plots of: (A) shear stress vs. shear rate and (B) viscosity vs. shear rate for a 50 wt% PCS+PSZ solution used in surface tension measurement.

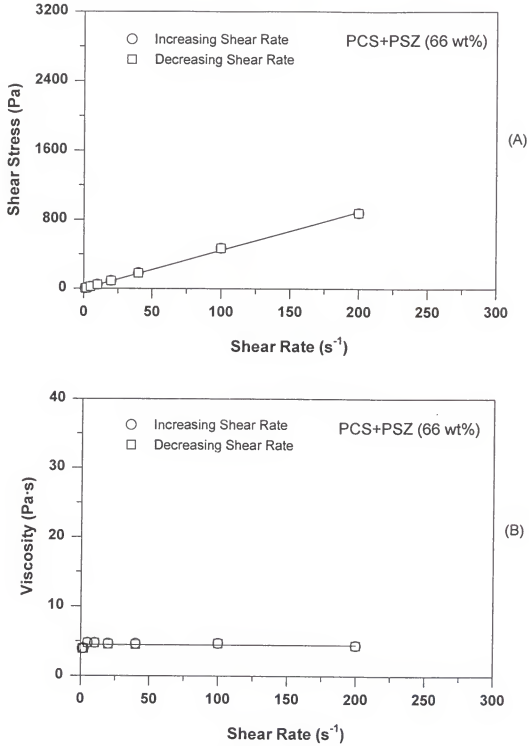

Figure 4.21. Plots of: (A) shear stress vs. shear rate and (B) viscosity vs.shear rate for a 66 wt% PCS+PSZ solution used in surface tension measurement.

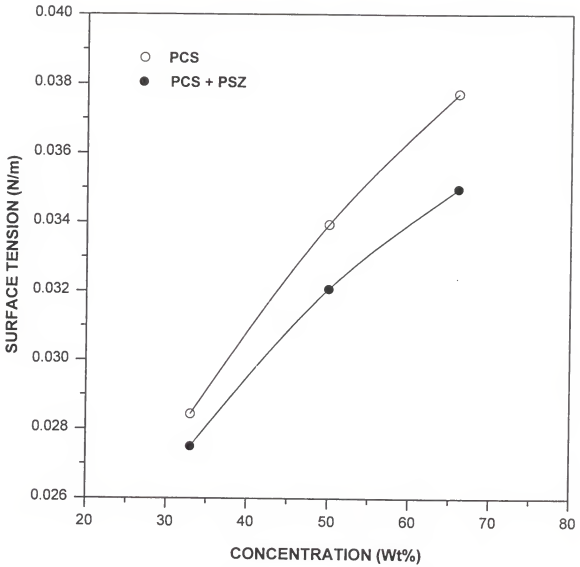

Figure 4.22. Surface tension as a function of concentration for PCS and PCS+PSZ solutions.

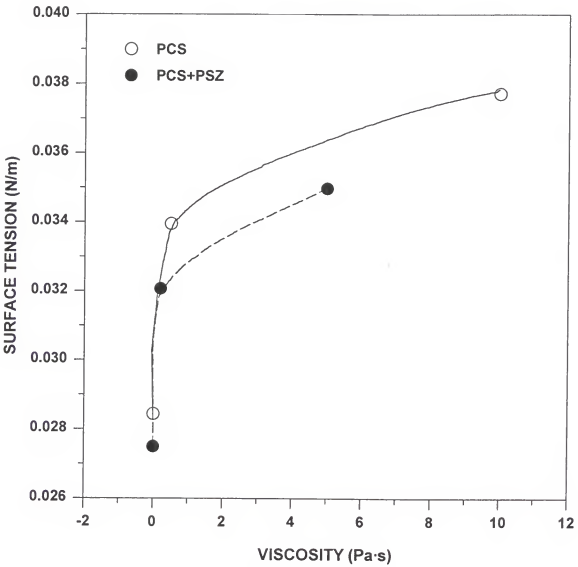

Figure 4.23. Surface tension as a function of viscosity for PCS and PCS+PSZ solutions.

in surface tension measurement by Wilhemy Plate technique. The first factor does not appear to be significant. This is suggested by the observation that the surface tension increased by ~0.002-0.004 N/m when the polymer concentration increased from 50 to 66 wt%. The amount of solvent loss during the measurement would be far less than this concentration change and, hence, solvent loss should have minimal effect on the surface tension value. On the other hand, any polymer remaining on the platinum blade during the surface tension measurement would cause the surface tension reading to be higher than the true value [Wu84]. It would be expected that more polymer would remain on the blade during the measurement when more concentrated (i.e., more viscous) polymer solutions are used. Hence, this may explain the increase in surface tension with increasing polymer concentration that was shown in Figure 4.22.

4.1.3 Characterization of fibers

PCS and PCS+PSZ fibers were characterized in the green state and after various heat treatments (in air at 180 ± 10°C and in nitrogen at temperatures in the range of 200-1150°C). Fibers were characterized using diffuse reflectance Fourier transform infrared spectroscopy (DRIFT) and tensile testing.

4.1.3.1 Characterization of fibers by FTIR

FTIR spectra of PCS-based fibers (green and heat-treated in air at 187°C) were collected at room temperature (25°C) and during heat treatment from 40-600°C in nitrogen. Figure 4.24 shows the room temperature FTIR spectra for green PCS fibers (batch UF-69s)(not containing any additives). The peak assignments for these fibers are shown in Table 4.4. The room temperature FTIR spectra (transmission mode) for polydimethylsilane (PDMS), the precursor for PCS, is shown in Figure 4.25. Table 4.5 shows a list of characteristic absorption bands for PDMS. Since PDMS consists of a Si-Si backbone with attached methyl groups, the major absorption bands in the FTIR

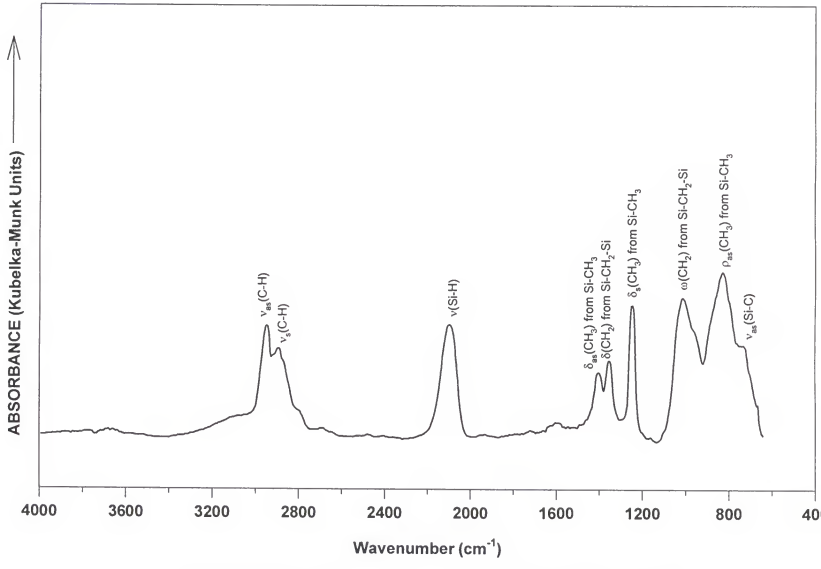

Figure 4.24. Room temperature FTIR spectra of green PCS fibers (batch 69s).

Table 4.4. FTIR peak assignments for polycarbosilane (PCS) fibers.

Peak (cm^{-1})	Assignment	References
2950	ν_{as} (C-H)	1,2
2894	ν_{s} (C-H)	1,2
2098	ν (Si-H)	1,4
1407	δ_{as} (CH_3) from Si-CH_3	2,3
1358	δ (CH_2) from Si - CH_2 - Si	1,3
1253	δ_{s} (CH_3) from Si-CH_3	2,3
1020	ω (CH_2) from Si - CH_2- Si	1,3
830	ρ_{as} (CH_3) from Si - CH_3	1,2,3
735	ν_{as} (Si-C)	1,2,3

ν = stretching ; δ = bending ; ω = bending ; ρ = rocking

(1) W. Kriner, *J. Org. Chem.*, 29, 1601 (1964).
(2) A.L. Smith, *J. Chem. Phys.*, 21, 1997 (1953).
(3) A.L. Smith, *Spectrochimica Acta*, 16, 87 (1960).
(4) A.L. Smith, *Spectrochimica Acta*, 15, 412 (1959).

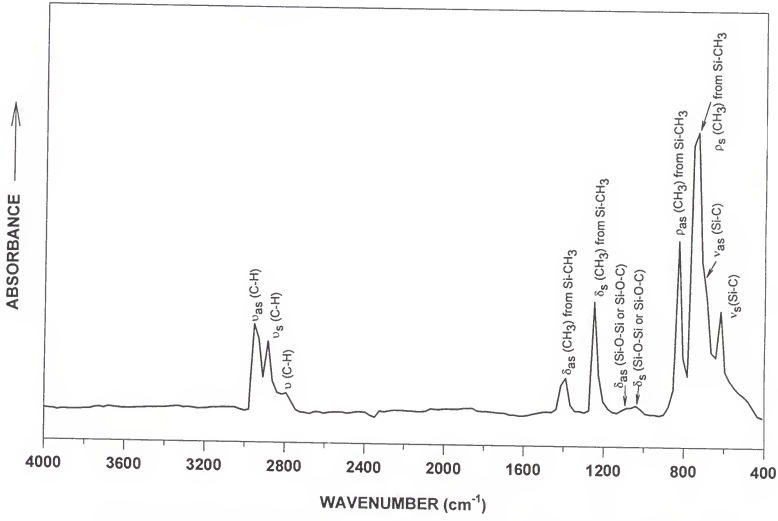

Figure 4.25. Room temperature FTIR spectra (transmission mode) of Polydimethylsilane (PDMS) (Nisso Corporation, Japan).

Table 4.5. FTIR peak assignments for polydimethylsilane(PDMS) polymer.

Peak (cm^{-1})	Assignment	References
2950	ν_{as} (C-H)	1,2
2894	ν_{s} (C-H)	1,2
1407	δ_{as} (CH_3) from Si-CH_3	2,3
1253	δ_{s} (CH_3) from Si-CH_3	2,3
1110	δ_{as} (Si-O-Si or Si-O-C)	1,3
1064	δ_{s} (Si-O-Si or Si-O-C)	1,3
830	ρ_{as} (CH_3) from Si - CH_3	1,2,3
745	ρ_{s} (CH_3) from Si - CH_3	1,2,3
689	ν_{as} (Si-C)	1,2,3
626	ν_{s} (Si-C)	1,2,3

ν = stretching ; δ = bending ; ω = bending ; ρ = rocking

(1) W. Kriner, *J. Org. Chem.*, 29, 1601 (1964)
(2) A.L. Smith, *J. Chem. Phys.*, 21, 1997 (1953)
(3) A.L. Smith, *Spectrochimica Acta*, 16, 87 (1960)
(4) A.L. Smith, *Spectrochimica Acta*, 15, 412 (1959)

spectra are due to various modes of vibrations of Si-CH_3 groups. In the case of PCS, it is possible that some residual Si-Si bonds may be remaining in the polymer structure depending on synthesis conditions. A comparison of FTIR spectra of PDMS and PCS will enable determination of whether the PDMS to PCS conversion is essentially complete. A mostly converted PCS shows an intense absorption band at 2100 cm^{-1} due to Si-H bond. This absorption band is absent in PDMS due to the lack of Si-H bonds in the structure of PDMS. A comparison of absorption bands at 1407 cm^{-1} and 1355 cm^{-1} for PDMS and PCS will also enable determination of the extent of conversion to PCS. In the case of PDMS, there is an absorption band at 1407 cm^{-1} and none at 1355 cm^{-1}. This is consistent with the structure of PDMS, which shows CH_3 groups attached as side groups to the main Si-Si backbone. After conversion to PCS, one of the side groups (CH_3) is replaced by CH_2, which attaches in the main chain as a Si-CH_2-Si linkage, and H which is attached to Si as side group. Hence, the contribution from Si-CH_2-Si also shows up in the FTIR spectra for PCS as an absorption band at 1355 cm^{-1}. Since the CH_2 group is attached to the Si atom in the backbone, its absorption intensity is higher than that of the Si-CH_3 in which the CH_3 is attached to a Si atom as a side group. Thus, in a mostly converted PCS, the absorption intensity at 1355 cm^{-1} is greater than the absorption intensity at 1407 cm^{-1}. It was expected that the absorption intensities at 2950 cm^{-1} and 2850 cm^{-1} would be higher for PDMS because two CH_3 groups are attached to each Si atom in the backbone of the repeating unit (R.U) compared to PCS, where only one CH_3 group is attached to each Si atom in the backbone of the R.U. However, this was not observed from Figures 4.24 and 4.25. (It is not clear if this is related to the fact that the PCS fibers were analyzed in the diffuse reflectance mode, while the PDMS sample was analyzed in the transmission mode.)

4.1.3.1.1 FTIR spectra of PCS fibers during heat treatment in N_2

The changes in the structure of PCS fibers during pyrolysis to 600°C in nitrogen are shown in Figure 4.26. The relative changes in intensities of various peaks as a function of temperature are shown in Figure 4.27. No significant changes were observed in the absorption bands for PCS up to ~300°C. The intensity of the absorption band for Si-H increased steadily, reached a maximum at ~500°C and then started to decrease. The initial increase in intensity is possibly due to the formation of additional Si-H groups as a result of methylene insertion reactions (also known as Kumada rearrangement reactions [Shi58]). Methylene insertion reaction (equation (4.1)) is the mechanism by which conversion of polydimethylsilane (PDMS) to polycarbosilane (PCS) takes place.

(4.1)

Schmidt et al. [Sch91] have also observed similar increases in intensities of the Si-H absorption band between the temperatures of 200-400°C during the pyrolytic conversion of vinylic polysilane to silicon carbide and have suggested that the mechanism responsible for this observation is the methylene insertion reaction. (This conclusion was based on ^{1}H CRAMPS (Combined Rotation and Multiple Pulse Spectroscopy), ^{13}C MAS NMR (Magic Angle Spinning Nuclear Magnetic Resonance), and ^{29}Si MAS NMR spectra.) Figure 4.27 also shows that the absorption band at 1020 cm^{-1} (due to ω (CH_2) of Si-CH_2-Si) started to increase relative to the absorption band at 1407 cm^{-1} (due to δ_{as} (CH_3) of Si-CH_3) in the temperature regime of 300-500°C. In addition, Figure 4.27 shows that the intensity of absorption band due to $\omega(CH_2)$ of Si-CH_2-Si increases relative to

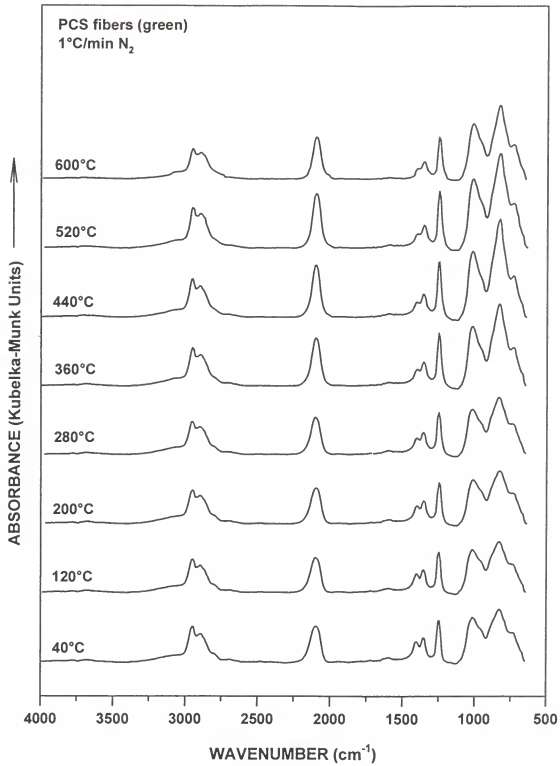

Figure 4.26. FTIR spectra for PCS fibers (batch 69s) during heat treatment to 600°C at 1°C/min in nitrogen atmosphere.

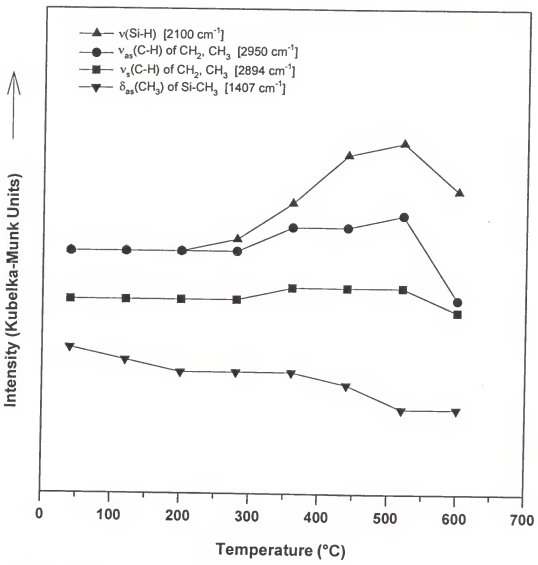

Figure 4.27. Intensity vs. temperature from FTIR spectra for PCS (green) fibers (batch 69s).

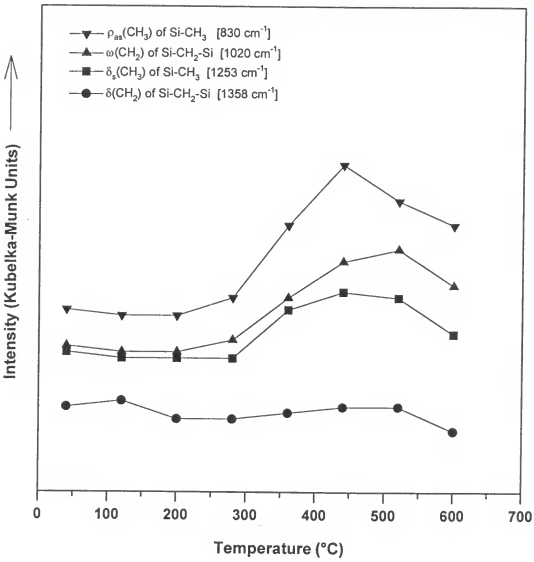

Figure 4.27. (Cont'd.)

$\delta(CH_2)$ of Si-CH_2-Si. This is also consistent with the methylene insertion reactions that occur in the PDMS to PCS conversion. (In the latter case, the intensity of the absorption band $\omega(CH_2)$ of Si-CH_2-Si formed during the PDMS to PCS conversion is significantly greater than the intensity of the absorption band $\delta(CH_2)$ of Si-CH_2-Si, as indicated in Figure 4.24.) However, Figure 4.27 shows that the $\rho_{as}(CH_3)$ of Si-CH_3 absorption band (at 830 cm^{-1}) increased significantly and the $\delta_s(CH_3)$ of Si-CH_3 absorption band (at 1253 cm^{-1}) increased slightly in this temperature range. This observation seems to be inconsistent with the occurrence of methylene insertion reactions. However, the relative intensity ratios for $\rho_{as}(CH_3)$ with respect to $\nu_{as}(CH)$ and $\delta_{as}(CH_3)$ with respect to $\nu_{as}(CH_3)$ increase only slightly during heat treatment. This is consistent with what is observed in the methylene insertion reactions, where these ratios are expected to increase slightly during heat treatment.

Hasegawa et al. [Has83] suggested that the main reason for the increase in intensity of Si-H absorption band during heat treatment between 200°C and 500°C was the existence of a polysilane skeleton in PCS. The residual polysilane skeleton gets converted to polycarbosilane skeleton in this temperature regime. (Such a conversion mechanism corresponds to an increase in Si-H and Si-CH_2-Si bonds with an increase in heat treatment temperature.) Hasegawa's FTIR spectra showed a decrease in intensity of Si-H absorption band beyond 500°C. This is possibly due to cross-linking by dehydrogenation reactions of Si-H bonds. Mocaer et al. [Moc93] have also reported similar decreases in intensity of Si-H absorption band in the pyrolysis of polycarbosilazane polymer. The evidence for dehydrogenation was obtained by gas chromatography which showed the evolution of H_2. In this temperature range, the Si-H

functionality appears to be the radical source for the pyrolytic conversion to silicon carbide, since it has the lowest bond energy in the PCS skeleton.

Subtraction spectra of PCS fibers before and after heat treatment in nitrogen at 600°C (i.e., 600 - 40°C) is shown in Figure 4.28. A direct comparison of the spectra at these temperatures is shown in Figure 4.29. The absorbance of band due to $\delta_s(CH_3)$ from Si-CH_3 at 1250 cm^{-1} increased only slightly up to 600°C whereas the absorbance of bands due to ν_s (C-H) at 2894 cm^{-1}, $\delta_{as}(CH_3)$ from Si-CH_3 at 1407 cm^{-1} and $\delta(CH_2)$ from Si-CH_2-Si at 1358 cm^{-1} decreased slightly. The absorbance of ν(Si-H) at 2100 cm^{-1}, $\omega(CH_2)$ from Si-CH_2-Si at 1020 cm^{-1}, and $\rho_{as}(CH_3)$ of Si-CH_3 at 830 cm^{-1} increased significantly, and these changes may be attributed to the methylene insertion reactions as explained previously.

Hasegawa et al. and Buoillon et al. [Buo91] studied the changes in the FTIR absorption spectra of PCS upon pyrolysis to 1000°C. They reported that intensities of most absorption bands changed only slightly during heat treatment to 400°C, similar to observations made in the present study. No significant gas evolution was detected (by gas chromatography) in this temperature range. Methylene insertion reactions took place between 400°C and 550°C, resulting in increases in intensities of absorption bands due to ν(Si-H) at 2100 cm^{-1} and ν (CH_2) of Si-CH_2-Si at 1358 cm^{-1}. There was no significant change in the intensities of other absorption bands in the FTIR spectra until 550°C. This is indicative of the fact that polymer degrades slowly up to 550°C (i.e., few organosilicon bonds are broken). After 550°C, decomposition of the side chains of the polymer started to take place, leading to the formation of an amorphous inorganic material. This was manifested by a rapid decrease in intensities of all absorption bands

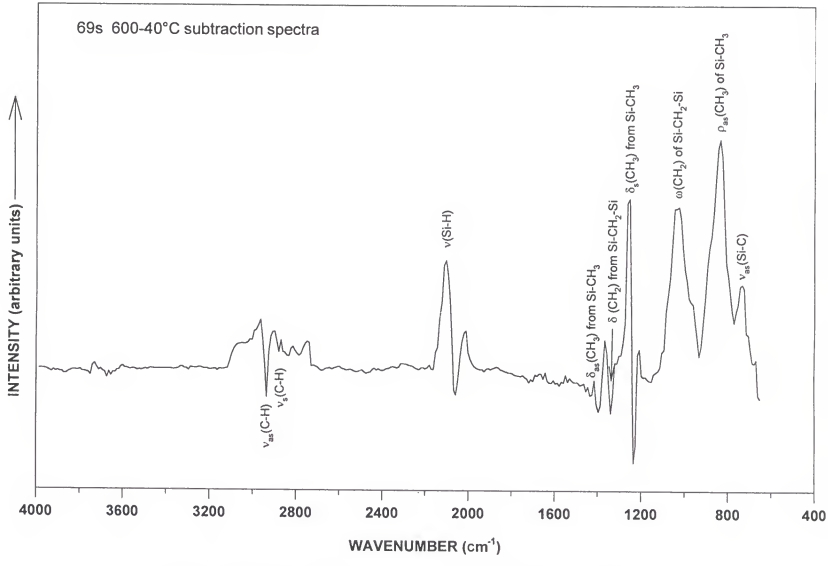

Figure 4.28. Subtraction spectra for PCS fibers (batch 69s) heat treated in N_2; 600-40°C.

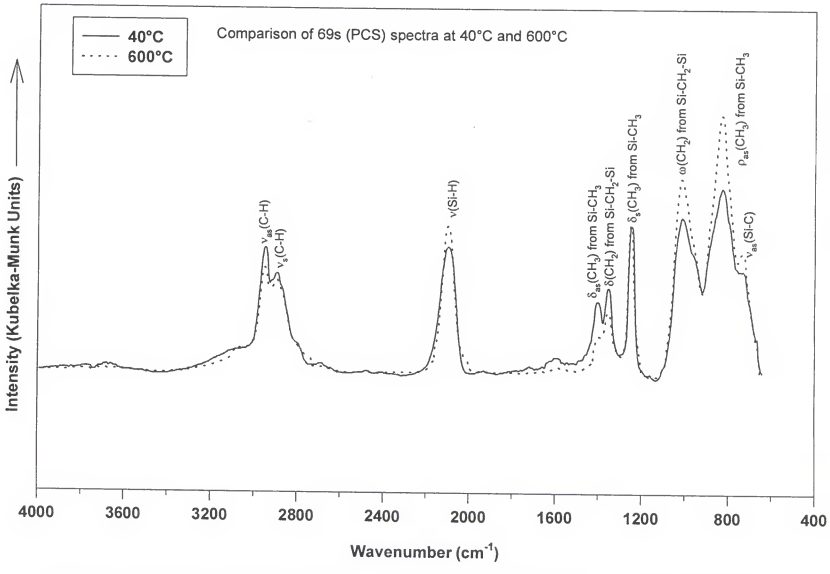

Figure 4.29. Comparison of FTIR spectra of PCS fibers(batch 69s) before and after heat treatment at 600°C in nitrogen.

in the FTIR spectra. At ~800°C, a well-defined absorption band due to ν_{as} (Si-C) at 735 cm^{-1} formed.

4.1.3.1.2 FTIR spectra of PCS fibers heat-treated in air

Figure 4.30 shows FTIR spectra at 40°C of PCS fibers after heat treatment in air at 187°C for 1 h. (The fibers had a weight gain of 8.5 wt% after this treatment.) Table 4.6 shows peak assignments for PCS fibers heat-treated in air. In addition to the characteristic absorption bands for normal PCS as described above (section 4.1.3.1.1), the spectra also shows absorption bands at 3650 cm^{-1} and 3600-3400 cm^{-1} (due to free -OH and bonded -OH, respectively), 1720 cm^{-1} (due to C=O), and a broad absorption band at 1000-1100 cm^{-1} (due to Si-O-Si or Si-C-O)[†]. The absorption band at 3220 cm^{-1} could not be identified. (It is suspected that this peak may have been due to some contamination of the sample during vacuum drying prior to loading the sample in the FTIR hot stage.) During heat treatment of PCS fibers in air, Si-H, $Si-CH_3$ and $Si-CH_2-Si$ groups get oxidized, resulting in the formation of Si-OH, Si-O-Si, Si-C-O, Si-O-C, and C=O linkages.

In the case of PCS fibers before heat treatment in air, the intensity of the absorption band δ (CH_3) from $Si-CH_3$ at 1407 cm^{-1} was less than that due to $\delta(CH_2)$ from $Si-CH_2-Si$ at 1358 cm^{-1}. After the air-heat treatment, it can be clearly seen that the absorption band due to δ (CH_3) from $Si-CH_3$ became higher in intensity than the absorption band $\delta(CH_2)$ from $Si-CH_2-Si$. This is attributed to the conversion of $Si-CH_2-Si$ bonds to Si-C-O bonds during heat treatment in air. (Hasegawa et al. argue that $Si-CH_2\bullet$ radicals form when the $Si-CH_2-Si$ chain is severed and that these radicals are oxidized easily and form Si-C-O networks [Has89].) Figure 4.31 shows a subtraction

[†] There would still be contributions from ω (CH_2) of $Si-CH_2-Si$ vibrations at ~1020 cm^{-1}.

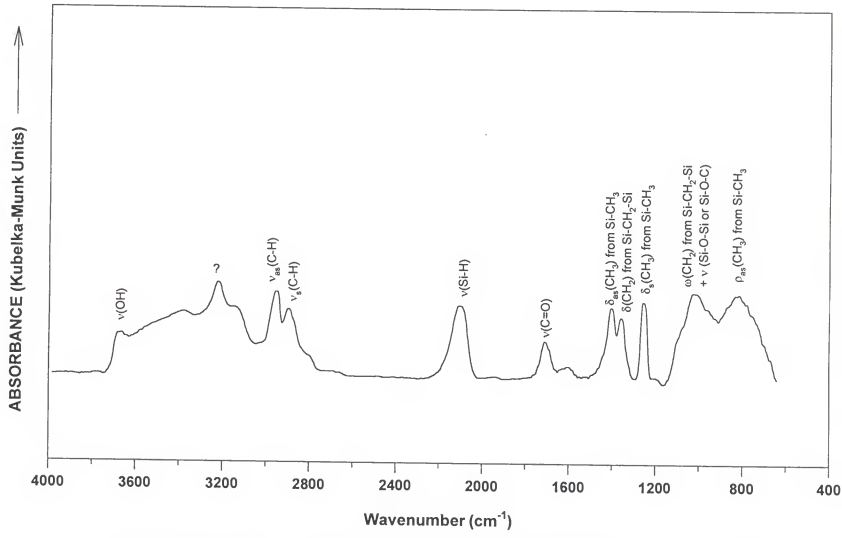

Figure 4.30. Room temperature FTIR spectra for PCS fibers (batch 65s) heat-treated in air at 187°C.

Table 4.6. FTIR peak assignments for PCS fibers (batch 65s) heat-treated in air at 187°C.

Peak (cm^{-1})	Assignment	References
3650	ν (OH)	1,2
2950	ν_{as} (C-H)	1,2
2894	ν_{s} (C-H)	1,2
2098	ν (Si-H)	1,4
1720	ν (C=O)	2,3
1407	δ_{as} (CH_3) from Si-CH_3	2,3
1358	δ (CH_2) from Si - CH_2 - Si	1,3
1253	δ_{s} (CH_3) from Si-CH_3	2,3
1000-1100	δ (Si-O-Si or Si-O-C)	1,3
1020	ω (CH_2) from Si - CH_2- Si	1,3
830	ρ_{as} (CH_3) from Si - CH_3	1,2,3
735	ν_{as} (Si-C)	1,2,3

ν = stretching ; δ = bending ; ω = bending ; ρ = rocking

(1) W. Kriner, *J. Org. Chem.*, 29, 1601 (1964)
(2) A.L. Smith, *J. Chem. Phys.*, 21, 1997 (1953)
(3) A.L. Smith, *Spectrochimica Acta*, 16, 87 (1960)
(4) A.L. Smith, *Spectrochimica Acta*, 15, 412 (1959)

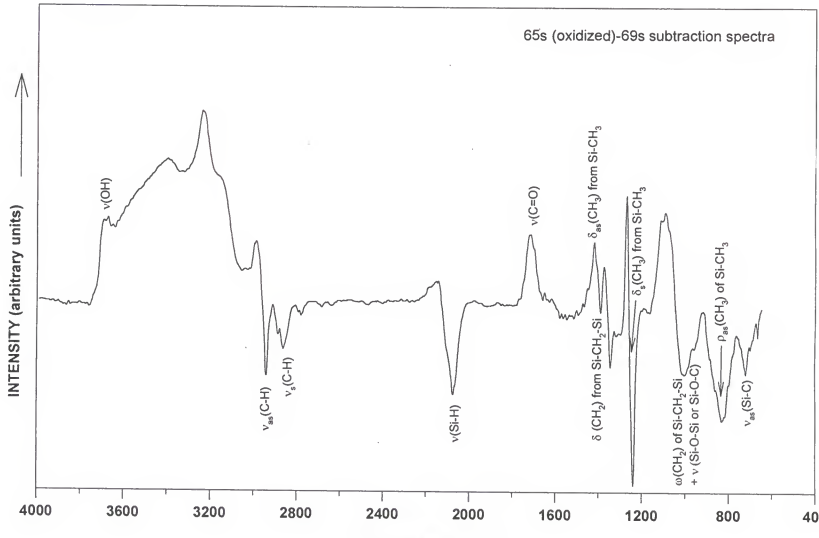

Figure 4.31. Subtraction spectra for PCS fibers heat-treated in air at 187°C (batch 65s) and PCS green fibers (batch 69s).

spectra (at 40°C) of fibers before and after air-heat treatment. Figure 4.32 shows a comparison of spectra at 40°C before and after air-heat treatment. It can be seen that all the original absorption bands, except $\delta_{as}(CH_3)$ from Si-CH_3 at 1407 cm^{-1}, decreased in intensity after air-heat treatment. The spectrum for the air-heat treated fibers also shows the formation of ν(C=O) groups (at 1722 cm^{-1}) due to oxidation of methyl groups and ν(OH) groups due to oxidation of Si-H groups.

4.1.3.1.3 FTIR spectra of air-heat treated PCS fibers during heat treatment in N_2

Figure 4.33 shows FTIR spectra of oxidized PCS fibers (batch UF-65s) during heat treatment to 600°C in nitrogen atmosphere. Figure 4.34 shows the changes in intensities of specific absorption bands as a function of temperature. In the range ~300-600°C, the intensities associated with the Si-OH and Si-H absorptions decreased significantly and that associated with the Si-O-Si absorptions increased significantly. This suggests that Si-OH and Si-H groups are involved in condensation reactions to form -Si-O-Si- linkages as indicated below:

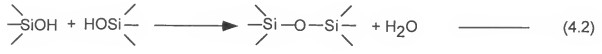

Ichikawa et al. [Ich90] have also observed a rapid decrease in intensity of Si-OH groups during heat treatment of air-heat treated PCS[§] (low molecular weight) in nitrogen to 500°C. Figure 4.35 shows Ichikawa et al.'s FTIR spectra of air-heat treated PCS polymer as a function of heat treatment temperature. They report that the absorption

[§] Nippon Carbon Company, Japan.

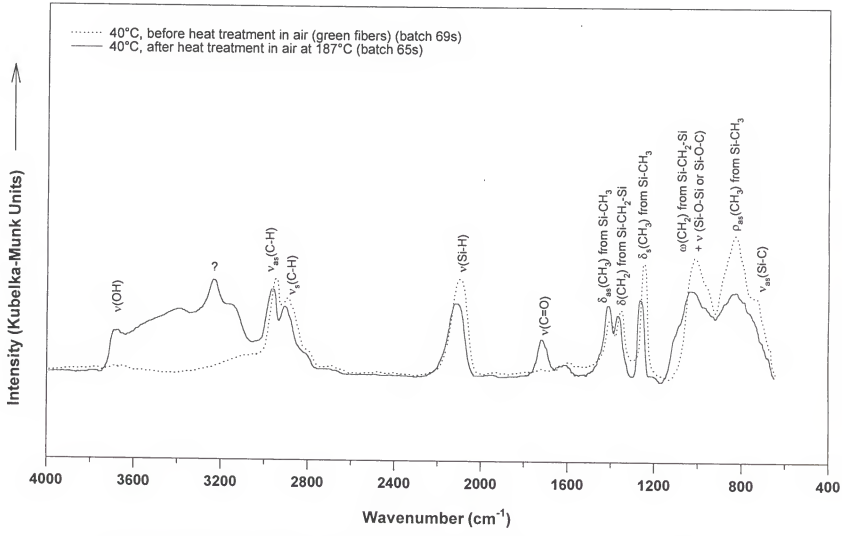

Figure 4.32. Comparison of FTIR spectra of PCS fibers at 40°C before and after heat treatment in air.

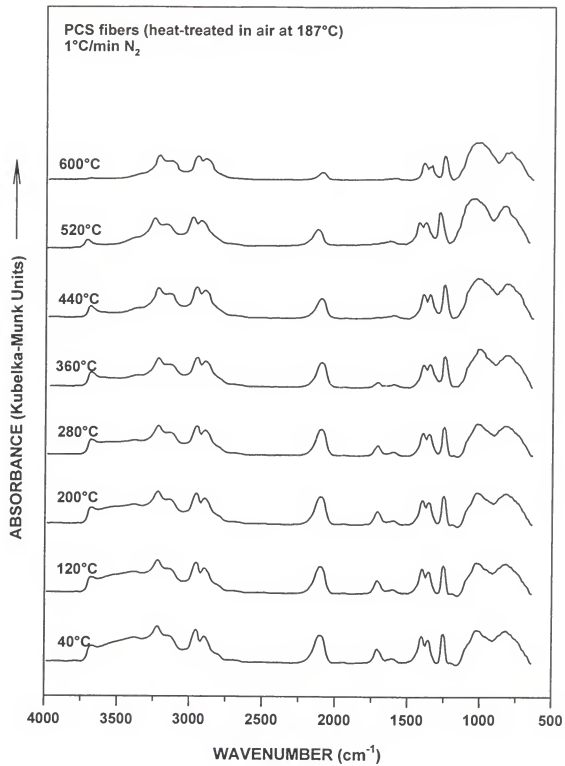

Figure 4.33. FTIR spectra for air-heat treated (187°C) PCS fibers (batch 65s) during heat treatment to 600°C at 1°C/min in nitrogen atmosphere.

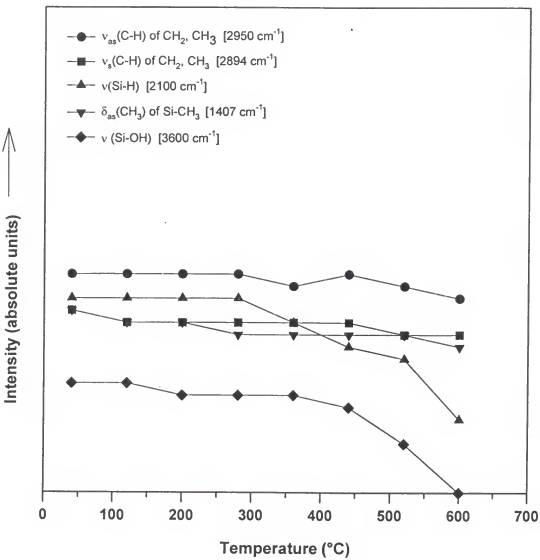

Figure 4.34. Intensity vs. temperature from FTIR spectra for PCS (air-heat treated at 187°C) fibers (batch 65s) during heat treatment in N_2 to 600°C.

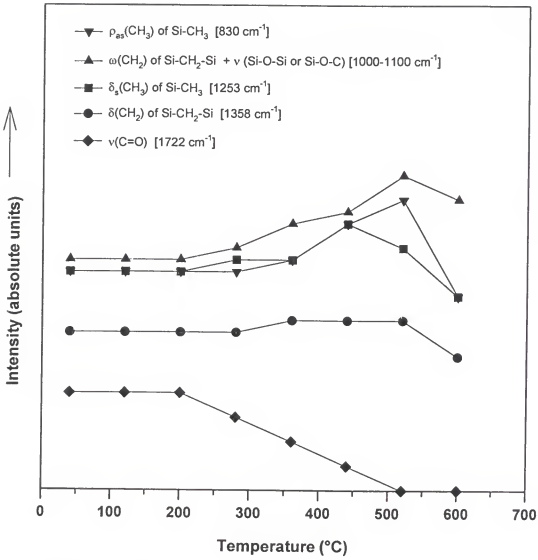

Figure 4.34. (Cont'd.)

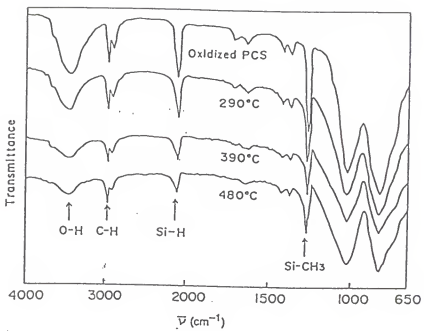

Figure 4.35. FTIR spectra of air-heat treated Nippon PCS fibers during heat treatment in nitrogen to 500°C (from Ichikawa et al. [Ich90]).

intensity of Si-H groups decreased after 300°C, similar to the observation made in this study, presumably due to reaction of Si-H groups with Si-OH groups (equation (4.3)).

Figure 4.34 shows that the band δ_s (CH_3) of Si-CH_3 (at 1253 cm^{-1}) increased slightly around 300°C and then started to decrease beyond 440°C for the PCS. In addition, the intensity of absorption band ρ_{as} (CH_3) of Si-CH_3 (at 830 cm^{-1}) showed an increase at around 400°C and decrease beyond 500°C. These trends are similar to those observed during heat treatment of the fibers prepared without air heat treatment, although the magnitude of the increases in intensity are considerably smaller (see Figure 4.27). In contrast to these results, Ichikawa et al. [Ich90] observed continuously decreasing intensity for these absorption bands (δ_s (CH_3) and ρ_{as} (CH_3) from Si-CH_3) up to 480°C (Figure 4.35). Ichikawa et al. attributed the decrease in the intensities of the absorption bands to reactions (4.4) and (4.5) shown below:

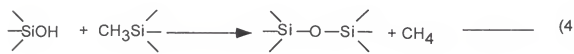

(4.4)

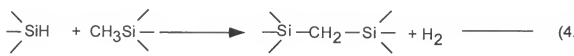

(4.5)

Figure 4.34 also shows that (1) the absorption intensity at ~1020 cm^{-1}, which represents a combination of the absorption intensities of $\omega(CH_2)$ of Si-CH_2-Si and ν(Si-O-Si/ Si-C-O), increased steadily up to 500°C, (2) the absorption intensity at 1358 cm^{-1} (δ (CH_2) of Si-CH_2-Si) remained unchanged all the way to 500°C, and (3) the absorption due to ν(C=O) group observed at 1722 cm^{-1} steadily decreased above ~200°C until it disappeared at ~520°C. All of the results are reasonably consistent with the results in Figure 4.35 from the study by Ichikawa et al.

Figure 4.36 shows a direct comparison of the spectra for oxidized fibers heat treated at 40°C and 600°C. Figure 4.37 shows the spectra obtained by subtracting the 40°C spectrum from the 600°C spectrum. It can be seen that after heat treatment at 600°C, the absorption bands due to oxidation have completely disappeared.

4.1.3.1.4 FTIR spectra of PSZ during heat treatment in N_2

Figure 4.38 shows the FTIR spectra for polyvinylsilazane (PSZ, batch 0831A) at 40°C. The characteristic absorption bands for PSZ are shown in Table 4.7. Figure 4.39 shows the FTIR spectra for PSZ heat-treated to 600°C in nitrogen. The changes in intensities of various groups in PSZ as a function of temperature are shown in Figure 4.40. Figure 4.40 shows that the intensities for all absorption bands of PSZ reached a maximum at 120°C and then started to decrease. Recall from section 3.1.1 that the PSZ was prepared by polymerizing a tri-functional vinylic silazane monomer at 120°C for 18 h in the presence of a radical initiator (dicumyl peroxide). The increase in FTIR peak intensities between 40 and 120°C indicates that there is continued polymerization and cross-linking of the as-prepared PSZ. For example, the largest increase in intensity occurs for the δ (Si-N-Si) absorption at 930 cm^{-1}. An increase in Si-N bonds is consistent with increased polymerization and cross-linking of the PSZ polymer.

As heat treatment of PSZ was continued above 120°C, the absorption intensities decreased rapidly, indicative of the transition from an organosilicon polymer to an inorganic ceramic. After heat treatment at 600°C, the residual absorption peaks were the ν_{as} (CH) of CH_3 at 2950 cm^{-1}, ν_s (CH) of CH_3 at 2894 cm^{-1}, δ_s (CH_3) of Si-CH_3 at 1253 cm^{-1}, 930 cm^{-1} due to δ (Si-N-Si) (broad peak), δ (N-H) at 1180 cm^{-1}, δ_s (CH=CH_2) at 1000 cm^{-1}, and ρ_s(CH_3) of Si-CH_3 at 776 cm^{-1}. The absorption band at 1000 cm^{-1} due to δ_s (CH=CH_2) showed a slight increase in intensity between 360-600°C.

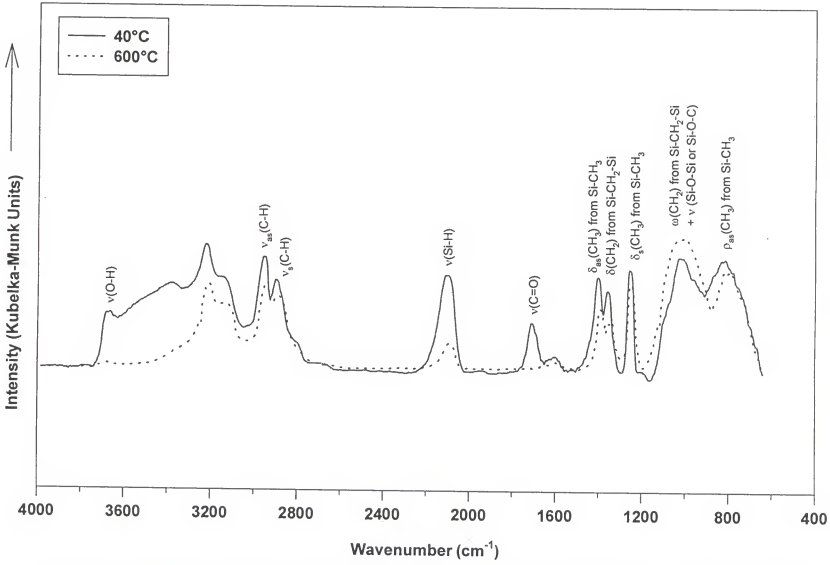

Figure 4.36. Comparison of spectra of air-heat treated (187°C) PCS fibers (batch 65s) before and after heat treatment at 600°C in N_2

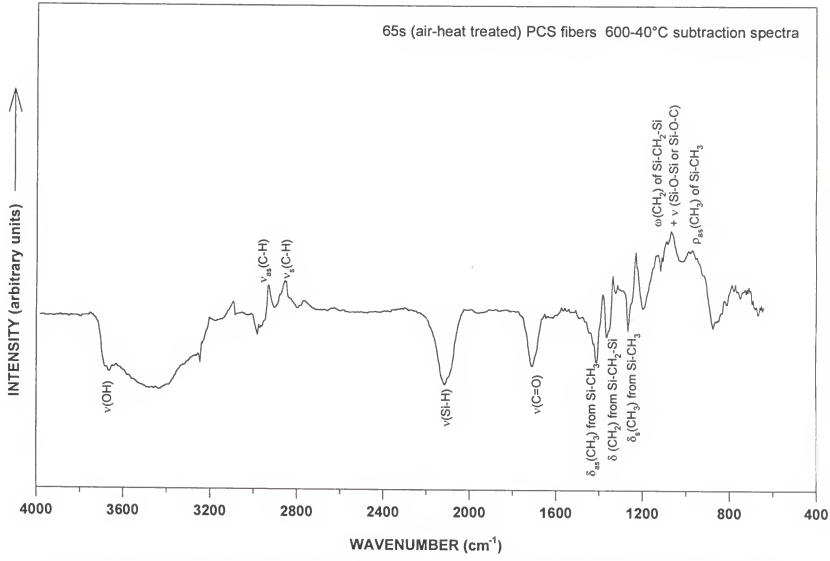

Figure 4.37. Subtraction spectra for air-heat treated (187°C) PCS fibers (batch 65s) heat-treated in N_2; 600-40°C.

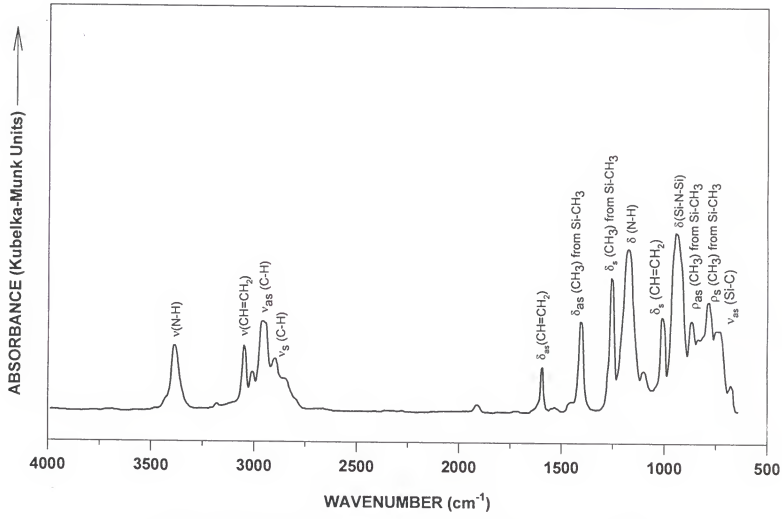

Figure 4.38. Room temperature FTIR spectra for PSZ polymer (batch 0831A).

Table 4.7. FTIR peak assignments for polyvinylsilazane (PSZ) polymer.

Peak (cm^{-1})	Assignment	References
3390	ν (N-H)	5,7
3040	ν ($CH=CH_2$) from $Si-CH=CH_2$	6,7
2950	ν_{as} (C-H)	1,2
2894	ν_s (C-H)	1,2
1592	δ ($CH=CH_2$) from $Si-CH=CH_2$	6
1407	δ_{as} (CH_3) from $Si-CH_3$	2,3
1253	δ_s (CH_3) from $Si-CH_3$	2,3
1180	δ (N-H)	5,7
1000	δ ($CH=CH_2$) from $Si-CH=CH_2$	6,7
930	δ (Si-N-Si)	5
865	ρ_{as} (CH_3) from $Si-CH_3$	1,2
776	ρ_s (CH_3) from Si - CH_3	1,2,3
735	ν_{as} (Si-C)	1,2,3

ν = stretching ; δ = bending ; ρ = rocking

(1) W. Kriner, *J. Org. Chem.*, 29, 1601 (1964).
(2) A.L. Smith, *J. Chem. Phys.*, 21, 1997 (1953).
(3) A.L. Smith, *Spectrochimica Acta*, 16, 87 (1960).
(4) A.L. Smith, *Spectrochimica Acta*, 15, 412 (1959).
(5) D. Seyferth, G.H. Wiseman, and C. Prud'homme, *J. Am.Ceram. Soc.*,1, C13-C14 (1983).
(6) W. Toreki, N.A. Creed, and C.D. Batich, *Polymer Preprints*, Am. Chem. Soc., 31 [2], 611-612 (1990).
(7) R.M. Silverstein, G.C. Bassler, and T.C. Morrill, Spectrometric Identification of Organic Compounds, John Wiley, New York (1981).

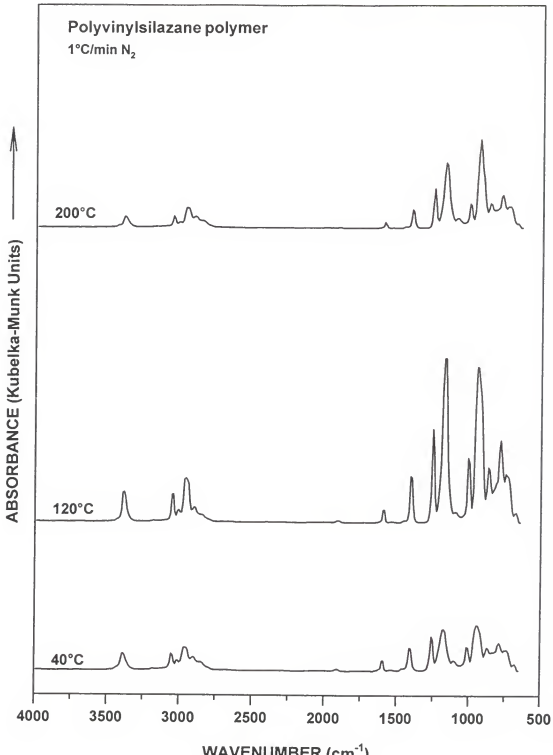

Figure 4.39. FTIR spectra for polyvinylsilazane polymer during heat treatment to 600°C at 1°C/min in nitrogen atmosphere.

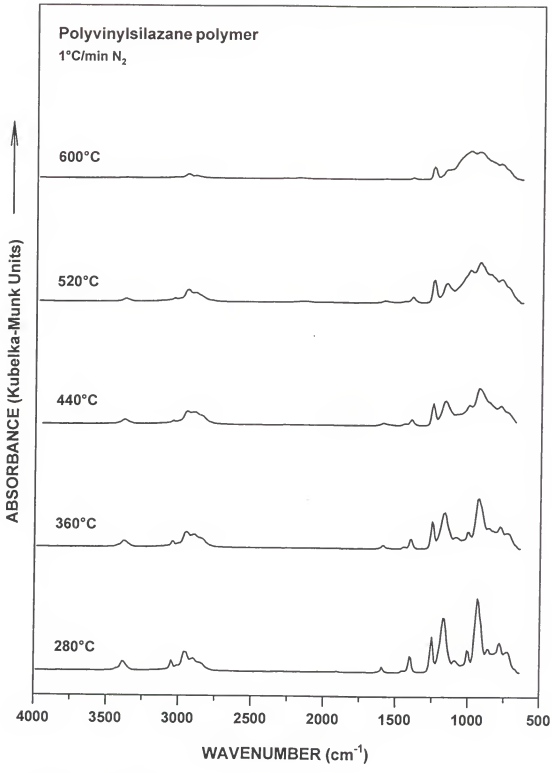

Figure 4.39. (Cont'd.)

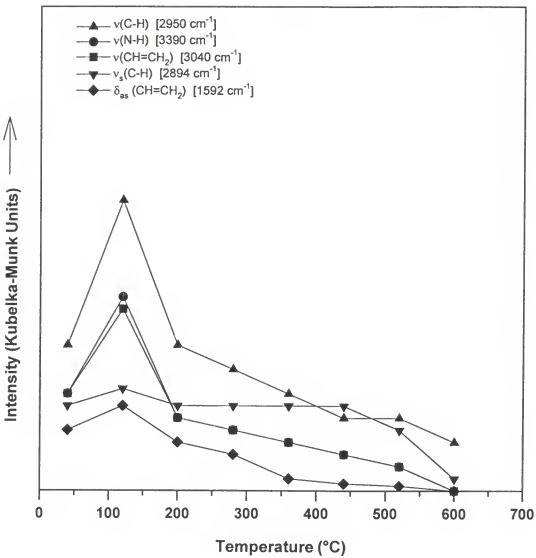

Figure 4.40. Intensity vs. temperature from FTIR spectra of PSZ.

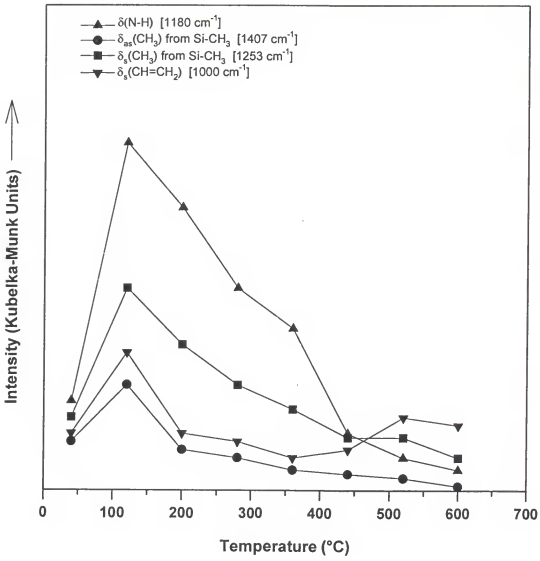

Figure 4.40. (Cont'd.)

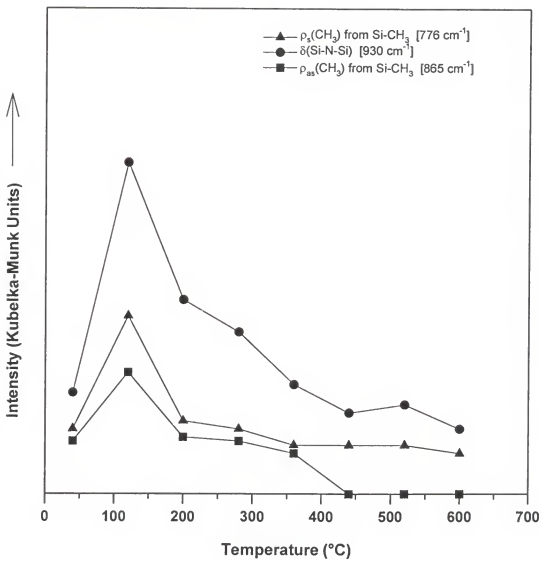

Figure 4.40. (Cont'd.)

4.1.3.1.5 FTIR spectra of PCS+PSZ fibers during heat treatment in N_2

Figure 4.41 shows FTIR spectra of PCS fibers containing 14.5 wt% PSZ (PCS+PSZ) at 40°C. Table 4.8 shows FTIR peak assignments for PCS+PSZ fibers. The spectra shows all the major characteristic absorption bands due to PCS as well as a few major absorption peaks due to PSZ, viz., the absorption peak at 1180 cm^{-1} (due to δ (N-H)), 3040 cm^{-1} (due to ν ($CH=CH_2$) from Si-$CH=CH_2$), 1592 cm^{-1} (due to δ_{as} ($CH=CH_2$) of Si-$CH=CH_2$), 1180 cm^{-1} (due to δ (N-H)), and 930 cm^{-1} (due to δ (Si-N-Si)).

Figure 4.42 shows the FTIR spectra of PCS+PSZ during heat treatment to 600°C in nitrogen. Figure 4.43 shows plots of the intensities of various absorption peaks vs. temperature for PCS+PSZ fibers. The absorption intensity of the Si-H groups increased only slightly up to ~275°C, remained constant until 440°C and then started to decrease. The intensity of the absorption band δ (CH_2) of Si-CH_2-Si decreased slightly beyond 275°C. The absorption intensity at 1020 cm^{-1} (due to ω (CH_2) of Si-CH_2-Si) also decreased at around ~300°C. The intensity of absorption band at 1407 cm^{-1} (due to δ_{as} (CH_3) of Si-CH_3) decreased rapidly starting at 300°C.

Figure 4.44 shows a direct comparison of PCS+PSZ spectra before and after heat treatment in nitrogen at 600°C. Figure 4.45 shows the subtraction spectra for the same. It can be seen that the absorption intensity of δ_{as} (CH_3) of Si-CH_3 at 1407 cm^{-1} decreased significantly after the heat treatment. In addition, the absorption intensities of all bands due to PSZ disappeared after heat treatment at 600°C. This observation is also supported by the subtraction of the spectra for PCS fibers (69s) from the spectra for the PCS+PSZ fibers (70s) at 40°C (Figure 4.46) and 600°C (Figure 4.47). At 40°C, the subtraction spectra clearly shows the presence of absorption bands due to PSZ. After 600°C heat treatment in nitrogen, the absorption bands due to PSZ were absent.

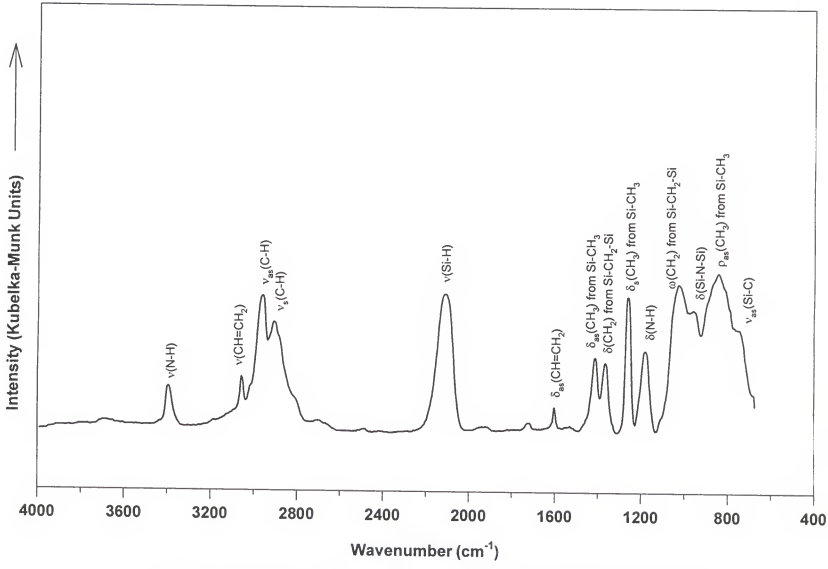

Figure 4.41. Room temperature FTIR spectra of green PCS+PSZ fibers (batch 70s).

Table 4.8. FTIR peak assignments for PCS+PSZ fibers.

Peak (cm^{-1})	Assignment	References
3390	ν (N-H)	1,2
3040	ν ($CH=CH_2$) from Si-$CH=CH_2$	5,6
2950	ν_{as} (C-H)	1,2
2894	ν_s (C-H)	1,2
2098	ν (Si-H)	1,4
1592	δ ($CH=CH_2$) from Si - $CH=CH_2$	6
1407	δ_{as} (CH_3) from Si-CH_3	2,3
1358	δ (CH_2) from Si - CH_2 - Si	1,3
1253	δ_s (CH_3) from Si-CH_3	2,3
1180	δ (N-H)	5,7
1020	ω (CH_2) from Si - CH_2- Si	1,3
930	δ (Si-N-Si)	5
830	ρ_{as} (CH_3) from Si - CH_3	1,2,3
776	ρ_s (CH_3) from Si - CH_3	1,2,3
735	ν_{as} (Si-C)	1,2,3

ν = stretching ; δ = bending ; ω = bending ; ρ = rocking

(1) W. Kriner, *J. Org. Chem.*, 29, 1601 (1964).
(2) A.L. Smith, *J. Chem. Phys.*, 21, 1997 (1953).
(3) A.L. Smith, *Spectrochimica Acta*, 16, 87 (1960).
(4) A.L. Smith, *Spectrochimica Acta*, 15, 412 (1959).
(5) D. Seyferth, G.H. Wiseman, and C. Prud'homme, J. Am.Ceram. Soc., 1, C13-C14 (1983)
(6) W. Toreki, N.A. Creed, and C.D. Batich, Polymer Preprints, Am. Chem. Soc., 31 [2], 611-612 (1990).
(7) R.M. Silverstein, G.C. Bassler, and T.C. Morrill, Spectrometric Identification of Organic Compounds, John Wiley, New York (1981).

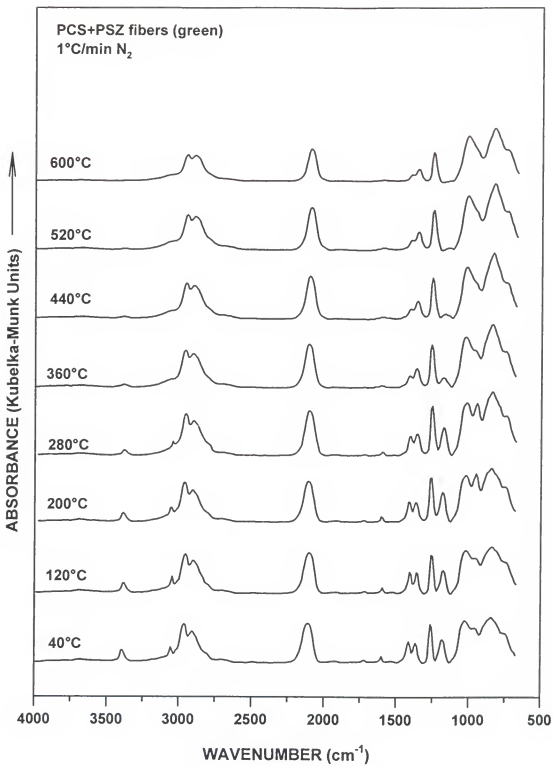

Figure 4.42. FTIR spectra of PCS+PSZ green fibers (batch 70s) during heat treatment to 600°C in nitrogen atmosphere.

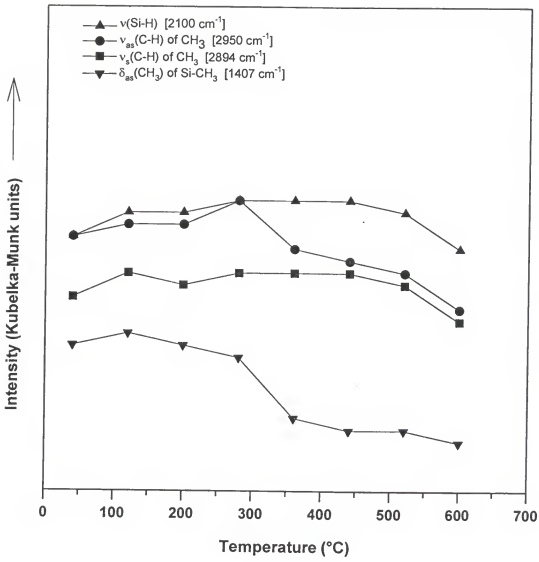

Figure 4.43. Intensity vs. temperature from FTIR spectra of PCS+PSZ fibers (batch 70s).

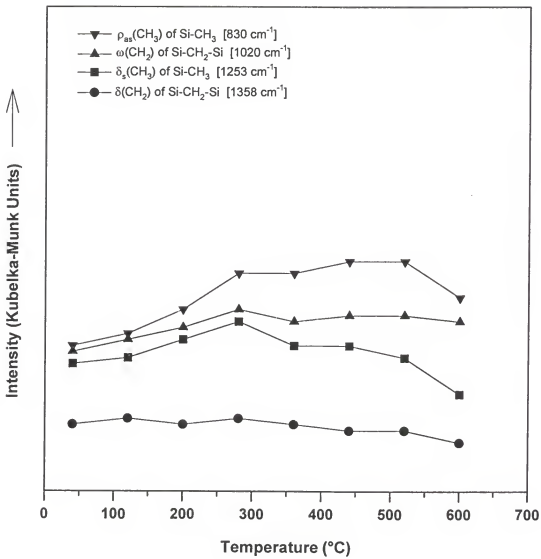

Figure 4.43. (Cont'd.)

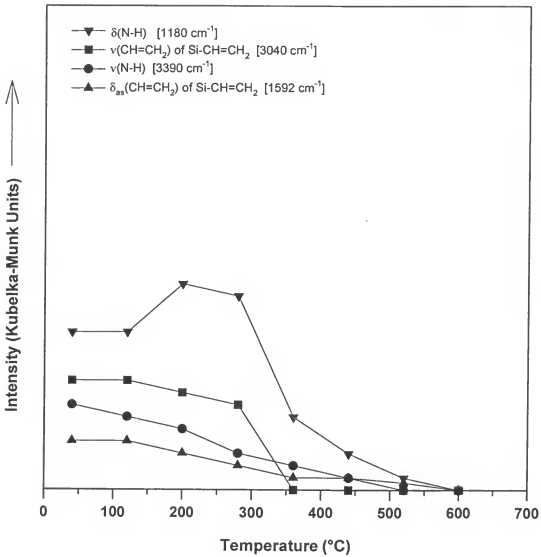

Figure 4.43. (Cont'd.)

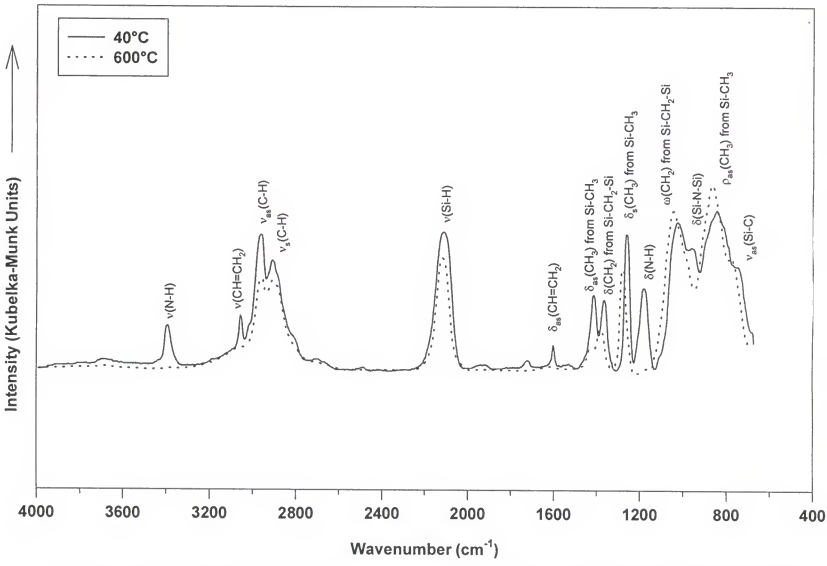

Figure 4.44. Comparison of FTIR spectra of PCS+PSZ fibers (70s) before and after heat-treatment at 600°C in nitrogen.

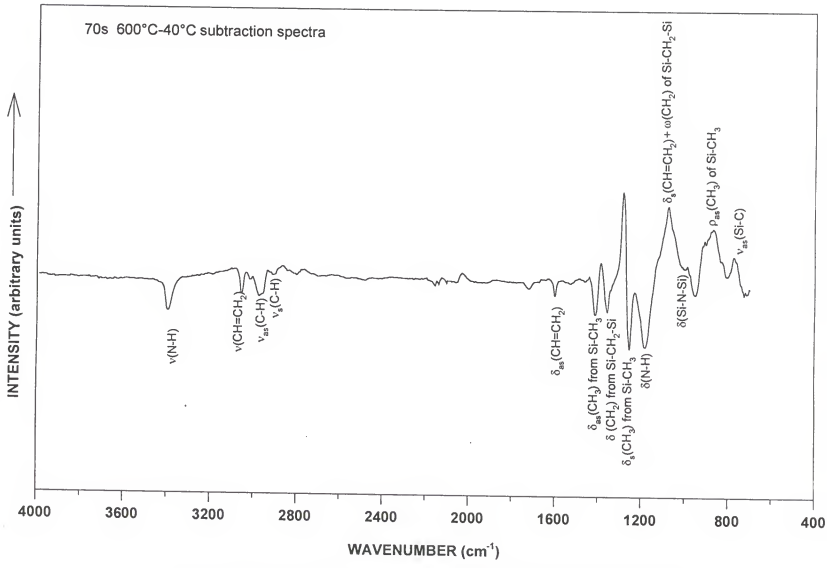

Figure 4.45. Subtraction spectra for PCS+PSZ fibers (batch 70s), 600-40°C

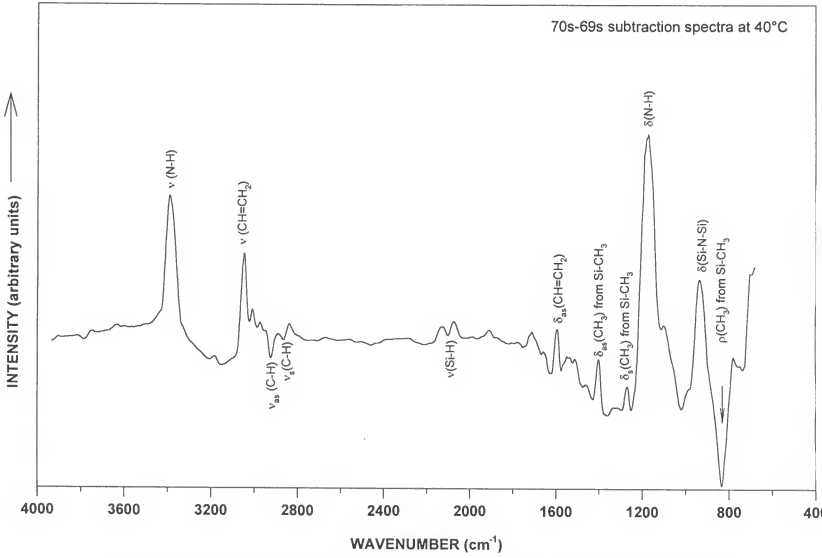

Figure 4.46. Subtraction spectra for PCS+PSZ (batch 70s) and PCS (batch 69s) fibers at 40°C.

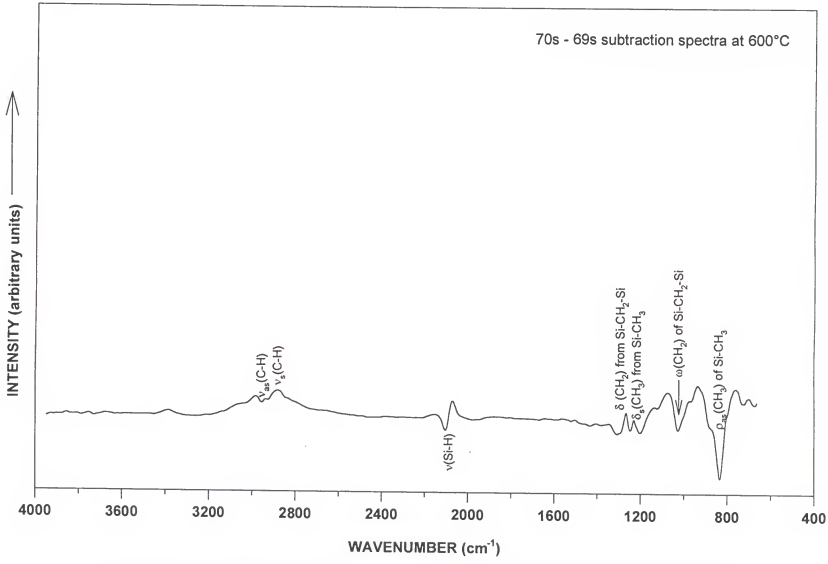

Figure 4.47. Subtraction spectra for PCS+PSZ (batch 70s) and PCS (batch 69s) fibers at 600°C.

The influence of PSZ on cross-linking of PCS can be ascertained by comparing the FTIR spectra (Figures 4.27 and 4.43) and the subtraction spectra for PCS and PCS+PSZ during the heat treatment from 40°C to 600°C in nitrogen (Figures 4.28 and 4.45). In the case of PCS, the absorption intensity for Si-H groups increased significantly until 520°C (presumably due to methylene insertion reactions) and then started to decrease (see Figure 4.27). The subtraction spectra for PCS fibers before and after heat treatment in nitrogen (Figure 4.28) also show the presence of a strong Si-H absorption band after 600°C. This was not the case for PCS+PSZ. The absorption intensity of Si-H groups increased only marginally up to ~275°C, remained constant till 440°C and then started to decrease (Figure 4.43). The absorption intensity at 1358 cm^{-1} (δ (CH_2) from Si-CH_2-Si) decreased very slightly beyond 275°C for PCS+PSZ while it remained essentially constant up to 600°C for PCS. The intensity of absorption peak at 1407 cm^{-1} (due to δ_{as} (CH_3) of Si-CH_3) decreased much more rapidly starting at 300°C for PCS+PSZ compared to PCS. All of these observations suggest that methylene insertion reactions are inhibited in the case of PCS+PSZ, most likely due to the interaction of PSZ with PCS.

Recall that the FTIR spectra for PSZ alone (Figure 4.40) showed a rapid increase in the intensities of all the absorption peaks during heat treatment from 40 to 120°C. This was attributed to continued polymerization/cross-linking of the PSZ during the initial heat treatment. With further heat treatment above 120°C, rapid decreases in peak intensities were observed for all the absorption peaks (Figure 4.40). Significantly different behavior was observed for the absorption peak intensities associated with the PSZ during heat treatment of the PCS+PSZ fibers. First, there were no increases in the absorption intensities between 40 and 120°C (Figure 4.43). Second, the peak intensities

either decreased more gradually (i.e., for ν ($CH=CH_2$) of Si-$CH=CH_2$ (at 3040 cm^{-1}), ν (N-H) (at 3390 cm^{-1}), and δ_{as} ($CH=CH_2$) of Si-$CH=CH_2$ (at 1592 cm^{-1})) or increased slightly (i.e., for δ (N-H) (at 1180 cm^{-1})) between 120 and 280°C. These results suggest that PSZ does not undergo continued polymerization/cross-linking when present in the PCS+PSZ fibers. Possible reasons might include : (I) The PSZ is diluted (i.e., it is only 14.5% of the polymer) in the PCS "matrix" and this limits the physical contact between PSZ molecules. (ii) The PSZ interacts with the PCS polymer. An interaction between PSZ and PCS was also indicated by observations that solutions prepared with PCS became cloudy about 30 minutes after PSZ was added to the solutions[¶].

4.1.3.1.6 FTIR spectra of air-heat treated PCS+PSZ fibers during heat treatment in N_2

Figure 4.48 shows the FTIR spectra of air-heat treated (177°C) PCS+PSZ fibers (batch 70s) at 40°C. Table 4.9 shows peak assignments for the same. The fibers showed a weight gain of 6.5% after heat treatment in air at 177°C/1h. The spectra clearly shows the absorption bands due to oxidation, viz., at 3650 cm^{-1} (free -OH stretching), 3600-3200 cm^{-1} (bonded -OH stretching), and 1720 cm^{-1} (due to C=O stretching), in addition to all the major absorption bands for PCS. However, peaks due to PSZ, which were clearly seen in the spectra of green PCS+PSZ fibers (Figure 4.41) are mostly masked by the oxidation peaks. (For example, the absorption peak at 3375 cm^{-1} due to ν (N-H) is not observed.) The only distinct peaks due to PSZ are the δ_{as} ($CH=CH_2$) at 1592 cm^{-1} and δ (N-H) at 1180 cm^{-1}.

[¶] A 0.1 µm filtered solution of 25 wt% PSZ in toluene was added to a 0.1 µm filtered solution of 33 wt% PCS in toluene. (The amount of PSZ solution added gave a PSZ/PCS weight ratio of 14.5/85.5.) The solution changed from an initially clear appearance to a cloudy state in ~30 min, i.e., indicative of microgel formation. This solution can still be filtered through a 0.1 µm filter, although this occurs more slowly when compared to filtration of similar amounts of PCS or PSZ solution.

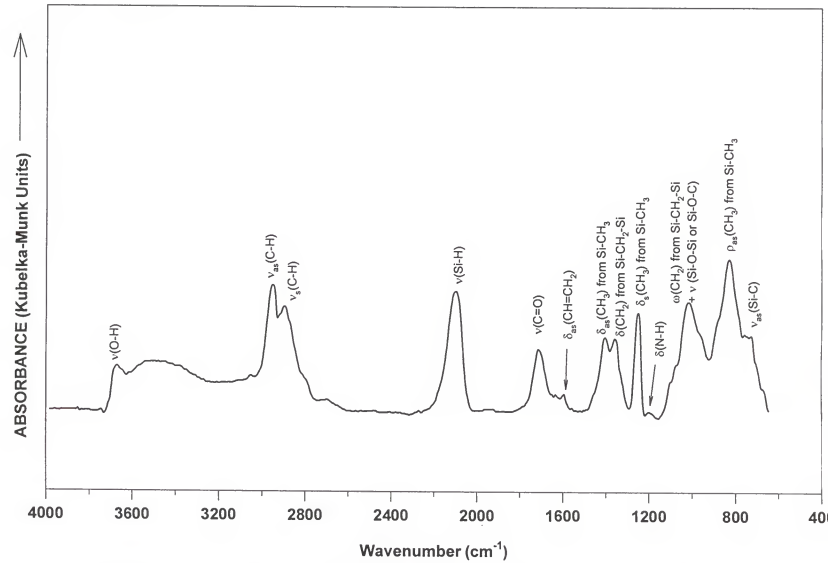

Figure 4.48. Room temperature FTIR spectra of PCS+PSZ fibers (batch 70s) heat-treated in air at 177°C.

Table 4.9. FTIR peak assignments for PCS+PSZ fibers (batch 70s) heat-treated in air at 177°C.

Peak (cm^{-1})	Assignment	References
3650	ν (OH)	1,2
3390	ν (N-H)	1,2
3040	ν ($CH=CH_2$) from Si-$CH=CH_2$	5,6
2950	ν_{as} (C-H)	1,2
2894	ν_s (C-H)	1,2
2098	ν (Si-H)	1,4
1720	ν (C=O)	2,3
1592	δ ($CH=CH_2$) from Si - $CH=CH_2$	6
1407	δ_{as} (CH_3) from Si-CH_3	2,3
1358	δ (CH_2) from Si - CH_2 - Si	1,3
1253	δ_s (CH_3) from Si-CH_3	2,3
1180	δ (N-H)	5,7
960-1100	δ (Si-O-Si or Si-O-C)	1,3
1020	ω (CH_2) from Si - CH_2- Si	1,3
930	δ (Si-N-Si)	5
830	ρ_{as} (CH_3) from Si - CH_3	1,2,3
776	ρ_s (CH_3) from Si - CH_3	1,2,3
735	ν_{as} (Si-C)	1,2,3

ν = stretching ; δ = bending ; ω = bending ; ρ = rocking

(1) W. Kriner, *J. Org. Chem.*, 29, 1601 (1964).
(2) A.L. Smith, *J. Chem. Phys.*, 21, 1997 (1953).
(3) A.L. Smith, *Spectrochimica Acta*, 16, 87 (1960).
(4) A.L. Smith, *Spectrochimica Acta*, 15, 412 (1959).
(5) D. Seyferth, G.H. Wiseman, and C. Prud'homme, J. Am.Ceram. Soc., 1, C13-C14 (1983).
(6) W. Toreki, N.A. Creed, and C.D. Batich, Polymer Preprints, Am. Chem. Soc., 31 [2], 611-612 (1990).
(7) R.M. Silverstein, G.C. Bassler, and T.C. Morrill, Spectrometric Identification of Organic Compounds, John Wiley, New York (1981).

Figure 4.49 shows FTIR spectra of air-heat treated PCS+PSZ fibers during heat treatment to 600°C in nitrogen. Figure 4.50 shows plots of the intensities of various absorption peaks for these fibers. Figure 4.51 shows a direct comparison between spectra of air-heat treated PCS+PSZ fibers before and after heat treatment in nitrogen at 600°C. Figure 4.52 shows the subtraction spectra for the same. It can be seen that intensities of absorption bands due to Si-OH (at 3650 cm^{-1}) and C=O (at 1722 cm^{-1}) gradually decreased starting above 120°C and completely disappeared by 600°C. The ν(Si-H), $\rho_{as}(CH_3)$, and δ_{as} (CH_3) absorption peaks show small decreases in intensity upon heating to 600°C. The decrease in Si-OH and Si-H bonds would be expected to be accompanied by an increase in siloxane bonds (Si-O-Si), i.e., according to equations (4.2) and (4.3). The slight increase in intensity of the absorption band in the range of ~960-1100 cm^{-1} (Figure 4.50) is consistent with the formation of Si-O-Si bonds. The rest of the absorption peaks associated with PCS showed little change during the heat treatment. This could mean that methylene insertion reactions are inhibited during heat treatment, as suggested previously for the case of green PCS+PSZ fibers (with no air heat treatment) undergoing the same heat treatment in nitrogen.

Figures 4.53 and 4.54 show comparison plots of FTIR spectra of air-heat treated PCS+PSZ and PCS fibers at 40°C, and after heat treatment in N_2 at 600°C, respectively. It is evident that Si-H peak intensity decreased considerably for PCS fibers than PCS+PSZ fibers. Also, the intensity of absorption band at 960-1100 cm^{-1}, due to ω (CH_2) from Si-CH_2-Si + ν (Si-O-Si or Si-O-Si) is greater for air-heat treated PCS than PCS+PSZ fibers. Thus, these observations also suggest that methylene insertion reactions are inhibited for air-heat treated PCS+PSZ fibers relative to air-heat treated PCS fibers.

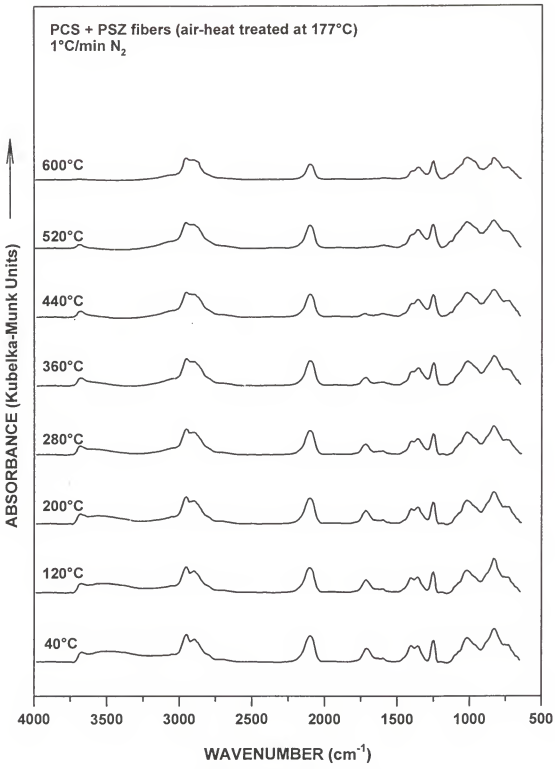

Figure 4.49. FTIR spectra of air-heat treated (177°C) PCS+PSZ fibers (batch 70s) during heat treatment to 600°C in nitrogen.

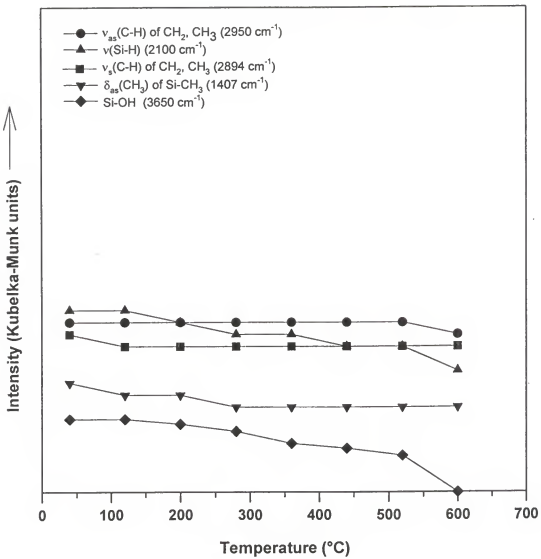

Figure 4.50. Intensity vs. temperature from FTIR spectra of air-heat treated (177°C) PCS+PSZ fibers (batch 70s).

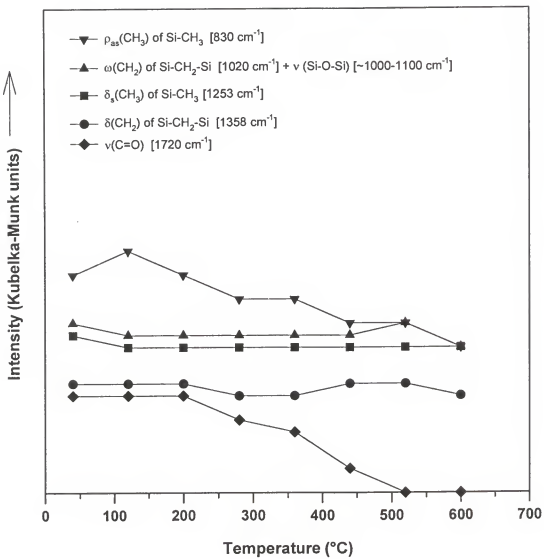

Figure 4.50. (Cont'd.)

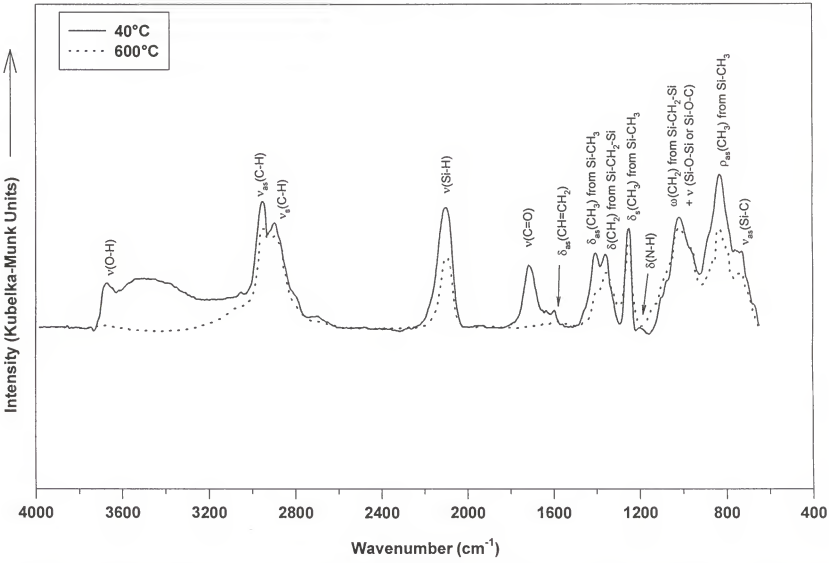

Figure 4.51. Comparison of spectra of air-heat treated PCS+PSZ fibers (batch 70s) (177°C) before and after heat treatment at 600°C in nitrogen.

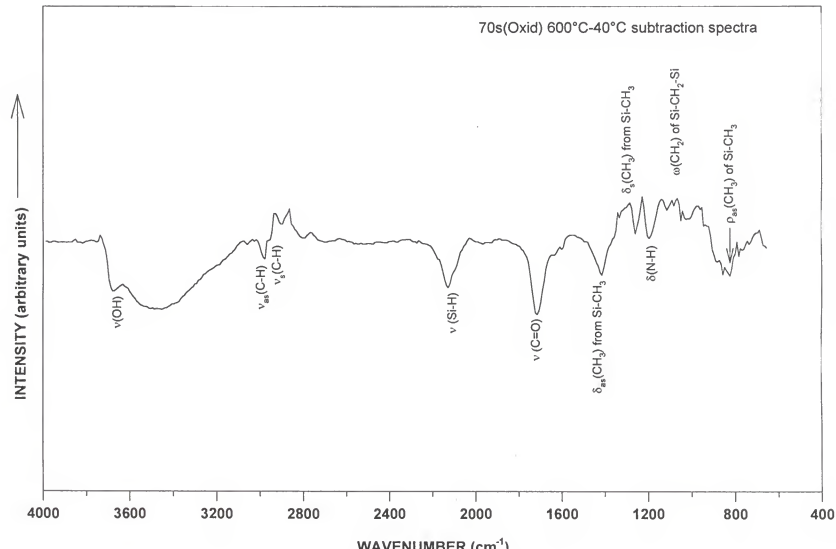

Figure 4.52. Subtraction spectra for air-heat treated (177°C) PCS+PSZ fibers (batch 70s), 600-40°C.

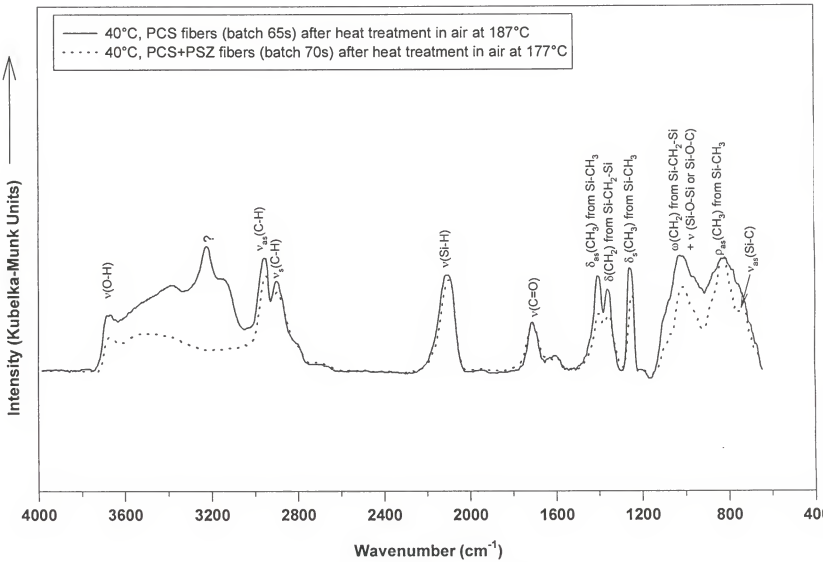

Figure 4.53. Comparison of spectra of air-heat treated PCS fibers (batch 65s) and PCS+PSZ fibers (batch 70s) at 40°C.

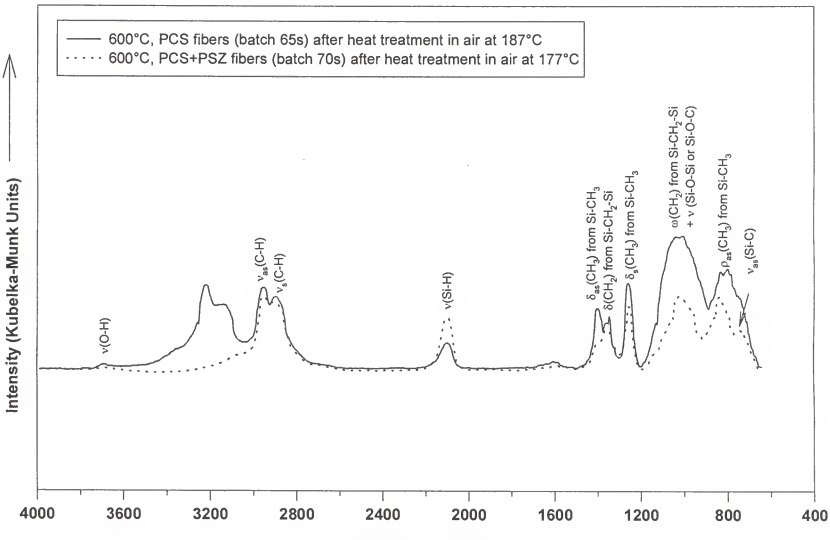

Figure 4.54. Comparison of spectra of air-heat treated PCS fibers (batch 65s) and PCS+PSZ fibers (batch 70s) after heat treatment in N_2.

4.1.3.2 Mechanical properties of fibers

Tensile stress-strain measurements were carried out on green and heat-treated fibers from different PCS and PCS+PSZ spin batches. Fibers were tested as-spun and after various heat treatments (air at 180 ±10°C/1 h and/or nitrogen at 400°C/1 h). Appendix F shows weight gains after heat treatment in air at 180 ±10°C for PCS and PCS+PSZ fibers.

Table 4.10 shows average tensile strengths and rupture strains for different batches of PCS and PCS+PSZ fibers. Figures 4.55 and 4.56 show bar charts of average tensile strengths and average rupture strains for the same. PCS and PCS+PSZ green fibers had similar strengths and rupture strains (~14-22 MPa and 0.6-1%, respectively). However, after heat treatment at 400°C in nitrogen, PCS+PSZ fibers showed much larger increases in tensile strength (~55-61 MPa) and rupture strain (~5.6-6.5%) compared to PCS fibers. Two 400°C - heat treated PCS fiber batches (63s and 64s) showed similar tensile strength and rupture strain as the green fibers, while two other 400°C batches (65s and 69s) showed relatively small increases in tensile strengths (~31 and ~43 MPa, respectively) and rupture strain (~1.45 and ~2.1%, respectively). PCS and PCS+PSZ fibers heat-treated in air at 180 ±10°C showed much higher strengths (~50-51 and ~58 MPa, respectively) and rupture strains (~2.9-3.2% and ~4.3%, respectively) compared to green fibers. PCS and PCS+PSZ fibers heat-treated in air at 180 ±10°C and subsequently heat-treated in nitrogen at 400°C showed even higher tensile strengths (~110 and ~105 MPa, respectively) and rupture strains (~5.0 and ~7.4%, respectively) compared to fibers given just one of the heat treatments.

Other studies [Has80] have also shown that the tensile strength and rupture strain both increase after cured (oxidized) green fibers are heat-treated. Hasegawa et al. reported a rupture strain of ~4.5% and a tensile strength of ~4 kg/mm^2 (~36 MPa) for

Table 4.10. Average tensile strengths and rupture strains for PCS and PCS+PSZ fibers (green, heat treatment in air at 180 ±10°C, heat treatment in nitrogen at 400°C, and heat treatment in air at 180 ±10°C followed by heat treatment in nitrogen at 400°C).

PCS fibers			PCS+PSZ fibers		
Fiber batch	Tensile strength (GPa)	Rupture strain (%)	Fiber batch	Tensile strength (GPa)	Rupture strain (%)
Green					
63s	0.020 ± 0.007	0.87 ± 0.31	67s	0.018 ± 0.008	0.83 ± 0.42
64s-A	0.014 ± 0.008	0.63 ± 0.34	68s	0.016 ± 0.007	0.76 ± 0.37
64s-B	0.022 ± 0.006	1.02 ± 0.38	70s	0.016 ± 0.005	0.63 ± 0.23
(*Average for 64s*)	0.018 ± 0.007	0.83 ± 0.36			
65s	0.018 ± 0.008	0.81 ± 0.37			
69s	0.018 ± 0.007	0.80 ± 0.36			
180°C ±10°C/Air					
65s	0.051 ± 0.009	3.23 ± 1.31	70s	0.058 ± 0.013	4.33 ± 1.27
69s	0.050 ± 0.008	2.92 ± 0.70			
400°C/Nitrogen					
63s	0.019 ± 0.010	0.88 ± 0.52	67s	0.055 ± 0.011	5.64 ± 1.52
64s-A	0.026 ± 0.009	1.25 ± 0.44	68s	0.061 ± 0.008	6.50 ± 1.19
64s-B	0.015 ± 0.006	0.62 ± 0.28	70s	0.058 ± 0.007	5.99 ± 1.19
(*Average for 64s*)	0.021 ± 0.008	0.95 ± 0.36			
65s-A	0.029 ± 0.010	1.35 ± 0.51			
65s-B	0.020 ± 0.006	0.83 ± 0.26			
65s-C	0.044 ± 0.006	2.16 ± 0.32			
(*Average for 65s*)	0.031 ± 0.007	1.45 ± 0.36			
69s	0.043 ± 0.003	2.12 ± 0.20			
180°C ±10°C/Air + 400°C/Nitrogen					
69s	0.11 ± 0.014	5.01 ± 0.97	70s	0.105 ± 0.014	7.38 ± 1.49

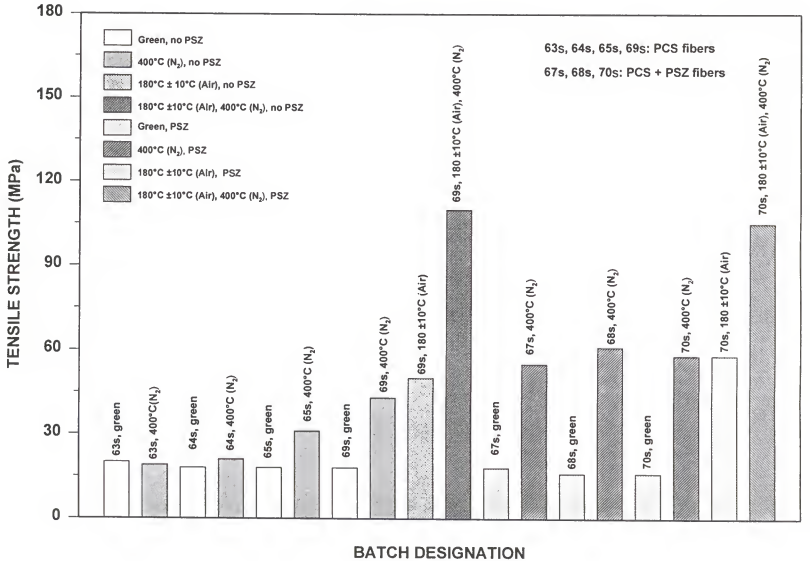

Figure 4.55. Average tensile strengths for PCS, PCS+PSZ fibers, as-spun and after heat treatment in (i)nitrogen at 400°C, (ii) air at 180 ±10°C, and (iii) air at 180 ±10°C, followed by N_2 at 400°C.

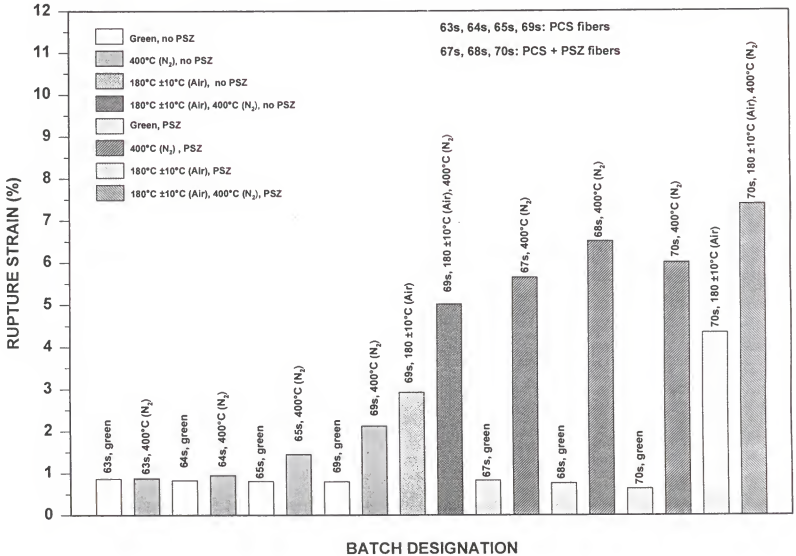

Figure 4.56. Average rupture strains for PCS, PCS+PSZ fibers, as-spun and after heat treatment in (i)nitrogen at 400°C, (ii) air at 180 ±10°C, and (iii) air at 180 ±10°C, followed by N_2 at 400°C.

low- molecular-weight PCS fibers which were first heat-treated in air (at ~200°C) and then heat-treated at 400°C in nitrogen.

The observation of increased tensile strength *and* rupture strain is not generally observed for organic polymeric materials which undergo cross-linking. An increase in tensile strength almost always results in decreased rupture strain. For example, unvulcanized elastomers exhibit low tensile strengths and large strain (~1200%). After vulcanizing (cross-linking) these elastomers with sulfur, the tensile strength increases many times, but a decrease in strain (to ~700-800%) is observed [Bil83]. Mathur et al. [Mat92] measured the tensile strength and rupture strain of polyacrylonitrile (PAN) fibers (a precursor for carbon fibers) upon heat treatment in air (i.e., in order to achieve oxidative cross-linking). Figure 4.57 shows that the rupture strain initially increased, but the tensile strength decreased upon heat treatment to ~220°C.

It is not clear what mechanism(s) are responsible for the simultaneous increases in tensile strength and rupture strain which were observed in this study for the various PCS and PCS+PSZ fibers. The original structure of the PCS consists mostly of relatively low-molecular-weight polymer chains which are cross-linked to a minimal extent. This results in green fibers with relatively low initial tensile strength and rupture strain. It is speculated that the increases in tensile strength upon heat treatment arise primarily from increases in the extent of cross-linking between the polymer chains. It is also speculated that the increases in rupture strain upon heat treatment arise primarily from increases in molecular weight that are associated with linear extension of the individual polymer chains (in contrast to increases in molecular weight arising from branching and cross-linking of the polymer chains).

On this basis, it is suggested that heat treatment in nitrogen alone (to 400°C) leads to only a limited increase in molecular weight, including some branching and

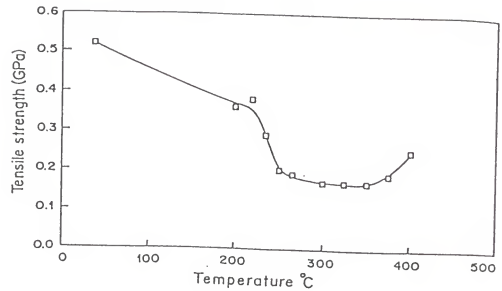

(A)

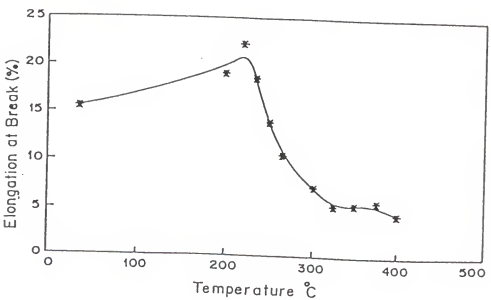

(B)

Figure 4.57. Plots of (a) tensile strength vs. heat treatment temperature (b) % elongation vs. temperature for polyacrylonitrile (PAN) fibers [Mat92].

cross-linking reactions, for the PCS fibers used in this study.[†] (Thus, only relatively small increases in tensile strength and rupture strain were observed.) In contrast, heat treatment in air results in the formation of a significant amount of Si-O-Si, Si-O-C, and Si-C-O bonds (e.g., see the schematic illustration in Figure 4.58) which allows for much more extensive increases in molecular weight through chain extension, as well as much more extensive cross-linking. Hence, larger increases in tensile strength and rupture strain were observed. (The extension of the chains may occur as a result of oxygen incorporation in the Si-C backbone. In regard to cross-linking, the results of this study and prior studies [Has83, Ich90] suggest that Si-H groups are oxidized to form Si-OH which subsequently condense to form the Si-O-Si linkages illustrated in Figure 4.58.)

The significant increase in both tensile strength and rupture strain for the PCS+PSZ fibers heat treated in nitrogen only (to 400°C) indicates that PSZ is also effective in increasing the polymer molecular weight and the extent of cross-linking. The PSZ contains many unsaturated carbon-carbon double bonds[‡] which can presumably react with PCS to form additional Si-C groups in the polymer backbone. (Recall that the FTIR spectra (Figure 4.43 in section 4.1.3.1.5) for PCS+PSZ fibers showed a slight increase in the intensity of the absorption peaks associated with ω ($Si-CH_2-Si$) upon heat treatment in nitrogen.) In addition, it is presumed that the vinyl groups in the PSZ also promote cross-linking by reaction with the PCS side groups.

Tables 4.11 and 4.12 show tensile properties of PCS and PCS+PSZ fibers (both as-spun and air-heat treated at 180 ±10°C) heat-treated to various temperatures in the

---

[†] Hasegawa et al. [Has83] used gel permeation chromatography to confirm that the molecular weight of PCS does increase upon heat treatment in nitrogen to 400°C. (The PCS used by Hasegawa et al. had lower molecular weight than the PCS used in the present study.)

[‡] PSZ contains a number of unreacted vinyl ($CH=CH_2$) groups. This is evidenced by the presence of vinyl absorptions at 3040 cm^{-1}, 1592 cm^{-1}, and 1000 cm^{-1} in the FTIR spectra of the polymer (see section 4.1.3.2.4).

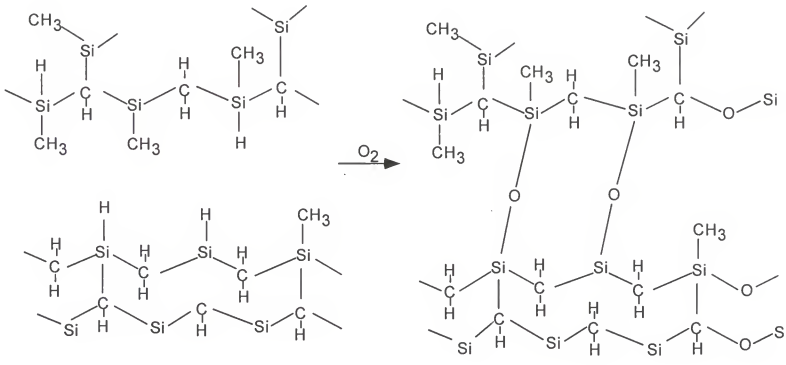

Figure 4.58. Schematic of structural changes taking place in PCS during heat treatment in air at 180 ±10°C [Oka87]

Table 4.11. Tensile properties of as-spun and air-heat treated (187°C) PCS fibers, heat treated to various temperatures between 200-1150°C in nitrogen.

Temperature of heat treatment (°C)	# of fibers tested	Diameter (μm)	Rupture strain (%)	Tensile strength (MPa)
PCS fibers (69s)				
None	17	16.8 ± 0.89	0.80 ± 0.36	18 ± 7
200	22	17.9 ± 0.52	0.81 ± 0.33	19 ± 8
400	19	15.2 ± 0.81	2.12 ± 0.20	43 ± 3
500	23	17.1 ± 1.43	3.23 ± 1.24	75 ± 25
600	24	14.9 ± 0.95	2.75 ± 0.88	174 ± 56
800	20	14.3 ± 1.41	1.43 ± 0.43	1771 ± 544
1000	20	12.6 ± 1.31	1.44 ± 0.38	2554 ± 726
1150	110	12.4 ± 1.16 [a]	1.36 ± 0.42 [a]	2700 ± 800 [a]
PCS fibers heat treated in air at 187°C (65s)				
None	19	17.7 ± 1.17	3.23 ± 1.31	51 ± 9
300	19	18.4 ± 1.15	5.45 ± 1.43	78 ± 11
500	16	17.9 ± 1.03	2.81 ± 0.89	97 ± 27
600	18	17.5 ± 0.80	2.07 ± 0.36	147 ± 28
800	20	14.8 ± 0.82	1.29 ± 0.26	1089 ± 274
1150	18	11.5 ± 0.24	1.37 ± 0.45	2138 ± 667

[a] Average for four separate heat treatments (individual results are provided in Appendix H).

Table 4.12. Tensile properties of as-spun and air-heat treated (177°C) PCS+PSZ fibers heat treated to various temperatures between 200-1150°C in nitrogen.

Temperature of heat treatment (°C)	# of fibers tested	Diameter (μm)	Rupture strain (%)	Tensile strength (MPa)
PCS+PSZ fibers (70s)				
None	23	17.5 ± 1.02	0.63 ± 0.23	16 ± 5
200	22	17.5 ± 1.17	0.57 ± 0.20	15 ± 5
300	20	17.4 ± 0.99	1.43 ± 0.58	29 ± 10
400	21	17.9 ± 2.01	5.99 ± 1.19	58 ± 7
500	21	18.1 ± 1.76	5.63 ± 1.00	77 ± 14
600	24	16.6 ± 1.11	2.19 ± 0.69	288 ± 107
700	23	15.7 ± 1.43	1.81 ± 0.47	900 ± 462
800	22	13.5 ± 0.66	1.60 ± 0.26	2292 ± 335
1000	22	13.1 ± 0.58	1.88 ± 0.28	3466 ± 543
1150	72	12.7 ± 0.98 [b]	1.61 ± 0.47 [b]	3250 ± 970 [b]
PCS+PSZ fibers heat treated in air at 177°C (70s)				
None	26	17.2 ± 1.51	4.33 ± 1.27	58 ± 13
200	25	17.5 ± 1.38	4.75 ± 1.47	63 ± 10
300	23	16.4 ± 1.22	5.57 ± 1.12	76 ± 12
400	22	19.6 ± 1.89	7.38 ± 1.49	105 ± 14
500	22	18.1 ± 0.77	4.40 ± 1.23	117 ± 31
600	23	18.4 ± 3.50	3.39 ± 0.66	184 ± 48
700	22	16.0 ± 0.58	1.62 ± 0.51	621 ± 202
800	20	14.5 ± 0.76	1.76 ± 0.38	1475 ± 368
1000	20	15.0 ± 1.36	1.49 ± 0.38	1656 ± 404
1150	18	13.3 ± 1.11	1.37 ± 0.40	2469 ± 674

[b] Average for four separate heat treatments (Individual results are provided in Appendix H).

range 200-1150°C in nitrogen. (Appendix G shows the weight losses that occur upon pyrolysis of the fibers at 1150°C in nitrogen.) The data for as-spun PCS fibers (as-spun) is shown for the highest strength fiber batch, UF-69s. The data for PCS fibers which were initially heat-treated in air is shown for batch UF-65s. (The selection of a particular batch for air-heat treatment and/or heat treatment in nitrogen was, to some extent, determined by the amount of fibers available.) Figures 4.59a and 4.59b show a comparison of average rupture strains as a function of temperature for PCS and PCS+PSZ fibers heat-treated in nitrogen. In both cases, the average rupture strains reached maximum values after heat treatments in range of ~400-600°C, and then decreased rapidly after heat treatments at higher temperatures. The decrease in rupture strain is due to the transition from an organosilicon polymer to an inorganic SiC-based ceramic (i.e., the branched polymer chains lose methyl groups and hydrogen from the Si-C backbone and form an amorphous Si-C network). Such a rapid decrease in rupture strains beyond 400°C was also reported by Hasegawa et al. [Has80] for low-molecular-weight Nicalon-type fibers, where rupture strains decreased from 3.5% at 400°C to 1.25% at 800°C. Figures 4.60a and 4.60b show a comparison of average rupture strains as a function of heat treatment temperature (in nitrogen) for PCS and PCS+PSZ fibers which were initially heat-treated in air at ~180°C. The trends were similar to the fibers heat-treated only in nitrogen, except that the maximum rupture strains were higher and were reached at lower temperatures for the air-heat treated fibers.

Figures 4.61a and 4.61b show plots of average tensile strength vs. the heat treatment temperature (in nitrogen) for the PCS fibers (batch 69s) and PCS+PSZ fibers (batch 70s). These plots show the same data as in Tables 4.11 and 4.12. It was noted earlier that: (i) The addition of PSZ had essentially no effect on the green strength. (ii) Batches with PSZ showed somewhat greater increases in strength during heat

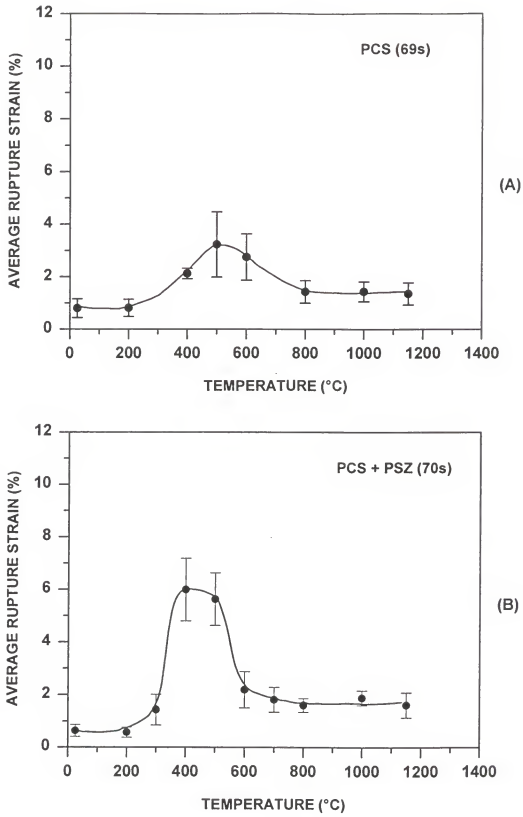

Figure 4.59. Average rupture strain vs. temperature for: (A) PCS fibers (batch 69s), and (B) PCS+PSZ fibers (batch 70s).

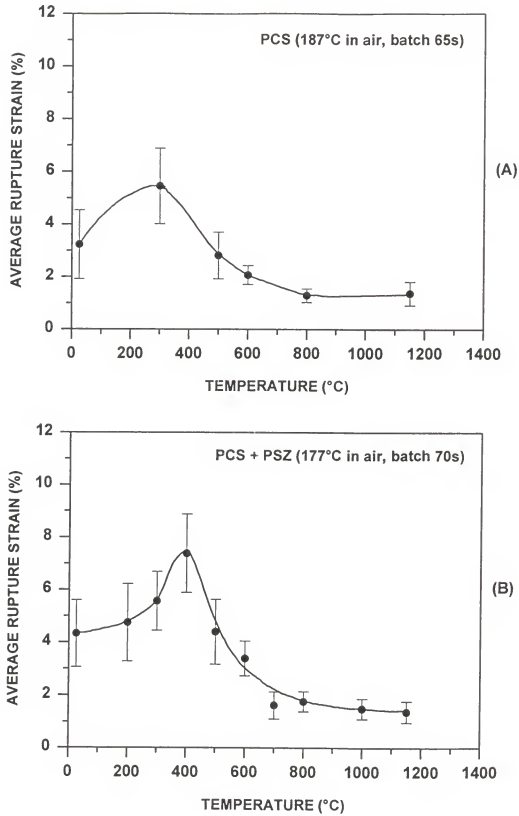

Figure 4.60. Average rupture strain vs. temperature for fibers heat-treated in air: (A) PCS (batch 65s/ 187°C air heat treatment), and (B) PCS+PSZ (batch 70s/ 177°C air heat treatment).

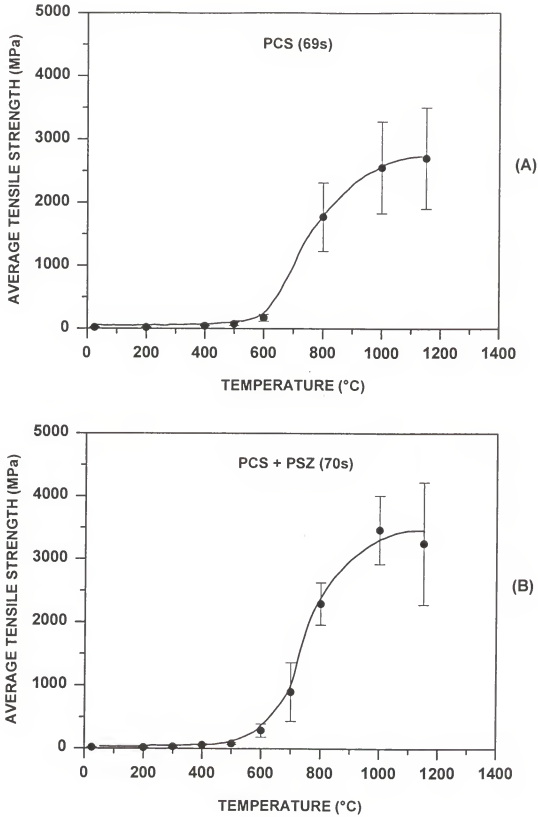

Figure 4.61. Average tensile strength vs. temperature for: (A) PCS fibers (batch 69s), and (B) PCS+PSZ fibers (batch 70s).

treatment at 400°C. (In this case, batch 69s had the highest strength for the batches prepared without PSZ and its strengths were close to that observed for the PCS+PSZ batch 70s.) This was attributed to a tendency for a greater degree of cross-linking during heat treatment in fibers which contain PSZ. The additional data in Tables 4.11 and 4.12 also show that: (i) There are no increases in strength upon heat treatment to 200°C for fibers prepared with and without PSZ. (ii) The differences in strength for the PCS and PCS+PSZ fibers remain relatively small for heat treatments up to at least 500°C.

The strength increases significantly as the organosilicon polymer fibers are heat-treated at temperatures above 600°C and become converted to ceramic-based fibers. The PCS+PSZ fibers develop higher strengths than the PCS fibers at these temperatures. The higher strengths are believed to be associated with the improved spinning behavior which, in turn, results in fiber bundles with fewer (and possibly smaller) defects. As shown in section 4.1.1, fibers spun without PSZ have more breaks during spinning and, therefore, more re-starts in the spinning are required. The breaks during spinning result in fibers with more variable diameters, including some fibers with significantly larger diameters. Larger fiber diameters normally result in lower tensile strength [Wyn87; Tor92A; Yaj78B]. (When there is a break in the spin line, part of the broken fiber may be incorporated in the bundle on the take-up wheel. Since this fiber was not under tension after the break, the fiber would be expected to develop a large diameter. Similarly, the fibers initially formed during the re-starting of the broken spin line will be under lesser tension and would be expected to have large diameter also.) In addition, broken fibers disrupt the uniformity of the fiber bundles when they are incorporated. This may result in the development of local breaks, snags, kinks, or other defects in the bundles.

Tables 4.13 and 4.14 show the average tensile strengths and diameters for various batches of PCS and PCS+PSZ fibers, respectively, which were pyrolyzed at 1150°C in nitrogen. (The tensile strength data for individual fiber batches are shown in Appendix H.) Histogram plots of the tensile strength and diameter distributions for the combined batches of the PCS and PCS+PSZ fibers are shown in Figures 4.62 and 4.63, respectively. As expected from the data shown for batches 69s and 70s (Table 4.11, Figure 4.61a and Table 4.12, Figure 4.61b, respectively), the tensile strengths are higher for batches prepared with PSZ. (As noted above, this is attributed to improved spinning behavior which in turn, should result in fewer large defects in the bundles.) Figure 4.61 shows that the average diameters for the two types of fibers were almost the same. The distribution is somewhat broader for the PCS fibers. This might be due to the increased frequency of breaks during spinning of the PCS fibers.

Figures 4.64a and 4.64b show plots of average tensile strength vs. temperature of heat treatment (in nitrogen) for the PCS fibers (batch 65s) and PCS+PSZ fibers (batch 70s) which were oxidized in air (180 ±10°C) prior to the heat treatments. These plots show the same data as in Tables 4.11 and 4.12. As noted earlier, fibers given the initial air-heat treatment have higher strengths in the green state and after heat treatment in nitrogen at 400°C compared to the corresponding fibers without the initial air heat treatment. Table 4.11 and 4.12 also show that this trend is observed after heat treatments in nitrogen at other temperatures up to 500°C. The PSZ has relatively little effect on the tensile strengths of the air-heat treated fibers during the early stages of heat treatment in nitrogen. Although Tables 4.11 and 4.12 show that the strengths of the PCS+PSZ fibers are slightly higher than the PCS fibers up through the 500°C heat treatments, the differences are within experimental error of the measurements. Hence, the strengths that develop as a result of these relatively low temperature heat

Table 4.13. Properties of SiC fibers spun from PCS[1].

Fiber batch	# of fibers tested	Diameter (μm)	Tensile strength (GPa)
63s	35	11.81 ± 1.32	2.26 ± 0.56
64s	87	9.45 ± 0.66	2.38 ± 1.02
65s	92	11.89 ±1.19	2.08 ± 0.82
69s	110	12.44 ± 1.16	2.70 ± 0.80

Table 4.14. Properties of SiC fibers spun from PCS + PSZ[1].

Fiber batch	# of fibers tested	Diameter (μm)	Tensile strength (GPa)
67s	121	10.62 ± 0.70	2.81 ± 0.80
68s	90	12.49 ± 0.84	2.97 ± 0.63
69s	72	12.74 ±0.98	3.25 ± 0.97

[1] Pyrolysis conditions: 1150°C, nitrogen atmosphere

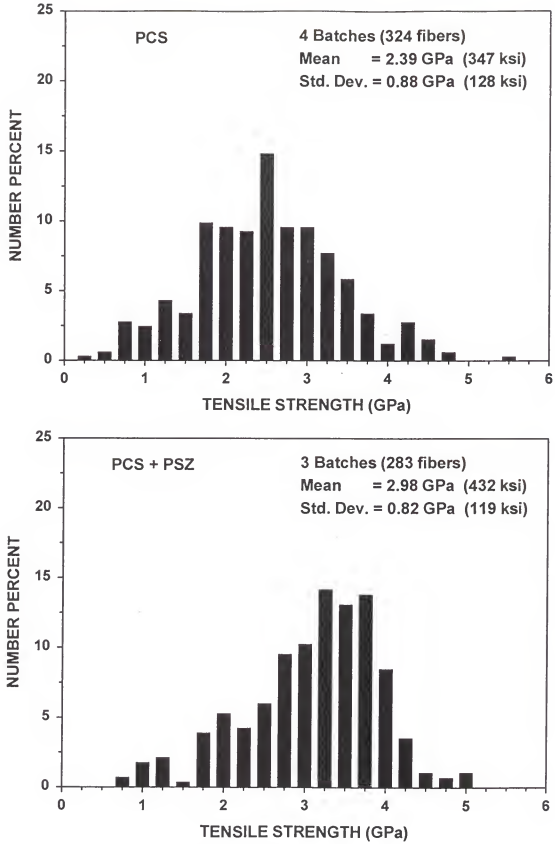

Figure 4.62. Distribution of tensile strengths of fibers after pyrolysis at 1150°C in nitrogen: (A) PCS (B) PCS+PSZ.

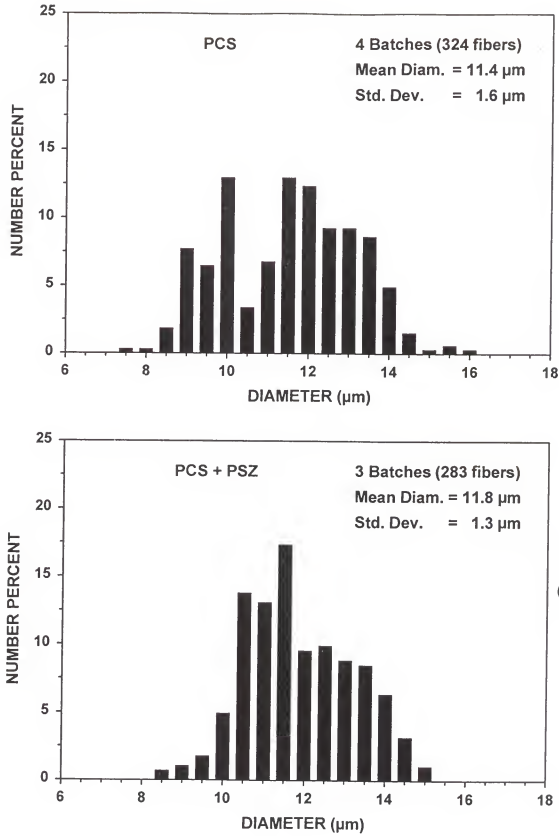

Figure 4.63. Distribution of diameters for fibers after pyrolysis at 1150°C in nitrogen: (A) PCS (B) PCS+PSZ.

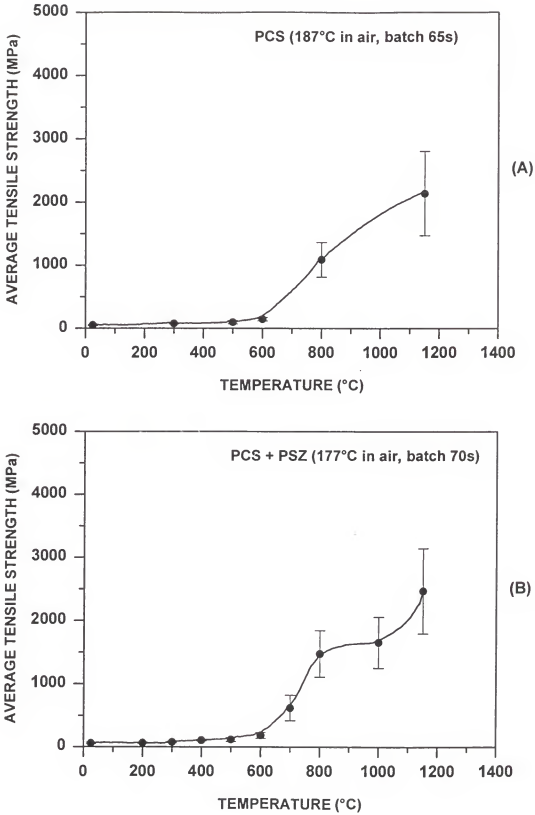

Figure 4.64. Average tensile strength vs. temperature for fibers heat-treated in air: (A) PCS (batch 65s/ 187°C air heat treatment, and (B) PCS+PSZ (batch 70s/ 177°C air heat treatment).

treatments in nitrogen appear to be controlled largely by the effects of the initial oxidative cross-linking.

With further heat treatment (≥ 600°C) in nitrogen, the air-heat treated PCS+PSZ fibers have somewhat higher strengths than the air-heat treated PCS fibers. As in the case of the corresponding fibers which were not given the initial air-heat treatment, this difference is attributed to the improved spinning behavior which results in fewer large defects in the pyrolyzed bundles. It is also noted that the air-heat treated fibers (both PCS and PCS+PSZ) have lower strengths than the corresponding fibers without the air heat treatment for samples pyrolyzed in nitrogen in the range of 600-1150°C. The reason for this behavior is not clear, but may reflect differences in phase composition. (The 1150°C-pyrolyzed fibers prepared without air heat treatment consist mostly of very weakly crystalline β-SiC and amorphous carbon. The corresponding air-heat treated fibers contain these phases, but also contains an amorphous silica-like and/or silicon oxycarbide material.)

4.2 Synthesis and Characterization of Polymethylsilane (PMS) Polymers

The requirements for preparing SiC fibers from PMS polymers are described in detail in section 4.3. At this point, it is simply noted that it would be desirable to have PMS polymers which are solid at room temperature, soluble in appropriate solvents for dry spinning, and infusible upon heat treatment to pyrolyze the polymer to SiC. Wurtz-coupling polymerization usually leads to low molecular weight polymers which are liquids [Sey92; Qiu89A]. Therefore, it is desirable to increase the molecular weight and/or degree of cross-linking of the polymers by modifying the synthesis conditions. The degree of cross-linking is enhanced by using a mixture of monomers of different functionalities [Qiu89A, Bil83]. For example, when a trifunctional monomer is added to a difunctional monomer in Wurtz-coupling polymerization, the resulting polymer becomes cross-linked due to the introduction of additional branching sites. This is illustrated schematically for Wurtz polymerization of methyldichlorosilane (MDCS, functionality=2) and methyltrichlorosilane (MTCS, functionality =3) with sodium in Figure 4.65. In the present study, PMS synthesis was carried out by using Wurtz polymerization in sodium using MDCS and MTCS in 70:30 wt% proportion. (The selection of this ratio was based on observations that mixtures prepared with higher MTCS contents show lower reaction rates and/or lower reaction yields [Qiu89A; Sal93].) Polymers were also synthesized using MDCS monomer alone for comparison.

The polymer yields in the Wurtz-coupling polymerization of MDCS and MDCS:MTCS (e.g., 70:30 wt%) with Na are typically low. There may be several reasons for the observed low yields: (1) There may be insoluble polymer product formed during polymerization. Wood [Woo84] has reported the formation of up to 15% of insoluble polymer product in the polymerization of MDCS with Na in hexane:THF (7:1 by volume). (2) Some soluble polymer could be trapped in the precipitating Na/NaCl colloids during

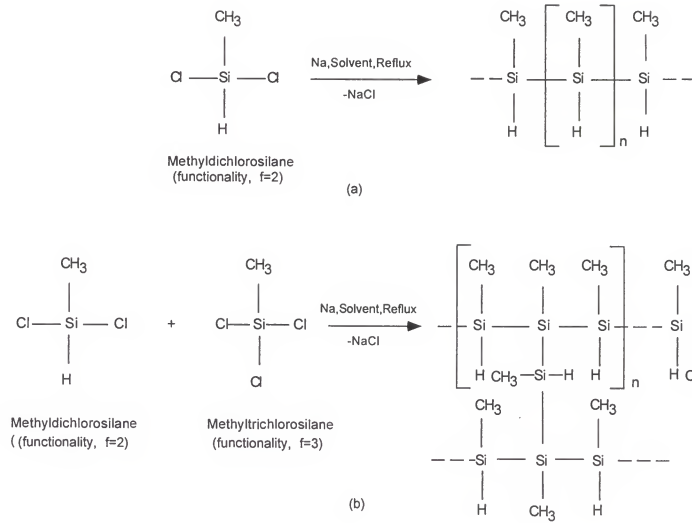

Figure 4.65. Schematic for Wurtz polymerization of (a) methyldichlorosilane and (b) methyldichlorosilane/methyltrichlorosilane mixture

polymerization. (3) If the rate of polymerization is slow (as in the case of polymerization of MDCS:MTCS with Na in toluene), some monomers could be lost due to evaporation. (It may be recalled that MDCS and MTCS have relatively low boiling points, 40 and 68°C, respectively.) (4) MDCS is known to undergo disproportionation under vigorous reaction conditions employed in Wurtz polymerization [Att72]. This could result in the loss of some monomer as volatile Si-containing products. Wood [Woo84] has shown by ^1H NMR of evolved gases during polymerization that MDCS disproportionated into methylsilane (CH_3SiH_3) and methylchlorosilane (CH_3SiH_2Cl) gases.

It was shown in section 2.2.1.4 that the type of solvent used in the Wurtz-coupling polymerization of dichlorosilanes with sodium had an effect on the polymer yield [Mil91; Mil93]. Polar solvents are sometimes added in Wurtz-coupling polymerization to increase the polymer yield. Based on prior investigations [Qiu89A; Mil93; Gau89; Gau90], THF and 1,4-dioxane were selected as the polar solvent additives for this study. Wurtz coupling polymerizations were carried out using solvent mixtures of 95:5 vol% toluene:THF and 50:50 vol% toluene:1,4-dioxane. (THF has a low boiling point (66°C) and use of THF in amounts > 5 vol% would cause the reflux temperature of the solvent mixture to be less than the melting point of Na (97.8°C) and would lead to incomplete melting of Na. Dioxane, on the other hand, has a relatively high boiling point (101.2°C) and would not cause such problems if used in higher amounts.)

Table 4.15 shows the synthesis conditions and characteristics of various polymers prepared. (Detailed synthesis characteristics for individual polymers are shown in Appendices L and M.) Six different monomer/solvent combinations were studied: (1) MDCS, toluene (batch A) (2) MDCS, toluene-THF mixture (95:5 % by volume) (batch B) (3) MDCS, toluene-1,4-Dioxane (50:50 % by volume) (batch C) (4) MDCS:MTCS

Table 4.15. Synthesis conditions and characteristics for PMS polymers[†].

Batch designation	Monomer(s)	Solvent(s)	Reaction conditions[§]	Polymer yield (%)	M_n	M_w	PDI	Ceramic yield (%)
A	MDCS	Toluene	40 h, Reflux	41 [a]	639 [a]	812 [a]	1.27	40.1
B	MDCS	Toluene:THF (95:5 vol%)	40 h, Reflux	48	760	1156	1.52	45.0
C	MDCS	Toluene:1,4-Dioxane (50:50 vol%)	14 h, Reflux	41 [b] ± 2.5	1397 [b] ± 62	2842 [b] ± 232	2.03 [b] ± 0.1	49.7 [b] ± 4.6
D	MDCS:MTCS (70:30 wt%))	Toluene	40 h, Reflux	15 [a]	813 [a]	1142 [a]	1.43	55.0
E	MDCS:MTCS (70:30 wt%))	Toluene:THF (95:5 vol%)	40 h, Reflux	36.8 [c] ± 3.9	906 [b] ± 42	1655 [b] ± 81	1.83 [b] ± 0.04	52.2 [b] ± 1.0
F	MDCS:MTCS (70:30 wt%))	Toluene:1,4-Dioxane (50:50 vol%)	14 h, Reflux	46.2 [d] ± 4.0	1087 [d] ± 183	2228 [d] ± 461	2.06 [d] ± 0.26	51.5 [b] ± 0.53

[a] Average for 2 batches
[b] Average for 3 batches
[c] Average for 15 batches
[d] Average for 15 batches
[†] Individual results are shown in Appendices L and M
[§] Oil bath temperature was maintained at 110°C for all syntheses reactions

mixture (70:30 % by weight), toluene (batch D) (5) MDCS:MTCS mixture (70:30 % by weight), toluene-THF (95:5 % by volume) (batch E) (6) MDCS:MTCS mixture (70:30 % by weight), toluene-1,4-Dioxane (50:50 % by volume) (batch F). Batches A,B,D, and E required 40 h for completion of reaction whereas batches C and F required 14 h for completion. (Reactions were considered essentially complete when the solutions were no longer acidic, i.e., according to the method described in section 3.2.2.) It has been reported that [Zei86; Wes86] that prolonged refluxing of the reaction mixture beyond completion of reaction leads to degradation of polymer molecular weight. Hence, batches C and F were not refluxed for 40 h for direct comparison with batches A,B,D, and E.

4.2.1 Effect of synthesis conditions on molecular weight

Figures 4.66a and 4.66b show representative GPC molecular weight distributions of the six classes of polymers prepared. It can be seen that all the molecular weight distributions are skewed towards low molecular weight end, indicating the presence of a significant amount of low molecular weight fractions. Figures 4.67 and 4.68 show bar plots of number-average and weight-average molecular weights for the same polymers. These figures show that the polymer molecular weights increased when THF and dioxane were used as cosolvents.

This observation can be explained by mechanisms based on the "poor solvent vs. good solvent" concept in Zeigler's model [Zei86]. Prior to a discussion of these mechanisms, it will be helpful to illustrate that a toluene-1,4-dioxane mixture is a poorer solvent for PMS polymers compared to toluene alone. This was accomplished by intrinsic viscosity measurements. In a poor solvent, the polymer chains are tightly coiled. This results in polymer chains with smaller radii and, hence, the polymer solution has lower intrinsic viscosity. In a good solvent, polymer chains assume an expanded

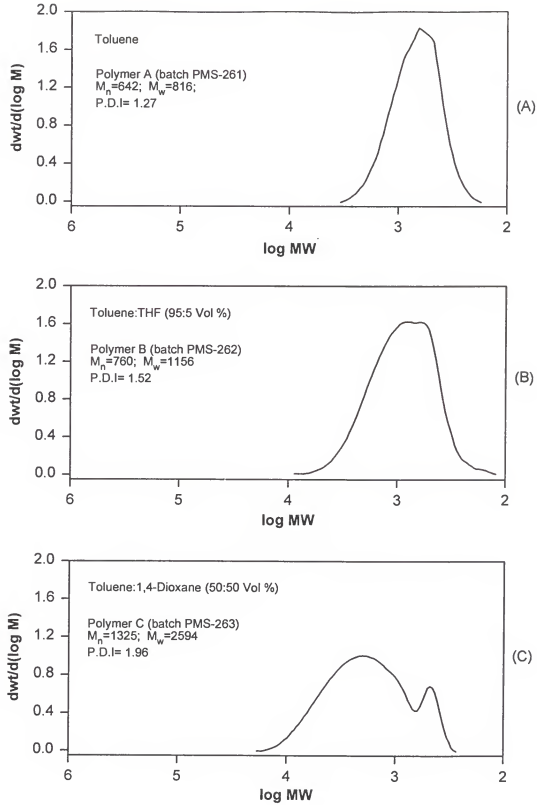

Figure 4.66. (a) Gel permeation chromatograms for polymers prepared from MDCS. (A)Toluene, (B) Toluene,THF(95:5 vol%), (C) Toluene, Dioxane (50:50 vol%).

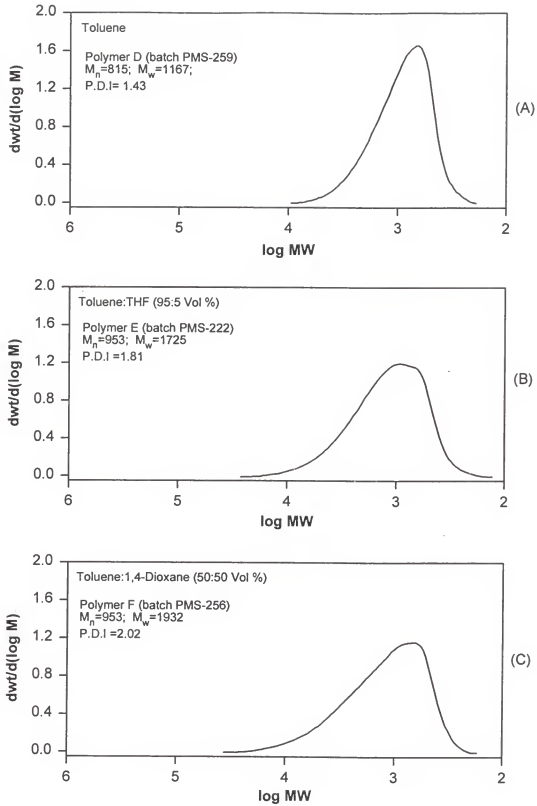

Figure 4.66. (b) Gel permeation chromatograms for polymers prepared from MDCS and MTCS(70:30 wt%). (A) Toluene (B) Toluene:THF (95:5 vol%) (C) Toluene:1,4-Dioxane(50:50 vol%).

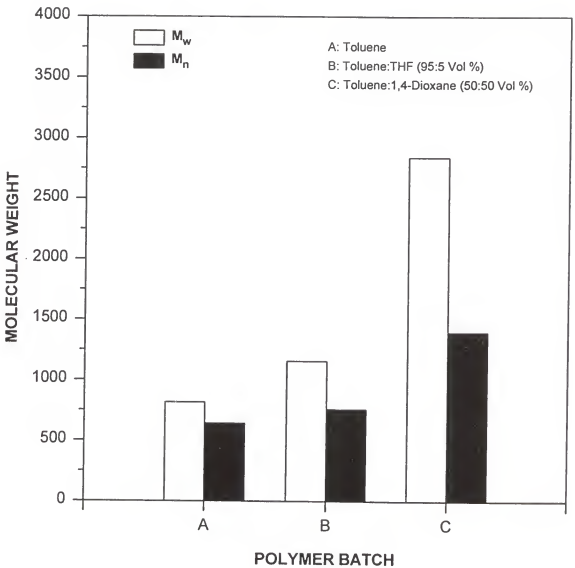

Figure 4.67. Effect of cosolvents on molecular weight of PMS polymers A,B, and C (prepared using 100% MDCS).

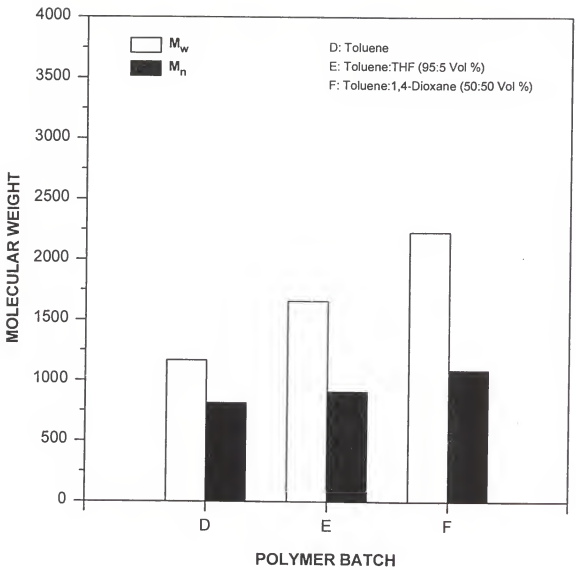

Figure 4.68. Effect of cosolvents on molecular weight of PMS polymers D,E, and F (prepared using MDCS/MTCS (70/30 wt%)).

configuration, and hence, the hydrodynamic radii are larger and the intrinsic viscosity of the polymer solution is higher. Figures 4.69 and 4.70 show that the intrinsic viscosity of PMS polymer in pure toluene (2.52 ml/g) is higher than in toluene-1,4-dioxane mixture (2.10 ml/g). In a separate experiment, it was observed that nearly pure dioxane (i.e., 10 ml of dioxane and 0.20 ml of toluene) acts as a nonsolvent for the polymer. (A cloudy yellow precipitate formed when 10 ml of dioxane was added to 0.5 g of concentrated polymer solution (70 wt% in toluene).)

Consider the Wurtz-coupling polymerization of MDCS in toluene (schematically illustrated in Figure 4.71a). Toluene is a good solvent for the PMS polymer, so the polymer molecules tend to remain in the solvent (i.e., as opposed to adsorbing on the Na particles). This allows the remaining monomer molecules to diffuse toward Na particles unimpeded, thereby resulting in the creation of new polymer chains. This limits the chain extension that can take place by collision of monomer molecules with the chain-ends. Hence, the polymer product after complete reaction has a low molecular weight (Table 4.15). Now consider the polymerization of MDCS in a mixture of toluene/dioxane (50:50 % by volume) (schematically illustrated in Figure 4.71b). As indicated by intrinsic viscosity measurements (Figures 4.69 and 4.70), the toluene/1,4-dioxane mixture is a poorer solvent for PMS (compared to toluene alone). Hence, it might be expected that more polymer chains are adsorbed on the Na particle surfaces. The monomer molecules would be forced to diffuse through polymer chains to access Na surface. Hence, it is more likely that extension of existing polymer chains will occur and that less chains will be formed. Thus, polymerization of MDCS in the toluene/dioxane mixture leads to higher molecular weight (Table 4.15). A similar trend was observed for polymerization of MDCS:MTCS monomers (70:30 wt%) in toluene and toluene/dioxane solvent mixture.

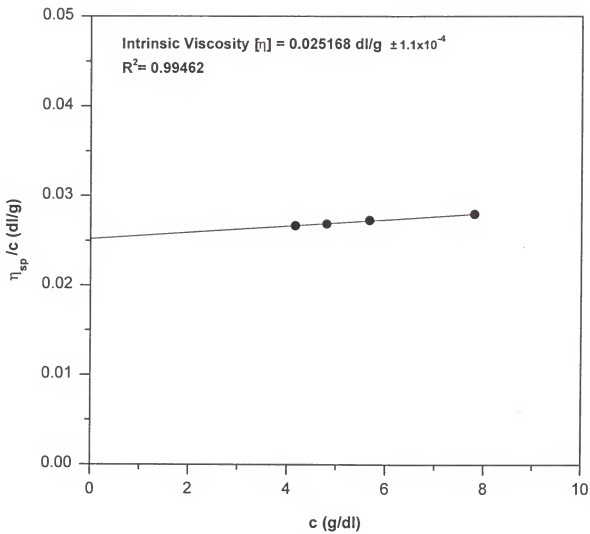

Figure 4.69. Plot of η_{sp}/c vs. c for polymer F (batch PMS-256) (MDCS/MTCS (70/30 wt%); toluene/1,4-dioxane (50/50)) in toluene.

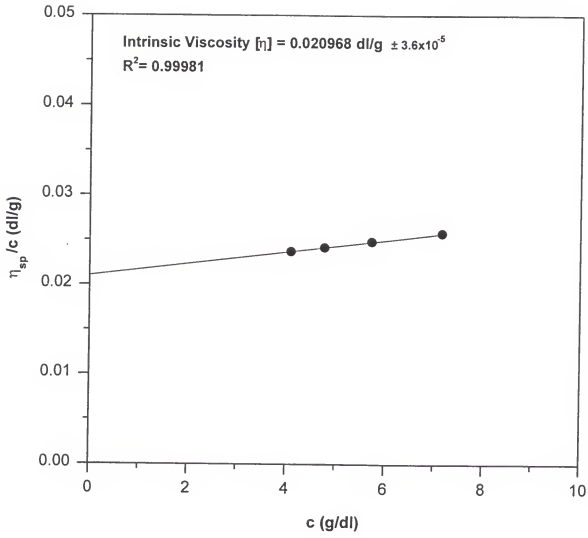

Figure 4.70. Plot of η_{sp}/c vs. c for polymer F (batch PMS-256) (MDCS/MTCS (70/30); toluene/1,4-dioxane (50/50)) in a mixture of toluene and 1,4-dioxane (50:50 vol%).

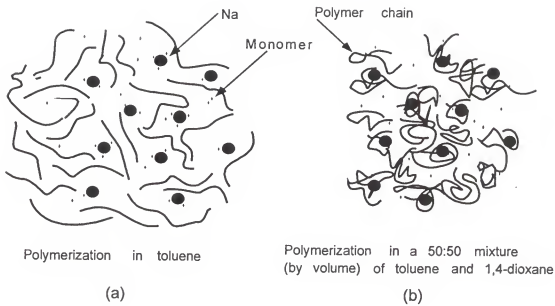

Figure 4.71. Schematic illustration for solvent effects for polymerization of MDCS (a) in toluene and (b) in a 50:50 mixture of toluene:1,4-dioxane.

4.2.2 Effect of synthesis conditions on polymer yield

As discussed earlier, the purpose of adding a trifunctional monomer (MTCS) to a difunctional monomer (MDCS) was to increase the degree of cross-linking in the polymer. (A higher degree of cross-linking will result in increased ceramic yield, which is desirable.) However, the addition of MTCS to MDCS also results in a significant decrease in the polymer yield in the absence of cosolvents. For example, Table 4.15 shows that yield for polymerization of MDCS in toluene was 41% (of theoretical yield) whereas the yield decreased to 15% when 30 wt% MTCS was added to MDCS. It is, therefore, necessary to add a polar solvent such as THF or 1,4-dioxane to toluene to increase yield for the polymerization reaction. (It is well-known in literature that polar and dipolar solvents (such as THF and dioxane) promote anionic polymerization, aiding the transfer of electrons from Na to the monomers and favoring the formation of silyl anion radicals ([Mil91]; [Gau89]).) As shown in Figure 4.72 and Table 4.15, when a 5 vol% of THF/95 vol% toluene mixture was used in the polymerization of MDCS:MTCS, the polymer yield increased ~2.5 times (from 15% to 37%) compared to polymerization in toluene alone. The polymer yield increased ~3 times (from 15% to 46%) when a 50 vol% dioxane/50 vol% toluene mixture was used for polymerization (Figure 4.72 and Table 4.15).

The higher yields for polymerization of MDCS/MTCS mixtures with the addition of polar solvents are apparently associated with a higher reaction rate. (As noted earlier, prolonged reaction times can result in lower yields due to the loss of Si-containing volatiles.) The correlation between the polymer yield and the reaction rate is suggested from observations of color changes that occurred during the reactions. As discussed in section 2.2.1.3, there is a change in color (to purple) during Wurtz-coupling

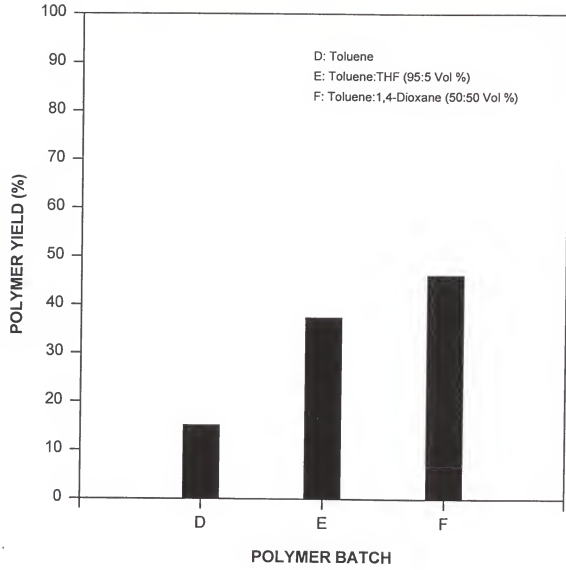

Figure 4.72. Effect of cosolvents on yield for PMS polymers D,E, and F (prepared from MDCS/MTCS (70/30 wt%)).

polymerization reactions[‡]. In this study, the purple color appeared in ~5, ~15, and ~40 minutes for polymerization of MDCS/MTCS (70/30 wt. ratio) in toluene/dioxane (50/50 vol. ratio), toluene/THF (95/5 vol. ratio), and toluene, respectively. (Note that this correlates with decreasing yields of ~46, ~37, and ~15%, respectively.) It was also observed that the reaction was essentially complete (i.e., as indicated by the acidity test described earlier) in 14 h for the polymerization carried out in toluene/dioxane (50/50 vol. ratio), while 40 h was required for the polymerization carried out in toluene alone.

In contrast to the results discussed above, there was a negligible effect of the solvent on the polymer yield when the polymerization reactions were carried out using MDCS alone (see Figure 4.73 and Table 4.15). This apparently reflects the high reaction rate for polymerizations carried out with MDCS (i.e., regardless of the solvent). The purple color appeared in ~5 min with each type of solvent used in the polymerization. The relatively high reaction rates are again consistent with the relatively high polymer yields (i.e., ~41-48% for polymers A, B, and C prepared with MDCS alone).

To further confirm the above trends, a polymerization reaction was carried out using a mixture of 70 wt% MTCS and 30 wt% MDCS in toluene. As expected, the reaction occurred more slowly and the polymer yield decreased with the higher proportion of MTCS. The purple color change did not occur until 2 h after the start of the reaction (i.e., compared to 40 and 5 minutes for the polymerizations carried out using 30 wt% MTCS/70 wt% MDCS in toluene and 100% MDCS in toluene, respectively). The polymer yield was only ~10% (i.e., compared to 15% and 41% for the polymerizations

[‡] It is well-known in Wurtz-coupling polymerization that a color change to purple indicates significant polymerization ([Ben92]; [Zei86A]; [Mil89]; [Mil93]). Miller et al. [Mil93] reported that in the case of Wurtz-coupling polymerization of aryldichlorosilanes, the purple color appeared within ~10 min of monomer addition to Na, at which point, 80% of monomer was consumed.

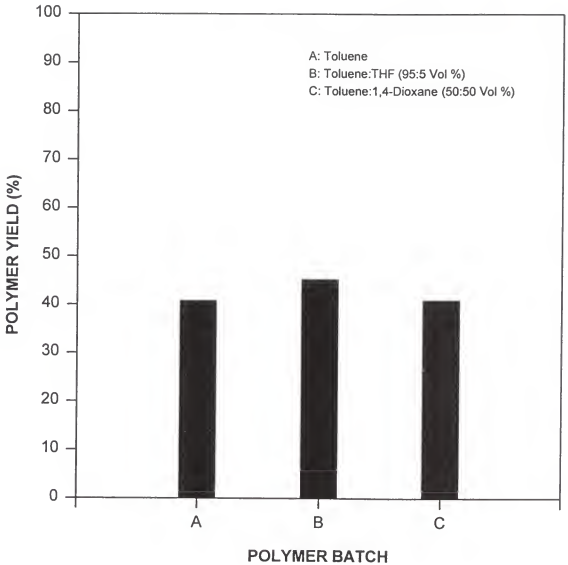

Figure 4.73. Effect of cosolvents on polymer yield for PMS polymers A,B, and C (prepared from 100% MDCS).

carried out using 30 wt% MTCS/70 wt% MDCS in toluene and 100% MDCS in toluene, respectively).

4.2.3 Characterization of PMS polymers and ceramic residues resulting from pyrolysis

4.2.3.1 Weight loss behavior

The weight loss behavior of PMS polymers A-F were studied by Thermal Gravimetric Analysis (TGA). The data on ceramic yield are presented in Table 4.15. Figure 4.74 shows TGA plots for polymers prepared by polymerization of MDCS in toluene (polymer A), toluene-THF (95:5 vol%) (polymer B), and toluene-1,4 dioxane (50:50 vol%) (polymer C). The use of cosolvents (THF and dioxane) resulted in polymers with slightly higher ceramic yields. Wood [Woo86] also reported a beneficial effect on ceramic yield when using a polar solvent in Wurtz-coupling polymerization. When polymerization was carried out in a mixture of hexane and THF (7:1 by volume), the ceramic yield was only ~25 wt%. However, when polymerization was carried out entirely in THF, the resultant polymer had a ceramic yield of 55 wt%. The increase in ceramic yield for polymers synthesized in polar solvents can be linked to the increase in molecular weight (and presumably an increased degree of polymer cross-linking).

Figure 4.75 shows TGA plots for polymers prepared by polymerization of MDCS/MTCS (70:30 wt%) in the presence of toluene (polymer D), toluene-THF (95:5 vol%) (polymer E), and toluene-1,4 dioxane (50:50 vol%) (polymer F). It can be seen from the figure that ceramic yields for all the three polymers are approximately the same and that the addition of polar solvents such as THF and 1,4-dioxane did not produce an increase in ceramic yield even though it resulted in an increase in molecular weight. This is contrary to what was observed in the case of polymerization of MDCS. It is presumed that the ceramic yield is primarily determined by degree of cross-linking brought about by addition of MTCS rather than the increase in molecular weight resulting from the use

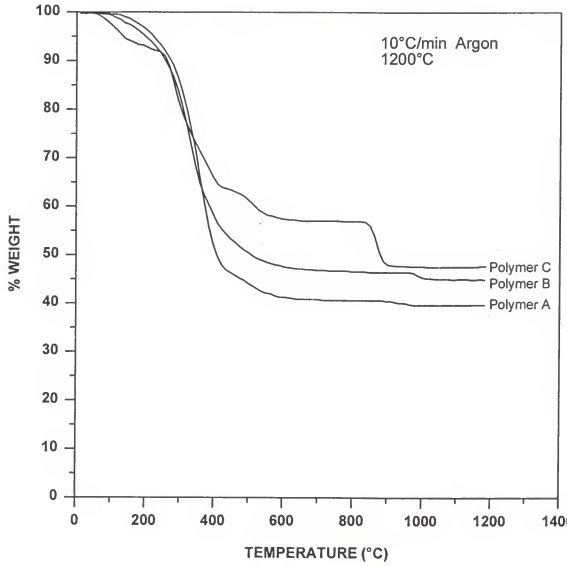

Figure 4.74. TGA plots (% weight vs. temperature) for polymers prepared with 100% MDCS. The solvents used in polymerization were toluene (polymer A, batch PMS-261), toluene/THF (95/5 vol. ratio) (polymer B, batch PMS-262), and toluene/1,4-dioxane (50/50 vol. ratio) (polymer C, batch PMS-257).

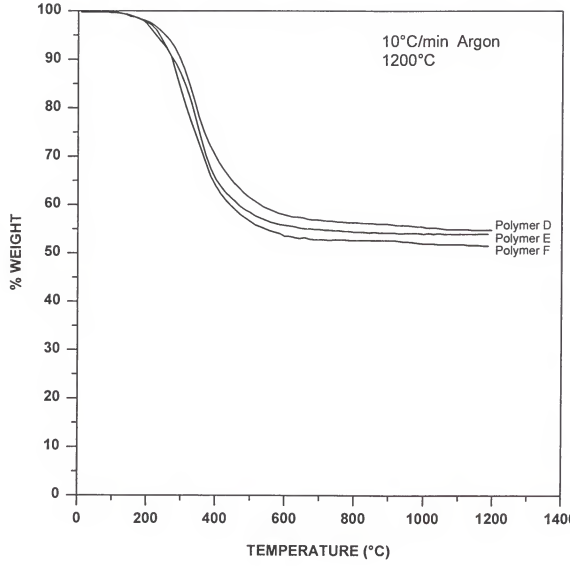

Figure 4.75. TGA plots (% weight vs. temperature) for polymers prepared with 70:30 wt% MDCS:MTCS. The solvents used in polymerization were toluene (polymer D, batch PMS-259), toluene/THF (95/5 vol. ratio) (polymer E, batch PMS-222), and toluene/1,4-dioxane (50/50 vol. ratio) (polymer F, batch PMS-256).

of the more polar solvents. This is also suggested by the fact that the ceramic yields are all higher for the polymers prepared from the MDCS/MTCS mixtures (i.e., compared to the polymers prepared with MDCS alone).

Figure 4.74 shows that polymer C has an abrupt weight loss of ~10 wt% starting at 860°C. Polymer B shows a weight loss of about 3% starting at 977°C. A similar (~10 wt%) high temperature weight loss was observed by Zhang et al. [Zha91] during TGA analysis of PMS polymers. It is suggested that these high temperature weight losses are attributed to the evolution of hydrogen arising from the decomposition of (Si-H)-containing structures. It is noted that this type of high temperature weight loss was not observed during the heat treatment of polymers prepared from MDCS/MTCS mixtures (Figure 4.75). This is consistent with the expectation that less Si-H groups are retained in these polymers since these groups are likely to be consumed during cross-linking reactions promoted by the use of the trifunctional monomer, MTCS.

4.2.3.2 FTIR spectroscopy studies on PMS polymers

FTIR spectra on PMS polymers C (batch PMS-263) and F (batch PMS-256) (polymers synthesized from MDCS and MDCS/MTCS in (70:30 wt. ratio), respectively in toluene/dioxane solvent) were collected in the diffuse reflectance mode at room temperature and during heat treatment from 40-600°C in nitrogen atmosphere. Figure 4.76 and 4.77 show the room temperature spectra of polymers PMS-C and PMS-F, respectively. The peak assignments for these polymers are shown in Table 4.16 and Table 4.17. Polymer C (prepared from MDCS) may be richer in Si-H groups compared to polymer PMS-F (prepared from mixture of MDCS/MTCS). This is suggested from the splitting of the Si-H absorption into the asymmetric stretching peak (at 2133 cm^{-1}) and symmetric stretching peak (at 2053 cm^{-1}). (As noted earlier, it is believed that the high temperature (above 800°C) weight losses in the polymers B and C prepared from

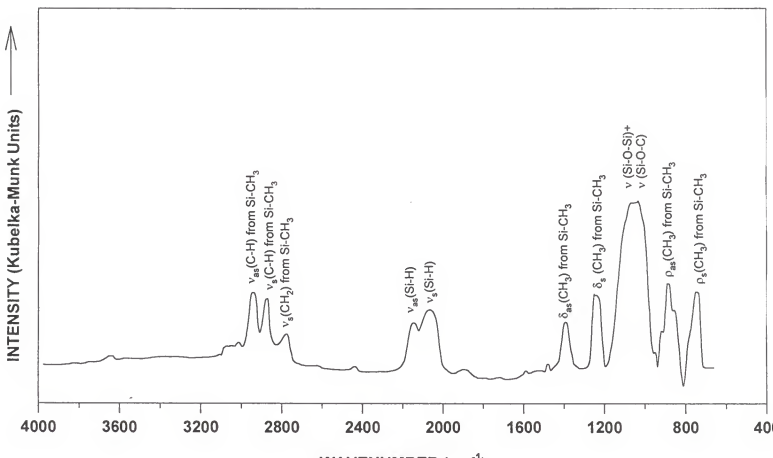

Figure 4.76. Room temperature FTIR spectra of PMS polymer C (batch PMS-263) (prepared from 100% MDCS in toluene/dioxane solvent).

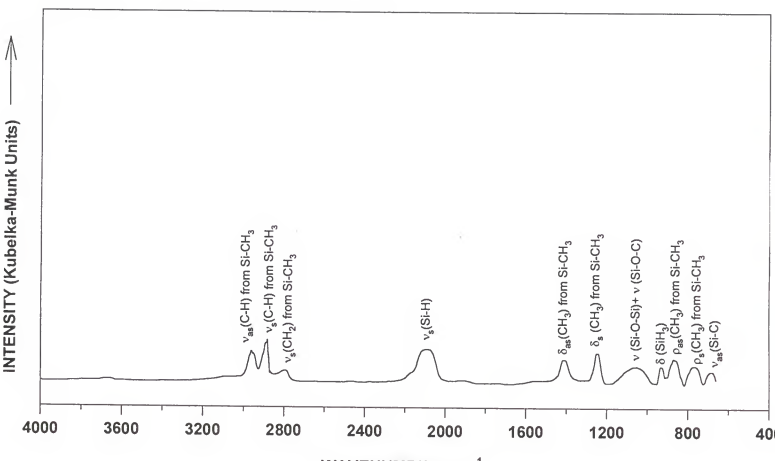

Figure 4.77. Room temperature FTIR spectra of PMS polymer F (batch PMS-256) (prepared from 70:30 wt% MDCS:MTCS in toluene/dioxane solvent).

Table 4.16. FTIR peak assignments for polymethylsilane (PMS) polymer PMS-C (batch PMS-263).

Peak (cm^{-1})	Assignment	References
2950	ν_{as} (C-H) from Si-CH_3	1,2
2894	ν_{s} (C-H) from Si-CH_3	1,2
2800	ν_{s} (CH_2) from Si-CH_3	1,2,5
2133	ν_{as} (Si-H)	1,4
2053	ν_{s} (Si-H)	1,4
1407	δ_{as} (CH_3) from Si-CH_3	2,3
1253	δ_{s} (CH_3) from Si-CH_3	2,3
1056	ν (Si-O-Si) + ν (Si-O-C)	1,3,5
838	ρ_{as} (CH_3) from Si - CH_3	1,2,3
770	ρ_{s} (CH_3) from Si - CH_3	6

ν = stretching ; δ = bending ; ρ = rocking

(1) W. Kriner, *J. Org. Chem.*, 29, 1601 (1964)
(2) A.L. Smith, *J. Chem. Phys.*, 21, 1997 (1953)
(3) A.L. Smith, *Spectrochimica Acta*, 16, 87 (1960)
(4) A.L. Smith, *Spectrochimica Acta*, 15, 412 (1959)
(5) R.M. Silverstein, G.C. Bassler, and T.C. Morrill, *Spectroscopic Identification of Organic Compounds*, John Wiley, New York (1981)
(6) J.R. Durig, and C.W. Hawley, *J. Chem. Phys.*, 59(1),1(1973)

Table 4.17. FTIR peak assignments for polymethylsilane (PMS) polymer PMS-F (batch PMS-256).

Peak (cm^{-1})	Assignment	References
2962	ν_{as} (C-H) from Si-CH_3	1,2
2886	ν_s (C-H) from Si-CH_3	1,2
2798	ν_s (CH_2) from Si-CH_3	1,2,5
2096	ν_s (Si-H)	1,4
1410	δ_{as} (CH_3) from Si-CH_3	2,3
1248	δ_s (CH_3) from Si-CH_3	2,3
1057	ν (Si-O-Si) + ν (Si-O-C)	1,3,5
930	δ (SiH_3)	7
841	ρ_{as} (CH_3) from Si - CH_3	1,2,3
771	ρ_s (CH_3) from Si - CH_3	6
676	ν_s (Si-C)	1,2,3

ν = stretching ; δ = bending ; ρ = rocking

(1) W. Kriner, *J. Org. Chem.*, 29, 1601 (1964)
(2) A.L. Smith, *J. Chem. Phys.*, 21, 1997 (1953)
(3) A.L. Smith, *Spectrochimica Acta*, 16, 87 (1960)
(4) A.L. Smith, *Spectrochimica Acta*, 15, 412 (1959)
(5) R.M. Silverstein, G.C. Bassler, and T.C. Morrill, *Spectroscopic Identification of Organic Compounds*, John Wiley, New York (1981)
(6) J.R. Durig, and C.W. Hawley, *J. Chem. Phys.*, 59(1),1(1973)
(7) N.B. Colthup, L.H. Daly, and S.E. Wiberley, *Introduction to Infrared and Raman Spectroscopy*, Academic Press, New York, 1964

MDCS reflects higher Si-H contents.) The FTIR spectrum for polymers C and F show an absorption band in the range of ~1000-1160 cm^{-1}. This absorption is attributed to Si-O-Si and Si-O-C bands arising from oxygen contamination (e.g., during polymer synthesis, FTIR sample preparation, etc.) The absorption is considerably more intense (relative to the other peaks) in polymer C. This is attributed to a greater amount of reactive Si-H groups. (This is consistent with the earlier suggestion, based on the TGA results in section 4.2.3, that the MDCS-derived polymers have more residual Si-H groups compared to the polymers prepared from MDCS/MTCS mixtures.)

Figure 4.78 shows the FTIR spectra for polymer PMS-C during heat treatment from 40 to 600°C in nitrogen atmosphere at 1°C/min. The changes in intensities of various absorption bands as a function of temperature are shown in Figure 4.79. No significant changes in intensities for absorption bands are observed for all groups up to ~200°C. The intensity of absorption band at 2053 cm^{-1} (due to symmetric stretch vibration of Si-H) increases starting at 300°C, reaches a maximum around 500°C and then decreases. This is possibly due to the formation of additional Si-H groups as a result of methylene insertion reactions. Schmidt et al. [Sch91] have also reported similar increases in Si-H absorption intensities between 200-400°C during the pyrolytic conversion of vinylic polysilane to silicon carbide and have suggested the methylene insertion reaction as the mechanism for the increase in intensity of absorption band.

The methylene insertion reaction occurring in PMS (i.e., conversion to a polycarbosilane structure) can be represented as shown in equation (4.6). Accompanying the increase in the intensity of Si-H absorption band is the onset of absorption band due to δ_s (CH_2) of Si-CH_2-Si (1358 cm^{-1}) at ~440°C, which corresponds to the insertion of -CH_2 groups in the main Si-Si chain. This was also reported by Zhang et al. [Zha91] in the pyrolytic conversion of PMS (prepared by

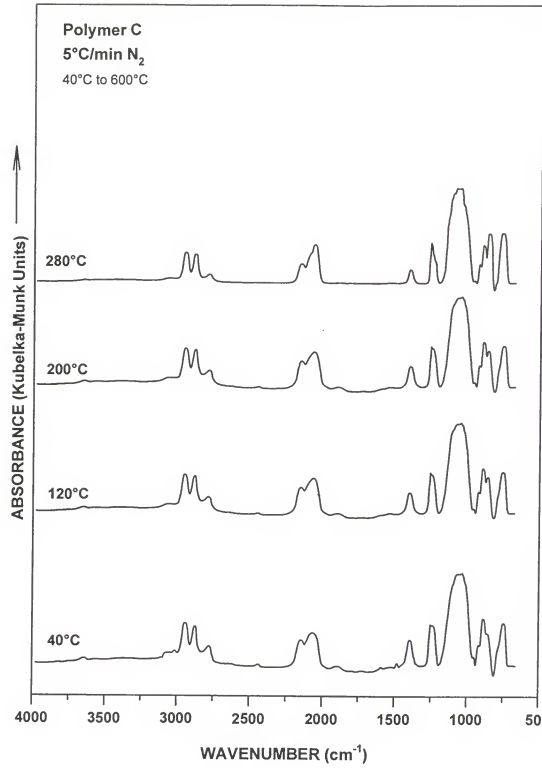

Figure 4.78. FTIR spectra of PMS polymer C (100% MDCS; toluene, dioxane (50:50 vol%)), 40°C to 600°C at 5°C/min in nitrogen.

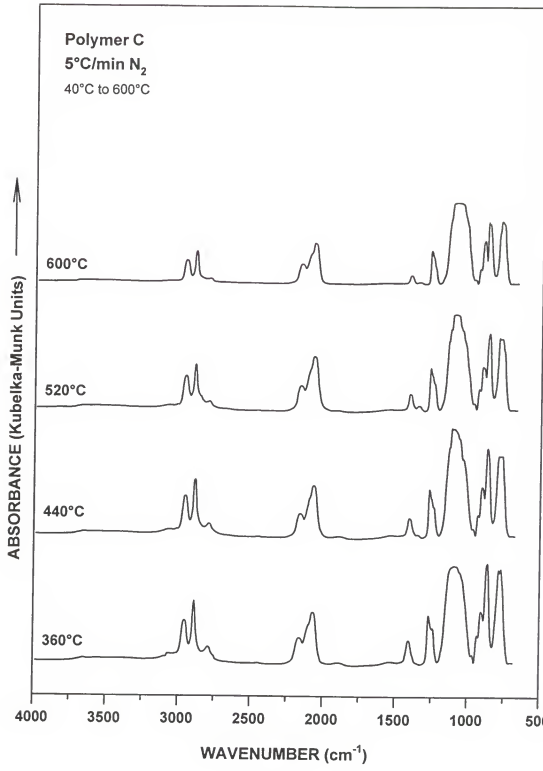

Figure 4.78. (cont'd.).

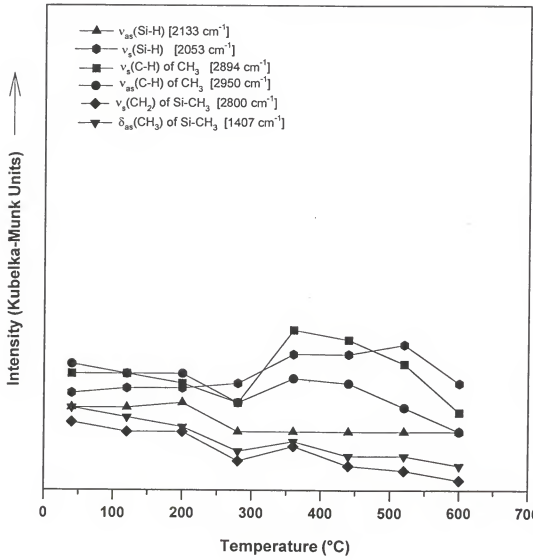

Figure 4.79. Intensity vs. temperature from FTIR spectra for PMS polymer C (100% MDCS; toluene, dioxane (50:50 vol%)).

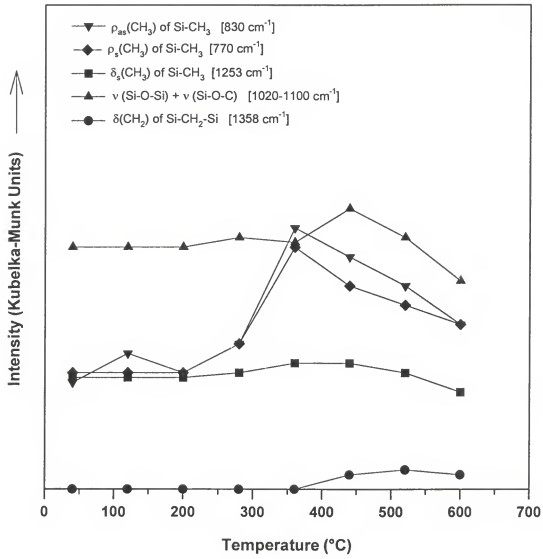

Figure 4.79. (Cont'd.).

dehydrocoupling of methylsilane) to silicon carbide at 400°C. While these changes can be attributed to formation of a PCS-type backbone from PMS during pyrolysis, it is unclear why the absorption intensities due to the symmetric ρ_s (CH_3) vibration of Si-CH_3 at 770 cm^{-1}, asymmetric ρ_{as} (CH_3) vibration of Si-CH_3 at 830 cm^{-1} and symmetric stretch of C-H of Si-CH_3 at 2894 cm^{-1} first increase (from below 300°C to at least 350°C) and then decrease at higher temperatures.

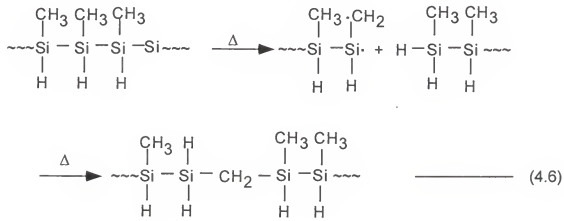

(4.6)

The intensities of most of the original absorption bands from PMS-C have decreased by 600°C. By 750°C, the well-defined peaks originally associated with the organosilicon polymer have mostly disappeared, leaving broad peaks associated with C-H stretching (~2800 cm^{-1}), Si-H stretching (~2140 cm^{-1}), and β-SiC (~1000 cm^{-1}) (see Figure 4.80). After heat treatment at 1050°C, the only remaining peaks are those associated with β-SiC. These peaks are at 1000 cm^{-1} (ν SiC) and 1528 cm^{-1} (unidentified vibration mode) [Gre72; Fen94; Han97; Zha94B].

Figure 4.81 shows FTIR spectra of polymer PMS-F collected during heat treatment from 40-600°C in nitrogen atmosphere at 1°C/min. The changes in intensities of various absorption bands as a function of temperature are shown in Figure 4.82.

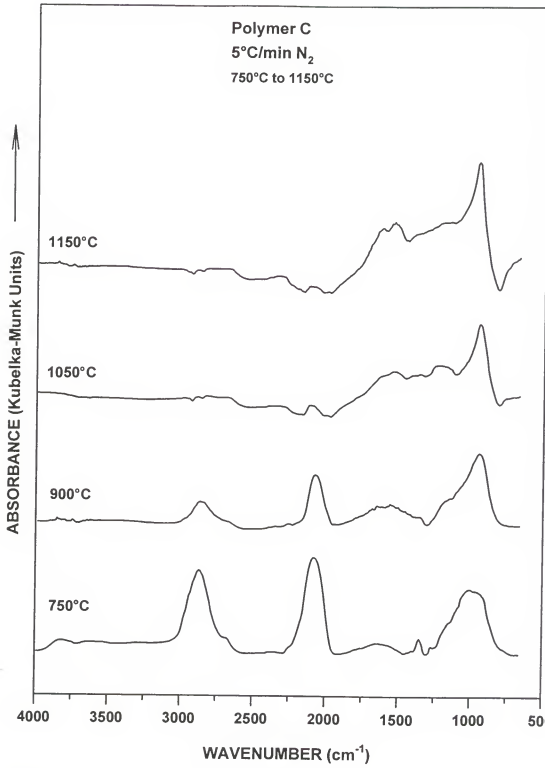

Figure 4.80. FTIR spectra of PMS polymer C (100% MDCS; toluene, dioxane (50:50 vol%)),750°C to 1150°C at 5°C/min in nitrogen.

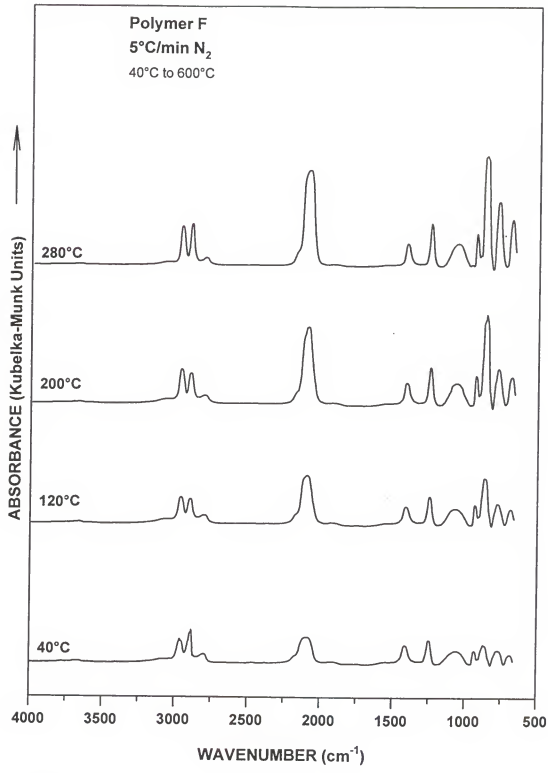

Figure 4.81. FTIR spectra of PMS polymer F (MDCS,MTCS (70:30 wt%)), toluene, dioxane (50:50 vol%), 40°C to 600°C at 5°C/min in nitrogen.

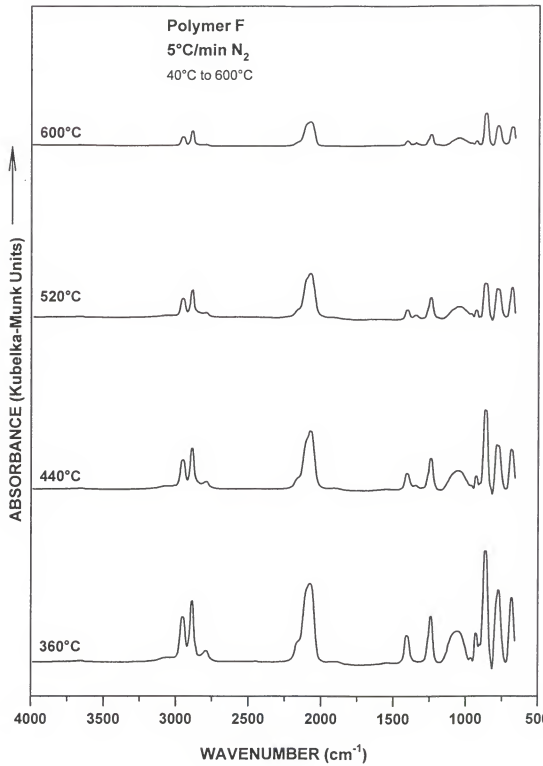

Figure 4.81. (Cont'd.).

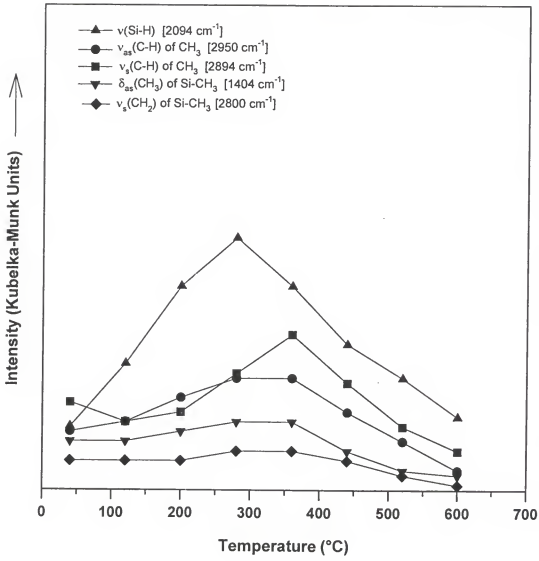

Figure 4.82. Intensity vs. temperature from FTIR spectra of PMS polymer F (MDCS, MTCS (70:30 wt%); toluene, dioxane (50:50 vol%)).

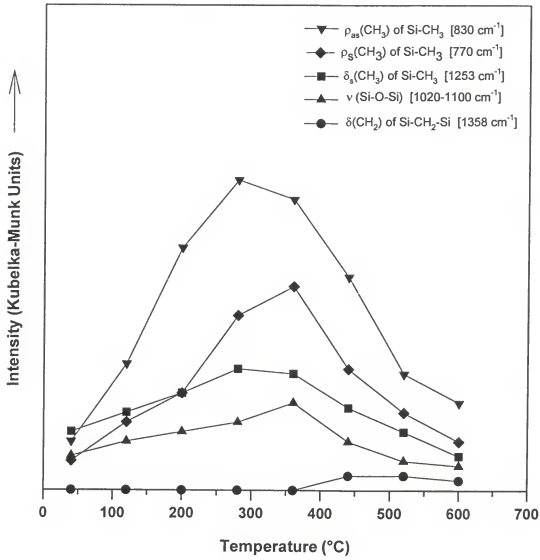

Figure 4.82. (Cont'd.).

Unlike polymer PMS-C, where no significant changes were observed for most of the absorption bands up to 200°C, polymer PMS-F showed changes early on in the heat treatment. The intensity due to the stretching vibration of Si-H (at 2096 cm^{-1}) increased from 40°C, reached a maximum at around 300°C and then started to decrease. This increase is again attributed to methylene insertion reaction shown in equation (4.6). This was also suggested by the onset of the absorption band due to δ_s (CH_2) of Si-CH_2-Si at ~360°C, which corresponds to the insertion of -CH_2 groups in the main Si-Si chain. However, some results are inconsistent with the hypothesis that methylene insertion reaction occurs. First, the increase in the ν (Si-H) vibration is considerably greater than the increase in the δ_s (CH_2) vibration and the increase occurs at much lower temperature. Second, the intensities due to symmetric ρ_s (CH_3) vibration of Si-CH_3 at 770 cm^{-1}, asymmetric ρ_{as} (CH_3) vibration of Si-CH_3 at 830 cm^{-1} and symmetric stretch of C-H of Si-CH_3 at 2894 cm^{-1} increase, starting at relatively low temperatures and increasing up to ~350°C.

The FTIR spectra after heat treatment of PMS-F at temperatures in the range of 750-1150°C are similar to those observed in PMS-C (see Figure 4.83). Above 750°C, the intensity of absorption band due to stretching vibration of β-SiC (at 750-1000 cm^{-1}) is broader compared to that of polymer PMS-C. This may be due to a lesser degree of crystallization for the SiC formed from polymer PMS-F. (This is suggested by XRD results for heat-treated PMS-F and PMS-C samples, as discussed below in section 4.2.3.3.)

4.2.3.3. XRD characteristics

Figures 4.84 and 4.85 show representative XRD patterns of the residues obtained from various MDCS-derived and MDCS/MTCS-derived polymers after heat

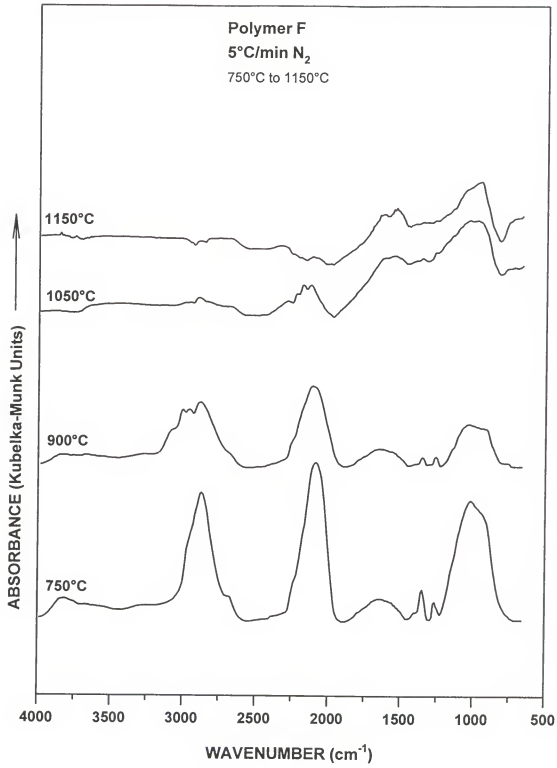

Figure 4.83. FTIR spectra of PMS polymer F (MDCS, MTCS (70:30 wt%)), toluene-dioxane (50:50 vol%), 750°C to 1150°C at 5°C/min in nitrogen.

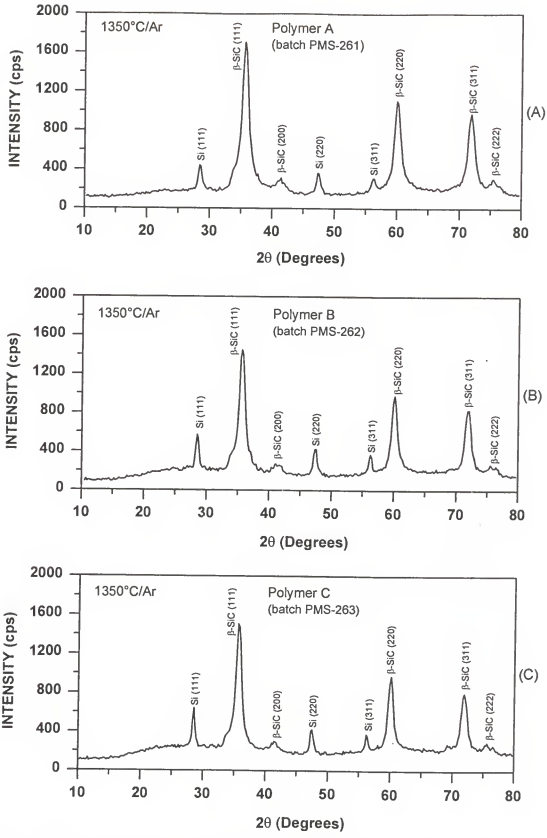

Figure 4.84. XRD Patterns for PMS polymers prepared from monomer MDCS. (A) 100% toluene (B) toluene:THF (95:5 Vol%) (C) toluene:dioxane (50:50 Vol%).

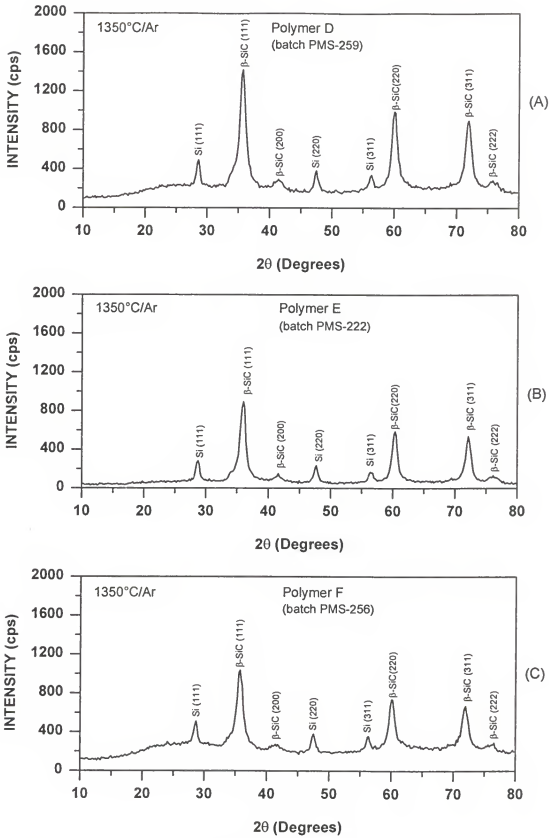

Figure 4.85. XRD Patterns for PMS polymers prepared from monomers MDCS/MTCS (70:30 wt%) (A) 100% toluene (B) toluene:THF (95:5 Vol%) (C) toluene: dioxane (50:50 Vol%).

treatment at 10°C/min to 1350°C (no hold time) in argon. The d-spacings, 2θ Bragg angles, and the corresponding intensities of diffraction planes are shown in Table 4.18. The XRD patterns were essentially the same for all samples. The major phase in these samples is β-SiC. Silicon is present as a minor phase. The pyrolytic decomposition of PMS polymers to a SiC/Si mixture was reported by several previous workers [Sey92; Zha94A].

The crystallite sizes for the Si and SiC phases were determined by the line broadening method using Scherrer's formula (described in section 3.2.6) and the results are tabulated in Table 4.19. The SiC crystallite sizes are virtually the same (in the range of 8.1-9.3 nm) for all samples. The Si crystallite sizes are slightly smaller for the samples prepared from the MDCS/MTCS polymers (i.e., compared to the samples prepared from MDCS alone). However, the differences are not particularly significant given the range of experimental variability observed when multiple samples were analyzed.

4.2.3.4 EMA analysis

Table 4.20 shows results of Electron Microprobe Analysis (EMA) for samples obtained after pyrolysis of PMS polymers at 1000°C in nitrogen. Results are shown for samples prepared from polymer PMS-245-A (an as-synthesized batch of polymer F) and polymer PMS-245-F-1 (a higher molecular weight portion of PMS-245-A prepared by fractional precipitation; see section 4.3.1.2). The former sample showed a Si-rich composition compared to that of stoichiometric SiC. (Stoichiometric SiC has a composition of 70 wt% Si/30 wt% C.) PMS polymers with Si-rich composition have been reported previously by other researchers [Sey92; Zha94A; Zha94B]. The result in this study is also consistent with the observation of free Si in the XRD pattern for a similar PMS sample (polymer F, batch PMS-256) which was pyrolyzed at 1350°C (in argon), as shown in Figure 4.85.

Table 4.18. d-spacings and 2θ Bragg angles.

Si (structure: diamond cubic)[a]

d-spacing, Å	2θ, degrees	Intensity	h k l index
3.138	28.42	100	1 1 1
1.920	47.31	60	2 2 0
1.638	56.10	35	3 1 1
1.357	69.17	8	4 0 0
1.246	76.37	13	3 3 1
1.108	88.06	17	4 2 2

β-SiC (structure: simple cubic)[b]

d-spacing, Å	2θ, degrees	Intensity	h k l index
2.51	35.74	100	1 1 1
2.17	41.58	20	2 0 0
1.54	60.03	63	2 2 0
1.31	72.03	50	3 1 1
1.26	75.37	5	2 2 2
1.09	89.93	6	4 0 0

[a] JCPDS Card # 5-565, International Diffraction Committee, Swarthmore, PA (1988)

[b] JCPDS Card # 5-565, International Diffraction Committee, Swarthmore, PA (1988)

Table 4.19. Crystallite sizes for Si and SiC calculated by Scherrer's formula for various polymers pyrolyzed at 1350°C in nitrogen at 10°C/min with no hold.

Polymer	Monomer(s)	Solvents(s)	Si crystallite size (nm)	SiC crystallite size (nm)
A	MDCS	Toluene	17.4	8.1
B	MDCS	Toluene/THF (95/5)	21.7	8.6
C	MDCS	Toluene/Dioxane (50/50)	23.3 ±5.0 (3 batches)	8.8 ±0.25 (3 batches)
D	MDCS/MTCS (70/30)	Toluene	15	8.6
E	MDCS/MTCS (70/30)	Toluene/THF (95/5)	19.4 ±3.9 (5 batches)	9.3 ±1.3 (5 batches)
F	MDCS/MTCS (70/30)	Toluene/Dioxane (50/50)	15.0	8.1

Table 4.20. Results of Electron Microprobe Analysis (EMA) on pyrolyzed ceramic from PMS polymers.

Batch	Sample description	# of points analyzed	Elemental composition						
			As-measured				Normalized		
			Si %	C%	O%	Total%	Si%	C%	O%
PMS-245-A-1000	As prepared, then pyrolyzed to 1000°C in N_2	10	69.41 ± 1.6	26.00 ± 3.7	2.15 ±1.8	97.57 ±3.4	71.18 ±1.47	26.57 ±2.85	2.25 ±1.88
PMS-245-F-1000	Fractionated in acetone, then pyrolyzed to 1000°C in N_2	10	70.63 ±1.1	30.44 ±0.5	0.20 ±0.4	101.27 ±1.1	69.74 ±0.5	30.06 ±0.40	0.20 ±0.41
PMS-238-A-1000	Oxidized in static air, then pyrolyzed to 1000°C in N_2	6	48.90 ±1.1	29.88 ±0.9	20.63 ±1.8	99.36 ±0.44	49.22 ±1.1	30.04 ±1.0	20.74 ±1.8

The sample prepared from PMS-245-F-1 polymer showed a composition close to that of stoichiometric SiC. This suggests that the higher molecular weight (and presumably more cross-linked) portions of the PMS polymers either are compositionally different (i.e., have lower Si/C ratio) or have different pyrolysis behavior (i.e., which leads to the lower Si/C ratio) compared to the lower molecular weight portions in the as-synthesized PMS polymers.

The oxygen present in the sample prepared from the PMS-245-A polymer is presumably due to contamination by exposure to air during handling. This may have occurred when the as-prepared polymer was initially concentrated and recovered after the Wurtz-coupling polymerization reaction (i.e., prior to storage as a dilute solution in toluene). However, this seems unlikely since PMS-245-F-1 was prepared from PMS-245-A and yet the pyrolyzed sample from PMS-245-F-1 showed very little oxygen contamination. Another possibility is that the oxygen contamination resulted from exposure to air when the PMS-245-A sample was removed (from the dilute storage solution), dried, and transferred to the pyrolysis furnace.

4.2.4. Sensitivity of PMS polymers to oxygen contamination

It is well known that PMS polymers are sensitive to contamination from exposure to oxygen and water vapor [Zha91B; Woo84; Qiu89A; Abu92]. This was observed for PMS polymers prepared in this study. Figure 4.86 shows FTIR spectra as a function of time for polymer PMS-C (prepared from MDCS in toluene/dioxane) which was exposed to air at room temperature. Figure 4.87 shows plots of intensity vs. time for various absorption peaks. It is evident that substantial oxygen contamination occurred within the first hour of air exposure. A substantial increase in intensity is observed for the Si-OH stretching vibration (~3198-3735 cm^{-1}). This correlates with the disappearance of asymmetric Si-H stretching vibration at 2131 cm^{-1}. (The symmetric Si-H stretching

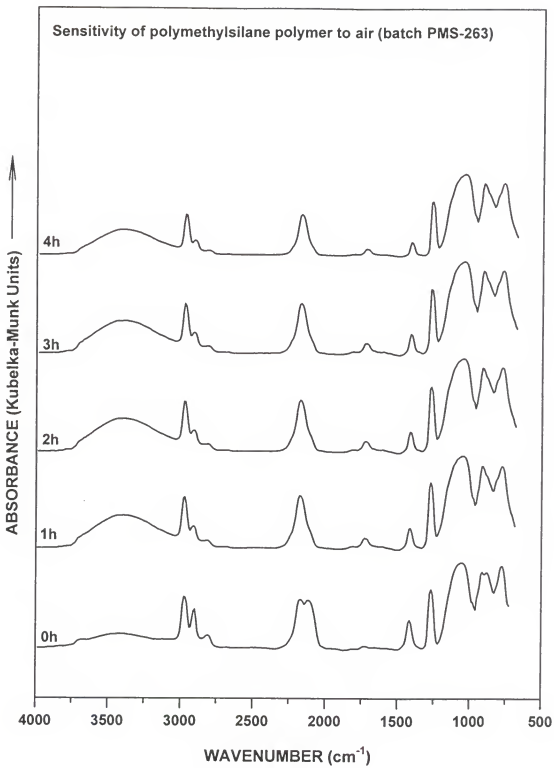

Figure 4.86. FTIR spectra of polymer PMS-C (100% MDCS; toluene/dioxane (50:50 vol%)) exposed to air, shown as a function of time.

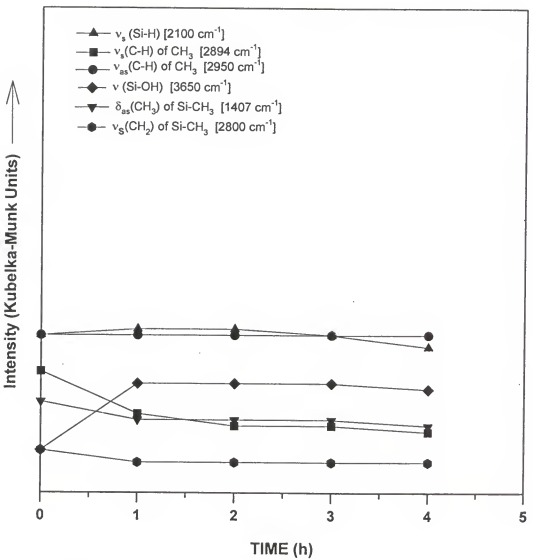

Figure 4.87. Intensity vs. time of exposure to air from FTIR spectra for PMS polymer PMS-C (100% MDCS; toluene, dioxane (50:50 vol%)).

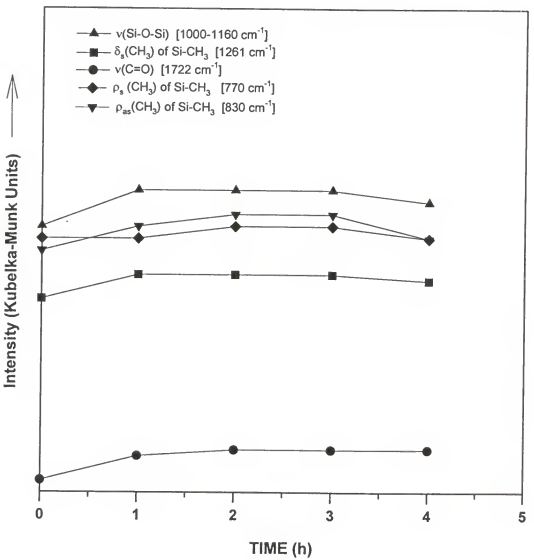

Figure 4.87. (Cont'd.).

vibration at 2100 cm^{-1} only decreases slightly over the 4 h exposure period.) The absorption peak associated with the Si-O-Si stretching vibration (~1000-1160 cm^{-1}) also increases. (It is presumed that this peak may develop due to both condensation reactions between Si-OH and direct oxidation of the Si-Si backbone of the PMS polymers.) The C=O stretching vibration (~1720 cm^{-1}) also increases significantly during the first hour of air exposure. This correlates with the decreases in intensity for the absorptions associated with the C-H stretching and deformation vibrations (from $Si-CH_3$ groups) at ~2894, ~2800, and ~1407 cm^{-1} and indicates that direct oxidation of methyl groups occurs.

In a separate experiment, a PMS polymer (PMS-238, polymer E in Table 4.15) sample was exposed to static air for 24 h. The sample changed color during this period from transparent yellow to cloudy white. The polymer was then pyrolyzed to 1000°C for 1 h in a nitrogen atmosphere and analyzed by EMA. Table 4.20 shows that the sample contained ~21 wt% oxygen. Hence, it is clear that extensive precautions must be taken to avoid oxygen contamination by atmosphere exposure if the PMS polymers prepared in this study are to be useful as precursors for the fabrication of SiC fibers.

4.3 Preparation of Silicon Carbide Fibers from Polymethylsilane Polymers

There are several requirements for successful conversion of PMS polymers to SiC fibers. They are as follows:

(i) Fiber formation/Infusibility. The polymer should be a solid at room temperature or should solidify during the course of fiber spinning to prevent fibers from sticking to the spinning wheel or to each other. In addition, even if the polymer is solid at room temperature, it should not melt at higher temperatures (i.e., during conversion to ceramic). Any melting could cause the fibers to stick to each other. Prior experience with some PMS polymers has shown that if the molecular weight becomes too low (e.g., <4,000), it will melt upon pyrolysis. Such polymers could be rendered infusible by carrying out a cross-linking (or curing) treatment below the melting temperature of the polymer. Alternatively, the molecular weight/degree of cross-linking of the polymer could be increased prior to spinning. (However, this would reduce the maximum concentration of polymer that could be dissolve in solvents used in solution spinning.)

(ii) Solubility. If fibers are formed by dry or wet spinning, then the solid polymer must have good solubility in an appropriate solvent. Good solubility is desired to achieve high polymer concentration in the spin dope, so that less solvent needs to be removed during spinning. Common solvents for organosilicon polymers include toluene, xylene, THF, etc. (In dry or wet spinning, a viscous spin dope is prepared and is extruded through a spinneret to form fibers.)

(iii) Molecular weight/ degree of cross-linking. If the polymer molecular weight is too high (e.g., >10,000 for some organosilicon polymers) or if it is highly cross-linked, the polymer will not be readily soluble in common organic solvents. This will lead to difficulties in spin dope preparation and fiber spinning (e.g., difficulty in filtration of

the polymer solution to remove any microgels present, low concentration of polymer in the spin dope which necessitates greater removal of solvent in forming the fiber).

(iv) Viscosity. The spin dope should have optimum viscosity for preparation of useful fibers. For example, if the viscosity is too high, it will be difficult to extrude spin dope through the spinneret. This tends to result in discontinuous brittle fibers with rough surfaces. If the viscosity is too low, fibers will not maintain their shape after exiting the spinneret and fibers may also stick together. (At greater extremes in viscosity, it will not even be possible to form fibers.)

(v) Solvent evaporation/ fiber "solidification". In dry spinning, the rate of solvent evaporation from fibers exiting from spinneret must be high enough so that fibers remain separable (i.e., they do not stick together) when they are collected on a winding drum. The rate of evaporation during fiber spinning depends on many factors such as the vapor pressure of the solvent, temperature of the spin dope, temperature in the spinning column, spinneret geometry, extrusion pressure, winding pressure, etc. Conditions which promote the formation of fine-diameter fibers are helpful in allowing fibers to "solidify" quickly (i.e., prior to the fibers reaching the winding drum). This is because a smaller quantity of solvent needs to be removed during spinning, i.e., assuming other factors (such as the number of fibers spun) remains consistent. (In addition, finer fibers will have a greater specific surface area available for evaporation, so the evaporation rate may be higher.) Process variables which lead to finer-diameter fibers include smaller hole diameter in the spinneret and higher winding speed.

(vi) Stability. The polymer should be stable at room temperature or at the temperature of storage. The polymer should not show latent reactivity to form gel-like particles or react with the environment. In some cases, such problems can be avoided by storing

the polymer (or polymer solution) at low temperature under an inert atmosphere. A major problem with PMS polymers is their high affinity to react with oxygen. It is well known that the presence of oxygen is detrimental to the thermomechanical stability of SiC-based fibers at high temperatures (>1200°C) [Ish94]; [Mah84]; [Sim84]; [Cla85]. As reported in section 4.2.4, FTIR spectroscopy (Figure 4.86) showed that a PMS polymer synthesized in this study picked up a substantial amount of oxygen within 1 h of exposure to air. Oxygen contamination was also demonstrated from EMA results carried out on a sample which was pyrolyzed under an inert atmosphere. (The PMS polymer was first exposed to air for 24 h and then pyrolyzed at 1000°C in nitrogen. EMA (Table 4.19) showed an oxygen content of ~21 wt% in the pyrolyzed product.) Oxygen contamination can be minimized by carrying out all polymer synthesis and handling operations in an inert atmosphere (e.g., nitrogen). (This may not be practical beyond the laboratory setting, especially since other fiber processing steps (spin dope preparation, fiber spinning, and fiber pyrolysis) would also have to be conducted in an inert environment to avoid oxygen contamination.)

(vii) Composition. In order to prepare near-stoichiometric SiC fibers, it would be desirable to have a polymer with an elemental Si:C ratio of 1:1. It is well-known that fibers prepared from polycarbosilane (PCS) polymers have a significant amount of excess carbon ([Has83A]; [Yaj78B]; [Tor92B]). As-synthesized PCS polymers have a Si:C ratio of ~1:2. After pyrolysis, Si:C ratios are typically in the range 1: 1.23-1.78 ([Has83A]; Tor92B]). In contrast, PMS polymers have an ~1:1 atomic ratio of Si:C. It is known that pyrolysis of these polymers results in either near-stoichiometric SiC or SiC with an excess of Si ([Sey92]; [Zha91A]; [Mu91A]). It is hypothesized that mixtures of PMS and PCS could be used to prepare near-stoichiometric SiC fibers.

The PMS polymers prepared in this study have low molecular weight in the as-prepared state (M_n ~800-1,000, and M_w ~1,100-2,500) and are viscous liquids at room temperature. The molecular weight needs to be increased in order for the polymers to be useful for fiber processing. Two approaches were utilized to raise the molecular weight of the polymer: (i) further polymerization and cross-linking by heat treatment with and without additives and (ii) fractional precipitation of higher molecular weight fractions. The results from these approaches are described in section 4.3.1. Section 4.3.2 describes the results of fiber spinning experiments from these polymers.

4.3.1. Methods to increase molecular weight of PMS polymers

4.3.1.1 Heat treatment of PMS polymers

Heat treatment of PMS polymers resulted in increased molecular weight and cross-linking of the polymers. This is presumed to occur by dehydrogenation reactions involving Si-H groups. Si-H groups are believed to have the lowest bond energy in the PMS polymers ([Sch91]; [Has83A]). Hasegawa et al. [Has83A] have studied heat treatment of PCS polymers by IR spectroscopy and proposed that dehydrogenation reactions involving Si-H occurred at temperatures ~400°C. Schmidt et al. [Sch91] have also suggested from IR results that dehydrogenation reactions involving Si-H groups take place during low temperature heat treatment of vinylic polysilane polymers. FTIR spectra showed a decrease in the absorption peak due to the Si-H vibration for polymers heated at < 200°C.

All polymers used for heat treatment in this study were synthesized from a mixture of methyldichlorosilane (MDCS) and methyltrichlorosilane (MTCS) monomers (in 70:30 wt% proportion). The solvent used in the synthesis was a mixture of toluene and tetrahydrofuran (95:5 vol%). Polyvinylsilazane (PSZ) (0.5-14.5 wt%), dicumyl peroxide, DCP, (0.05-1 wt%), and decaborane ($B_{10}H_{14}$) were investigated as potential cross-linking

aids for the PMS polymers. The polymer solution viscosity was generally monitored before and after heat treatment. Increases in viscosity indicated that polymer molecular weight increased. In most cases, the molecular weight was also directly determined (by GPC) before and after heat treatment.

Table 4.21 shows the heat treatment conditions for different PMS polymer batches (with and without additives) and the resulting effects on viscosity and molecular weight. The nomenclature of the PMS polymers used in this study is shown in Table 4.22. The main problems in the heat treatment approach to raising molecular weight of PMS polymers were poor control over the molecular weight increases and lack of reproducibility (i.e., the increase in molecular weight was not uniform from batch to batch). The poor control over the molecular weight increases meant that it was difficult to avoid microgel formation and, in some cases, complete gelation of the solution. (Microgel formation is highly undesirable because it causes difficulty in filtering solutions and results in lower solids loading in the solutions (or higher viscosities for a fixed solids loading).) The lack of reproducibility may have been due to the variation in the characteristics of as-prepared polymers from batch to batch. The monomers used in the polymer synthesis (MDCS and MTCS) are highly reactive (e.g., they are highly sensitive towards moisture) and may age with time, even though samples were stored after backfilling with nitrogen and all handling operations were carried out under argon in a glove bag. In addition, it is speculated that the polymers may age (i.e., undergo increases in molecular weight with time) due to latent reactivity of Si-H groups.

The lack of reproducibility in the polymer syntheses is indicated by the initial characteristics of polymer PMS-231, PMS-235, and PMS-236 in Table 4.21. Although synthesized under identical conditions, PMS-231 showed a much higher initial molecular weight compared to PMS-235 and PMS-236. Also, the changes in viscosity and

Table 4.21. Conditions for heat treatment of PMS polymers¶ containing PSZ, DCP, and DB.

Initial polymer batch	Additives (wt%)			Heat treatment conditions	Initial viscosity	Final viscosity	% viscosity	Initial	Initial	Initial	Final	Final	Final
	PSZ	DCP	DB	time(h)(temp°C)	mPa·s	mPa·s	change	M_n †	M_w †	PDI	M_n	$\cdot M_w$	PDI
PMS-214-A	5	0.5	0	1 (100, 115, 125, 130, 145)	*	*	*	1493	6449	4.32	2614	27039	10.34
PMS-216-A	5	0.5	0	1 (55, 70, 85)	1.84	2.59	41	1263	3760	2.97	1461	7580	5.18
PMS-216-A2	5	0.5	0	1 (105)	1.90	3.43	80	*	*	*	2076	11213	5.40
PMS-217-A	5	0.5	0	1 (100)	1.90	2.84	49	1156	3351	2.89	1768	8213	4.64
PMS-218-A	10	1	0	1 (85, 95, 105, 115, 130)	1.52	4.27	181	*	*	*	*	*	*
PMS-219-A	14.5	1.5	0	1 (140); 94(150)	1.50	12.0	700	1293	4552	3.51	2496	24044	9.63
PMS-223-AD	0.25	0	6	1 (100, 120, 130, 140, 150)	1.90	27.5-12.5	800	*	*	*	*	*	*
PMS-223-AD2	0.25	0	6	1 (120,130); 2(140)	1.80	4.2	130	1629	2626	1.61	1671	3087	1.84
PMS-224-AD	0.25	0	6	2 (130)	1.80	solution gelled		*	*	*	*	*	*
PMS-225-AD	0.25	0	6	1 (100,120,130); 2.75(140)	1.80	7.5	320	*	*	*	1037	1846	1.78
PMS-225-AD2	0.25	0	3	1 (130); 4(140)	1.90	24	1100	*	*	*	1337	2231	1.67
PMS-226-AD	3	0	3	3.5 (140)	1.90	36	1700	close to gel point					
PMS-227-AD	3	0	3	4.5 (130)	1.90	solution gelled		*	*	*	*	*	*
PMS-231	0	0	0	28 (130)	3.00	38-26	800	2991	21041	7.03	6884	69404	10.1
PMS-235	0	0	0	168 (130)	*	*	*	863	1531	1.77	2237	3859	1.73
PMS-236	0	0	0	109 (130)	3.8-3.0	8	160	967	1149	1.19	4634	17456	3.77

¶ solids-loading of starting polymer solution was 33 wt% ; * Data not available ; † Molecular weights of PMS with additives

Table 4.22. Nomenclature of PMS polymers used in the heat treatment experiments.

Polymer designation[a]	Description
PMS-XXX	As-synthesized polymer (no additives)
PMS-XXX-H	Heat-treated PMS-XXX polymer
PMS-XXX-A	As-prepared PMS-XXX with PSZ and DCP additives
PMS-XXX-A-H	Heat-treated PMS-XXX-A
PMS-XXX-A2	A second portion of as-prepared PMS-XXX-A with PSZ and DCP additives
PMS-XXX-A2-H	Heat-treated PMS-XXX-A2
PMS-XXX-AP	As-prepared PMS-XXX which contains PCS and PSZ as polymer additives. It also contains DCP
PMS-XXX-AP-H	Heat-treated PMS-XXX-AP
PMS-XXX-AP2[b]	A second portion of as-prepared PMS-XXX which contains PCS and PSZ additives. It also contains DCP
PMS-XXX-AP2-H	Heat-treated PMS-XXX-AP2
PMS-XXX-AD	As-prepared PMS-XXX which contains DB and PSZ polymer as additives. It may also contain DCP as an additive
PMS-XXX-AD-H	Heat-treated PMS-XXX-AD
PMS-XXX-AD2	A second portion of PMS-XXX-AD which contains DB and PSZ polymer as additives. It may also contain DCP as an additive
PMS-XXX-AD2-H	Heat-treated PMS-XXX-AD2
PMS-XXX-APD	As-prepared PMS-XXX which contains DB, PCS polymer, and PSZ polymer as additives. It may also contain DCP as an additive
PMS-XXX-APD-H	Heat-treated PMS-XXX-APD
PMS-XXX-APD-a	As-prepared PMS-XXX with the same additives as PMS-XXX-APD but with different concentrations of the additives
PMS-XXX-APD-a-H	Heat-treated PMS-XXX-APD-a

[a] XXX refers to the batch number (e.g., 216, 217, etc.)

[b] PMS-217-AP2 and PMS-219-AP2 were prepared from the original stock solutions PMS-217-AP and PMS-219-AP, respectively; PMS-218-AP2 was prepared by increasing the amount of PSZ in the solution to 14.5 wt% and DCP to 1 wt%; PMS-220-AP2 and PMS-221-AP2 contained type C PCS whereas PMS-220-AP and PMS-221-AP contained type B PCS;

molecular weight with heat treatment were much different among these polymers. PMS-235 showed a relatively small increase in molecular weight after holding for 168 h at 130°C. Despite an initial molecular weight similar to PMS-235, PMS-236 showed a much larger increase in molecular weight after heat treatment. (PMS-231 showed an even larger increase in molecular weight with heat treatment, but this is not surprising considering the high initial molecular weight.)

The occurrence of aging in the polymers is shown by the observation that the molecular weight of PMS polymer (PMS-231) increased significantly upon storage at room temperature (under nitrogen) for 260 days. M_n increased from 1350 to 3,000 and M_w from 3,000 to 21,000 (see Figure 4.88).

Table 4.21 shows conditions for heat treatment of PMS polymers containing both PSZ and DCP additives (first six entries). Heat treatment was carried out at temperatures in the range of 50-150°C in a teflon container encased in a pressure bomb, as described in section 3.2.4. Increases in molecular weight were obtained, but there were also increases in polydispersity. This was true for almost all heat treatments which resulted in significant increases in molecular weight. (An exception was for the heat treatment of PMS-235, as shown in Table 4.21.) Although data is limited, the increases in the molecular weight and polydispersity after heat treatment appeared to be greater when the PSZ (5-14.5 wt%)/DCP (0.5-1.5 wt%) additives were used. Figure 4.89 shows a plot of polydispersity index vs. weight average molecular weight for these polymers before and after heat treatment. Figures 4.90a and 4.90b show GPC molecular weight distributions of polymer PMS-214-A and PMS-214-A-H (before and after heat treatment, respectively). The heat-treated polymer shows a bimodal distribution. The modes for the low molecular weight portions of the polymers remain in nearly the same position before and after heat treatment. It is clear from these

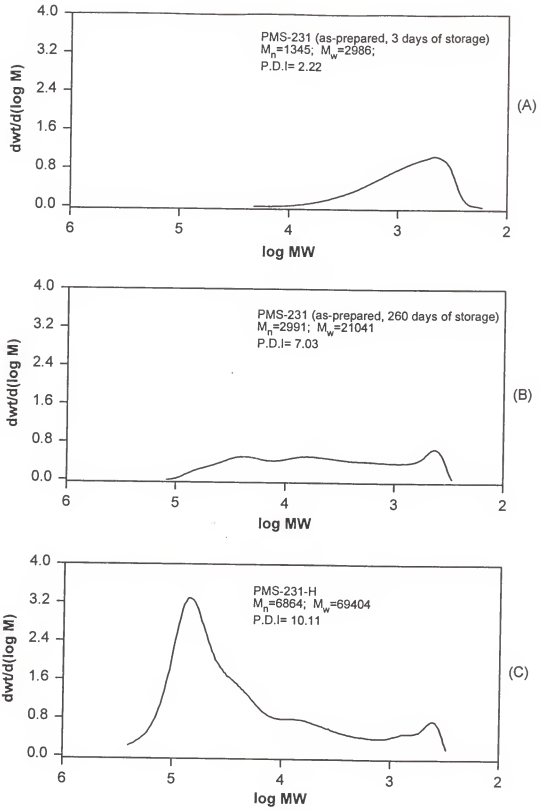

Figure 4.88. Gel permeation chromatograms for PMS-231 polymer: (A) after 3 days of storage, (B) after 260 days of storage, and (C) after heat treatment (PMS-231-H).

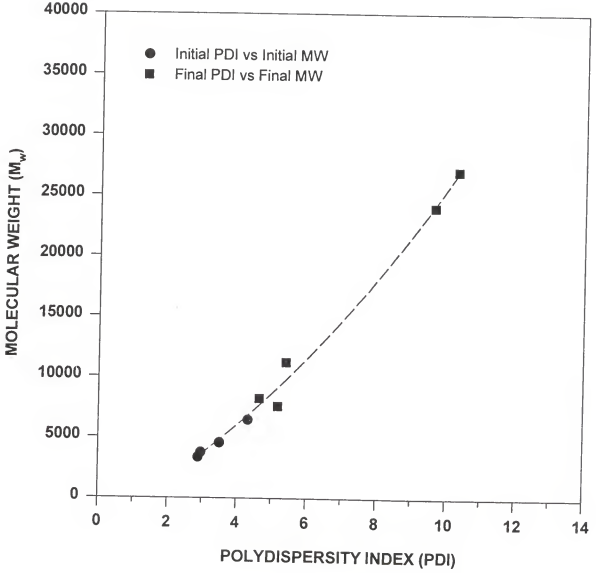

Figure 4.89. Polydispersity index vs. molecular weight for PMS polymers containing 5-14.5 wt% PSZ (and 0.5-1.5 wt% DCP) as additives.

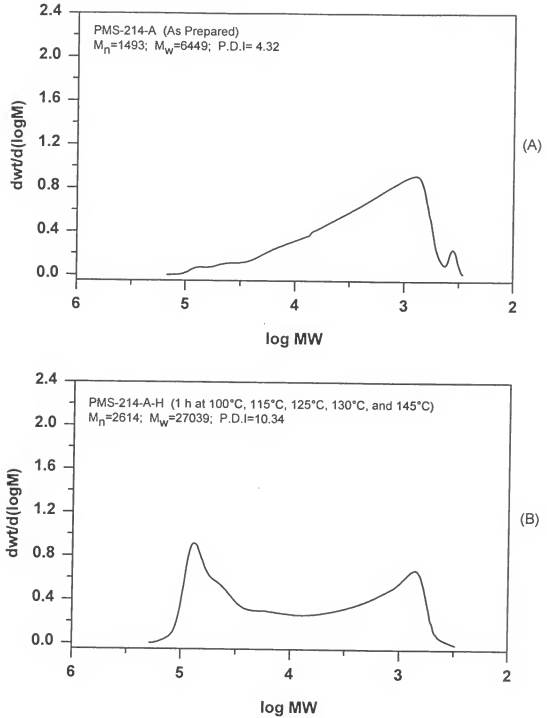

Figure 4.90. GPC molecular weight distributions for: (A) PMS-214-A and (B) PMS-214-A-H.

observations that not all of the molecules which form during the initial polymerization reaction participate in the polymerization/cross-linking reactions that lead to the increased average molecular weight after heat treatment.

Figures 4.91a, 4.91b, and 4.92 show GPC molecular weight distributions for PMS-216-A, PMS-216-A-H, and PMS-216-A2-H, respectively. (PMS-216-A2 was prepared at the same time as PMS-216-A, and had a composition identical to that of PMS-216-A. These polymers contained 5 wt% PSZ and 0.5 wt% DCP as additives.) PMS-216-A2-H showed a larger increase in molecular weight than PMS-216-A-H. This is presumably due to higher heat treatment temperature (105°C vs. 85°C). As noted earlier, however, it was observed that PMS polymers can undergo aging during storage (e.g., molecular weight increases were observed upon room temperature storage.) Although the PMS-216-A and PMS-216-A2 listed in Table 4.21 are different portions of the same solution, heat treatment to produce PMS-216-A2-H was carried out 28 days after the heat treatment was carried out to produce PMS-216-A-H. (Thus, PMS-216-A2 solution was aged for 28 days longer than PMS-216-A prior to heat treatment.) Hence, it is possible that the initial molecular weight for PMS-216-A2 may have been higher than that of PMS-216-A. (In fact, this is suggested from the higher initial viscosity (1.90 mPa•s vs. 1.84 mPa•s), although the difference may be within the experimental error of the measurement.) Therefore, the higher final viscosity and molecular weight for the PMS-216-A2-H may reflect not only the higher heat treatment temperature, but also a higher initial molecular weight due to the longer aging time prior to heat treatment.

The molecular weight distributions remained essentially monomodal for the heat-treated PMS-216-A-H and PMS-216-A2-H polymers. This may be due to the fact that overall increases in molecular weight for these samples were much smaller than the PMS-214-A-H sample. The changes in molecular weight upon heat treatment (100°C, 1

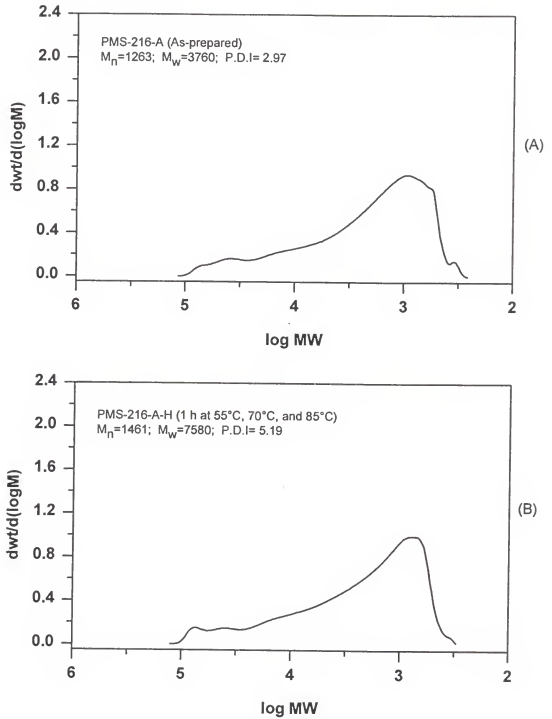

Figure 4.91. GPC molecular weight distributions for: (A) PMS-216-A and (B) PMS-216-A-H.

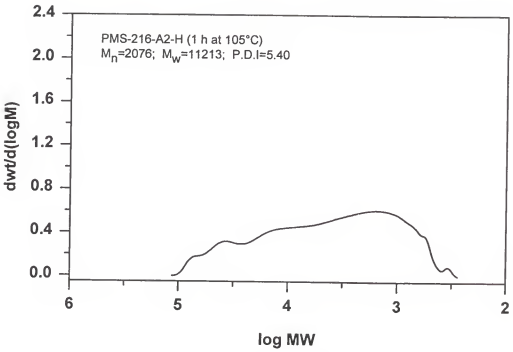

Figure 4.92. GPC molecular weight distribution for PMS-216-A2-H.

h) of PMS-217-A with 5 wt% PSZ were similar to PMS-216-A. Figures 4.93a and 4.93b show GPC molecular weight distributions before and after heat treatment for a PMS-219-A solution (which contained 14.5 wt% PSZ and 1.5 wt% DCP as additives). The increase in molecular weight upon heat treatment was similar in magnitude to that observed in the PMS-214-A-H sample. (Hence, the bimodality in the molecular weight distribution was clearly observed.) The large increase in molecular weight upon heat treatment of the PMS-219-A solution probably reflects the high temperatures used (i.e., 140 and 150°C, which is similar to the maximum temperature used with PMS-214-A). (There is no clear evidence from this study if the higher PSZ and DCP concentrations had any effect on the extent of the molecular weight increase during heat treatment.)

Table 4.21 also shows results of heat treatment for PMS polymers containing 3-6 wt% DB and 0.25-3.0 wt% PSZ. When DB was present, the polymer solutions showed significant increases in viscosity and often gelled. The polymer solution often changed in color from yellow to brown during the heat treatment. The molecular weight distributions were determined before and after heat treatment in only one case (i.e., for samples prepared with PMS-223-AD2, as shown in Figures 4.94a and 4.94b). No significant difference in molecular weight distribution was observed upon heat treatment, despite the observed increase in viscosity for the heat-treated solution. The reason for this behavior is not known.

Table 4.23 shows the heat treatment conditions used and the resulting effects on the solution viscosity and the polymer molecular weight for PMS/PCS polymer blends (70:30 proportion by weight) containing various additives (PSZ, DCP, and/or DB). The molecular weights of the PCS polymers used in the heat treatment experiments are given in Table 4.24. First consider the results for PMS-216-AP, PMS-217-AP, and PMS-217-AP2. The starting solutions for these samples all contained the same type and

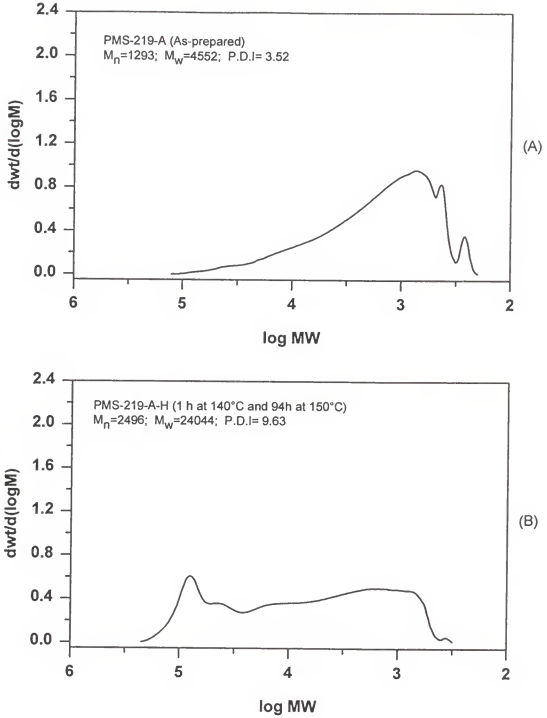

Figure 4.93. GPC molecular weight distributions for: (A)PMS-219-A and (B) PMS-219-A-H.

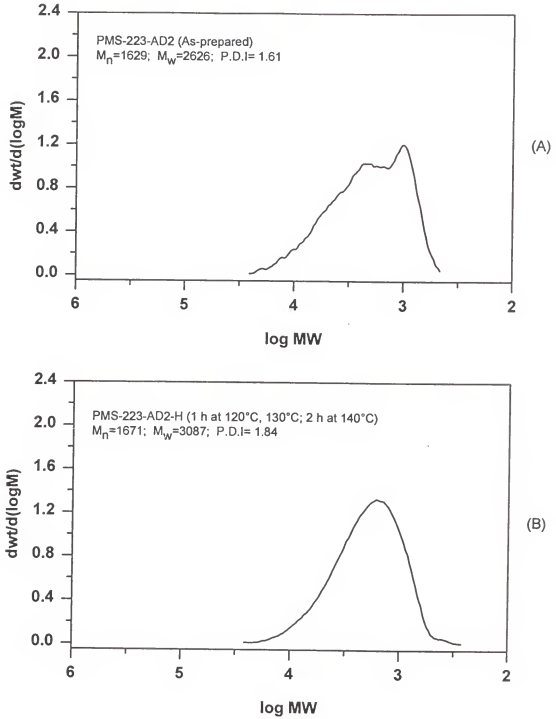

Figure 4.94. GPC molecular weight distributions for: (A) PMS-223-AD2 and (B) PMS-223-AD2-H.

Table 4.23. Conditions and results of heat treatment for PMS/PCS polymer blends¶.

Polymer batch	Additives (wt%)				Heat treatment conditions time(h)(temp°C)	Initial viscosity mPa·s	Final viscosity mPa·s	% viscosity change	Initial M_n †	Initial M_w †	Initial PDI	Final M_n	Final M_w	Final PDI
	PCS§	PSZ	DB	DCP										
PMS-216-AP	30 [A]	5	-	0.5	1 (85)	1.78	2.29	29	1303	3431	2.63	1577	8104	5.13
PMS-217-AP	30 [A]	5	-	0.5	1 (100)	1.93	2.71	41	1216	3279	2.69	1779	9340	5.25
PMS-217-AP2††	30 [A]	5	-	0.5	1 (105,115)	2.16	4.13	80	*	*	*	2230	16164	7.24
PMS-218-AP	30 [B]	10	-	1	1 (85, 95, 110, 130, 140)	2.15	7.13	49	1320	5437	4.11	1977	22873	11.5
PMS-218-AP2	30 [B]	14.5	-	1.5	1 (140); 80 (150)	2.00	solution gelled		**					
PMS-219-AP	30 [B]	14.5	-	1.5	1 (150)	2.20	solution gelled		**					
PMS-219-AP2	30 [B]	14.5	-	1.5	1 (100)	2.00	solution gelled		**					
PMS-220-AP	30 [B]	14.5	-	1.5	1 (50, 65, 70)	1.87	solution gelled		**					
PMS-220-AP2	30 [C]	14.5	-	1.5	5 (70)	2.00	16.00	700	1347	6643	4.93	1789	12940	7.23
PMS-221-AP	30 [B]	14.5	-	1.5	4 (70)	2.00	solution gelled		**					
PMS-221-AP2	30 [C]	14.5	-	1.5	5.5 (70)	2.00	16.4	722	1304	5379	4.12	2316	26872	11.6
PMS-222-APD	30 [C]	1	1	1.5	1 (50)	1.90	1.95‡	3	1311	3732	2.85	1386	3977	2.87
PMS-222-APD-a †††	30 [C]	0.5	3	0.05	1 (50, 60, 70, 80, 90, 100, 110, 120, 130)	2.00	8.50	325	*	*	*	2683	12845	4.79
PMS-224-APD	30 [D]	0.25	6	0	2 (130)	1.80	solution gelled		**					
PMS-225-APD	30 [D]	0.25	6	0	1 (120, 130); 2.75 (140)	1.80	16	740	*	*	*	*	*	*

¶ solids-loading of starting polymer solution was 33 wt%

* Data not available

‡ Heat-treatment stopped after 1h as the solution turned cloudy

§ [A]: PCS143; [B]: PCS145; [C]: PCS144; [D] PCS213; the characteristics of these PCS polymers are shown in Table 4.24

† Molecular weight of PMS:PCS blend with additives

†† Molecular weight not measured separately for the second portion of PMS-217-AP

††† Molecular weight not measured separately for the second portion of PMS-222-APD

** Data not collected for gelled samples

Table 4.24. Molecular weight distributions of PCS polymers used in the heat treatment of PMS/PCS blends.

PCS batch	Molecular weight distribution		
	M_n	M_w	Polydispersity
PCS-143 (A)	2581	5912	2.29
PCS-145 (B)	2507	11049	4.41
PCS-144 (C)	1888	7870	4.17
PCS-213 (D)	2608	11220	4.30

amount of PCS (30 wt%, type A) and PSZ (5 wt%). The molecular weight distributions for the heat-treated polymers are shown in Figures 4.95, 4.96, and 4.97, respectively. The molecular weights increase with increasing heat treatment temperature (i.e., the maximum heat treatment temperatures were 85, 100, and 115°C, respectively). It is also observed from Figure 4.97 that the increase in molecular weight for the PMS-217-AP2 sample was large enough that the bimodality of the distribution became more pronounced. (PMS-217-AP and PMS-217-AP2 also showed a similar effect as noted in regard to PMS-216-A and PMS-216-A2, i.e., the solution which was aged longer before heat treatment (PMS-217-AP2) had a higher initial viscosity.)

PMS-218-AP had higher molecular weight (see Figure 4.98) compared to the PMS-216-AP, PMS-217-AP, and PMS-217-AP2. In addition, PMS-218-AP2 gelled upon heat treatment. One factor responsible for these effects was presumably the higher heat treatment temperatures (140-150°C); however, there were many other variables that were changed so it is not possible to draw any definitive conclusions. The initial molecular weight of the PMS/PCS blend, the molecular weight of the PCS, the amount of PSZ, and the amount of DCP were all higher for these two PMS-218 samples, i.e., compared to the corresponding PMS-216 and PMS-217 samples listed in Table 4.23. All of these could be factors contributing to the higher molecular weight of the heat-treated PMS-218-AP samples.

There is some evidence to indicate that using a PCS with higher molecular weight results in a heat-treated polymer with higher molecular weight. PMS-220-A solution was prepared from PMS-220 polymer with 14.5 wt% PSZ and 1.5 wt% DCP. PMS-220-AP was prepared by adding 30 wt% type B PCS to some PMS-220-A solution. PMS-220-AP2 was prepared by adding 30 wt% type C PCS to some PMS-220-A solution. Type C PCS has a lower molecular weight than type B PCS. (Despite this, the

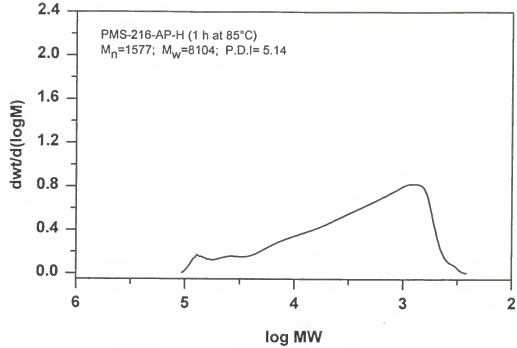

Figure 4.95. GPC molecular weight distribution for PMS-216-AP-H.

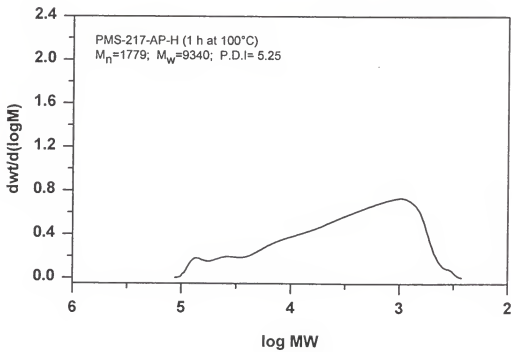

Figure 4.96. GPC molecular weight distribution for PMS-217-AP-H.

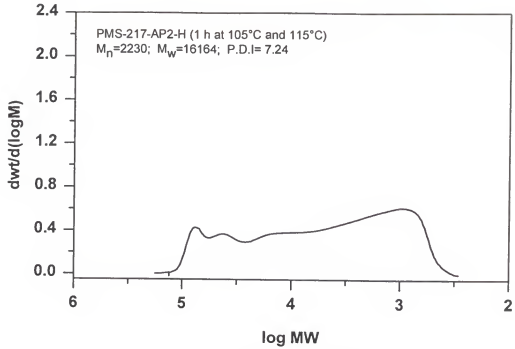

Figure 4.97. GPC molecular weight distribution for PMS-217-AP2-H.

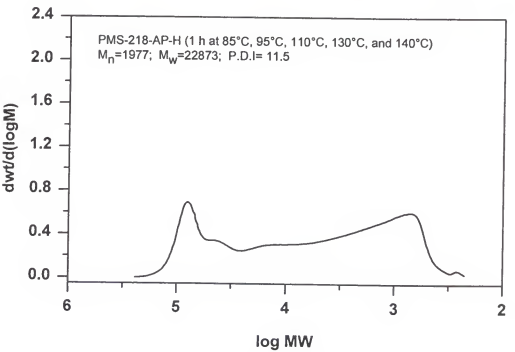

Figure 4.98. GPC molecular weight distribution for PMS-218-AP-H.

PMS-220-AP2 sample has a slightly higher initial viscosity compared to the PMS-220-AP sample. This may reflect the longer aging time for the PMS-220-A solution before the addition of the PCS.) After heat treatment, the sample prepared with higher-molecular-weight PCS (i.e., PMS-220-AP-H) gelled, even though the heat treatment time at the maximum temperature (70°C) was only 1 h. In contrast, the sample prepared with lower-molecular-weight PCS (i.e., PMS-220-AP2-H) had a molecular weight of only ~13,000, despite a heat treatment time of 5 h at 70°C. The molecular weight distribution for this sample is shown in Figure 4.99. The same effect was observed upon heat treatment of the PMS-221-AP and PMS-221-AP2 samples, i.e., the samples prepared with higher-molecular-weight PCS gelled despite a shorter heat treatment time at the maximum temperature. The molecular weight distribution for the heat-treated sample which was prepared with lower molecular weight PCS (i.e., sample PMS-221-AP2-H) is shown in Figure 4.100. (It is also noted that the bimodality in the distribution is more pronounced for PMS-221-AP2-H compared to PMS-220-AP2-H, which again is consistent with the higher overall average molecular weight for the former sample.)

It is noted that most of the samples in Table 4.23 that contained 14.5 wt% PSZ either gelled or showed significant increases in molecular weight, even at heat treatment temperatures as low as 70°C. Nevertheless, it is not possible to draw a definitive conclusion that high PSZ concentrations promote increases in molecular weight upon heat treatment because too many other variables were changed simultaneously in these experiments. For example, the DCP concentrations were also higher in these solutions. Furthermore, it is likely that there were significant variations in the characteristics of the starting PMS polymers.

In summary, heat treatment is effective in increasing the polymer molecular weight, but it was not possible to achieve these increases reproducibly. Furthermore,

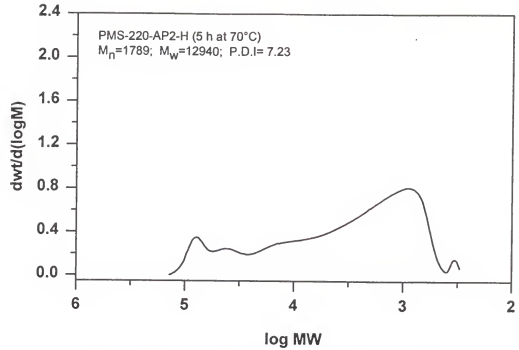

Figure 4.99. GPC molecular weight distribution for PMS-220-AP2-H.

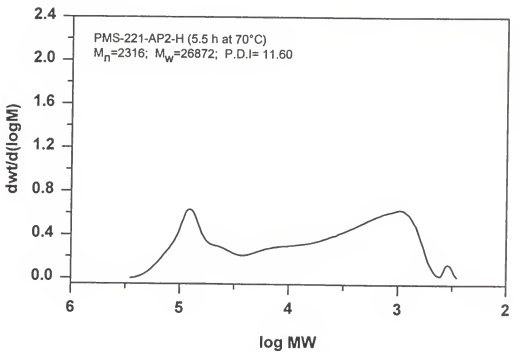

Figure 4.100. GPC molecular weight distribution for PMS-221-AP2-H.

heat-treated polymers have bimodal molecular weight distributions. This is undesirable for two reasons: First, the low-molecular-weight portions of the polymers would presumably be liquids (if they were isolated from the high-molecular-weight portions). As noted earlier, solid polymers are needed for fiber formation. Second, the higher molecular weight portions tend to make filtration of the polymer solutions difficult and tend to make the polymer solutions unstable toward gelation. Hence, these polymers are not particularly suitable for fiber formation.

4.3.1.2 Fractional precipitation

Fractional precipitation was carried out on polymer batches that were synthesized by reacting a mixture of MDCS and MTCS (in 70:30 wt% proportion) with sodium in a mixture of toluene and 1,4-dioxane at the reflux temperature of the solvent mixture. The toluene:1,4 dioxane volume ratios used were 60:40 for PMS-240, 40:60 for PMS-241, and 50:50 for PMS-242-F through PMS-255-F. (Toluene/dioxane was used for the synthesis because the polymer yields were much higher compared to polymers synthesized using toluene alone or a toluene/THF mixture, as reported in section 4.2.2.)

Qiu and Du [Qiu89] have reported that addition of a polar solvent such as tetrahydrofuran (THF) to a PMS polymer solution prepared with a less polar solvent (e.g., toluene) aids in the fractional precipitation of the polymer. They fractionally-precipitated the PMS polymer by adding a 50:50 (by volume) mixture of methanol and 2-propanol to the polymer dissolved in THF. Following this approach, the as-prepared polymer solutions in this study were first subjected to rotary evaporation under vacuum in order to remove the toluene and 1,4-dioxane solvents. After rotary evaporation, the flask containing the polymer was vented to N_2 to minimize contamination from air. Then, THF was added to the polymer in the proportions listed in Table 4.25.

Table 4.25. Conditions of fractional precipitation of PMS polymers.

Fractionated polymer designation	Polymer, non-solvents proportion	Non-solvent/ polymer ratio (ml/g)	THF/ polymer ratio (ml/g)	Non-solvent/ THF ratio (ml/g)	Initial M_n	Initial M_w	Initial PDI	Final M_n	Final M_w	Final PDI	Yield %	Melted Yes/ No
PMS-240-F	PMS-240 (6.73g) 2-propanol (150ml) methanol (150ml)	44.5	7.4	6.0	960	2395	2.49	2821	8443	2.99	44.5	No
PMS-241-F	PMS-241 (9.00g) 2-propanol (300ml) methanol (300ml)	66.7	5.5	12.0	899	1865	2.07	2119	4512	2.13	22.0	No
PMS-242-F	PMS-242 (8.33g) 2-propanol (150ml) methanol (150ml)	36.0	6.0	6.0	1653	3631	2.20	2200	5018	2.28	35.0	Yes (partial)
PMS-243-F	PMS-243 (10.5g) 2-propanol (150ml) methanol (150ml)	28.6	6.0	4.8	1004	2438	2.43	2555	5830	2.28	33.2	No
PMS-245-F-1	PMS-245 (4g) Acetone (100ml)	25.0	8.2	3.1	1055	2028	1.92	3153	6235	1.98	21.5	Yes (partial)
PMS-245-F-2	PMS-245 (5.45g) Acetone (110ml)	20.1	8.3	2.4	1126	2419	2.15	4493	11287	2.51	22.6	No
PMS-246-F	PMS-246 (8.15) Acetone (164.5ml)	20.1	7.7	2.6	1069	2469	2.31	5317	16370	3.08	19.2	No
PMS-247-F	PMS-247 (7.47g) Acetone (152ml)	20.3	8.8	2.3	1097	2276	2.07	7721	16719	2.17	7.0	No
PMS-248-F	PMS-248 (9.05g) Acetone (208ml)	23.0	4.5	5.1	1027	2287	2.33	2572	8734	3.40	26.1	No

Table 4.25. (cont'd.)

Polymer designation	Polymer, non-solvents proportion	Non-solvent/ polymer ratio (ml/g)	THF/ polymer ratio (ml/g)	Non-solvent/ THF ratio (ml/g)	Initial M_n	Initial M_w	Initial PDI	Final M_n	Final M_w	Final PDI	Yield %	Melted Yes/ No
PMS-249-F-1	PMS-249 (8.91g) Acetone (205ml)	23.0	6.4	3.6	977	2329	2.38	3635	6197	1.70	18.4	Yes (slight)
PMS-249-F-2‡	PMS-249 (8.28g) Acetone (166ml)	20.0	6.1	3.3	...	...	...	5700	10800	1.89	17.9	No
PMS-250-F	PMS-250 (9.00) Acetone (216ml)	24.0	4.5	5.3	1207	1919	1.59	2990	6173	2.06	19.2	No
PMS-251-F	PMS-251 (8.25g) Acetone (234ml)	28.4	4.5	6.3	1174	1981	2.01	2736	5513	2.01	27.7	No
PMS-252-F	PMS-252 (9.00g) Acetone (234ml)	26.0	4.5	5.7	1133	2118	1.87	2579	4488	1.74	27.1	No
PMS-253-F	PMS-253 (8.00g) Acetone (208ml)	26.0	4.5	5.8	975	1725	1.77	2691	7796	2.90	15.5	No
PMS-254-F	PMS-254 (8.00g) Acetone (208ml)	26.0	4.5	5.8	887	1857	2.09	2366	5270	2.23	21.8	No
PMS-255-F	PMS-255 (8.00g) Acetone (208ml)	26.0	4.5	5.8	971	2017	2.08	2280	5892	2.58	28.7	No

‡ PMS-249-F-1 was redissolved and fractional precipitation was attempted again.

Fractional precipitation was accomplished by using alcohols (for polymers PMS-240-F through PMS-243-F) and acetone (for polymers PMS-245-F-1 through PMS-255-F) as non-solvents. The alcohols used were 2-propanol and methanol in a 50:50 volume ratio. Fractional precipitation was carried out by adding the propanol/methanol mixture dropwise to the PMS polymer/THF solutions (which were vigorously stirred during the alcohol additions). Table 4.25 shows the proportions of PMS, non-solvent, and THF used in the fractionation experiments. Also shown are the initial and final PMS molecular weights (i.e., before and after fractionation), the polymer yield (i.e., the percentage of initial polymer which was recovered after fractionation), and the results of the "melt test" (see section 3.2.4).

Figures 4.101a and 4.101b show the GPC molecular weight distribution of PMS-240 before and after fractional precipitation using alcohols. The GPC molecular weight distributions for other alcohol-fractionated polymers are shown in Appendix I. It is evident from the figures that chromatogram of the fractionally-precipitated polymer is less skewed towards lower molecular weight end compared to the as-prepared polymer.

The as-prepared PMS polymers are viscous liquids. As noted earlier, it is necessary in SiC fiber preparation to use polymers which are solids at room temperature and which do not melt upon pyrolysis (i.e., so that the fiber retains its shape throughout the various processing steps). Table 4.25 shows that three of the four samples fractionated with the alcohol mixture did not melt upon pyrolysis, while one of the sample underwent partial melting.[¶]

[¶] A melt test was carried out by pyrolyzing chunks of dried polymer to 1000°C in a nitrogen atmosphere at 5°C/min. The polymer was considered to have undergone no melting if the pyrolyzed polymer retained sharp corners and edges. It was considered partially melted if some rounding of edges and corners occurred and if the pyrolyzed chunks were stuck to the alumina boat used for pyrolysis.

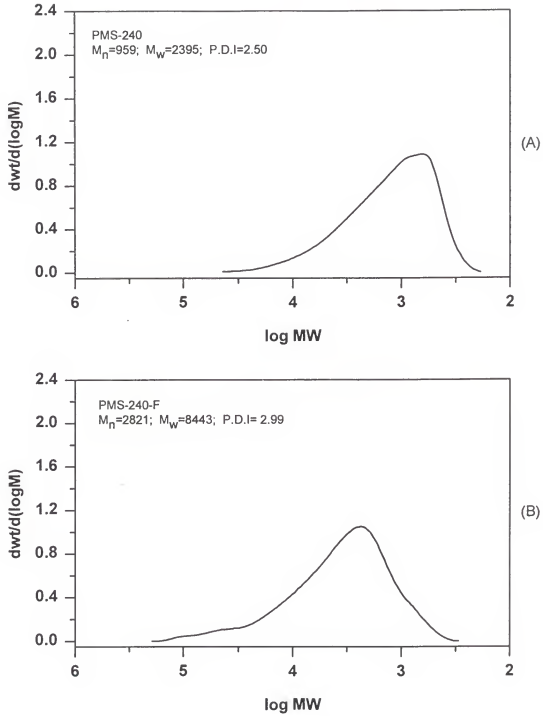

Figure 4.101. GPC molecular weight distributions for PMS-240 polymer (A) before and (B) after fractional precipitation with alcohol mixture.

Although fractional precipitation with the alcohol mixture allowed the preparation of PMS polymers with sufficiently high molecular weight for fiber processing, the method turned out to be unsatisfactory because it resulted in large amounts of oxygen contamination in the polymers. This was determined from EMA results that were obtained on a sample prepared by pyrolysis (1150°C in nitrogen) of PMS-243-F. Table 4.26 shows that the pyrolyzed sample contained ~30 wt% oxygen. It is presumed that this high oxygen content resulted from reactions that occurred between the alcohols and the PMS during the fractionation process. (Such reactions would incorporate hydroxyl groups (i.e., in the form of Si-OH groups) in the polymer. It is expected that the silanol groups would condense upon heat treatment to form siloxane bonds.)

The oxygen contents of the different polymers prepared by fractional precipitation with the alcohol mixture were not determined. However, it is speculated the oxygen content may be a factor that affects the melting behavior. The formation of siloxane bonds during the early stages of heat treatment would presumably result in a more highly cross-linked polymer which, in turn, would make the polymer less likely to melt upon pyrolysis. It is possible that the oxygen content of the precipitated polymers might vary due to differences in the starting PMS polymers (e.g., differences in the reactive Si-H groups) and/or the amount of alcohol (e.g., the alcohol/polymer ratio) used in the precipitation process.

Fractional precipitation was carried out using acetone because of the large amount of oxygen contamination that occurred when the alcohol mixture was used. Table 4.25 shows that the polymer yields obtained using acetone were in the range of 7-29%, i.e., less (in most cases) than yields obtained by using the alcohol mixture. However, the method was successful in producing PMS polymers with increased molecular weight. Figure 4.102 shows a plot of the average molecular weight after

Table 4.26. Results of Electron Microprobe Analyses (EMA) on fractionally-precipitated, 1000°C- pyrolyzed (nitrogen) polymers.

Sample	Description	Elemental composition						
		As-measured (wt%)				Normalized (wt%)		
		Si	C	O	Total	Si	C	O
PMS-243-F	Precipitated using alcohols	49.3 ±1.6	16.7 ±1.1	28.2 ±1.5	94.2 ±1.2	52.5 ±1.4	17.6 ±0.8	29.9 ±2.0
PMS-245-A	As-prepared polymer	69.4 ±1.6	26.0 ±3.7	2.2 ±1.8	97.6 ±3.4	71.2 ±1.5	26.6 ±2.9	2.3 ±1.9
PMS-245-F	Precipitated with acetone	70.6 ±1.1	30.4 ±0.5	0.20 ±0.4	101.2 ±1.1	69.7 ±0.5	30.1 ±0.4	0.20 ±0.4

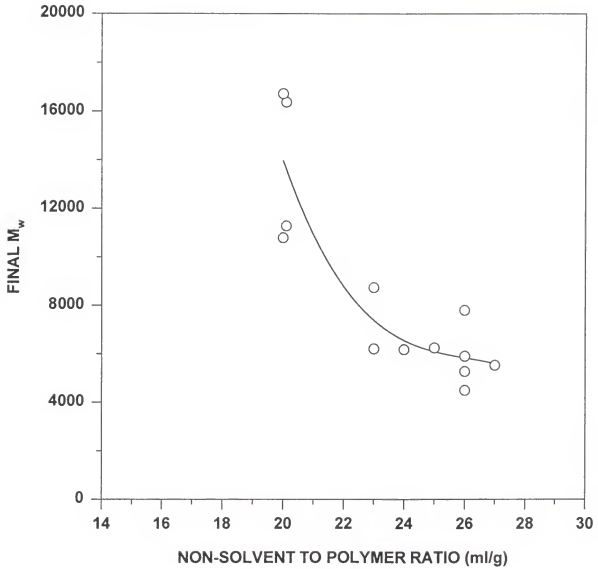

Figure 4.102. Plot of non-solvent to polymer ratio vs. final M_w for polymers precipitated using acetone as non-solvent.

fractional precipitation vs. the acetone/polymer ratio used in the process. The molecular weight generally increased as the acetone/PMS ratio decreased. (This is consistent with observations made for other fractional precipitation processes [Bil83].) Figure 4.103 shows an example of the change in the GPC molecular weight distribution after fractionation. (The GPC results for the other polymers fractionated with acetone are shown in Appendix J.)

The fractionated polymers prepared using acetone were not contaminated with oxygen[§]. This was illustrated by EMA measurements which were carried out on a pyrolyzed (1150°C in nitrogen) sample. Table 4.26 shows that the oxygen content of a sample pyrolyzed from PMS-245-F-1 was only 0.2 wt%. (Table 4.26 indicates that this is less than the oxygen content of a pyrolyzed sample prepared from the as-synthesized PMS-245 polymer. It is inconceivable that low-molecular-weight (e.g., oligomeric) portions of the PMS polymers (which are removed during fractionation) are the most susceptible to oxygen incorporation during exposure to oxygen and water vapor in the atmosphere. However, the difference in oxygen content observed between PMS-245 and PMS-245-F-1 is probably within experimental error. First, variations of at least 1-2% in the oxygen content have been observed in SiC fibers (prepared by pyrolysis of organosilicon polymers) when the same sample was re-analyzed by EMA at different times [Sal95]. Second, oxygen variations may occur due to differences in sample preparation. For example, different amounts of oxygen contamination may have occurred during pyrolysis of the polymers. More samples would need to be analyzed to

[§] There was some concern that the THF used in the precipitation process could adsorb some atmospheric moisture. In turn, this could lead to some hydrolysis reactions which incorporate hydroxyl groups in the PMS polymers. However, this apparently did not occur to any significant extent in the present study. This conclusion is based on the low oxygen content that was obtained for the pyrolyzed PMS-245-F-1 sample prepared by fractional precipitation using acetone.

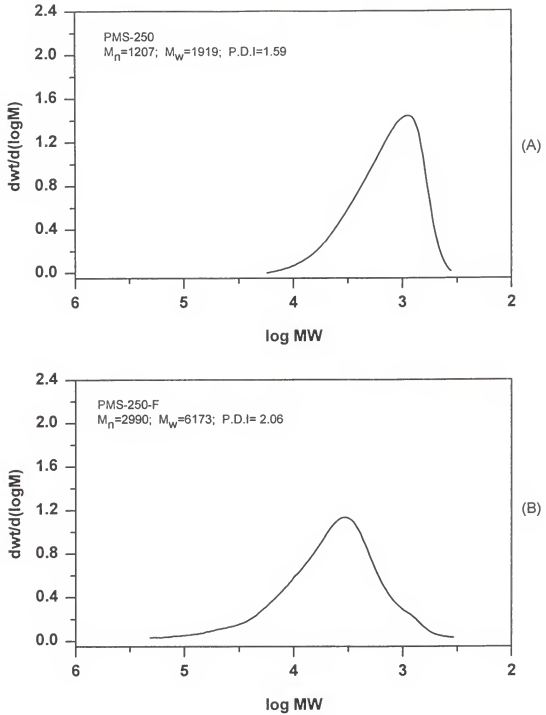

Figure 4.103. GPC molecular weight distributions for PMS-250 polymer (A) before and (B) after fractional precipitation with acetone.

determine if there really is a trend of lower oxygen content for the acetone-fractionated polymers.)

Table 4.25 shows that most of the acetone-fractionated polymers did not melt upon pyrolysis. However, some melting was observed for PMS-245-F-1 and PMS-249-F-1. It is unclear why these two polymers showed some melting, while several polymers with lower molecular weight (e.g., PMS-251-F, PMS-252-F, PMS-254-F, and PMS-255-F) did not. Even though starting molecular weights were all similar, there may be other differences in PMS characteristics (e.g., degree of branching, amount of Si-H groups) which affect the fractionation behavior and the precipitated polymer characteristics.

4.3.2. Spinning of fibers from PMS-based polymers

4.3.2.1 Spinning of fibers from as-prepared blends of PMS:PCS polymers

The earliest work on spinning of fibers in this study was carried out using blends of as-prepared (non-heat-treated) PMS and PCS polymers. Table 4.27 shows the conditions for fiber spinning experiments from PMS/PCS polymer blends (non-heat treated). Three PMS:PCS ratios were used in the spin dope preparation, viz., 25:75, 40:60, and 50:50. The amount of spinning additive, PSZ, used in all the fiber batches was 14.5 wt% (based on total amount of polymer, i.e., PMS+PCS+PSZ).

The PMS polymers used in these blends were stored in concentrated form. It was subsequently learned that these polymers were subject to significant aging effects (especially when stored in concentrated form) which was indicated by visual observations of "microgel" formation over time. ("Microgel" formation is attributed to latent polymerization and cross-linking reactions at reactive sites in PMS polymers.) Due to the microgel formation, most of the polymer solutions were either difficult to filter through 0.45 μm filters (e.g., spin batches UF-14s, UF-16s, UF-18s, UF-21s, and UF-22s) or they were filterable only through 1.0 μm filters (e.g., UF-24s through UF-27s).

Table 4.27. Conditions for fiber spinning experiments from as-prepared PMS:PCS polymer blends (non-heat treated).

Batch	Amount of PCS (g)	Amount of PMS (g)	PMS/PCS ratio (wt%)	PSZ[§] wt%	Filtration condition[¶] Filter (μm)/time (min)	Flow test time[‡] (s)	Final solids loading (%)	Viscosity (Pa·s)	Spin speed (rpm)	Pressure (psi)	Remarks
UF-11s	1.28	0.43	25:75	14.5	0.45/ 2	*	*	*	54	400	Spinning average
UF-21s	1.50	0.50	25:75	14.5	0.45/120 (3 sets)	45	*	*	84	260	Spun well
UF-25s	1.92	0.63	25:75	14.5	1/30	45	*	*	41	340	Spun poorly
UF-18s	0.98	0.65	40:60	14.5	0.45/30	40	*	*	54	360	Spun well
UF-22s	1.20	0.80	40:60	14.5	0.45/120 (3 sets)	60	*	*	54	450	Spun poorly
UF-24s	1.20	0.80	40:60	14.5	1.0/30	20	*	*	119	360	Spun well
UF-26s	1.20	0.80	40:60	14.5	1.0/30	44	*	*	119	360	Spun well
UF-27s	1.20	0.80	40:60	14.5	1.0/90	54	*	*	41	360	Spun poorly
UF-28s	2.10	0.80	40:60	14.5	0.45/1	48	91.3	182-154	41	400	Spun poorly
UF-12s	0.85	0.85	50:50	14.5	0.45/2	*	*	*	54	360	Spun poorly
UF-14s	0.78	0.78	50:50	14.5	0.45/30	11	*	*	54	200	Spun well
UF-16s	1.06	1.06	50:50	14.5	0.45/30	19	*	*	41	230	Spun well

‡ Flow test time is the time taken by the polymer solution to travel 2.5 cm at 45° angle. The measurement was done in a capped vial. The procedure is described in more detail in section 3.2.1.

* Data not available.

¶ Time taken for filtration through specified filter at 20 psi nitrogen pressure.

§ Percentage based on total amount of polymer (PMS+PCS+PSZ).

Flow test times were measured for spin batches as an indicator of the viscosity of the spin dopes. (See section 3.2.1 for the details of the flow test measurement.) The flow test was used instead of viscosity measurements for two reasons. First, the test does not consume material. (Rheological tests result in less material being available for spinning.) Second, rheological measurements result in additional exposure of the air-sensitive spin dope to the ambient atmosphere. The initial basis for choosing the flow test time was the prior experience with PCS polymer solutions. As discussed in section 4.1, flow times on the order of 10 s (with corresponding viscosities of ~35-40 Pa·s) were typically used for spinning. It was subsequently discovered (see below), however, that higher flow times (and viscosities) were required for spin dopes prepared with PMS/PCS in order to obtain both good spinning behavior and green fibers which were not stuck together after spinning.

Table 4.27 shows that three batches with 25:75 PMS:PCS composition were spun, i.e., UF-11s, UF-21s, and UF-25s. Only UF-21s spun well[‡] . UF-11s was the earliest spin batch prepared and spinning techniques were not yet perfected. (For example, winding of fibers was difficult due to air draft effects in the laboratory. Thus, subsequent experiments were carried out in a glove box.) UF-25s also spun poorly, but this was probably due to microgel particles in the spin dope. (The solution was only filterable through 1 μm (but not 0.45 μm) filters.)

Six batches of fibers were spun with the 40:60 PMS:PCS composition. Batches with high flow test times (i.e., ~48-60 s) did not spin well (e.g., UF-22s, UF-27s, and UF-28s). The remaining three fiber batches with relatively lower viscosity (i.e., flow test times of ~20-44 s) spun well. UF-24s, which had a flow test time of only 20 s, spun well,

[‡] Fiber spinning behavior was considered 'good' when there were: (i) fewer fiber breaks during spinning, (ii) the polymer easily fiberized and stretched, and (iii) a larger amount of fibers was collected.

but the as-spun fibers were stuck together. Figure 4.104 shows SEM micrographs fibers which illustrate 'necking' between the as-spun fibers. This may have been caused by insufficient solvent removal prior to collection of fibers on the winding drum. (The low flow test time indicates that more solvent was probably present in the spinning solution. This could lead to difficulties in removing enough solvent to "solidify" the fibers prior to collection on the winder.) The necking may also have been caused by flow of a liquid portion of the PMS polymer in the spin batch. (Lower molecular weight portions were liquids at room temperature.) However, the latter explanation seems less likely because adhesion of as-spun fibers were not observed for spin batches which had higher flow test times. Fibers from some of the spin batches (i.e., UF-18s and UF-26s) were flexible and easily separable after spinning, but became brittle and stuck together after pyrolysis. This was probably caused by melting of portions of PMS polymers. Figure 4.105 shows that necks formed after pyrolysis of the UF-26s fibers.

Batches prepared with a 50:50 PMS:PCS composition (UF-12s, UF-14s, and UF-16s in Table 4.27) developed severe problems with adhesion between as-spun fibers and between as-spun fibers and the winding drum. This may have been due to flow of the liquid portion of the PMS polymers in the spin batches. It is also possible that the solvent evaporation rate was slower in these batches. (This would result in flow of the fibers due to a high residual liquid content.)

Table 4.28 shows the fiber diameters and tensile strengths of SiC fibers prepared by spinning PMS/PCS polymer blends (non-heat treated) and pyrolyzing the as-spun fibers under the conditions indicated. The fiber tensile strengths decreased with increasing amount of PMS in the spin batch. Fiber batches prepared with 50% PMS were too weak and brittle to be tested. Table 4.28 shows that fiber batches prepared with 25:75 PMS:PCS, and pyrolyzed at 1000°C, had an average tensile strength of 1.85

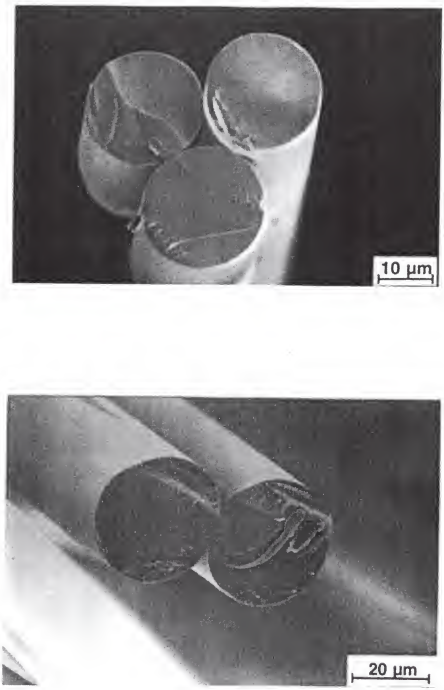

Figure 4.104. SEM micrographs of as-spun fibers (batch UF-24s) prepared from PMS/PCS blends (non- heat treated) showing necking.

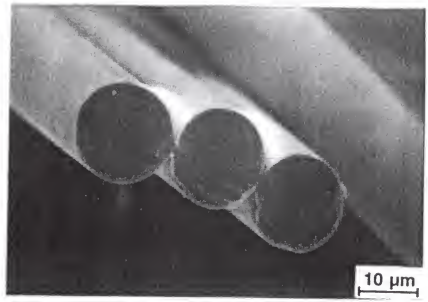

Figure 4.105. SEM micrographs of pyrolyzed fibers (batch UF-26s) prepared from PMS/PCS blends (non-heat treated) showing necking.

Table 4.28. Tensile strengths of SiC fibers spun from as-prepared PMS:PCS polymer blends.

Designation	PMS/PCS ratio (wt%)	Heat treatment temperature (°C)	Heat treatment atmosphere	# of fibers tested	Fiber diameter (μm)	Tensile strength (GPa)
UF-11s	25:75	1000	N_2	14	13.9 ± 2.0	2.11 ± 0.46
UF-11s	25:75	1500	Ar	10	14.3 ± 1.1	1.53 ± 0.38
UF-21s	25:75	1000	N_2	14	14.4 ± 1.9	1.92 ± 0.57
UF-25s	25:75	1000	N_2	15	14.4 ± 1.1	1.65 ± 0.38
UF-18s	40:60	1000	N_2	11	19.2 ± 8.3	0.96 ± 0.51
UF-22s	40:60	1500	Ar	8	18.9 ± 2.1	0.33 ± 0.13
UF-24s	40:60	1000	N_2	12	13.6 ± 1.9	1.48 ± 0.47
UF-24s	40:60	1500	Ar	10	13.5 ± 1.5	1.03 ± 0.51
UF-26s	40:60	1000	N_2	12	15.0 ± 2.2	1.33 ± 0.51

GPa, whereas fiber batches prepared with 40:60 PMS:PCS ratio (and also pyrolyzed at 1000°C) had an average tensile strength of 1.26 GPa. (Some of the fiber batches with 40:60 PMS:PCS ratio, such as UF-27s and UF-28s, were too weak to be tested.) Table 4.28 also shows that fibers heat-treated at 1500°C had lower strengths than the corresponding fibers heat-treated to 1000°C.

In summary, it was not possible to prepare high strength SiC fibers from as-prepared PMS/PCS polymer blends. A higher molecular weight (more cross-linked), infusible PMS polymer was needed to avoid adhesion problems between as-spun fibers and melting of fibers during pyrolysis.

4.3.2.2 Spinning of heat-treated PMS polymers and PMS/PCS polymer blends

Table 4.29 shows conditions and some qualitative results for fiber spinning experiments carried out using heat-treated polymers. PMS:PCS blends of 40:60, 60:40, 70:30, 90:10, and 100:0 were used in making spin dopes. The blends were prepared by two methods: (1) PMS polymers were heat-treated separately and mixed with as-prepared PCS in the desired ratio and (2) As-prepared PMS and PCS were mixed initially in the desired proportions and then the mixture was heat-treated.

Three spin dopes (UF-33s, UF-35s, and UF-36s) were prepared by method 1 using a 40:60 PMS:PCS mixture. The rheological flow behavior of these spin dopes is shown in Figures 4.106, 4.107, and 4.108. All three batches spun well. However, the UF-33s spin dope, which had a significantly lower viscosity (19-25 Pa·s) compared to the UF-35s (110-118 Pa·s) and UF-36s (55-71 Pa·s) spin dopes, produced as-spun fibers which were stuck together. In contrast, fibers from the other two spin dopes were easily separated. It is interesting to note UF-33s had much higher solids loading (87.1 wt%) despite the lower viscosity compared to the other two batches (which had solids loadings of 69.7 and 73.0 wt%, respectively). This is attributed to a lower molecular

Table 4.29. Conditions and qualitative results for fiber-spinning experiments from heat-treated PMS and PMS/PCS blends.

Batch	PMS used	PCS added		PMS: PCS ratio	Wt% PSZ added[a]	Wt% DB added		Filtration behavior[b]	Flow test time(s)	Solids loading (%)	Viscosity (Pa·s)	Spin speed (rpm)	Spin pressure (psi)
		Before heat-treatment	After heat-treatment			Before heat treatment	After heat treatment	Filter (μm)/ time(min)					
UF-33s	PMS-217-A-H	*	PCS 143	40:60	5	0	0	0.45/ 10	46	87.1	25-19	41	350
	Spun well; as-spun fibers stuck together.												
UF-35s	PMS-216-A2-H	*	PCS 145	40:60	5	0	0	1.0/10	31	69.7	118-110	119	300
	Spun well; as-spun and pyrolyzed fibers separable.												
UF-36s	PMS-218-A-H	*	PCS 145	40:60	10	0	0	0.45/35	37	73.0	71-55	54-69	300-325
	Spun well; as-spun and pyrolyzed fibers separable.												
UF-39s	PMS-219-A-H	*	PCS 145	60:40	14.5	0	0	1.0/15	24	66.4	*	69-84	200
	Spun well; as-spun fibers and pyrolyzed fibers separable.												
UF-31s	PMS-216-AP-H	PCS 143	*	70:30	5	0	0	0.45/10	48	75.0	59-55	41	450
	Spun well; as-spun fibers separable but pyrolyzed fibers stuck together.												
UF-32s	PMS-217-AP-H	PCS 143	*	70:30	5	0	0	0.45/60 (3 sets)	49	90.0	82-78	41	450
	Spun well; as-spun fibers separable but pyrolyzed fibers stuck together.												
UF-34s	PMS-217-AP2-H	PCS 143	*	70:30	5	0	0	1.0/10	42	69.0	78-70	54-84	450-500
	Spun poorly; as-spun fibers but pyrolyzed fibers were brittle.												

Table 4.29. (Cont'd.)

Batch	PMS used	PCS added		PMS: PCS ratio	Wt% PSZ added[a]	Wt% DB added		Filtration behavior[b] Filter (μm)/ time(min)	Flow test time(s)	Solids loading (%)	Viscosity (Pa·s)	Spin speed (rpm)	Spin pressure (psi)
		Before heat-treatment	After heat-treatment			Before heat treatment	After heat treatment						
UF-37s	PMS-218-AP-H	PCS 145	*	70:30	10	0	0	0.45/10	32	69.7	57-45	28	350-375
	Spun well; as-spun fibers separable but pyrolyzed fibers were brittle.												
UF-40s	PMS-220-AP-H	PCS 145	*	70:30	14.5	0	0	0.45/40	24	87.0	38	*	*
	Spin dope gelled during storage												
UF-41s	PMS-219-AP-H	PCS 145	*	70:30	14.5	0	0	1.0/10	*	*	*	*	*
	Spin dope gelled during solution preparation												
UF-42s	PMS-220-AP2-H	PCS 145	*	70:30	14.5	0	0	0.45/180 (3 sets)	30	70.0	125-50	194	200
	Spun well; as-spun and pyrolyzed fibers were separable.												
UF-43s	PMS-221-AP2-H	PCS 144	*	70:30	14.5	0	0	0.45/35	*	*	*	*	*
	Spin dope gelled during solution preparation.												
UF-44s	PMS-222-APD-H	PCS 144	*	70:30	1	0	1	0.45/20	34	77.4	23-19.5	69-84	350
	Spun well; as-spun fibers separable but pyrolyzed fibers stuck together.												
UF-45s	PMS-222-APD-a-H	PCS 144	*	70:30	0.5	3	3	0.45/8	31	62.3	52-20	*	300-450
	Spun poorly; only fragments of fibers collected.												

Table 4.29. (cont'd.)

Batch	PMS used	PCS added		PMS: PCS ratio	Wt% PSZ added[a]	Wt% DB added		Filtration behavior[b] Filter (μm)/ time(min)	Flow test time(s)	Solids loading (%)	Viscosity (Pa·s)	Spin speed (rpm)	Spin pressure (psi)
		Before heat-treatment	After heat-treatment			Before heat treatment	After heat treatment						
UF-53s	PMS-225-APD-H	PCS 213	*	90:10	0.25	0	6	0.1/35 (2 sets)	43	63.6	50-30	*	350
	Spun poorly; no fibers collected.												
UF-56s	PMS-225-AD2-H	*	PCS 213	90:10	0.25	3	3	0.45/90	38	62.2	41-16	119	200-250
	Spun poorly; as-spun fibers separable but pyrolyzed fibers brittle.												
UF-57s	PMS-226-AD-H	*	PCS 213	90:10	0.25	3	3	0.45/90	48	57.5	48-10	*	150-175
	Not spinnable												
UF-29s	PMS-214-A-H	*	*	100:0	5	0	0	0.45/10	46	87.1	25-18.6	28	450
	Spun poorly; as-spun fibers stuck together.												
UF-30s	PMS-216-A-H	*	*	100:0	5	0	0	0.45/10	41	82.0	23	54	450
	Spun poorly; as-spun fibers stuck together												
UF-38s	PMS-219-A-H	*	*	100:0	14.5	0	0	Centri-fuged[c]	18	69.1	*	54	300
	Spun well; as-spun fibers stuck together.												
UF-49s	PMS-223-AD-H	*	*	100:0	0.25	6	0	0.45/45 (3 sets)	*	*	*	*	*
	Spin dope gelled during processing.												

Table 4.29. (Cont'd.)

Batch	PMS used	PCS added		PMS: PCS ratio	Wt% PSZ added[a]	Wt% DB added		Filtration behavior[b] Filter (μm)/ time(min)	Flow test time(s)	Solids loading (%)	Viscosity (Pa·s)	Spin speed (rpm)	Spin pressure (psi)
		Before heat-treatment	After heat-treatment			Before heat treatment	After heat treatment						
UF-52s	PMS-223-AD2-H	*	*	100:0	0.25	6	0	0.45/45 (3 sets)	27	69.6	29-21	164-179	225-250
	Spun well; as-spun fibers separable but pyrolyzed fibers brittle.												
UF-54s	PMS-225-AD-H	*	*	100:0	0.25	6	0	0.1/35 (2 sets)	42	67.9	60-21	*	200-500
	Not spinnable.												

[a] PSZ added before heat-treatment.
[b] Time taken for filtration through specified filter at 20 psi nitrogen pressure.
[c] To conserve material, this particular heat-treated polymer solution was centrifuged at 20,000 rpm for 20 min to remove microgels.

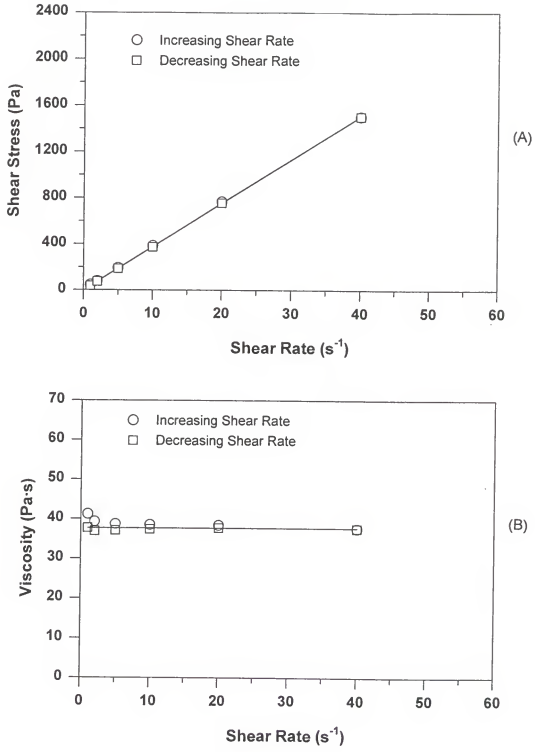

Figure 4.106. Plots of (A) shear stess vs. shear rate and (B) viscosity vs. shear rate for UF-33s spin dope.

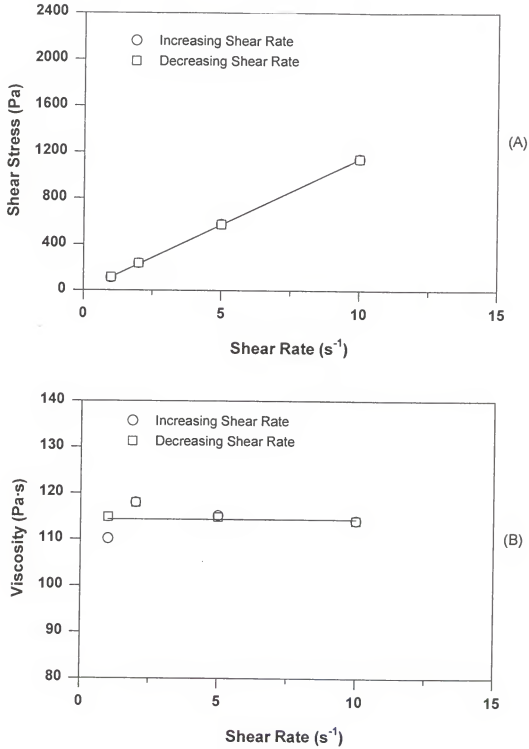

Figure 4.107. Plots of (A) shear stress vs. shear rate (B) viscosity vs. shear rate for UF-35s spin dope.

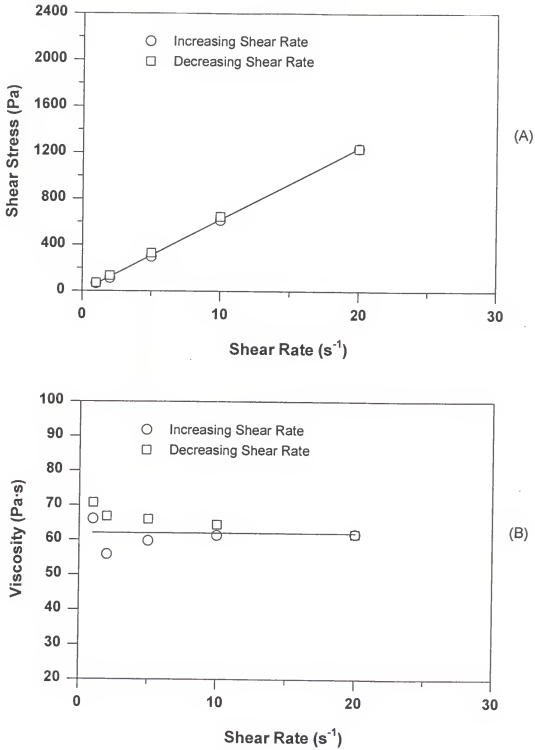

Figure 4.108. Plots of (A) shear stress vs. shear rate (B) viscosity vs. shear rate for UF-36s spin dope.

weight for the PMS polymer. (For example, as discussed in section 4.3.1.1 (Table 4.21), PMS-217-A-H (used in UF-33s) has lower molecular weight than PMS-216-A2-H (used in UF-35s) .)

One spin batch (UF-39s) was prepared by method 1 using a 60:40 PMS:PCS composition. It spun well but had a relatively low solids loading (66.4%). (This is presumably due to the high molecular weight of the starting PMS (PMS-219-A-H), see section 4.3.1.1.) The GPC plot in Figure 4.93 shows the typical bimodal molecular weight distribution observed in PMS polymers which have been heat-treated to effect significant increases in average molecular weight. The high molecular weight portion of the polymer resulted in difficulties in filtering the spin batch. (The solution could pass through 1.0 μm filters but not 0.45 μm filters.)

Table 4.29 also shows characteristics of 10 spin batches prepared by method 2 using 70:30 PMS:PCS compositions. As noted previously, concentrated PMS solution tends to age (i.e., increase in viscosity and/or gel) upon storage. Hence, several of the spin dopes (UF-40s, UF-41s, and UF-49s) gelled during spin batch preparation or during storage prior to fiber spinning. The PMS used in spin batches UF-31s and UF-32s, viz., PMS-216-AP-H and PMS-217-AP-H, had similar molecular weight characteristics (see the GPC plots - Figure 4.95 (PMS-216-AP-H) and Figure 4.96 (PMS-217-AP-H), respectively, in section 4.3.1.1). UF-32s had a higher solids loading (~90%). In addition, it was much more difficult to filter the polymer solution (PMS-217-AP-H) through 0.45 μm filters. (The reason for these observations is not clear. UF-32s was prepared with a higher viscosity but it is unlikely that this alone would account for such a large difference in solids loading and filtration behavior.) Both UF-31s and UF-32s batches spun well. The as-spun fibers of these batches were separable but they stuck together after pyrolysis. This is likely due to the fact that low molecular weight components in the

starting PMS polymers (for both UF-31s and UF-32s) melted during pyrolysis and caused the fibers to stick together. Spin batch UF-37s also spun well, but the pyrolyzed fibers were brittle after pyrolysis. This is also presumably due to melting of low molecular weight components in the polymer. (It may be recalled from the discussion in section 4.3.1.1 that even though the average molecular weight of PMS-218-AP-H was high ($M_w \approx 23{,}000$), it had a bimodal molecular weight distribution. Hence, melting of low molecular weight components in the polymer could still have occurred.)

Spin batches UF-34s and UF-45s spun poorly. The polymer used in UF-34s (PMS-217-AP2-H) had a high starting molecular weight ($M_w \approx 16{,}200$), and the spin dope was also not filterable through sub-micron filters. The solids loading was also relatively low (69%) for this spin dope. In the case of UF-45s, the starting polymer used (PMS-222-AD-H) had a molecular weight of ≈12,800 (i.e., lower than the molecular weight of the polymer used in UF-34s) and the spin dope filtered through 0.45 μm filter relatively easily. However, the spin dope was shear thinning (i.e., the viscosity decreasing from ~52 to ~20 Pa·s as shear rate increased from 1 to 40 s^{-1}, respectively) (see Figure 4.109). Also, the spin dope had a low solids loading (62.3%). The low solids loading suggests that the polymer is highly cross-linked. As indicated in Table 4.23, the starting polymer used for this spin dope contained 3 wt% DB. It is possible that DB led to the development of polymers which have a highly branched, network-type structure. Weakly associated polymers in such a structure may break apart under shear and, hence, shear thinning flow behavior would be observed in rheological measurements. The structure (i.e., network character) in these solutions imparts a more elastic character which is apparently related to the poor spinnability. Similar observations (i.e., difficulty in spinning

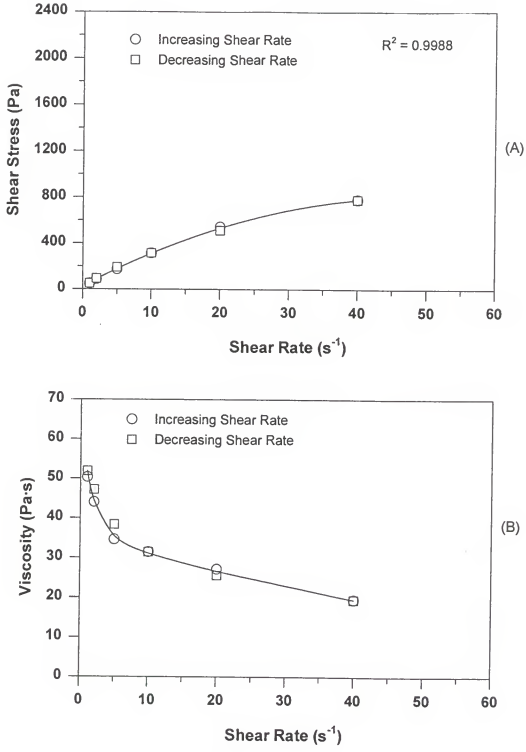

Figure 4.109. Plots of (A) shear stress vs. shear rate (B) viscosity vs. shear rate for UF-45s spin dope.

fibers from shear thinning and thixotropic solutions) have been reported previously [Sac86].

Spin batch UF-42s also exhibited highly shear thinning rheological flow behavior (Figure 4.110). However, unlike UF-45s, this batch spun well. The UF-42s batch was prepared with no DB and the PMS polymer used in the batch had been prepared with 14.5 wt% PSZ during heat treatment. In contrast, the UF-45s batch was prepared with 3 wt% DB and the PMS polymer used in the batch had 0.5 wt% PSZ and 3 wt% DB during heat treatment. The higher solids loading in batch UF-42s suggests that the polymers develop a less cross-linked structure. However, it is not understood why the solution still shows such highly shear thinning behavior.

Three spin batches (UF-53s, UF-56s, and UF-57s) were prepared with 90:10 PMS:PCS polymer blends. These spin batches either spun poorly or could not be spun at all. The spin batches had low solids loading and rheological flow behavior was highly shear thinning (typical rheological flow behavior is shown in Figure 4.111 for UF-56s). As discussed earlier in the case of the UF-45s spin batch, the poor spinning behavior may have been caused by highly shear thinning behavior of the spin dopes.

Six spin batches were prepared with 100% heat-treated PMS polymer. Fiber batches UF-29s and UF-30s spun poorly. The spin dopes used for these batches had low viscosities (~25 Pa·s) and the as-spun fibers stuck together. Fiber batch UF-38s spun well, but the as-spun fibers also stuck together. Rheological measurements were not made (due to limited amount of spin dope) for this spin batch but the low flow test time indicated that the viscosity was probably too low. Spin batches UF-49s, UF-52s, and UF-54s were prepared using PMS polymers which were heat-treated with 6 wt% DB. As discussed in section 4.3.1.1, these polymers had a tendency towards gelation. Hence, it was not surprising that it was difficult to prepare stable spin dopes with these

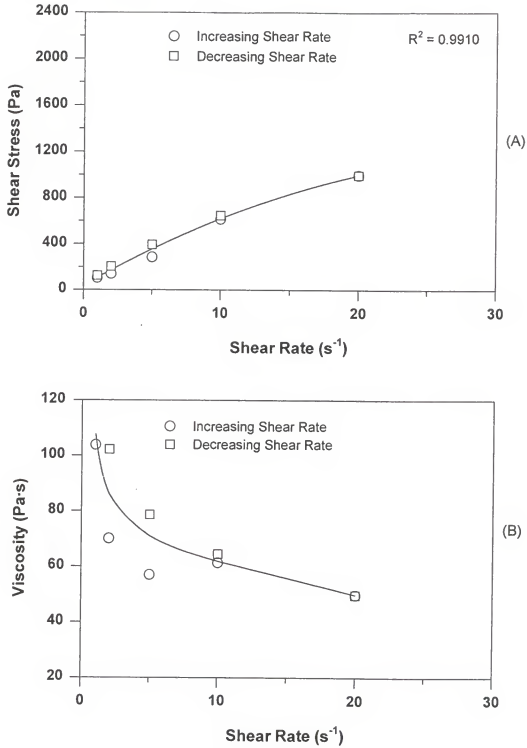

Figure 4.110. Plots of (A) shear stress vs. shear rate (B) viscosity vs. shear rate for UF-42s spin dope.

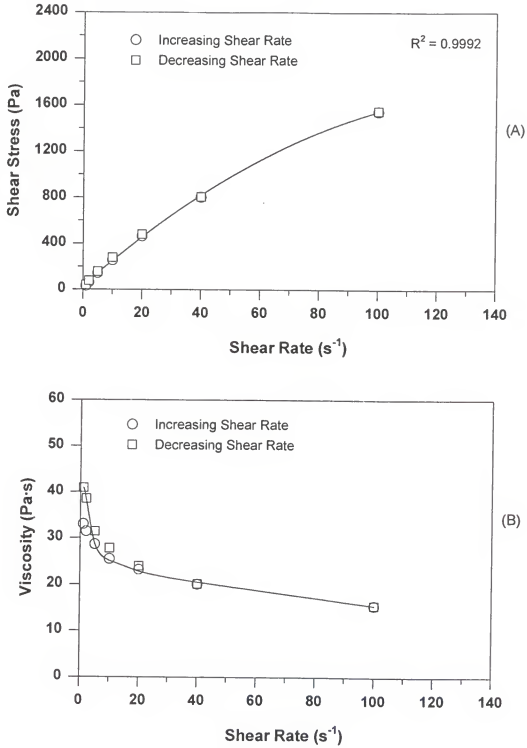

Figure 4.111. Plots of (A) shear stress vs. shear rate (B) viscosity vs. shear rate for UF-56s spin dope.

polymers. UF-49s gelled during spin dope preparation. The UF-54s spin dope was shear thinning (see Figure 4.112) and it was not spinnable at all. Spin batch UF-52s was the only batch in this group which spun well. The spin dope had relatively low viscosity (29-21 Pa·s) and the flow behavior was only slightly shear thinning (Figure 4.113). Despite the relatively low viscosity, the fibers remained separable after spinning. This may be related to the tendency for the batches prepared with DB-containing PMS to gel more readily. (Hence, less solvent would need to be removed during spinning in order to "solidify" the fibers.)

Table 4.30 gives the tensile strengths for fiber batches spun from heat-treated polymers. Table 4.30 shows results obtained only for batches prepared with 40:60, 60:40, and 70:30 PMS:PCS compositions. Fiber batches prepared with 100% heat-treated PMS polymer could not be tested. As discussed previously (also see Table 4.29), fibers prepared from 100% heat-treated PMS were generally stuck together after spinning. Upon pyrolysis (at 1000°C in nitrogen), all the batches became extremely brittle (and too weak to test). The batches prepared with 90% PMS polymer either could not be spun or the spinning behavior was poor (see Table 4.29); therefore, no fibers with this composition were pyrolyzed (and thus no fibers were available for testing).

Most of the fiber batches prepared with 70% PMS polymer could not be tested. As discussed previously (also see Table 4.29), as-spun fibers were generally separable but the fibers became stuck together after pyrolysis (at 1000°C in nitrogen). Hence, the fibers became brittle and too weak to be tested. It was possible to separate and test pyrolyzed fibers from one batch (UF-42s), but strengths were low (~1.2 GPa). Despite the ability to separate the fibers for testing, SEM observations, in conjunction with low tensile strengths, suggested that many fibers indeed stuck together during pyrolysis. Figure 4.114 shows SEM micrographs of the bonding between two pyrolyzed fibers in

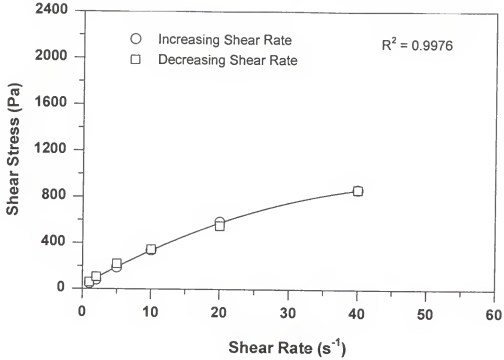

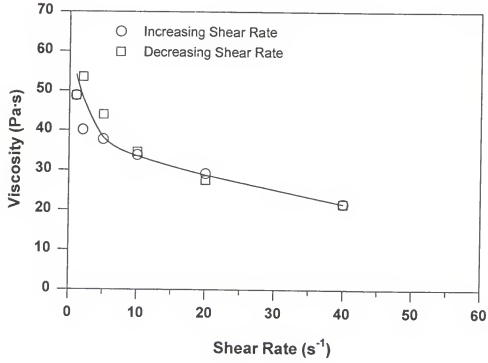

Figure 4.112. Plots of (A) shear stress vs. shear rate (B) viscosity vs. shear rate for UF-54s spin dope.

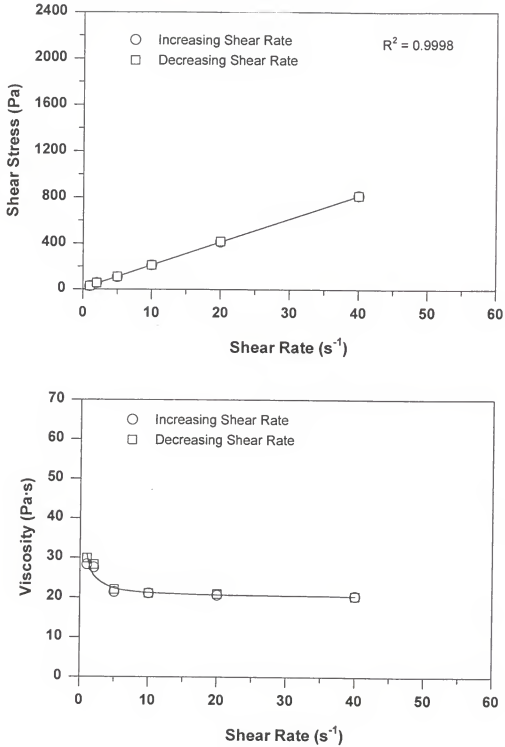

Figure 4.113. Plots of (A) shear stress vs. shear rate (B) viscosity vs. shear rate for UF-52s spin dope.

Table 4.30. Tensile strengths of SiC fibers spun from heat-treated PMS polymers and PMS/PCS polymer blends.

Designation	PMS/PCS ratio (wt%)	Heat treatment temperature (°C)	Heat treatment atmosphere	# of fibers tested	Fiber diameter (μm)	Tensile strength (GPa)
UF-35s	40:60	1000	N_2	11	13.9 ± 1.5	2.22 ± 0.83
UF-35s	40:60	1500	Ar	13	14.2 ± 1.4	2.07 ± 0.45
UF-35s	40:60	1700	Ar	12	14.0 ± 1.0	1.28 ± 0.40
UF-36s	40:60	1000	N_2	12	16.1 ± 1.4	1.22 ± 0.31
UF-39s	60:40	1000	N_2	17	27.7 ± 6.1	0.84 ± 0.39
UF-42s	70:30	1000	N_2	17	18.4 ± 1.7	1.22 ± 0.46

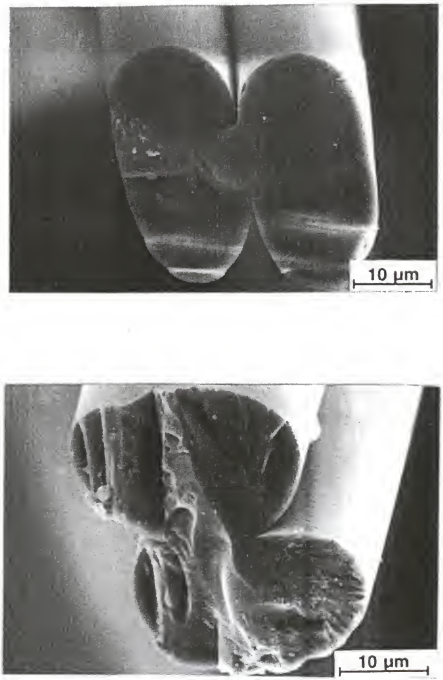

Figure 4.114. SEM micrographs of pyrolyzed fibers (batch 42s) prepared from heat-treated PMS/PCS polymer blends showing necking between fibers.

this batch. As discussed earlier, this bonding is attributed to melting of low molecular weight portions of the PMS polymer used in the spin batch.

A fiber batch prepared with 60% PMS (UF-39s) also had low strength. SEM observations were not carried out, but it is possible that bonding between pyrolyzed fibers was also a problem in this batch. In addition, the pyrolyzed fiber diameters were very large (average of ~28 μm). (It has been observed that fiber strengths usually decrease with increasing diameter [Tor92B].)

Tensile strengths of ~2.2 GPa and ~1.2 GPa were measured for two pyrolyzed fiber batches (UF-35s and UF-36s, respectively) prepared with 40% PMS. The spin dopes used in these batches both showed good spinning behavior and the as-spun and pyrolyzed fibers appeared separable for both batches. The reason for the lower strength for UF-36s is not known.

The UF-35s fibers were heat-treated in argon at 10°C/min to 1500°C and 1700°C (1 h hold). The fiber tensile strengths after heat treatment were ~2.1 GPa and ~1.3 GPa, respectively. SEM observations were carried out on the 1700°C-heat-treated UF-35s fibers. Figure 4.115 indicates that fiber surfaces are relatively smooth and no obvious fiber degradation occurred as a result of the heat treatment. The fiber cross-section (Figure 4.115C) also showed no large defects. More detailed SEM observations were made on the fracture surfaces of fiber fragments collected during tensile testing. Many of the fracture surfaces showed the presence of submicrometer pores (Figures 4.116 A-F). These pores may be the reason for the low tensile strengths for these fibers. These pores may have developed as a result of the processing conditions used in preparation of the spin batch. As indicated in Table 4.29, a 1.0 μm filter was the smallest size used in the filtration operation. (In contrast, the smallest filter used in most batches was 0.45 μm and, in some cases, the smallest filter was 0.1 μm.) Hence, it would be expected

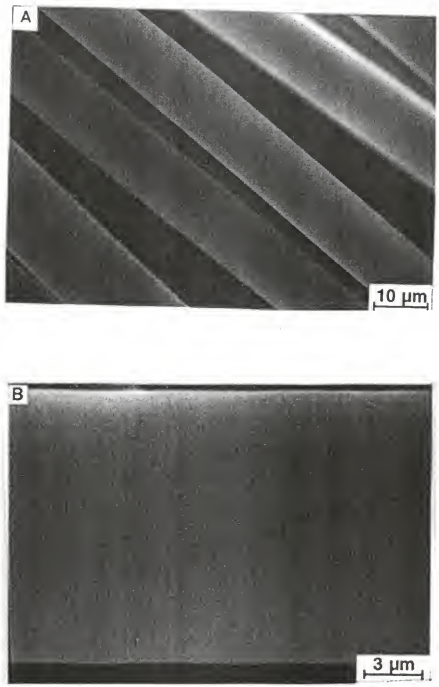

Figure 4.115. SEM micrographs of UF-35s fibers after heat treatment at 1700°C in argon.

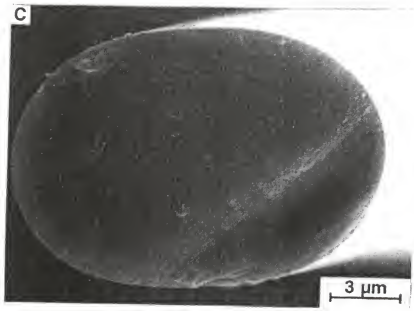

Figure 4.115. (Cont'd.)

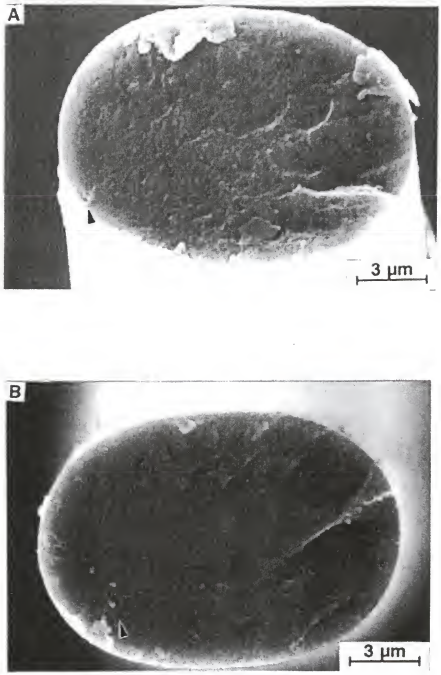

Figure 4.116. SEM micrographs of fracture surfaces of UF-35s fibers after heat treatment at 1700°C in argon.

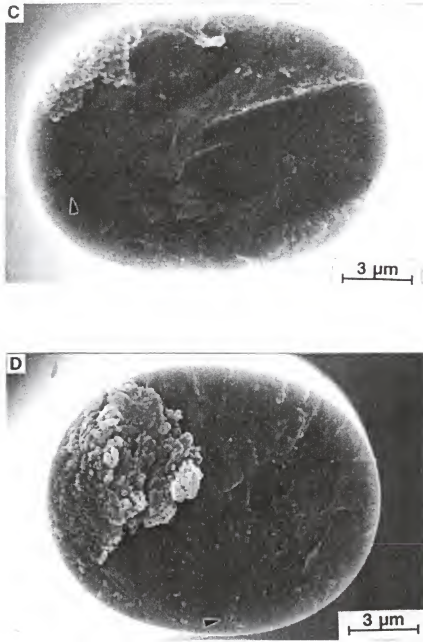

Figure 4.116. (Cont'd.).

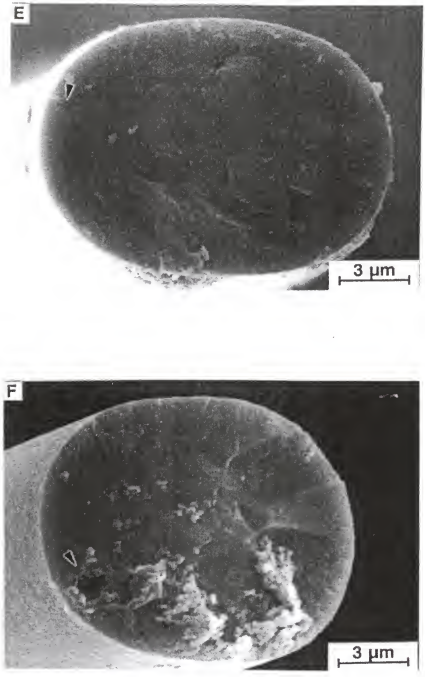

Figure 4.116. (Cont'd.)

that relatively large particulate defects were introduced into the UF-35s spin batch. (Hard inorganic, or preceramic, particulates might interfere with fiber shrinkage/densification during pyrolysis, thereby creating "crack-like" voids. Organic particulates could partially or fully "burnout" during pyrolysis which would result in pores with shapes and sizes somewhat comparable to the original particulates.)

Table 4.31 shows the results of elemental analyses (Si,C, and O) on 1150°C-pyrolyzed (in nitrogen) UF-35s, UF-42s, and UF-52s fibers, as determined by Electron Microprobe Analysis (EMA). UF-52s fibers, spun using 100% heat-treated PMS, had a Si-rich composition (2.2 wt% excess Si). (Details of calculation of excess Si are shown in Appendix K.) Recall from section 4.2.4 that free Si was detected after pyrolysis of PMS at 1350°C in argon. XRD was used to show the presence of crystalline Si in the pyrolysis product. UF-42s fibers, spun using a 70:30 PMS:PCS composition, had 10.4 wt% excess carbon[¶]. (The details of calculation of excess C are shown in Appendix K.) This is not surprising since it is well-known that PCS pyrolyzes to a highly carbon-rich composition. The amount of excess carbon increased as the PMS:PCS ratio in the spin dope decreased.

4.3.2.3 Spinning of fibers from fractionally-precipitated PMS polymers

Table 4.32 shows conditions for fiber spinning experiments and some qualitative results using fractionally-precipitated PMS polymers. Fiber batch UF-73s was spun from PMS-243-F ($M_w \approx 8400$) polymer (precipitated by adding alcohols) using a 70 μm hole diameter, 4-hole spinneret. Although the fibers spun well (0.25 breaks per minute per hole), the green fibers were slightly stuck together and this resulted in brittle fibers after pyrolysis. The sticking between green fibers was most likely caused by inadequate

[¶] This is low compared with the excess carbon (i.e., ~15-20 wt%) found in Nicalon™ fibers.

Table 4.31. Elemental analysis by Electron Microprobe for SiC fibers prepared from heat-treated PMS/PCS polymer blends[a].

Fiber batch	PMS:PCS ratio	Additives used	Composition						
			As-measured				Normalized (to 100%)[b]		
			Si %	C %	O %	Total %	Si %	C %	O %
UF-35s-1700	40:60	5 wt% PSZ	58.93 ±0.49	38.99 ±0.27	...	97.92 ±0.63	60.18 ±0.21	39.82 ±0.21	...
UF-39s-1000	60:40	14.5 wt% PSZ	58.99 ±0.66	35.37 ±0.31	2.50 ±0.32	96.86 ±0.95	60.90 ±0.29	36.51 ±0.35	2.58 ±0.32
UF-42s-1000	70:30	14.5 wt% PSZ	61.59 ±0.58	36.13 ±0.30	1.68 ±0.61	99.40 ±0.91	61.96 ±0.53	36.35 ±0.37	1.69 ±0.61
UF-52s-1000	100:0	0.25 wt% PSZ, 6 wt% DB	70.04 ±0.93	27.78 ±0.28	3.36 ±0.67	101.19 ±0.75	69.22 ±0.54	27.46 ±0.31	3.32 ±0.67

[a] Nitrogen and B were below the detection limit of the Electron Microprobe Analyzer used.
[b] Normalized Si, C, and O to 100% total.
[c] Added to polymer solution prior to heat treatment.

Table 4.32. Conditions and qualitative results of fiber spinning experiments for fractionally-precipitated PMS polymers.

Batch	Amount of PMS	M_n	M_w	Spin. additive (wt%)	Filtration condition Filter/press/time	Flow test time (s)	Solids loading (%)	Viscosity (Pa·s)	Spin speed (rpm)	Pressure (psi)
UF-73s	2.60g PMS-243-F	2821	8443	10% PSZ	0.1μm/30psi/5 min	27	84.7	39-38	84	425
	Spun well; green fibers were partially stuck together especially in the middle portion of the bundle.									
UF-74s	1.23g PMS-245-F1 (37%), 1.56g PMS-246-F (48%), 0.50g PMS-247-F (15%)	4872[a]	12672[a]	10% PSZ	0.1μm/30psi/ 90min (4sets)	40.5	73.2	37-35	…	…
	Not spinnable as the spinneret got clogged as soon as the spinning started. Used 40μm, 3hole spinneret.									
UF-75s	1.50g PMS-250-F (46%), 0.87g PMS-251-F (27%), 0.87g PMS-248-F (27%)	2810[a]	6686[a]	10% PSZ	0.1μm/30psi/ 3-10min	30.1	79.5	47-43	54	500-600
	Spun well. Used 40μm, 3-hole spinneret. Fibers separable in green state and after pyrolysis.									
UF-76s	0.78g PMS-250-F (29%), 0.74g PMS-251-F (28%), 1.15g PMS-248-F (43%)	2739[a]	7089[a]	10% PSZ 2% DB	0.1μm/30psi/ 3-10min	…	…	…	…	…
	Polymer solution gelled during processing.									
UF-77s	0.81g PMS-252-F (30%), 0.41g PMS-253-F (15%), 0.58g PMS-254-F (22%), 0.86g PMS-255-F (33%)	2450[a]	5620[a]	6% PSO 2% DB 0.5% PSZ	0.1μm/30psi/ 5min	25	78.0	37-31	134	500
	Spun well but two holes clogged and only one spun. Green fibers were separable but not as separable as UF-75s. Used 40μm,3-hole spinneret.									
UF-78s	0.81g PMS-252-F (30%), 0.41g PMS-253-F (15%), 0.58g PMS-254-F (22%), 0.86g PMS-255-F (33%)	2450[a]	5620[a]	6% PSO 2% DB 0.5% PSZ	0.1μm/30psi/ 5min	34	77.1	47-41	84	500
	Spun well; repeat of UF-77s. Fibers highly separable both in green and pyrolyzed state. Used 40μm, 3hole spinneret.									

[a] Calculated based on rule of mixtures using individual component molecular weight information.

solvent removal prior to winding of the fibers. (The fractionated PMS polymers appeared to be solids at room temperature, so sticking in the green state did not result because of flow of the polymer. In addition, no melting was observed for a sample of PMS-243-F in a 1000°C-melt test.)

Some changes in processing conditions were made in order to avoid sticking of the as-spun fibers. First, a spinneret with smaller diameter holes (40 μm diameter, 3-holes) was used in subsequent batches. (This was done so that a greater proportion of the solvent would be evaporated by the time the fibers reached the winding drum.) Second, some of the batches were prepared with a higher viscosity. (This was done so that less liquid removal would be needed before the fibers would "solidify".)

Spin batch UF-74s was prepared from a mixture of polymer solutions PMS-245-F-1 ($M_w \approx 6200$), PMS-246-F ($M_w \approx 16400$), and PMS-247-F ($M_w \approx 16700$) (in a 38:47:15 wt% proportion). It was not spinnable because the spinneret holes became clogged at the start of fiber spinning. This may have been an indication that the polymer solution was close to the point of gelation. This is suggested because it was difficult to filter the solution prior to concentration (see Table 4.32). Two of the polymers used in this batch (PMS-246-F and PMS-247-F) had very high molecular weights and may have contained gel-like fractions.

UF-75s fibers was prepared from polymer batches PMS-250-F ($M_w \approx 6200$), PMS-251-F ($M_w \approx 5500$), and PMS-248-F ($M_w \approx 8700$) in a 46:27:27 wt% proportion. These fibers spun well and were highly separable both in the green state and after pyrolysis.

UF-76s spin batch was prepared from polymer batches PMS-250-F ($M_w \approx 6200$), PMS-251-F ($M_w \approx 5500$), and PMS-248-F ($M_w \approx 8700$) in a 29:28:43 wt% proportion. The spin dope also contained 2 wt% DB. Previous work [Cho93] has shown that DB and

PSZ react with each other, and at sufficiently high concentration, spinning solutions with these additives either undergo gelation or some precipitates form from the solutions. Hence, it is not too surprising that the UF-76s batch underwent gelation during spin dope preparation.

Fiber batches UF-77s and UF-78s were prepared from PMS-252-F ($M_w \approx 4500$), PMS-253-F ($M_w \approx 7800$), PMS-254-F ($M_w \approx 5300$), and PMS-255-F ($M_w \approx 5900$) in proportions of 30:15:22:33 by wt%. The spin batch additives were PSZ (0.5 wt%), DB (2 wt%), and polysiloxane, PSO, (6 wt%). (PSO has been reported to be an excellent spinning aid in the spinning of fibers from PCS polymers [Sac95].) UF-77s fibers were slightly stuck together in green state, while the UF-78s fibers were highly separable both after spinning and pyrolysis. The improved separability of the UF-78s fibers was probably due to the higher spin batch viscosity (48-41 Pa·s compared to 37-31 Pa·s for UF-77s).

The UF-75s fibers had high tensile strength (2.72 GPa) after pyrolysis at 1150°C in nitrogen (Table 4.33). The 1150°C-pyrolyzed fibers had a near-stoichiometric composition of 66.5 wt% Si, 32.0 wt% C, and 1.5 wt% O, as determined by electron microprobe analysis (EMA) (Table 4.34). These fibers showed unexpectedly poor thermal stability upon further heat treatment. The fibers had total weight losses of 8%, 12 wt%, and 22 wt% after heat treatments of 1480°C for 1 h (in argon), 1480°C for 10 h (in argon), and 1845°C for 1 h (in argon), respectively. The composition of fibers after 1480°C/1 h was determined to be somewhat more carbon-rich (Si:64.5 wt%, C:35.5 wt%, O: 0 wt%) compared to the 1150°C-pyrolyzed fibers.

The pyrolyzed 1150°C UF-78s fibers had reasonably good tensile strength (~2.35 GPa, Table 4.33) but showed poor thermal stability at higher temperature. The weight loss for these fibers was ~25% after heat-treatment at 1480°C for 1 h in argon.

Table 4.33. Tensile strengths of SiC fibers spun from fractionally-precipitated PMS polymers.

Fiber batch	Heat treatment temperature (°C)	Heat treatment atmosphere	# of fibers tested	Fiber diameter (μm)	Tensile strength, (GPa)
UF-75s	1150	N_2	18	11.0 ± 1.8	2.72 ± 0.36
UF-78s	1150	N_2	18	11.0 ± 1.2	2.35 ± 0.69

Table 4.34. Elemental analysis by Electron Microprobe for SiC fibers prepared from fractionally-precipitated PMS polymers[a].

Fiber batch	Composition						
	As-measured				Normalized (to 100%)[b]		
	Si %	C %	O %	Total %	Si %	C %	O %
UF-75s-1150	67.93 ±0.35	32.66 ±1.00	1.60 ±0.70	102.19 ±1.59	66.49 ±0.94	32.00 ±0.62	1.5 ±0.67
UF-75s-1150-1480	65.70 ± 1.51	36.20 ± 1.39	0.00	101.90 ±1.68	64.48 ± 1.16	35.52 ± 1.16	0.00
UF-78s-1150	67.64 ±0.49	24.64 ±0.69	5.84 ±1.67	98.12 ±0.98	68.95 ±1.04	25.12 ±0.85	5.94 ±1.63

[a] Nitrogen and B were below the detection limit of the Electron Microprobe Analyzer used.
[b] Normalized Si, C, and O to 100% total.

The electron microprobe analysis on pyrolyzed (1150°C) UF-78s fibers revealed a silicon-rich composition (Si: 69.0 wt%, C: 25.1 wt%, and O:5.9 wt%) (Table 4.34). The reason(s) for the high oxygen content in the fibers are unclear. The PSO addition would result in some oxygen in the pyrolyzed fiber, but not to the level measured.

The reason for the observed large weight losses at these temperatures is not clear. It is possible that carbothermal reduction reactions occur which result in a more carbon-rich fiber. The following carbothermal reduction reactions are possible [Dan93]:

$$2\ SiC + SiO_2 \rightarrow 3\ Si + 2\ CO \qquad (4.7)$$

$$SiC + 2SiO_2 \rightarrow 3SiO + CO \qquad (4.8)$$

$$SiO_2 + C \rightarrow SiO + CO \qquad (4.9)$$

The weight losses based on these reactions (equations (4.7), (4.8), and (4.9)) and stoichiometry change can be determined for each of these reactions as shown below:

Consider UF-75s fibers. The initial composition of the 1150°C-pyrolyzed fiber is: 66.5 wt% Si, 32 wt% C, and 1.5 wt% O. We have 91.3 wt% SiC, 4.1 wt% SiO_2, and 4.6 wt% C. Based on reaction (4.7), we have 1 mole of SiO_2 reacting with 2 moles of SiC, forming 3 moles of Si and 2 moles of CO. It is assumed that Si formed as a result of this reaction is volatilized at the heat treatment temperature (1480°C). (The melting point of Si is 1410°C.) This means that, for 0.0936 mole (or 4.1 g) of SiO_2, the total amount of volatile species formed (Si, CO) would be 11.6 g. Thus, the expected weight loss is ~11.6 %. (The observed weight loss was 8% after 1480°C/1 h.) The calculated stoichiometry based on loss of 7.5 wt% SiC due to reaction (7) is 66.3 wt% Si and 33.7

wt% C. (The composition of the fiber after 1480°C/1 h determined by EMA is 64.5 wt% Si and 35.5 wt% C.)

Based on reaction (4.8), we have 1 mole of SiO_2 reacting with 1/2 mole of SiC to produce 3/2 moles of SiO and 1/2 mole of CO. This means that 0.0936 mole (or 4.1 g) of SiO_2 reacts with 0.046 mole (or 1.8 g) of SiC to form 0.139 mole (or 5.0 g) of SiO and 0.046 mole (or 0.9 g) of CO. The total amount of volatile species (SiO, CO) is 5.9 g. Thus, the expected weight loss is 5.9%. The calculated stoichiometry for the fiber after heat treatment is 62.6 wt% Si and 31.4 wt% C.

Based on reaction (4.9), we have 1 mole of SiO_2 reacting with 1 mole of C forming 1 mole of SiO and 1 mole of CO or 0.09363 gmole of SiO_2 (4.1 g) reacting with 0.09363 gmole of C (or 1.1 g) forming 5.2 g of volatile species SiO and CO. Thus, the expected weight loss is ~5.2% (as opposed to the observed weight loss of 8%). The calculated stoichiometry (based on loss of 1.1 g of C) is 67.3 wt% Si and 32.7 wt% C.

Thus, reaction (4.8) predicts the weight loss closest to the observed weight loss for UF-75s fibers after 1480°C/1 h heat treatment. However, the large weight losses occurring after 1480°C/10 h and 1845°C/1 h cannot be adequately explained by this reaction. More investigations on thermal stability of these fibers would be needed.

The large weight loss in UF-78s fibers after heat treatment at 1480°C/1 h is likely due to the carbothermal reduction reaction shown by equation (4.8). The weight loss based on this reaction and stoichiometry change can be determined as follows: The initial composition of the 1150°C-pyrolyzed fiber is: 69.0 wt% Si, 25.1 wt% C, and 5.9 wt% O. Assuming that all O_2 is tied to Si as SiO_2, we have 83.7 wt% SiC, and 16.3 wt% SiO_2. Based on reaction (4.8), we have 1 mole of SiO_2 reacting with 1/2 mole of SiC, forming 3/2 moles of Si and 1/2 mole of CO. This means that, for 16.3 g of SiO_2 in the fiber (or 0.3704 gmole), the total amount of volatile species formed (SiO, CO) would be

23.7 g. Thus, the expected weight loss is ~23.7 %. (The observed weight loss was ~25 % after 1480°C/1 h.)

4.3.3. Fiber extension experiments on PMS polymer spin dopes containing PSZ

The lengths to which fibers can be slowly hand-drawn before they break were measured on "spin dopes" prepared using PMS, PSZ, and PMS/PSZ mixtures. (The technique for hand-drawing fibers is described in section 3.1.3.) These "fiber extension measurements" were considered an indication of the spinnability of the batch, i.e., the ability to spin fibers by extruding (under pressure) a spin dope through a spinneret having fine-diameter holes.

Fiber extension measurements were carried out on two PSZ polymers, i.e., PSZ 0908A with relatively high molecular weight ($M_n \approx 8,400$, $M_w \approx 748,000$) and PSZ 0831A with relatively low molecular weight ($M_n \approx 2,700$, $M_w \approx 13,600$). Both PSZ's are liquids at room temperature, so the initial experiments were carried out with no solvent additions. Table 4.35 shows that the fiber extension was almost three times greater for the high-molecular weight PSZ (i.e., extensions were 17.0 cm and 5.7 cm for the 0908A and 0831A polymers, respectively). It should be noted that PSZ 0908A had much higher viscosity than PSZ 0831A (see Table 4.35). Therefore, it was not clear from the initial experiments if the greater fiber extension was due to the higher molecular weight or the higher viscosity. Consequently, a solution was prepared in which the PSZ 0908A was diluted with toluene (i.e., 95 wt% PSZ 0908A/5 wt% toluene) in order to obtain approximately the same viscosity as 100% PSZ 0831A (i.e., ~20 Pa·s). Table 4.35 shows that the fiber extension of the 95 wt% PSZ0908A solution was still much greater than the PSZ 0831A polymer. Hence, the higher molecular weight was the primary factor responsible for greater fiber extension.

Table 4.35 shows fiber extension results for solutions prepared with fractionated PMS polymers PMS-240-F and PMS-242-F. The PMS-242-F solutions were prepared at a viscosity similar to the 100% PSZ 0831A polymer and the 95 wt% PSZ 0908A/5 wt% toluene solution. The PMS-240-F solutions were prepared with similar flow test times as the PMS-242-F solutions. (Unfortunately, viscosity measurements could not be made with PMS-240-F solutions due to the limited amount of material available.)

The fiber extension for PMS-240-F-0 solution was slightly greater than for the PMS-242-F-0 solution (13.5 cm vs. 12.5 cm). One possible reason for this observation is the higher molecular weight for the former polymer. (The average molecular weights were $M_w \approx 8{,}400$ and $M_w \approx 5{,}000$ for the PMS-240-F and PMS-242-F polymers, respectively[‡]. The GPC molecular weight distributions for the as-prepared PMS-240 and fractionated PMS-240-F polymers and the as-prepared PMS-242 and fractionated PMS-242-F polymers are shown in Figures 4.101a and 4.101b, and Figure 4.117a and 4.117b, respectively.) It should be noted, however, that the small difference in the fiber extension distances may also be due to a difference in viscosity. The PMS-240-F-0 solution had a slightly higher flow time, so the viscosity may have been higher also.

Table 4.35 also shows fiber extension measurements for solutions prepared with PMS/PSZ mixtures. The addition of 14.5 wt% PSZ 0831A to PMS-242-F clearly resulted in a decrease in fiber extension (9.8 cm for the mixed solution, PMS-242-F-1, vs. 12.5 cm for the PMS-242-F-0 solution with no PSZ). The mixed solution had essentially identical solution viscosity, flow test time, and solids loading to the solution with no PSZ.

[‡] It is interesting to note that solids loading for the PMS-242-F-0 solution was significantly lower compared to the PMS-240-F-0 solution (i.e., 78.2 wt% vs. 85.5 wt%). This was somewhat surprising since the former polymer has a lower molecular weight ($M_w \approx 5{,}000$ vs. $M_w \approx 8{,}400$ for PMS-240-F). There are at least two possible reasons for this observation. First, the PMS-240-F-0 solution may actually have a higher viscosity. (As shown in Table 4.31, the flow time is slightly higher.) In that case, the higher solids loading would be less surprising. Second, there may be differences in the polymer architecture.

Table 4.35. Results of fiber extension experiments for PMS polymers containing PSZ.

Polymer	PSZ batch	Amount of PSZ (wt%)	Viscosity (Pa·s)	Flow test time(s) †	Solids-loading (wt%)	Fiber extension (cm)
PMS-240-F-0	...	0	*	21	85.5	13.5 ± 2.1
PMS-240-F-1	0908A	4.0	*	20	84.5	15.0 ± 3.4
PMS-240-F-2	0908A	8.0	*	21	80.5	13.9 ± 2.1
PMS-240-F-3	0908A	14.5	*	23	80.1	12.1 ± 2.9
PMS-242-F-0	...	0	19-18	18	78.2	12.5 ± 3.0
PMS-242-F-1	0831A	14.5	19-17	18	78.1	9.8 ± 1.7
PSZ	0908A	100	180-130	*	100	17.0 ± 2.5
PSZ	0908A	95.0	22-19	14	95	14.4 ± 1.5
PSZ	0831A	100	19-18	8.5	100	5.7 ± 1.2

† Flow test time is the time taken by the polymer solution to travel 2.5cm at 45° angle. The measurement was done in a capped vial. (The detailed procedure for the flow test is given in section 3.2.1.)
* Data not available

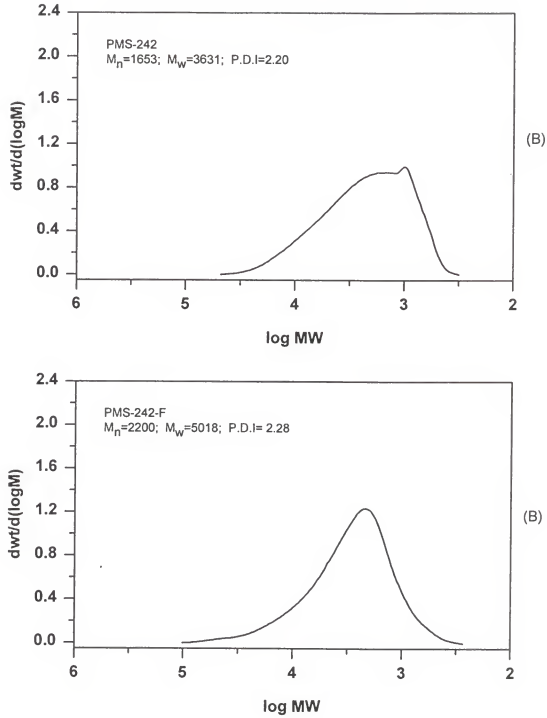

Figure 4.117. Gel permeation chromatograms for PMS-242 polymer: (A) before and (B) after fractional precipitation.

The decreased fiber extension can be attributed to the incorporation of a PSZ component (i.e., the relatively low molecular weight PSZ 0831A) which itself has relatively poor fiber extension.

In contrast to the above results, the addition of 4 wt% PSZ 0908A to PMS-240-F resulted in a small increase in fiber extension (i.e., 15.0 cm for the mixed solution, PMS-240-F-1, vs. 13.5 cm for the PMS-240-F-0 solution with no PSZ). The mixed solution had similar flow test time and solids loading to the solution with no PSZ. The increased fiber extension can be attributed to the incorporation of a PSZ component (i.e., the relatively high molecular weight PSZ 0908A) which had better fiber extension, as a pure component, than the PMS-240-F-0 solution. At higher concentrations of PSZ 0908A (i.e., 8 and 14.5 wt%), the trend reversed and the fiber extensions decreased for mixed solutions prepared with PMS-240-F (see Table 4.35 and Figure 4.118). The decreases are probably *not* associated with differences in viscosity since the flow test times were maintained approximately constant for these solutions. It is noted, however, that the solids loading decreased with increasing PSZ 0908A content in the mixed solutions. It is not clear if this is related to the observed decreases in fiber extension. The decreased solids loading is expected due to the high molecular weight of PSZ 0908A[†] . However, there is some evidence that the decreased solids loading may also have been related to a reaction between the PMS and PSZ. It was observed that the initially clear yellow-colored PMS-240-F solution became increasingly cloudier with successive additions of PSZ (i.e., 4 wt%, 8 wt%, and 14.5 wt%). It was not determined if any increases in molecular weights were associated with these changes. However, it was observed that the time required for filtration increased with increasing PSZ content of the solution.

[†] Recall that this PSZ has relatively high viscosity in pure form and that it must be diluted to 95 wt% in toluene to have a similar flow test time to the mixed solutions prepared with PMS-240-F.

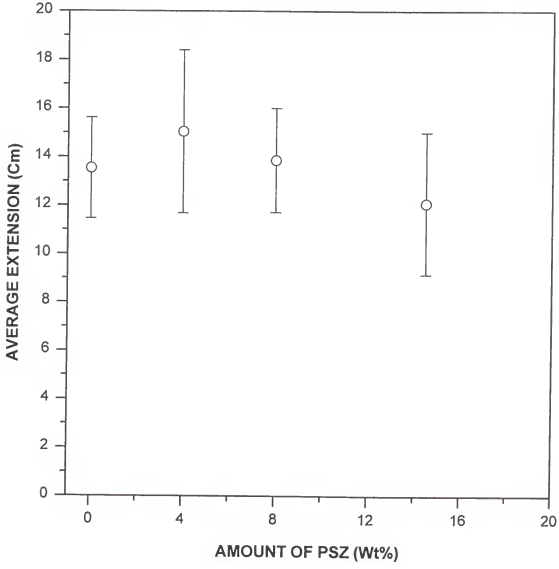

Figure 4.118. Average extension for fibers drawn from PMS-based polymers as a function of amount of PSZ 0908A added.

Solutions (~33 wt% solids) with 0, 4, 8, and 14.5 wt% PSZ required 3, 5, 9, and 12 min, respectively, for filtration through 0.45 μm filters. The observations of increased solution cloudiness and increased filtration time for the solutions with higher PSZ content suggest that some microgel may have been developing. This, in turn, would have an adverse effect on the ability to draw fibers (i.e., decreased fiber extension would be expected).

CHAPTER 5
SUMMARY AND CONCLUSIONS

1. SiC fibers were prepared by dry spinning of polycarbosilane (PCS) solutions. The effects of polyvinylsilazane (PSZ) on spinnability of PCS solutions and mechanical properties of green and heat-treated fibers were investigated. It was found that the addition of PSZ to PCS greatly improved fiber spinning by reducing the number of fiber breaks occurring during spinning. (This also allowed a considerably greater amount of fibers to be formed from the PCS solutions containing PSZ.) It was also observed qualitatively that fibers could be stretched more easily in the case of PCS+PSZ solutions than PCS solutions. Fiber extension experiments carried out separately confirmed this observation. It was determined that PCS+PSZ solution had an average fiber extension greater than PCS solution by ~20%.

Contact angle measurements for PCS and PCS+PSZ solutions (33 wt% solids loading) on stainless steel and teflon substrates revealed differences in wetting characteristics for these solutions. It was found that contact angles for PCS+PSZ solutions were lower than for PCS solutions on both stainless steel and teflon substrates. Contact angles for PCS solution on PCS-coated stainless steel and for PCS+PSZ solution on PCS+PSZ-coated stainless steel were also measured. The contact angles of the PCS solution on a PCS-coated stainless steel substrate were larger than the contact angles of PCS+PSZ solution on PCS+PSZ-coated stainless steel substrates.

Experiments were carried out on PCS and PCS+PSZ solutions to assess changes in rate of solvent evaporation as a result of addition of PSZ to PCS. (Changes in solvent evaporation rate influence the drying characteristics during fiber spinning.) The rate of solvent evaporation was monitored for PCS/toluene and PCS+PSZ/toluene solutions prepared with 68 wt% polymer. It was found that PCS+PSZ solution exhibited lower evaporation rate compared to PCS solution in the early stages of evaporation.

The effect of PSZ on the mechanical properties of fibers prepared from PCS and PCS+PSZ solutions was investigated. It was found that as-spun PCS and PCS+PSZ fibers developed similar tensile strengths and rupture strains. However, after heat treatment at 400°C in nitrogen, PCS+PSZ fibers showed higher tensile strength and rupture strain compared to PCS fibers. Air-heat treated (~180 ±10°C) PCS and PCS+PSZ fibers also showed considerably higher strengths and rupture strains than as-spun PCS and PCS+PSZ fibers. Air-heat treated PCS and PCS+PSZ fibers had higher tensile strengths and rupture strains after heat treatment at 400°C in nitrogen compared to as-spun PCS and PCS+PSZ fibers given only a 400°C heat treatment in nitrogen. It follows from these results that both oxygen and PSZ are effective cross-linking agents for PCS. The oxidative cross-linking of PCS occurs by oxidation of Si-H groups to form Si-OH groups and subsequent condensation to form Si-O-Si and Si-O-C networks. Since PSZ contains many carbon-carbon double bonds, cross-linking presumably occurs by a mechanism involving free radicals. FTIR spectra of as-spun and air-heat treated PCS and PCS+PSZ fibers collected during heat treatment to 600°C in nitrogen suggest that PSZ cross-links PCS.

PCS+PSZ fibers developed higher average tensile strengths compared to PCS fibers after heat treatments in nitrogen at various temperatures up to 1150°C.

2. SiC fibers were prepared from polymethylsilane (PMS) polymers and PMS/PCS polymer blends. PMS polymers were synthesized by Wurtz-coupling polymerization of methyldichlorosilane (MDCS) and methyltrichlorosilane (MTCS) (in 70:30 wt% proportion) with sodium in refluxing solvent mixtures. In order to address problems with low polymer yields (associated with Wurtz polymerization reactions), polar solvents THF and 1,4-dioxane were added to toluene. It was found that both THF and 1,4-dioxane caused an increase in polymer yield and molecular weight of the polymers. One of the major drawbacks of PMS polymers are that they are liquids at room temperature, and have low molecular weights. In order to form fibers from these polymers, an increased molecular weight and an increased extent of cross-linking are needed so that the polymers are solids at room temperature (and remain solids during pyrolysis). Two approaches were used to raise the molecular weight/cross-linking of the polymers: (1) polymerization and cross-linking by heat treatment of solutions with and without additives and (2) fractional precipitation of higher molecular weight fractions by addition of non-solvents. The additives for heat treatment consisted of polyvinylsilazane (PSZ), dicumyl peroxide (DCP), and decaborane (DB). It was found that heat treatment approach was effective in increasing the molecular weight but it was not possible to achieve these increases reproducibly. Furthermore, the heat-treated polymers tended to have bimodal molecular weight distributions which is undesirable. (The low molecular weight portion remains as a liquid.) Hence, these polymers are not particularly suitable for fiber formation.

Fractional precipitation of higher molecular weight fractions was an effective method of producing solid polymers. Use of alcohols as nonsolvents for fractional precipitation was undesirable since it incorporated a large amount of oxygen in the polymer. (This was indicated by analyses carried out on pyrolyzed samples which

showed oxygen contents up to 30 wt%.) This oxygen incorporation is primarily attributed to reaction of the polymer with alcohols (i.e., hydrolysis). This was not a problem in the case of polymers precipitated with acetone as nonsolvent.

It was possible to prepare high strength pyrolyzed SiC-based fibers from fractionally-precipitated polymers. Some changes in processing conditions were necessary in order to avoid sticking of as-spun fibers. First, a spinneret with smaller diameter holes (40 μm diameter, 3-holes) was needed to spin fibers. (This was done so that a greater portion of the solvent would be evaporated by the time the fibers reached the winding drum.) Second, some of the fiber batches were prepared with higher viscosity. (This was done so that less liquid removal would be needed before the fibers would "solidify".) The fibers had high tensile strength (~2.4-2.7 GPa) and a near-stoichiometric composition (66.5 wt% Si, 32.0 wt% C, and 1.5 wt% O) after pyrolysis at 1150°C. The fibers, however, showed poor thermal stability upon further heat treatment.

It was observed that PMS polymers were extremely sensitive towards air/moisture. This is due to the presence of a large number of Si-H groups in the Therefore, for many practical applications involving PMS polymers (except, for example, in applications involving use as photoresists in microlithography where sensitivity of PMS polymers towards oxygen is exploited), it would be necessary to take extensive precautions during handling to exclude oxygen and water vapor.

APPENDIX A
RHEOLOGICAL CHARACTERIZATION OF PCS AND PCS+PSZ SPIN DOPES

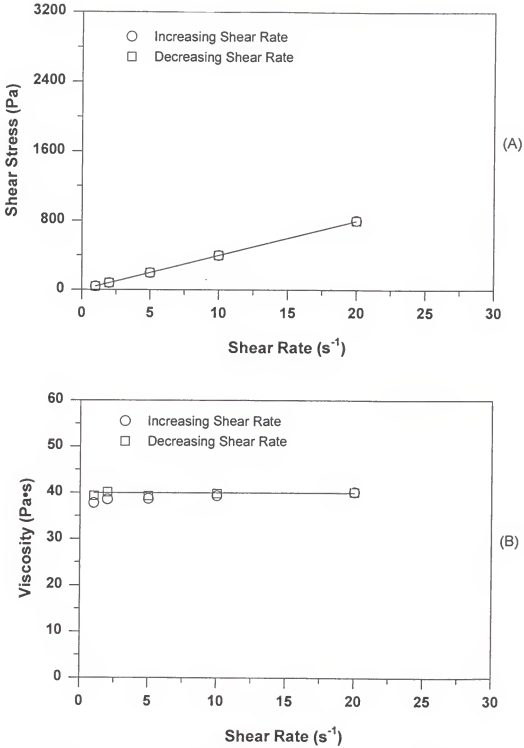

Figure A-1. Plots of (A) shear stress vs. shear rate (B) viscosity vs. shear rate for batch 64s spin dope (PCS) (solids concentration ~67 wt%).

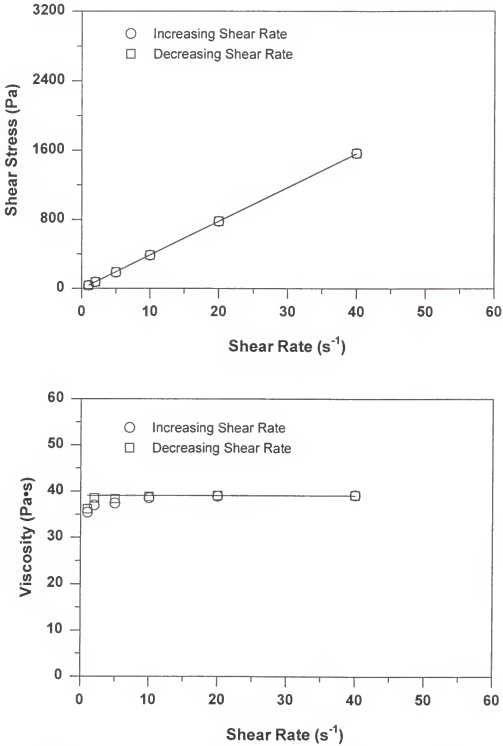

Figure A-2. Plots of (A) shear stress vs. shear rate (B) viscosity vs. shear rate for batch 65s spin dope (PCS) (solids concentration ~66 wt%).

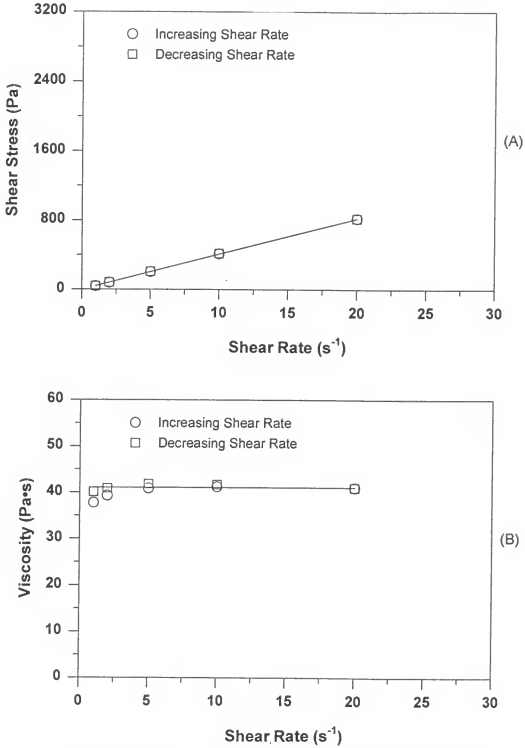

Figure A-3. Plots of (A) shear stress vs. shear rate (B) viscosity vs. shear rate for batch 69s spin dope (PCS) (solids concentration ~66 wt%).

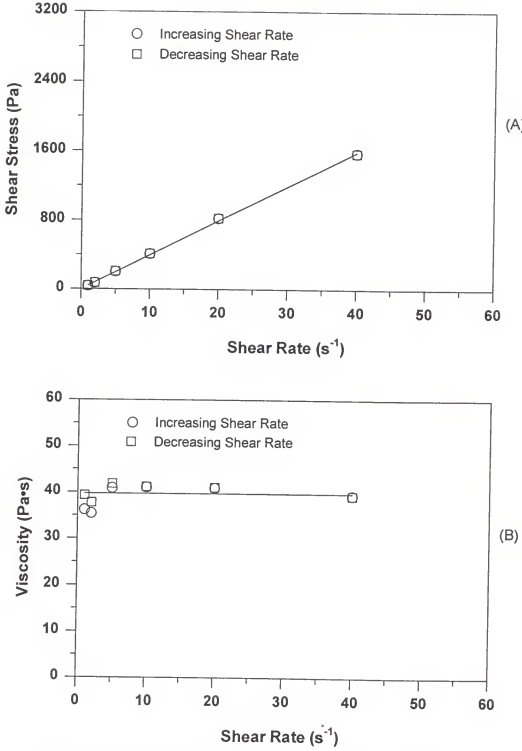

Figure A-4. Plots of (A) shear stress vs. shear rate (B) viscosity vs. shear rate for batch 67s spin dope (PCS+PSZ) (solids concentration ~69 wt%).

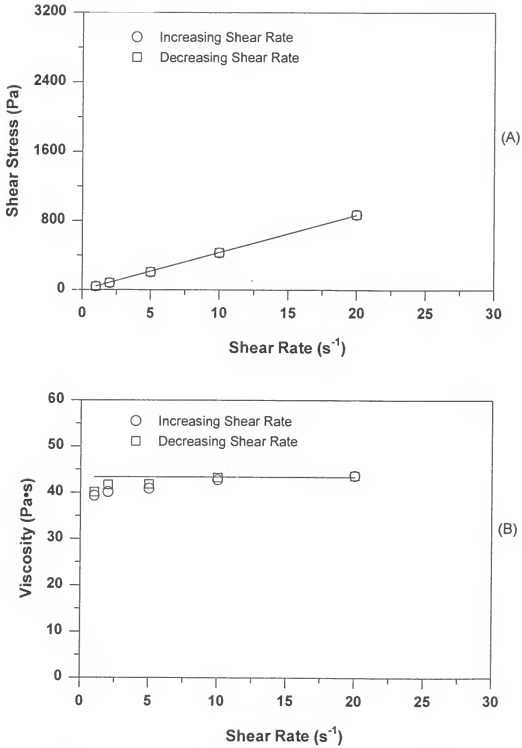

Figure A-5. Plots of (A) shear stress vs. shear rate (B) viscosity vs. shear rate for batch 68s spin dope (PCS+PSZ) (solids concentration ~70 wt%).

APPENDIX B
FIBER SPINNING CHARACTERISTICS FOR PCS AND PCS+PSZ SPIN DOPES

Fiber spinning characteristics for PCS and PCS+PSZ spin batches:

UF-63s (PCS)

t, min	Number of holes spun	Number of fiber breaks
0	-	-
1-2	2	12
3-7	1	10
8-9	1	4
10-13	1	20
14-17	0	0
Total number of fiber breaks = 46		
Number of breaks per minute per spinneret hole = 3.1		

UF-64s (PCS)

t, min	Number of holes spun	Number of fiber breaks
0	-	-
1-2	2	12
3-4	3	0
5-8	2	0
9-11	0	0
12-20	2	50
21	2	0
22	1	0
23	2	0
Total number of breaks = 62		
Number of breaks per minute per spinneret hole = 1.51		

UF-65s (PCS)

t, min	Number of holes spun	Number of fiber breaks
0	-	-
1	1	0
2-4	3	11
5	2	3
6	0	0
7-8	4	0
9	0	0
10-11	1	4
12-13	2	3
14	1	1
15-17	0	0
Total number of breaks = 22		
Number of breaks per minute per spinneret hole = 0.81		

UF-69s (PCS)

t, min	Number of holes spun	Number of fiber breaks
0	-	-
1	0	0
2-3	2	2
4	0	0
5	2	2
6	1	0
7-8	2	4
9-10	3	3
11-13	2	1
14	3	1
15-17	2	1
Total number of breaks = 14		
Number of breaks per minute per spinneret hole = 0.44		

UF-67s (PCS+PSZ)

t, min	Number of holes spun	Number of fiber breaks
0	-	-
1	0	0
2	3	1
3-5	2	0
6-8	3	3
9-10	3	4
11	3	0
12-13	3	2
14-18	3	0
19	3	1
20-21	3	0
22	3	4
23-24	3	5
Total number of breaks = 20		
Number of breaks per minute per hole = 0.29		

UF-68s (PCS+PSZ)

t, min	Number of holes spun	Number of fiber breaks
0	-	-
1	4	0
2	4	1
3-4	4	0
5-6	4	2
7-8	4	0
9	4	1
10-11	4	0
12	4	1
13	2	1
14	3	0
Total number of breaks = 6		
Number of breaks per minute per spinneret hole = 0.11		

UF-70s (PCS+PSZ)

t, min	Number of holes spun	Number of fiber breaks
0-1	-	-
2-5	4	0
6	4	1
7	4	0
8	4	1
9-10	4	0
11	4	1
12	4	2
Total number of breaks = 5		
Number of breaks per minute per spinneret hole = 0.11		

APPENDIX C
FIBER EXTENSION DISTANCES FOR PCS AND PCS+PSZ SPIN DOPES

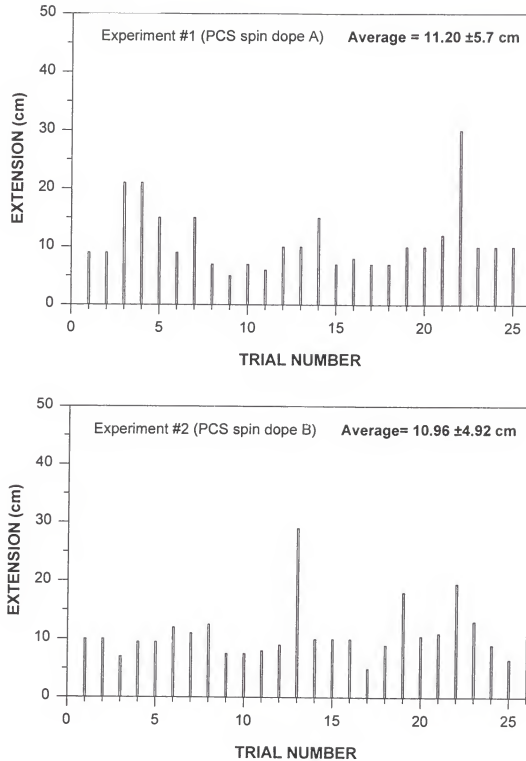

Figure C-1. Fiber extension distances for PCS spin dopes.

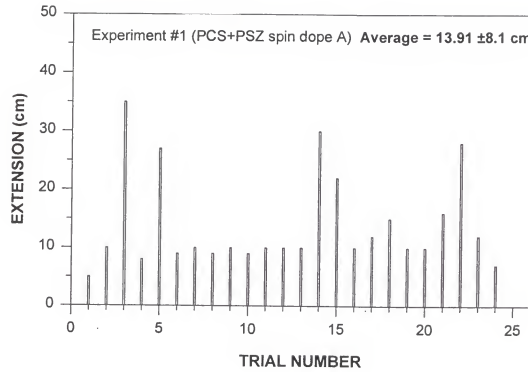

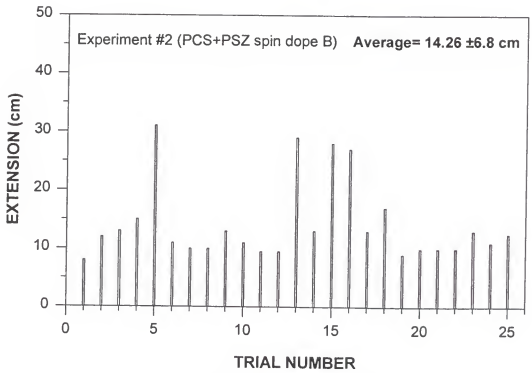

Figure C-2. Fiber extension distances for PCS+PSZ spin dopes.

APPENDIX D
INTRINSIC VISCOSITY CALCULATIONS FOR PCS, PCS+PSZ, PSZ, AND PMS POLYMERS

Table D-1. Intrinsic viscosity calculations for PCS and PCS+PSZ solutions in toluene (Ubhellode viscometer type OC).

PCS solution:

Set #1:

Concentration (g/dl)	Efflux times (s)				Ave. efflux time (s)
5.1235	277.97	277.87	277.90	278.11	277.96 ± 0.11
3.8426	265.06	265.12	264.90	264.94	265.01 ± 0.10
3.0741	257.68	257.78	257.59	257.42	257.62 ± 0.15
2.7124	254.34	254.40	254.12	254.40	254.32 ± 0.13

Set #2:-

Concentration (g/dl)	Efflux times (s)				Ave. efflux time (s)
4.5541	271.97	271.71	271.97	271.42	271.77 ± 0.26
3.4156	260.71	260.86	260.62	260.75	260.74 ± 0.10
2.9276	256.20	256.31	256.25	256.36	256.28 ± 0.07

Toluene:

Concentration (g/dl)	Efflux times (s) (t_o)				Ave. efflux time (s)
...	231.13	231.25	231.16	231.25	231.20 ± 0.06

Calculations:

$\eta_{rel} = t/t_o$; $\eta_{sp} = \eta_{rel} - 1$

c (g/dl)	t (ave)	η_{rel}	η_{sp}	η_{sp}/c (dl/g)
5.1235	277.96	1.2022	0.2022	0.03947
4.5541	271.77	1.1755	0.1755	0.03853
3.8426	265.01	1.1462	0.1462	0.03805
3.4156	260.74	1.1278	0.1278	0.03741
3.0741	257.62	1.1143	0.1143	0.03717
2.9276	256.28	1.1085	0.1085	0.03705
2.7124	254.32	1.1000	0.1000	0.03687

From a plot of η_{sp}/c vs c, $[\eta] = 0.03395$ dl/g ± 6.01×10^{-5}

Table D-1. (Cont'd.)

PCS + PSZ solution:

Set #1:

Concentration (g/dl)	Efflux times (s)				Ave. efflux time (s)
4.9257	276.47	276.37	276.78	276.80	276.61 ± 0.22
3.5447	261.96	262.49	262.50	262.41	262.34 ± 0.26
2.9864	257.08	257.19	257.13	257.03	257.11 ± 0.07
2.5801	253.54	253.27	253.22	253.22	253.31 ± 0.15

Set #2:-

Concentration (g/dl)	Efflux times (s)				Ave. efflux time (s)
4.6146	273.21	273.35	273.24	273.40	273.30 ± 0.09
3.6917	263.85	263.92	263.71	263.99	263.87 ± 0.12
3.0764	258.11	258.01	257.95	257.97	258.01 ± 0.07

Toluene:

Concentration (g/dl)	Efflux times (s) (t_o)				Ave. efflux time (s)
...	231.13	231.25	231.16	231.25	231.20 ± 0.06

Calculations:

$\eta_{rel}=t/t_o$; $\eta_{sp}=\eta_{rel}-1$

c (g/dl)	t (ave)	η_{rel}	η_{sp}	η_{sp}/c (dl/g)
4.9257	276.61	1.1964	0.1964	0.03987
4.6146	273.30	1.1821	0.1821	0.03946
3.6917	263.87	1.1431	0.1413	0.03828
3.5447	262.34	1.1347	0.1347	0.03799
3.0764	258.01	1.1160	0.1160	0.03769
2.9864	257.11	1.1121	0.1121	0.03752
2.5801	253.31	1.0956	0.0956	0.03706

From a plot of η_{sp}/c vs c, $[\eta] = 0.03394 dl/g \pm 1.73 \times 10^{-4}$

Table D-1. (Cont'd.)

PSZ solution (batch 0831A):

Set #1:

Concentration (g/dl)	Efflux times (s)				Ave. efflux time (s)
4.3762	267.50	267.15	267.10	267.19	267.24 ± 0.18
3.1827	257.38	257.37	257.59	257.28	257.41 ± 0.13
2.6930	252.87	253.35	253.18	253.22	253.16 ± 0.20
2.3334	249.85	249.75	250.28	250.03	249.98 ± 0.23

Set #2:-

Concentration (g/dl)	Efflux times (s)				Ave. efflux time (s)
3.4937	259.85	260.01	260.05	259.70	259.90 ± 0.16
2.7949	254.09	253.90	253.98	253.97	253.99 ± 0.08
2.1499	248.60	248.42	248.39	248.65	248.52 ± 0.13

Toluene:

Concentration (g/dl)	Efflux times (s) (t_o)				Ave. efflux time (s)
...	231.13	231.25	231.16	231.25	231.20 ± 0.06

Calculations:

$\eta_{rel}=t/t_o$; $\eta_{sp}=\eta_{rel}-1$

c (g/dl)	t (ave)	η_{rel}	η_{sp}	η_{sp}/c (dl/g)
4.3762	267.24	1.1559	0.1559	0.03562
3.4937	259.90	1.1241	0.1241	0.03553
3.1827	257.41	1.1134	0.1134	0.03562
2.7949	253.99	1.0986	0.0986	0.03527
2.6930	253.16	1.0950	0.0950	0.03527
2.3334	249.98	1.0812	0.0812	0.03481
2.1499	248.52	1.0749	0.0749	0.03485

From a plot of η_{sp}/c vs. c, $[\eta] = 0.0342$ dl/g ± 2.00×10^{-4}

Table D-2. Intrinsic viscosity calculations for PMS polymer in toluene (Ubhellode viscometer type OB)

Concentration (g/dl)	Efflux times (s)					Ave. efflux time (s)
7.8005	143.81	143.88	144.01	143.98	143.82	143.90 ±0.09
5.6731	136.56	136.36	136.41	136.39	136.28	136.40 ±0.10
4.8003	133.28	133.41	133.48	133.36	133.22	133.35 ±0.10
4.1603	131.40	131.21	131.17	131.11	131.21	131.22 ±0.11

Toluene:

Concentration (g/dl)	Efflux times (s)					Ave. efflux time (s)
-	118.06	118.10	118.13	118.13	118.13	118.11 ±0.03

Calculations:

$\eta_{rel}=t/t_o$; $\eta_{sp}=\eta_{rel}-1$

c (g/dl)	t (ave)	η_{rel}	η_{sp}	η_{sp}/c (dl/g)
7.8005	143.90	1.21835	0.21835	0.02799
5.6731	136.40	1.15485	0.15485	0.02729
4.8003	133.35	1.12903	0.12903	0.02688
4.1603	131.22	1.11099	0.11099	0.02668

From a plot of η_{sp}/c vs c, $[\eta] = 0.02516$ dl/g ± 1.1×10^{-4}; $R^2 = 0.9946$

Table D-3. Intrinsic viscosity calculations for PMS polymer in toluene-1,4 dioxane mixture (50:50 by volume) (Ubhellode viscometer type OB)

Concentration (g/dl)	Efflux times (s)					Ave. efflux time (s)
7.1640	180.72	180.92	180.62	180.78	180.85	180.78 ±0.11
5.7312	174.50	174.16	174.28	174.47	174.18	174.32 ±0.16
4.7760	170.25	170.19	170.22	170.16	170.25	170.21 ±0.04
4.0937	167.50	167.38	167.47	167.47	167.25	167.41 ±0.10

Toluene-1,4 dioxane mixture (50:50 Vol%):

Concentration (g/dl)	Efflux times (s)					Ave. efflux time (s)
-	152.44	152.50	152.62	152.75	152.62	152.59 ±0.12

Calculations:

$\eta_{rel}=t/t_o$; $\eta_{sp}=\eta_{rel}-1$

c (g/dl)	t (ave)	η_{rel}	η_{sp}	η_{sp}/c (dl/g)
7.1640	180.78	1.1847	0.1847	0.02578
5.7312	174.32	1.1424	0.1424	0.02485
4.7760	170.21	1.1155	0.1155	0.02417
4.0930	167.41	1.0971	0.0971	0.02372

From a plot of η_{sp}/c vs c, $[\eta] = 0.020968$ dl/g ± 3.6×10^{-5}; $R^2 = 0.9998$

APPENDIX E
RESULTS OF SURFACE TENSION MEASUREMENTS

Table E-1. Results of surface tension measurements (at 22°C).

Water (viscosity: 0.953 mPa·s at 22°C; published surface tension: 0.07258 N/m at 22°C) [Dea85]

Force (mg)	Surface tension (N/m)
387.20	0.07589
388.80	0.07620
387.00	0.07585
388.00	0.07605
387.00	0.07585
Average surface tension : 0.07597 ± 0.00015 [Deviation from published value: 4.6%]	

Acetone (viscosity: 0.337 mPa·s at 15°C; published surface tension: 0.0238 N/m at 22°C) [Dea85]

Force (mg)	Surface tension (N/m)
126.00	0.02470
126.40	0.02477
125.60	0.02462
127.00	0.02489
126.40	0.02477
Average surface tension : 0.02475 ± 0.00010 [Deviation from published value: 4.0%]	

Glycerol (viscosity ~0.6-0.58 Pa·s at 22°C; published surface tension: 0.06272 N/m at 22°C)

Force (mg)	Surface tension (N/m)
348.0	0.06821
348.4	0.06829
348.6	0.06833
348.4	0.06829
348.8	0.06836
Average surface tension : 0.06830 ± 0.00006 [Deviation from published value: 8.8%]	

Table E-1. (Cont'd.)

Polydimethylsiloxane (viscosity: 12.12 Pa·s (molecular weight~67,700) at 22°C; published surface tension: 0.0215 N/m)

Force (mg)	Surface tension (N/m)
122.0	0.02391
122.6	0.02384
121.8	0.02387
122.4	0.02399
122.4	0.02395
Average surface tension : 0.02391 ± 0.00006 [Deviation from published value: 11.2%]	

Toluene (viscosity: 0.587 mPa·s at 20°C; Published value of surface tension: 0.02828 N/m at 22°C) [Dea85]

Force (mg)	Surface tension (N/m)
152.40	0.02987
151.80	0.02975
152.00	0.02979
151.60	0.02971
151.00	0.02960
Average surface tension : 0.02974 ± 0.00010 [Deviation from publsihed value: 5.2%]	

PCS Solution (33 wt%)

Force (mg)	Surface tension (N/m)
144.60	0.02834
145.20	0.02846
145.80	0.02858
144.80	0.02838
145.20	0.02846
Average surface tension : 0.02844 ± 0.00009	

Table E-1. (Cont'd.)

PCS Solution (50 wt%)

Force (mg)	Surface tension (N/m)
172.60	0.03383
173.00	0.03391
174.00	0.03410
173.40	0.03399
173.00	0.03391
Average : 0.03395 ± 0.00010	

PCS Solution (66 wt%)

Force (mg)	Surface tension (N/m)
199.20	0.03728
191.40	0.03751
193.60	0.03795
194.20	0.03806
192.80	0.03770
Average: 0.03772 ±0.00032	

PCS+PSZ Solution (33 wt%)

Force (mg)	Surface tension (N/m)
140.00	0.02744
140.40	0.02752
140.80	0.02760
140.00	0.02744
140.40	0.02752
Average: 0.02750 ±0.00007	

Table E-1. (Cont'd.)

PCS+PSZ Solution (50 wt%)

Force (mg)	Surface tension (N/m)
163.00	0.03195
163.20	0.03199
164.60	0.03226
164.00	0.03214
163.60	0.03203
Average: 0.03207 ±0.00013	

PCS+PSZ Solution (66 wt%)

Force (mg)	Surface tension (N/m)
178.00	0.03489
178.40	0.03497
178.20	0.03493
179.60	0.03520
178.00	0.03489
Average: 0.03497 ±0.00013	

APPENDIX F
TEMPERATURE AND WEIGHT GAINS FOR HEAT TREATMENT OF PCS AND PCS+PSZ FIBERS IN AIR

Table F-1. Air-heat treatment temperatures and weight gains for PCS and PCS+PSZ fibers.

Fiber batch	PCS or PCS+PSZ	Amount of sample (mg)	Temperature (°C)	Weight gain (%)
UF-65s-AL187(1h)	PCS	36.6	187	8.5
UF-69s- AL180(1h)	PCS	33.8	180	4.7
UF-69s-AL187(1h)	PCS	13.4	187	5.2
UF-69s-AL190(1h)	PCS	33.5	190	9.3
UF-70s-AL170(1h)	PCS+PSZ	11.8	170	6.8
UF-70s-AL177(1h)	PCS+PSZ	158	177	6.5

APPENDIX G

WEIGHT LOSS DATA FOR PCS, PCS+PSZ FIBERS (AIR-HEAT TREATED AND NON-AIR HEAT TREATED) AFTER PYROLYSIS AT 1150°C IN NITROGEN

Table G-1. Weight loss data for air-heat treated and non-air heat treated PCS and PCS+PSZ fibers after pyrolysis at 1150°C in nitrogen.

Batch	Number of batches	Weight loss (%)	Standard deviation
PCS	18	22.7	2.3
PCS+PSZ	15	22.5	2.8
PCS (air-heat treated)	2	12.2	0.5
PCS+PSZ (air-heat treated)	3	15.3	0.2

APPENDIX H
TENSILE STRENGTH DATA FOR PYROLYZED PCS AND PCS+PSZ FIBERS

Table H-1. UF 63s-1150 (1150°C/1 h/N_2) (PCS)

Batch 1:

	d_1(μm)	d_2(μm)	d(avg.)	Load(g)	Strain	TS(GPa)	EM(GPa)
	11.00	11.00	11.00	28.27	0.0135	2.92	215.95
	12.50	13.00	12.75	21.37	0.0088	1.64	185.69
	11.00	11.50	11.25	31.77	0.0137	3.13	227.98
	11.00	11.00	11.00	19.67	0.0094	2.03	216.82
	12.00	13.00	12.50	32.06	0.0122	2.56	210.52
	12.50	13.00	12.75	27.59	0.0105	2.12	201.42
	12.00	12.00	12.00	24.43	0.0102	2.12	207.88
	13.00	13.00	13.00	31.67	0.0117	2.34	200.71
	13.00	13.00	13.00	34.73	0.0126	2.56	204.25
	12.00	12.00	12.00	18.07	0.0081	1.57	192.79
	13.00	13.00	13.00	30.94	0.0103	2.29	222.01
	12.00	12.00	12.00	34.73	0.0144	3.01	209.09
	13.00	13.00	13.00	10.00	0.0038	0.74	195.93
	11.50	11.50	11.50	31.28	0.0128	2.95	231.45
	12.00	12.00	12.00	25.79	0.0109	2.24	205.13
	12.00	12.00	12.00	28.85	0.0113	2.50	221.44
	12.00	12.50	12.25	39.30	0.0144	3.27	226.64
	12.00	12.00	12.00	30.55	0.0121	2.65	218.49
Average	**12.08**	**12.25**	**12.17**	**27.84**	**0.0112**	**2.37**	**210.79**
Std. Dev	**0.67**	**0.71**	**0.68**	**7.04**	**0.0026**	**0.63**	**12.80**

Batch 2:

	d_1(μm)	d_2(μm)	d(avg.)	Load(g)	Strain	TS(GPa)	EM(GPa)
	9.50	9.50	9.50	19.34	0.0142	2.67	186.49
	9.50	9.50	9.50	14.43	0.0111	2.00	179.55
	11.00	11.50	11.25	19.97	0.0117	1.97	167.85
	13.00	13.50	13.25	34.21	0.0140	2.43	174.35
	12.50	13.00	12.75	15.64	0.0078	1.20	154.26
	13.00	13.50	13.25	35.13	0.0132	2.50	188.70
	10.50	11.00	10.75	25.98	0.0140	2.81	200.01
	12.50	13.50	13.00	33.20	0.0140	2.46	174.92
	11.50	11.50	11.50	25.21	0.0135	2.38	176.20
	11.00	11.50	11.25	19.34	0.0102	1.91	185.95
	12.00	12.00	12.00	23.43	0.0128	2.03	158.13
	9.50	9.50	9.50	17.27	0.0130	2.39	184.23
	11.50	12.00	11.75	27.96	0.0135	2.53	187.86
	9.50	9.50	9.50	14.92	0.0110	2.06	186.67
	14.50	16.00	15.25	22.28	0.0061	1.20	195.43
	9.00	9.00	9.00	10.68	0.0094	1.65	175.14
	11.50	11.50	11.50	24.35	0.0124	2.30	185.86
Average	**11.26**	**11.62**	**11.44**	**22.55**	**0.0119**	**2.15**	**180.09**
Std. Dev	**1.55**	**1.89**	**1.72**	**7.19**	**0.0024**	**0.47**	**12.08**

Table H-2. UF 64s-1150 (1150°C/1 h/N_2) (PCS)

Batch 1:

	d_1(μm)	d_2(μm)	d(avg.)	Load(g)	Strain	TS(GPa)	EM(GPa)
	9.0	9.0	9.0	21.30	0.0153	3.28	215.07
	8.0	9.5	8.8	14.93	0.0125	2.45	196.07
	9.0	9.0	9.0	17.17	0.0132	2.65	199.96
	8.0	10.0	9.0	18.63	0.0128	2.91	227.22
	9.0	9.5	9.3	28.26	0.0171	4.12	241.16
	8.0	9.0	8.5	10.22	0.0080	1.77	221.40
	8.5	9.0	8.8	9.92	0.0080	1.62	202.40
	9.0	9.0	9.0	23.98	0.0164	3.69	225.71
	9.0	9.0	9.0	22.23	0.0149	3.42	229.99
	9.0	9.0	9.0	27.24	0.0174	4.20	241.41
	9.0	9.0	9.0	30.30	0.0191	4.67	244.45
	9.0	9.0	9.0	26.85	0.0180	4.14	229.65
	9.0	9.0	9.0	12.89	0.0091	1.99	219.29
	8.0	9.0	8.5	31.18	0.0201	5.40	269.18
	8.0	9.0	8.5	14.06	0.0106	2.44	230.84
	7.0	10.0	8.5	2.05	0.0023	0.37	158.10
	8.0	10.0	9.0	11.82	0.0095	1.84	193.89
	9.0	9.0	9.0	20.62	0.0139	3.18	228.37
	9.0	9.0	9.0	18.39	0.0134	2.83	211.52
	9.0	9.0	9.0	22.37	0.0159	3.45	216.30
Average	**8.53**	**9.22**	**8.88**	**19.09**	**0.0132**	**3.01**	**220.79**
Std. Dev	**0.61**	**0.39**	**0.23**	**8.10**	**0.0046**	**1.26**	**24.50**

Batch 2:

	d_1(μm)	d_2(μm)	d(avg.)	Load(g)	Strain	TS(GPa)	EM(GPa)
	9.00	10.00	9.50	10.17	0.0075	1.41	183.82
	9.50	9.50	9.50	16.79	0.0137	2.91	212.05
	8.50	11.50	10.00	14.07	0.0107	1.80	167.52
	7.00	12.50	9.75	10.08	0.0088	1.44	163.28
	9.50	10.00	9.75	21.32	0.0169	2.80	175.16
	9.50	10.00	9.75	18.92	0.0129	2.49	192.91
	10.00	10.00	10.00	19.97	0.0129	2.49	193.45
	9.50	9.50	9.50	14.31	0.0106	1.98	186.78
	10.00	10.00	10.00	23.19	0.0150	2.89	192.40
	9.50	10.50	10.00	21.65	0.0141	2.71	192.20
	8.50	12.00	10.25	9.65	0.0072	1.18	163.19
	9.50	9.50	9.50	20.21	0.0135	2.80	206.51
	9.50	9.50	9.50	17.48	0.0119	2.42	202.58
	9.50	9.50	9.50	17.38	0.0114	2.40	211.05
	9.50	9.50	9.50	12.24	0.0090	1.69	187.76
	9.50	10.00	9.75	16.95	0.0121	2.23	184.71
	9.50	10.00	9.75	16.95	0.0118	2.23	184.71
Average	**9.26**	**10.21**	**9.74**	**16.55**	**0.0118**	**2.23**	**188.24**
Std. Dev	**0.71**	**0.92**	**0.24**	**4.22**	**0.0026**	**0.55**	**15.01**

Table H-2. (Cont'd.)

Batch 3:

	d_1(μm)	d_2(μm)	d(avg.)	Load(g)	Strain	TS(GPa)	EM(GPa)
	10.50	11.50	11.00	18.70	0.0112	1.93	172.41
	9.50	11.00	10.25	12.30	0.0093	1.47	157.84
	10.50	11.00	10.75	29.20	0.0165	3.15	191.16
	9.50	10.00	9.75	16.25	0.0114	2.13	187.57
	6.00	8.50	7.25	7.68	0.0079	1.88	236.91
	8.00	11.50	9.75	12.06	0.0111	1.64	147.95
	9.00	10.50	9.75	19.47	0.0124	2.57	207.70
	8.00	14.50	11.25	11.10	0.0086	1.19	138.16
	9.50	10.00	9.75	19.52	0.0129	2.56	199.08
	10.00	10.00	10.00	18.99	0.0122	2.37	193.78
	8.50	12.00	10.25	13.26	0.0098	1.62	165.18
	9.50	10.50	10.00	20.53	0.0121	2.57	212.05
	9.00	11.00	10.00	6.47	0.0052	0.82	157.27
	9.00	11.00	10.00	18.56	0.0117	2.34	200.61
	9.50	10.00	9.75	24.96	0.0155	3.28	210.90
	9.50	10.50	10.00	16.78	0.0111	2.10	189.81
	8.50	11.00	9.75	1.66	0.0016	0.22	138.34
Average	**9.06**	**10.85**	**9.96**	**15.73**	**0.01**	**1.99**	**182.75**
Std. Dev	**1.07**	**1.23**	**0.83**	**6.84**	**0.00**	**0.79**	**28.41**

Batch 4:

	d_1(μm)	d_2(μm)	d(avg.)	Load(g)	Strain	TS(GPa)	EM(GPa)
	10.00	10.50	10.25	18.78	0.0102	2.23	218.65
	6.50	13.50	10.00	7.23	0.0074	1.03	139.51
	6.50	13.50	10.00	12.72	0.0094	1.81	191.39
	6.50	13.50	10.00	9.21	0.0085	1.31	153.97
	6.50	12.50	9.50	3.58	0.0032	0 55	171.69
	9.50	11.00	10.25	5.74	0.0036	0.69	189.20
	7.00	11.00	9.00	5.02	0.0037	0.81	222.77
	9.50	10.50	10.00	20.27	0.0115	2.54	221.39
	9.50	9.50	9.50	31.09	0.0189	4.30	227.73
	8.00	11.00	9.50	6.85	0.0052	0.97	186.13
	8.50	11.00	9.75	14.50	0.0095	1.94	202.66
	6.00	13.50	9.75	4.49	0.0045	0.69	154.76
	9.50	10.00	9.75	19.11	0.0120	2.51	209.76
	9.50	10.00	9.75	28.69	0.0160	3.77	235.12
	10.00	10.00	10.00	19.55	0.0109	2.44	223.49
	6.50	12.50	9.50	8.53	0.0068	1.31	192.08
	10.50	10.50	10.50	14.16	0.0083	1.60	191.97
Average	**8.24**	**11.41**	**9.82**	**13.50**	**0.0088**	**1.79**	**196.02**
Std. Dev	**1.60**	**1.43**	**0.36**	**8.38**	**0.0043**	**1.08**	**28.34**

Table H-2. (Cont'd.)

Batch 5:

	d_1(μm)	d_2(μm)	d(avg.)	Load(g)	Strain	TS(GPa)	EM(GPa)
	9.50	10.00	9.75	19.85	0.0122	2.61	219.83
	9.00	9.00	9.00	18.74	0.0118	2.89	244.92
	8.00	10.50	9.25	12.30	0.0086	1.83	211.55
	9.00	9.00	9.00	21.94	0.0127	3.38	266.07
	9.00	9.50	9.25	17.82	0.0124	2.60	208.92
	8.50	9.00	8.75	9.49	0.0061	1.55	252.49
	8.50	9.00	8.75	24.60	0.0167	4.01	240.52
	8.50	9.00	8.75	18.40	0.0117	3.00	257.06
	8.50	8.50	8.50	12.74	0.0087	2.20	253.91
	8.50	9.00	8.75	23.92	0.0147	3.90	266.15
	8.50	8.50	8.50	14.67	0.0103	2.53	246.37
	7.50	12.00	9.75	14.04	0.0097	1.95	200.05
	9.00	9.50	9.25	11.14	0.0067	1.63	240.93
	8.00	10.50	9.25	10.94	0.0070	1.63	233.01
	7.50	8.00	7.75	17.58	0.0122	3.66	300.07
	8.00	10.50	9.25	20.29	0.0140	3.01	215.19
	8.50	9.00	8.75	20.58	0.0131	3.36	257.16
Average	**8.47**	**9.44**	**8.96**	**17.00**	**0.0111**	**2.69**	**242.01**
Std. Dev	**0.54**	**0.98**	**0.49**	**4.68**	**0.0030**	**0.81**	**25.43**

Table H-3. UF 65s-1150 (1150°C/1 h/N_2) (PCS)

Batch 1:

	d_1(μm)	d_2(μm)	d(avg.)	Load(g)	Strain	TS(GPa)	EM(GPa)
	10.00	10.00	10.00	18.38	0.0102	2.29	223.99
	10.00	10.00	10.00	22.61	0.0121	2.82	238.57
	11.00	11.00	11.00	30.86	0.0146	3.18	218.36
	11.00	11.50	11.25	30.42	0.0134	3.00	223.65
	11.00	11.00	11.00	41.24	0.0184	4.25	231.41
	12.00	12.00	12.00	27.31	0.0122	2.37	194.29
	10.50	11.00	10.75	25.52	0.0134	2.76	205.23
	11.00	11.00	11.00	30.37	0.0148	3.13	211.38
	10.00	11.00	10.50	31.58	0.0156	3.58	229.62
	10.00	10.00	10.00	25.95	0.0147	3.24	220.94
	9.00	9.50	9.25	24.35	0.0156	3.55	227.16
	10.00	10.00	10.00	12.32	0.0075	1.54	206.02
	11.00	11.00	11.00	25.27	0.0135	2.61	193.37
	9.50	10.00	9.75	20.81	0.0126	2.73	213.95
	10.00	11.00	10.50	31.24	0.0151	3.54	234.93
	9.00	9.00	9.00	13.43	0.0096	2.07	214.56
	10.00	10.00	10.00	20.71	0.0122	2.58	211.22
	10.00	10.00	10.00	26.83	0.0148	3.35	226.49
	11.00	12.00	11.50	16.83	0.0072	1.59	220.20
	14.00	14.00	14.00	32.60	0.0098	2.08	212.53
Average	**10.50**	**10.75**	**10.63**	**25.43**	**0.01**	**2.81**	**217.89**
Std. Dev	**1.11**	**1.11**	**1.09**	**7.07**	**0.00**	**0.70**	**12.32**

Batch 2:

	d_1(μm)	d_2(μm)	d(avg.)	Load(g)	Strain	TS(GPa)	EM(GPa)
	11.50	11.50	11.50	14.03	0.0073	1.32	182.51
	11.50	12.00	11.75	11.86	0.0055	1.07	208.10
	12.00	12.00	12.00	27.65	0.0134	2.40	178.52
	13.00	13.00	13.00	8.86	0.0035	0.65	185.09
	12.50	13.50	13.00	15.48	0.0063	1.14	182.01
	12.50	13.00	12.75	23.40	0.0099	1.80	180.60
	12.50	12.50	12.50	12.97	0.0059	1.04	175.97
	13.00	13.50	13.25	26.00	0.0101	1.85	183.25
	12.00	12.50	12.25	36.43	0.0164	3.03	184.83
	12.00	12.00	12.00	20.40	0.0102	1.77	173.81
	11.00	11.00	11.00	22.48	0.0131	2.32	176.38
	12.00	12.50	12.25	18.91	0.0087	1.57	181.15
	11.00	11.50	11.25	17.22	0.0088	1.70	199.17
	13.00	13.50	13.25	31.22	0.0128	2.22	173.56
	12.50	12.50	12.50	19.68	0.0091	1.57	172.21
	11.50	12.00	11.75	30.83	0.0156	2.79	178.36
	13.00	13.00	13.00	42.71	0.0171	3.15	184.48
	11.50	12.50	12.00	26.15	0.0116	2.27	194.86
Average	**12.11**	**12.44**	**12.28**	**22.57**	**0.01**	**1.87**	**183.05**
Std. Dev	**0.68**	**0.73**	**0.68**	**8.96**	**0.00**	**0.71**	**9.32**

Table H-3. (Cont'd.)

Batch 3:

	d_1(μm)	d_2(μm)	d(avg.)	Load(g)	Strain	TS(GPa)	EM(GPa)
	11.00	13.50	12.25	13.15	0.0075	1.11	147.37
	12.00	14.50	13.25	21.82	0.0098	1.56	159.86
	9.00	13.00	11.00	6.07	0.0048	0.65	136.38
	13.00	13.50	13.25	8.53	0.0045	0.61	135.37
	9.50	11.50	10.50	14.50	0.0085	1.66	195.38
	11.00	14.00	12.50	22.44	0.0113	1.82	160.82
	11.50	14.50	13.00	13.05	0.0054	0.98	180.90
	11.50	13.50	12.50	14.40	0.0099	1.16	116.80
	11.50	12.00	11.75	26.10	0.0124	2.36	189.74
	14.00	14.50	14.25	36.50	0.0210	2.24	144.95
	14.00	14.50	14.25	14.02	0.0066	0.86	129.88
	12.50	15.00	13.75	16.38	0.0079	1.09	137.29
	12.00	13.50	12.75	15.17	0.0073	1.17	160.70
	9.00	10.50	9.75	18.93	0.0142	2.50	184.96
	12.00	14.50	13.25	20.28	0.0094	1.45	154.27
	12.50	14.50	13.50	8.67	0.0040	0.60	150.54
	10.50	15.00	12.75	24.99	0.0126	1.98	156.67
	13.00	15.50	14.25	37.03	0.0178	2.29	128.85
Average	**11.64**	**13.75**	**12.69**	**18.45**	**0.01**	**1.45**	**153.93**
Std. Dev	**1.48**	**1.31**	**1.27**	**8.66**	**0.00**	**0.63**	**22.33**

Batch 4:

	d_1(μm)	d_2(μm)	d(avg.)	Load(g)	Strain	TS(GPa)	EM(GPa)
	11.00	11.00	11.00	9.03	0.0047	0.93	198.68
	11.50	11.50	11.50	20.68	0.0097	1.95	201.74
	11.50	11.50	11.50	22.08	0.0102	2.08	203.61
	11.00	11.00	11.00	26.57	0.0124	2.74	220.75
	11.50	12.00	11.75	22.71	0.0102	2.05	201.56
	13.00	13.00	13.00	17.44	0.0062	1.29	206.82
	11.00	12.00	11.50	29.42	0.0118	2.78	236.10
	13.00	13.50	13.25	12.37	0.0055	0.88	160.24
	12.50	12.50	12.50	19.47	0.0073	1.56	212.83
	11.50	11.50	11.50	17.25	0.0077	1.63	210.86
	11.50	12.00	11.75	26.81	0.0109	2.42	221.75
	11.50	12.00	11.75	25.12	0.0104	2.27	217.84
	12.50	12.50	12.50	22.03	0.0080	1.76	220.76
	12.50	13.00	12.75	28.02	0.0102	2.15	211.37
	11.00	11.50	11.25	28.70	0.0121	2.83	233.22
	11.50	11.50	11.50	7.63	0.0038	0.72	191.77
	11.50	11.50	11.50	17.34	0.0076	1.64	214.30
	12.50	15.00	13.75	22.17	0.0072	1.48	204.57
Average	**11.78**	**12.14**	**11.96**	**20.82**	**0.0087**	**1.84**	**209.38**
Std. Dev	**0.69**	**1.00**	**0.80**	**6.45**	**0.0026**	**0.64**	**16.86**

Table H-3. (Cont'd.)

Batch 5:

	d_1(μm)	d_2(μm)	d(avg.)	Load(g)	Strain	TS(GPa)	EM(GPa)
	11.50	11.50	11.50	25.35	0.0102	2.39	233.90
	12.50	13.50	13.00	42.48	0.0157	3.14	199.55
	11.50	11.50	11.50	20.31	0.0084	1.92	228.61
	12.50	12.50	12.50	17.77	0.0064	1.42	222.75
	13.00	13.50	13.25	30.20	0.0096	2.15	223.57
	13.50	13.50	13.50	23.86	0.0074	1.63	220.07
	11.50	11.50	11.50	19.50	0.0082	1.84	225.08
	13.50	13.50	13.50	21.13	0.0077	1.45	188.21
	12.00	12.00	12.00	22.76	0.0086	1.97	228.23
	11.50	11.50	11.50	28.80	0.0118	2.72	230.52
	11.50	11.50	11.50	30.20	0.0119	2.85	239.18
	11.50	11.50	11.50	36.43	0.0155	3.44	225.74
	11.50	11.50	11.50	26.69	0.0105	2.52	239.26
	11.50	11.50	11.50	39.26	0.0152	3.71	243.81
	13.00	13.50	13.25	23.38	0.0075	1.66	221.10
	11.00	11.50	11.25	32.98	0.0134	3.25	242.11
	11.00	11.50	11.25	25.73	0.0109	2.54	232.29
	11.50	11.50	11.50	19.40	0.0084	1.83	217.02
Average	**11.97**	**12.14**	**12.06**	**27.01**	**0.01**	**2.36**	**225.61**
Std. Dev	**0.81**	**0.90**	**0.85**	**7.12**	**0.00**	**0.71**	**14.02**

Table H-4. UF-69s-1150: (1150°C/1 h/N_2) (PCS)

Batch 1

	d_1(μm)	d_2(μm)	d(avg.)	Load(g)	Strain	TS(GPa)	EM(GPa)
	12.00	12.00	12.00	28.58	0.0116	2.48	212.98
	10.00	11.00	10.50	14.80	0.0090	1.68	186.34
	9.50	10.00	9.75	12.59	0.0078	1.65	213.14
	10.00	10.50	10.25	14.61	0.0086	1.74	201.27
	12.50	14.00	13.25	18.95	0.0076	1.35	176.94
	9.00	10.50	9.75	17.89	0.0096	2.36	244.94
	11.00	11.50	11.25	29.98	0.0131	2.96	225.34
	10.00	10.00	10.00	27.71	0.0148	3.46	234.26
	12.50	12.50	12.50	30.51	0.0130	2.44	188.04
	10.00	11.50	10.75	28.63	0.0121	3.11	256.53
	11.00	11.00	11.00	32.96	0.0156	3.40	217.28
	11.00	11.50	11.25	11.63	0.0051	1.15	225.51
	10.50	11.50	11.00	9.70	0.0060	1.00	166.20
	11.50	12.50	12.00	27.81	0.0123	2.41	196.64
	10.50	11.00	10.75	28.00	0.0122	3.03	248.57
	12.00	13.00	12.50	21.64	0.0095	1.73	182.14
	10.00	11.50	10.75	32.63	0.0161	3.54	224.12
Average	**10.76**	**11.50**	**11.13**	**22.86**	**0.0108**	**2.32**	**211.78**
Std. Dev	**1.05**	**1.06**	**1.02**	**8.01**	**0.0033**	**0.83**	**26.50**

Batch 2

	d_1(μm)	d_2(μm)	d(avg.)	Load(g)	Strain	TS(GPa)	EM(GPa)
	12.50	12.50	12.50	39.07	0.0143	3.12	235.42
	11.50	12.00	11.75	4.80	0.0020	0.43	222.13
	13.00	13.00	13.00	27.57	0.0109	2.04	186.00
	11.50	12.00	11.75	24.79	0.0109	2.24	205.89
	12.50	12.50	12.50	20.01	0.0066	1.60	242.41
	13.50	13.50	13.50	25.91	0.0083	1.77	212.94
	13.00	13.50	13.25	48.05	0.0166	3.42	205.76
	11.50	11.50	11.50	32.54	0.0139	3.07	221.00
	12.50	12.50	12.50	33.76	0.0128	2.70	210.53
	13.50	14.00	13.75	44.58	0.0140	2.94	217.62
	13.50	13.50	13.50	29.96	0.0095	2.05	225.47
	13.50	13.50	13.50	15.96	0.0053	1.09	207.98
	13.00	13.50	13.25	24.11	0.0075	1.71	228.10
	13.50	13.50	13.50	40.29	0.0130	2.76	220.54
	12.00	12.50	12.25	29.27	0.0110	2.44	221.51
	11.50	11.50	11.50	23.37	0.0095	2.21	231.94
	12.50	12.50	12.50	36.00	0.0133	2.88	215.40
	11.50	12.00	11.75	43.37	0.0190	3.92	217.03
Average	**12.56**	**12.75**	**12.65**	**30.19**	**0.0110**	**2.35**	**218.20**
Std. Dev	**0.80**	**0.77**	**0.78**	**10.91**	**0.0042**	**0.85**	**12.85**

Table H-4. (Cont'd.)

Batch 3

	d_1(μm)	d_2(μm)	d(avg.)	Load(g)	Strain	TS(GPa)	EM(GPa)
	13.00	15.00	14.00	52.70	0.0168	3.37	201.15
	13.00	13.00	13.00	37.07	0.0163	2.74	167.49
	12.50	15.00	13.75	53.95	0.0180	3.59	199.82
	11.50	15.50	13.50	25.00	0.0086	1.75	204.65
	11.00	12.50	11.75	36.40	0.0154	3.30	214.65
	15.50	16.00	15.75	52.46	0.0192	2.64	141.62
	10.50	11.50	11.00	39.09	0.0163	4.04	247.65
	13.00	14.50	13.75	36.59	0.0129	2.42	187.62
	14.00	14.50	14.25	38.56	0.0155	2.37	153.07
	12.00	15.00	13.50	31.16	0.0117	2.16	184.05
	12.00	12.50	12.25	38.47	0.0164	3.20	195.59
	11.50	14.50	13.00	55.49	0.0187	4.15	221.73
	14.00	15.50	14.75	40.05	0.0130	2.30	176.82
	13.00	15.50	14.25	42.31	0.0162	2.62	162.23
	10.50	11.50	11.00	20.00	0.0094	2.07	219.71
	15.00	15.50	15.25	45.82	0.0152	2.46	161.74
	11.50	13.00	12.25	37.46	0.0158	3.13	197.37
	12.50	14.50	13.50	32.79	0.0112	2.26	201.27
Average	**12.56**	**14.17**	**13.36**	**39.74**	**0.0148**	**2.81**	**191.01**
Std. Dev	**1.42**	**1.45**	**1.33**	**9.67**	**0.0030**	**0.68**	**27.06**

Batch 4

	d_1(μm)	d_2(μm)	d(avg.)	Load(g)	Strain	TS(GPa)	EM(GPa)
	12.00	13.50	12.75	41.51	0.0173	3.20	184.40
	11.50	14.00	12.75	29.72	0.0126	2.30	182.24
	13.00	13.50	13.25	39.57	0.0160	2.81	184.65
	12.00	12.50	12.25	51.99	0.0212	4.33	211.66
	11.50	14.00	12.75	39.48	0.0166	3.06	196.23
	11.50	14.00	12.75	36.43	0.0163	2.82	173.53
	12.50	13.50	13.00	58.03	0.0236	4.29	181.73
	13.00	14.00	13.50	34.35	0.0134	2.36	187.98
	12.00	13.50	12.75	35.22	0.0149	2.71	181.78
	11.00	13.50	12.25	33.63	0.0123	2.83	244.32
	11.50	13.50	12.50	38.32	0.0163	3.08	189.33
	12.00	14.00	13.00	59.19	0.0232	4.40	189.25
	12.00	13.00	12.50	42.09	0.0175	3.37	192.71
	11.50	13.00	12.25	41.75	0.0177	3.48	205.79
	13.00	13.00	13.00	49.09	0.0190	3.63	209.43
	11.50	14.00	12.75	40.88	0.0173	3.17	182.94
	11.50	13.00	12.25	49.77	0.0205	4.15	203.05
Average	**11.94**	**13.50**	**12.72**	**42.41**	**0.0174**	**3.29**	**194.18**
Std. Dev	**0.61**	**0.47**	**0.36**	**8.45**	**0.0033**	**0.67**	**16.86**

Table H-4. (Cont'd.)

Batch 5

	d_1(μm)	d_2(μm)	d(avg.)	Load(g)	Strain	TS(GPa)	EM(GPa)
	14.00	14.00	14.00	37.77	0.0123	2.41	194.83
	12.50	12.50	12.50	19.63	0.0081	1.57	193.74
	11.50	12.00	11.75	26.95	0.0121	2.44	201.16
	14.00	14.00	14.00	44.27	0.0137	2.82	205.56
	12.00	12.50	12.25	30.06	0.0130	2.50	191.73
	12.00	12.00	12.00	30.35	0.0133	2.63	198.36
	12.00	12.00	12.00	41.31	0.0175	3.58	204.38
	12.50	12.50	12.50	37.09	0.0157	2.96	188.12
	14.00	14.00	14.00	52.86	0.0179	3.37	187.49
	14.00	14.00	14.00	31.37	0.0101	2.00	198.43
	12.00	12.00	12.00	24.91	0.0106	2.16	203.47
	14.00	14.00	14.00	34.18	0.0112	2.18	193.77
	13.50	13.50	13.50	27.34	0.0093	1.87	202.12
	14.00	14.00	14.00	30.40	0.0100	1.94	193.88
	13.50	14.00	13.75	53.78	0.0187	3.55	194.42
	14.00	14.00	14.00	38.45	0.0135	2.45	180.77
	14.00	14.00	14.00	53.97	0.0179	3.44	192.04
	12.00	12.00	12.00	28.60	0.0127	2.48	195.44
	11.50	12.00	11.75	26.27	0.0109	2.38	217.55
	11.50	11.50	11.50	29.72	0.0132	2.80	211.76
Average	**12.93**	**13.03**	**12.98**	**34.96**	**0.0131**	**2.57**	**197.45**
Std. Dev	**1.04**	**0.98**	**1.01**	**9.92**	**0.0031**	**0.58**	**8.53**

Batch 6

	d_1(μm)	d_2(μm)	d(avg.)	Load(g)	Strain	TS(GPa)	EM(GPa)
	12.50	14.00	13.25	27.33	0.0096	1.95	203.12
	11.00	11.00	11.00	20.23	0.0102	2.09	205.52
	11.50	12.00	11.75	17.51	0.0081	1.58	195.20
	11.50	12.00	11.75	41.62	0.0189	3.76	204.98
	13.50	13.50	13.50	62.04	0.0224	4.25	198.00
	11.50	11.50	11.50	29.86	0.0128	2.82	219.58
	11.50	11.50	11.50	21.79	0.0092	2.06	223.67
	11.50	11.50	11.50	47.90	0.0220	4.52	214.47
	11.50	12.00	11.75	32.48	0.0162	2.94	183.45
	11.50	12.00	11.75	33.02	0.0149	2.99	200.60
	11.50	11.50	11.50	28.40	0.0138	2.68	194.84
	11.00	11.50	11.25	30.83	0.0163	3.04	188.33
	11.50	12.00	11.75	28.60	0.0149	2.59	173.35
	12.00	12.00	12.00	25.09	0.0111	2.17	195.92
	11.50	12.00	11.75	31.90	0.0144	2.88	200.12
	11.50	11.50	11.50	35.40	0.0165	3.34	205.05
	11.50	11.50	11.50	19.26	0.0085	1.82	214.69
	11.50	11.50	11.50	33.21	0.0151	3.13	207.81
	11.50	12.00	11.75	27.62	0.0118	2.50	211.88
	11.50	12.00	11.75	49.01	0.0227	4.43	203.28
Average	**11.63**	**11.93**	**11.78**	**32.16**	**0.0145**	**2.88**	**202.19**
Std. Dev	**0.53**	**0.69**	**0.59**	**10.97**	**0.0045**	**0.85**	**12.07**

Table H-5. UF 67s-1150 (1150°C/1 h/N_2) (PCS+PSZ)

Batch 1:

	d_1(μm)	d_2(μm)	d(avg.)	Load(g)	Strain	TS(GPa)	EM(GPa)
	10.50	11.00	10.75	34.44	0.0191	3.72	194.80
	10.50	11.00	10.75	30.38	0.0177	3.28	185.87
	10.50	10.50	10.50	30.29	0.0177	3.43	193.93
	11.00	11.00	11.00	24.47	0.0141	2.52	179.35
	10.00	10.00	10.00	24.27	0.0140	3.03	215.63
	11.00	11.50	11.25	39.97	0.0208	3.94	189.32
	10.50	10.50	10.50	24.91	0.0146	2.82	192.94
	10.50	11.00	10.75	22.41	0.0145	2.42	167.43
	10.00	10.00	10.00	29.01	0.0190	3.62	190.98
	11.00	11.00	11.00	34.25	0.0178	3.53	197.95
	10.50	10.50	10.50	29.89	0.0175	3.38	193.34
	11.00	11.00	11.00	35.66	0.0183	3.68	200.91
	10.50	10.50	10.50	30.58	0.0173	3.46	199.82
	10.00	10.50	10.25	33.66	0.0199	4.00	201.23
	10.00	10.50	10.25	22.36	0.0141	2.66	188.03
	10.50	10.50	10.50	32.63	0.0189	3.69	195.11
	10.00	10.00	10.00	30.68	0.0180	3.83	212.40
	10.50	12.00	11.25	27.16	0.0148	2.69	182.22
Average	**10.47**	**10.72**	**10.60**	**29.83**	**0.0171**	**3.32**	**193.40**
Std. Dev	**0.36**	**0.52**	**0.40**	**4.88**	**0.0022**	**0.50**	**11.23**

Batch 2:

	d_1(μm)	d_2(μm)	d(avg.)	Load(g)	Strain	TS(GPa)	EM(GPa)
	10.50	10.50	10.50	25.64	0.0172	2.90	173.71
	11.50	11.50	11.50	23.65	0.0140	2.23	159.38
	10.50	10.50	10.50	25.30	0.0166	2.86	179.42
	11.00	11.50	11.25	18.65	0.0106	1.84	182.60
	10.50	10.50	10.50	25.30	0.0170	2.86	182.67
	11.50	12.00	11.75	30.98	0.0175	2.80	160.43
	10.50	11.00	10.75	27.29	0.0173	2.95	170.23
	10.50	10.50	10.50	29.72	0.0195	3.36	172.58
	10.00	11.00	10.50	28.17	0.0194	3.20	165.05
	11.00	11.50	11.25	17.88	0.0106	1.76	166.66
	10.50	10.50	10.50	23.07	0.0147	2.61	187.91
	10.50	10.50	10.50	27.15	0.0175	3.07	180.47
	10.50	10.50	10.50	21.81	0.0138	2.47	185.20
	11.00	11.50	11.25	12.05	0.0066	1.19	180.76
	11.50	12.00	11.75	36.61	0.0199	3.31	165.96
	10.50	10.50	10.50	27.68	0.0180	3.13	176.98
	10.50	10.50	10.50	26.76	0.0180	3.03	168.37
	10.50	10.50	10.50	18.22	0.0113	2.06	191.90
Average	**10.72**	**10.94**	**10.83**	**24.77**	**0.0155**	**2.65**	**175.02**
Std. Dev	**0.43**	**0.57**	**0.48**	**5.65**	**0.0037**	**0.60**	**9.52**

Table H-5. (Cont'd.)

Batch 3:

	d_1(μm)	d_2(μm)	d(avg.)	Load(g)	Strain	TS(GPa)	EM(GPa)
	10.50	11.50	11.00	31.70	0.0189	3.28	173.16
	11.00	12.00	11.50	37.14	0.0190	3.51	184.80
	11.50	11.50	11.50	21.01	0.0121	1.98	163.19
	11.50	11.50	11.50	35.68	0.0194	3.37	173.65
	11.00	11.00	11.00	31.75	0.0199	3.27	164.70
	11.50	12.00	11.75	32.38	0.0180	2.93	162.33
	12.00	12.00	12.00	29.66	0.0162	2.57	164.50
	11.50	11.50	11.50	27.91	0.0162	2.63	170.37
	11.50	11.50	11.50	28.30	0.0153	2.67	178.68
	11.00	11.00	11.00	25.53	0.0153	2.63	184.94
	11.50	12.00	11.75	36.46	0.0195	3.30	177.19
	11.00	11.00	11.00	28.88	0.0183	2.98	187.79
	11.50	12.00	11.75	24.65	0.0131	2.23	188.09
	10.50	10.50	10.50	19.94	0.0128	2.26	176.76
	10.50	11.00	10.75	30.87	0.0197	3.34	169.38
	10.50	11.00	10.75	30.19	0.0184	3.26	177.48
Average	**11.16**	**11.44**	**11.30**	**29.50**	**0.0170**	**2.89**	**174.81**
Std. Dev	**0.47**	**0.48**	**0.44**	**4.98**	**0.0026**	**0.47**	**8.68**

Batch 4:

	d_1(μm)	d_2(μm)	d(avg.)	Load(g)	Strain	TS(GPa)	EM(GPa)
	9.00	10.00	9.50	26.53	0.0149	3.68	247.21
	5.50	15.00	10.25	5.55	0.0053	0.84	158.78
	6.00	12.00	9.00	6.65	0.0064	1.15	178.84
	7.00	11.50	9.25	10.64	0.0074	1.65	222.74
	7.00	12.50	9.75	10.69	0.0074	1.52	205.60
	10.50	11.00	10.75	22.16	0.0114	2.39	210.33
	9.50	11.00	10.25	18.94	0.0100	2.26	225.33
	6.50	11.00	8.75	6.27	0.0065	1.09	167.72
	6.50	12.00	9.25	7.81	0.0062	1.25	202.50
	10.00	10.50	10.25	21.92	0.0114	2.61	229.20
	10.00	10.50	10.25	18.27	0.0096	2.17	226.50
	10.50	11.00	10.75	16.06	0.0082	1.74	211.63
	6.00	11.00	8.50	5.12	0.0048	0.97	199.91
	10.00	11.00	10.50	20.91	0.0108	2.37	219.41
	10.00	10.00	10.00	9.29	0.0052	1.16	224.28
	10.50	10.50	10.50	20.62	0.0105	2.33	221.64
	8.00	9.50	8.75	5.79	0.0058	0.95	163.94
Average	**8.38**	**11.18**	**9.78**	**13.72**	**0.0083**	**1.77**	**206.80**
Std. Dev	**1.88**	**1.25**	**0.74**	**7.24**	**0.0028**	**0.77**	**25.45**

Table H-5. (Cont'd.)

Batch 5:

	d_1(μm)	d_2(μm)	d(avg.)	Load(g)	Strain	TS(GPa)	EM(GPa)
	11.00	11.50	11.25	35.76	0.0162	3.53	217.71
	10.00	10.50	10.25	29.46	0.0164	3.50	212.90
	11.00	11.50	11.25	25.57	0.0109	2.52	230.38
	11.00	11.50	11.25	29.03	0.0132	2.86	221.33
	11.00	11.00	11.00	33.93	0.0163	3.50	214.18
	10.00	10.50	10.25	23.03	0.0119	2.74	229.24
	11.00	11.50	11.25	27.06	0.0120	2.67	221.92
	11.00	11.00	11.00	34.12	0.0155	3.52	227.17
	7.50	11.00	9.25	12.46	0.0073	1.89	259.54
	11.00	11.50	11.25	19.67	0.0091	1.94	213.33
	10.50	11.50	11.00	34.46	0.0164	3.56	216.59
	10.00	10.50	10.25	31.05	0.0166	3.69	222.34
	10.00	10.00	10.00	32.11	0.0173	4.01	232.19
	10.00	10.50	10.25	23.60	0.0129	2.81	216.88
	11.00	12.00	11.50	32.73	0.0146	3.09	212.49
	10.00	10.50	10.25	24.42	0.0130	2.90	224.00
	10.00	10.00	10.00	28.89	0.0163	3.61	220.48
	11.00	11.50	11.25	12.41	0.0064	1.22	192.44
Average	**10.39**	**11.00**	**10.69**	**27.21**	**0.0135**	**2.98**	**221.40**
Std. Dev	**0.87**	**0.59**	**0.63**	**7.00**	**0.0033**	**0.74**	**13.11**

Batch 6:

	d_1(μm)	d_2(μm)	d(avg.)	Load(g)	Strain	TS(GPa)	EM(GPa)
	11.00	11.50	11.25	29.08	0.0153	2.87	187.10
	10.50	10.50	10.50	28.89	0.0163	3.27	201.16
	10.50	10.50	10.50	34.50	0.0173	3.91	225.51
	10.50	10.50	10.50	23.99	0.0127	2.72	213.71
	10.00	10.00	10.00	31.43	0.0180	3.92	217.71
	10.50	10.50	10.50	21.11	0.0135	2.39	177.55
	10.00	11.00	10.50	31.19	0.0149	3.54	237.18
	10.00	10.50	10.25	28.84	0.0165	3.43	207.40
	11.00	11.00	11.00	34.26	0.0169	3.53	208.66
	10.00	10.00	10.00	29.80	0.0170	3.72	218.14
	9.50	10.50	10.00	15.39	0.0094	1.93	204.37
	10.50	11.50	11.00	30.04	0.0151	3.10	205.13
	11.00	11.50	11.25	30.66	0.0173	3.02	175.07
	10.00	10.00	10.00	28.36	0.0166	3.54	212.55
	11.00	11.00	11.00	28.65	0.0140	2.95	211.47
	10.50	11.50	11.00	30.76	0.0148	3.18	214.95
	10.00	10.50	10.25	27.73	0.0155	3.30	212.63
Average	**10.38**	**10.74**	**10.56**	**28.51**	**0.0154**	**3.19**	**207.66**
Std. Dev	**0.45**	**0.53**	**0.45**	**4.66**	**0.0021**	**0.53**	**15.82**

Table H-5. (Cont'd.)

Batch 7:

	d_1(μm)	d_2(μm)	d(avg.)	Load(g)	Strain	TS(GPa)	EM(GPa)
	11.00	11.00	11.00	29.49	0.0148	3.04	205.50
	10.50	11.50	11.00	36.31	0.0176	3.75	213.35
	11.50	11.50	11.50	24.59	0.0124	2.32	186.66
	10.50	11.00	10.75	35.45	0.0171	3.83	224.50
	10.50	12.00	11.25	22.38	0.0115	2.22	192.85
	10.50	11.50	11.00	23.53	0.0115	2.43	211.08
	10.50	11.00	10.75	30.93	0.0149	3.34	224.42
	11.00	11.00	11.00	37.08	0.0177	3.82	216.43
	9.00	10.00	9.50	15.50	0.0104	2.15	206.45
	6.00	11.00	8.50	8.82	0.0072	1.67	231.24
	10.00	10.00	10.00	30.55	0.0149	3.81	254.97
	10.00	13.50	11.75	27.33	0.0139	2.53	182.26
	11.00	11.00	11.00	36.51	0.0180	3.77	208.99
	9.50	10.50	10.00	26.03	0.0149	3.26	218.84
	10.00	11.00	10.50	23.48	0.0114	2.66	234.02
	10.50	10.50	10.50	31.89	0.0182	3.61	197.88
	10.00	10.00	10.00	5.17	0.0038	0.65	170.97
Average	**10.12**	**11.06**	**10.59**	**26.18**	**0.0135**	**2.87**	**210.61**
Std. Dev	**1.22**	**0.85**	**0.80**	**9.32**	**0.0040**	**0.91**	**20.78**

Table H-6. UF-68s-1150: (1150°C/1 h/N_2) (PCS+PSZ)

Batch 1

	d_1(μm)	d_2(μm)	d(avg.)	Load(g)	Strain	TS(GPa)	EM(GPa)
	11.00	14.00	12.50	39.05	0.0146	3.16	217.14
	12.00	12.50	12.25	41.51	0.0181	3.45	190.92
	11.00	11.50	11.25	37.41	0.0198	3.69	186.69
	11.00	11.00	11.00	30.52	0.0163	3.15	193.66
	11.00	11.00	11.00	26.62	0.0150	2.75	186.23
	14.00	14.00	14.00	43.63	0.0164	2.78	169.13
	11.00	11.00	11.00	29.22	0.0144	3.01	208.56
	11.50	12.00	11.75	29.41	0.0151	2.66	176.64
	11.00	12.50	11.75	33.36	0.0159	3.03	190.18
	11.00	11.50	11.25	29.99	0.0144	2.96	205.52
	11.00	11.00	11.00	33.85	0.0195	3.49	192.03
	10.50	11.00	10.75	29.65	0.0147	3.20	217.31
	12.00	13.00	12.50	40.40	0.0166	3.23	195.04
	12.50	13.00	12.75	47.39	0.0199	3.64	188.01
	11.50	13.00	12.25	36.88	0.0168	3.08	183.39
	11.50	11.50	11.50	31.82	0.0154	3.00	195.05
	11.50	12.00	11.75	33.65	0.0162	3.04	187.34
	12.50	12.50	12.50	43.97	0.0188	3.51	186.69
Average	**11.53**	**12.11**	**11.82**	**35.46**	**0.02**	**3.16**	**192.75**
Std. Dev	**0.83**	**1.01**	**0.84**	**6.07**	**0.00**	**0.30**	**12.62**

Batch 2

	d_1(μm)	d_2(μm)	d(avg.)	Load(g)	Strain	TS(GPa)	EM(GPa)
	12.00	12.00	12.00	35.97	0.0193	3.12	161.64
	13.00	15.00	14.00	34.03	0.0139	2.18	156.23
	14.00	14.50	14.25	49.07	0.0198	3.02	152.20
	14.00	14.50	14.25	30.40	0.0118	1.87	158.83
	14.50	15.00	14.75	33.89	0.0131	1.94	156.07
	14.00	14.00	14.00	38.59	0.0160	2.46	165.95
	12.00	12.00	12.00	35.63	0.0180	3.09	171.72
	12.00	12.50	12.25	34.03	0.0177	2.83	160.06
	13.00	14.00	13.50	54.30	0.0206	3.72	181.14
	13.50	14.00	13.75	50.04	0.0215	3.30	172.63
	14.00	14.50	14.25	45.14	0.0170	2.78	162.73
	14.00	14.50	14.25	40.92	0.0157	2.52	159.77
	12.00	12.00	12.00	35.63	0.0179	3.09	172.59
	14.00	14.50	14.25	50.86	0.0187	3.13	166.78
	14.00	14.50	14.25	26.13	0.0104	1.61	154.38
	12.00	12.50	12.25	32.04	0.0165	2.67	170.91
	13.50	14.00	13.75	44.02	0.0169	2.91	180.48
	12.00	12.00	12.00	23.27	0.0123	2.02	164.26
Average	**13.19**	**13.67**	**13.43**	**38.55**	**0.02**	**2.68**	**164.91**
Std. Dev	**0.94**	**1.14**	**1.02**	**8.76**	**0.00**	**0.57**	**8.54**

Table H-6. (Cont'd.)

Batch 3

	d_1(μm)	d_2(μm)	d(avg.)	Load(g)	Strain	TS(GPa)	EM(GPa)
	13.00	13.00	13.00	37.38	0.0173	2.76	177.79
	12.50	13.50	13.00	38.11	0.0170	2.82	174.01
	12.50	13.50	13.00	42.81	0.0198	3.17	168.06
	11.50	12.50	12.00	43.30	0.0192	3.76	211.22
	12.50	14.00	13.25	45.43	0.0192	3.24	169.04
	12.50	13.00	12.75	48.54	0.0202	3.73	184.58
	13.50	13.50	13.50	29.91	0.0130	2.05	170.48
	13.00	13.50	13.25	35.93	0.0167	2.55	152.64
	13.50	13.50	13.50	43.93	0.0188	3.01	175.43
	12.50	13.50	13.00	38.93	0.0176	2.88	174.78
	12.50	13.00	12.75	46.26	0.0194	3.55	183.06
	13.00	13.00	13.00	33.60	0.0149	2.48	165.97
	13.50	13.50	13.50	42.96	0.0195	2.94	171.32
	12.00	12.00	12.00	44.61	0.0194	3.87	208.55
	12.50	13.00	12.75	36.51	0.0166	2.80	182.96
	13.00	13.50	13.25	34.13	0.0152	2.43	159.18
	13.00	13.50	13.25	47.33	0.0192	3.37	175.06
	12.50	14.00	13.25	47.28	0.0202	3.37	166.86
Average	**12.72**	**13.28**	**13.00**	**40.94**	**0.02**	**3.04**	**176.17**
Std. Dev	**0.52**	**0.49**	**0.44**	**5.50**	**0.00**	**0.50**	**14.67**

Batch 4

	d_1(μm)	d_2(μm)	d(avg.)	Load(g)	Strain	TS(GPa)	EM(GPa)
	12.50	13.00	12.75	35.21	0.0134	2.70	201.15
	13.00	13.00	13.00	42.75	0.0166	3.16	190.31
	11.50	12.00	11.75	37.67	0.0169	3.41	201.89
	11.00	11.50	11.25	32.31	0.0143	3.19	222.77
	13.00	13.50	13.25	51.11	0.0194	3.63	203.35
	11.00	11.50	11.25	38.21	0.0166	3.77	231.56
	12.00	12.50	12.25	35.64	0.0137	2.97	223.51
	11.00	12.00	11.50	24.04	0.0108	2.27	210.12
	13.00	13.00	13.00	32.31	0.0121	2.39	197.47
	12.50	13.00	12.75	29.89	0.0111	2.30	206.33
	12.50	13.00	12.75	18.92	0.0070	1.45	208.31
	11.50	12.00	11.75	38.83	0.0173	3.51	205.27
	11.50	11.50	11.50	19.79	0.0092	1.87	202.45
	11.50	11.50	11.50	35.64	0.0154	3.36	217.74
	13.50	13.50	13.50	24.82	0.0082	1.70	207.41
	11.50	11.50	11.50	19.45	0.0081	1.84	226.07
	13.50	14.00	13.75	39.08	0.0128	2.58	204.46
	12.50	13.00	12.75	51.21	0.0200	3.93	205.91
Average	**12.14**	**12.50**	**12.32**	**33.72**	**0.01**	**2.78**	**209.23**
Std. Dev	**0.85**	**0.82**	**0.83**	**9.70**	**0.00**	**0.77**	**10.85**

Table H-6. (Cont'd.)

Batch 5

	d_1(μm)	d_2(μm)	d(avg.)	Load(g)	Strain	TS(GPa)	EM(GPa)
	11.00	11.50	11.25	26.02	0.0139	2.57	184.71
	12.00	13.00	12.50	20.22	0.0078	1.62	207.66
	12.50	13.50	13.00	41.23	0.0151	3.05	201.78
	11.50	15.00	13.25	52.82	0.0189	3.82	210.57
	12.00	12.50	12.25	21.28	0.0082	1.77	215.49
	12.00	12.50	12.25	32.44	0.0130	2.70	210.53
	11.50	13.00	12.25	36.93	0.0129	3.08	238.18
	9.50	12.00	10.75	28.62	0.0135	3.13	237.22
	11.00	12.00	11.50	36.98	0.0169	3.50	209.37
	11.00	11.50	11.25	41.13	0.0193	4.06	218.75
	13.00	13.50	13.25	29.69	0.0101	2.11	209.01
	10.50	11.50	11.00	33.70	0.0149	3.48	240.46
	10.50	12.50	11.50	36.11	0.0164	3.43	213.80
	12.00	12.50	12.25	47.56	0.0204	3.96	211.38
	11.00	11.50	11.25	38.48	0.0174	3.80	225.87
	12.00	12.50	12.25	51.04	0.0221	4.25	197.76
	11.00	11.50	11.25	37.80	0.0169	3.73	223.52
	10.50	12.00	11.25	37.95	0.0177	3.76	219.51
Average	**11.36**	**12.44**	**11.90**	**36.11**	**0.02**	**3.21**	**215.31**
Std. Dev	**0.85**	**0.92**	**0.78**	**9.04**	**0.00**	**0.78**	**14.28**

Table H-7. UF70s-1150 (1150°C/1 h/N_2) (PCS+PSZ)

Batch 1:

	d_1(μm)	d_2(μm)	d(avg.)	Load(g)	Strain	TS(GPa)	EM(GPa)
	11.00	13.00	12.00	56.38	0.0209	4.92	235.74
	11.50	14.00	12.75	52.94	0.0192	4.10	213.26
	11.50	14.00	12.75	49.94	0.0186	3.87	207.98
	12.00	13.00	12.50	57.05	0.0207	4.56	220.91
	12.50	15.00	13.75	52.51	0.0198	3.49	176.51
	13.50	15.00	14.25	55.84	0.0202	3.44	170.67
	12.50	14.00	13.25	46.75	0.0177	3.33	188.32
	11.50	13.50	12.50	53.38	0.0196	4.29	218.62
	11.00	12.50	11.75	37.42	0.0175	3.40	193.95
	14.00	14.00	14.00	25.00	0.0096	1.59	165.49
	11.50	15.00	13.25	53.62	0.0196	3.88	197.67
	11.50	11.50	11.50	39.60	0.0180	3.74	208.02
	11.50	14.00	12.75	49.90	0.0195	3.87	198.42
	10.50	12.50	11.50	39.16	0.0173	3.72	214.91
	11.00	12.00	11.50	38.00	0.0177	3.59	203.49
	11.50	12.50	12.00	33.02	0.0142	2.87	201.71
	13.00	13.50	13.25	48.25	0.0181	3.43	189.52
	11.00	12.50	11.75	35.54	0.0159	3.23	202.41
Average	**11.81**	**13.42**	**12.61**	**45.79**	**0.0180**	**3.63**	**200.42**
Std. Dev	**0.94**	**1.05**	**0.88**	**9.42**	**0.0027**	**0.71**	**17.99**

Batch 2:

	d_1(μm)	d_2(μm)	d(avg.)	Load(g)	Strain	TS(GPa)	EM(GPa)
	11.50	13.50	12.50	38.57	0.0152	3.10	204.36
	11.50	14.00	12.75	46.50	0.0182	3.60	198.18
	11.50	12.50	12.00	42.82	0.0196	3.72	190.13
	11.00	12.00	11.50	43.74	0.0187	4.14	221.35
	11.00	11.50	11.25	43.26	0.0174	4.27	244.52
	11.50	13.00	12.25	39.49	0.0155	3.30	212.83
	12.00	14.50	13.25	51.47	0.0199	3.69	185.83
	11.50	14.00	12.75	54.37	0.0202	4.21	208.49
	12.00	14.00	13.00	55.63	0.0194	4.13	212.47
	11.50	14.00	12.75	51.67	0.0202	4.00	197.81
	11.00	13.00	12.00	41.32	0.0181	3.61	199.31
	13.00	14.00	13.50	56.35	0.0220	3.86	175.41
	11.50	13.00	12.25	45.92	0.0186	3.83	206.48
	11.50	13.50	12.50	56.69	0.0226	4.56	201.21
	13.50	14.00	13.75	11.22	0.0053	0.74	140.85
	14.00	15.50	14.75	61.14	0.0222	3.52	158.38
	11.50	13.00	12.25	38.33	0.0151	3.20	211.45
	11.00	12.50	11.75	53.50	0.0202	4.86	240.04
Average	**11.78**	**13.42**	**12.60**	**46.22**	**0.0182**	**3.68**	**200.51**
Std. Dev	**0.86**	**0.96**	**0.85**	**11.22**	**0.0039**	**0.87**	**25.16**

Table H-7. (Cont'd.)

Batch 3:

d_1(μm)	d_2(μm)	d(avg.)	Load(g)	Strain	TS(GPa)	EM(GPa)
12.00	12.50	12.25	34.37	0.0146	2.86	200.67
12.00	12.50	12.25	41.59	0.0140	3.46	247.10
14.00	14.00	14.00	59.19	0.0202	3.77	197.32
12.00	12.50	12.25	38.58	0.0159	3.21	204.96
12.00	12.50	12.25	43.87	0.0177	3.65	213.30
11.50	12.50	12.00	10.47	0.0041	0.91	224.28
12.50	12.50	12.50	27.72	0.0104	2.21	212.03
13.50	14.00	13.75	34.95	0.0113	2.31	203.46
13.50	14.00	13.75	13.52	0.0042	0.89	211.82
14.00	14.00	14.00	32.57	0.0097	2.07	213.92
13.00	14.00	13.50	26.27	0.0083	1.80	217.48
14.00	14.00	14.00	24.77	0.0079	1.58	199.47
14.00	14.00	14.00	27.05	0.0090	1.72	191.63
13.50	14.00	13.75	23.31	0.0075	1.54	204.58
14.00	14.00	14.00	41.64	0.0135	2.65	195.73
12.50	12.50	12.50	38.24	0.0153	3.05	199.50
14.00	14.00	14.00	28.11	0.0088	1.79	204.48
13.00	14.00	13.50	38.34	0.0124	2.63	211.74
13.06	**13.42**	**13.24**	**32.48**	**0.0114**	**2.34**	**208.53**
0.89	**0.75**	**0.80**	**11.43**	**0.0044**	**0.88**	**12.77**

Average
Std. Dev

Batch 4:

d_1(μm)	d_2(μm)	d(avg.)	Load(g)	Strain	TS(GPa)	EM(GPa)
13.00	13.50	13.25	49.70	0.0175	3.53	209.46
12.50	13.50	13.00	58.72	0.0202	4.34	229.33
10.50	12.00	11.25	30.83	0.0137	3.05	222.84
13.50	15.00	14.25	66.92	0.0240	4.12	183.52
10.50	12.50	11.50	31.84	0.0140	3.03	216.34
13.50	13.50	13.50	50.18	0.0181	3.44	205.85
10.50	12.00	11.25	40.92	0.0178	4.05	237.01
14.50	15.00	14.75	53.89	0.0182	3.09	176.30
12.50	14.00	13.25	35.80	0.0121	2.55	210.38
11.00	11.50	11.25	39.95	0.0170	3.94	231.21
11.00	12.50	11.75	31.12	0.0139	2.82	203.87
12.00	14.50	13.25	68.37	0.0255	4.90	209.07
10.50	12.00	11.25	19.06	0.0086	1.89	218.36
11.00	12.00	11.50	39.08	0.0178	3.69	211.08
11.50	13.00	12.25	38.31	0.0168	3.20	195.29
10.50	11.50	11.00	35.80	0.0150	3.70	251.84
12.50	13.00	12.75	25.57	0.0114	1.96	171.85
14.00	14.50	14.25	44.97	0.0169	2.76	173.23
11.94	**13.08**	**12.51**	**42.28**	**0.0166**	**3.34**	**208.71**
1.35	**1.17**	**1.22**	**13.54**	**0.0041**	**0.79**	**22.32**

Average
Std. Dev

APPENDIX I
GPC MOLECULAR WEIGHT DISTRIBUTIONS FOR PMS POLYMERS FRACTIONALLY- PRECIPITATED BY ADDITION OF ALCOHOLS

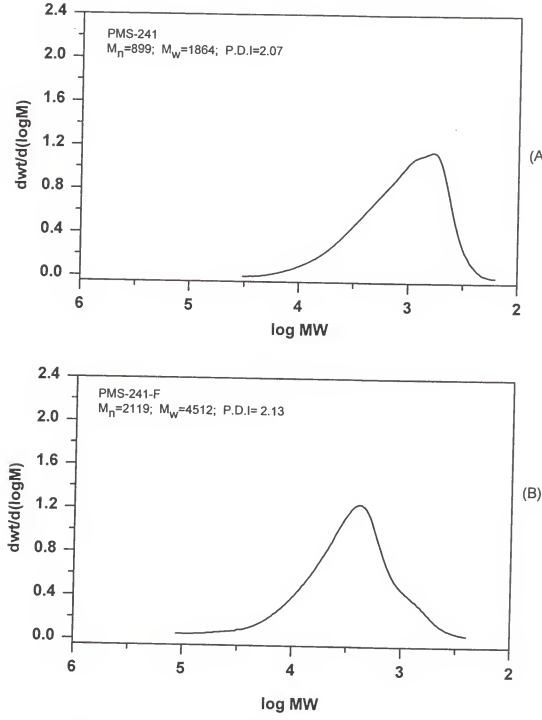

Figure I-1. GPC distributions for PMS-241 polymer: (A) before and (B) after fractional precipitation with alcohols.

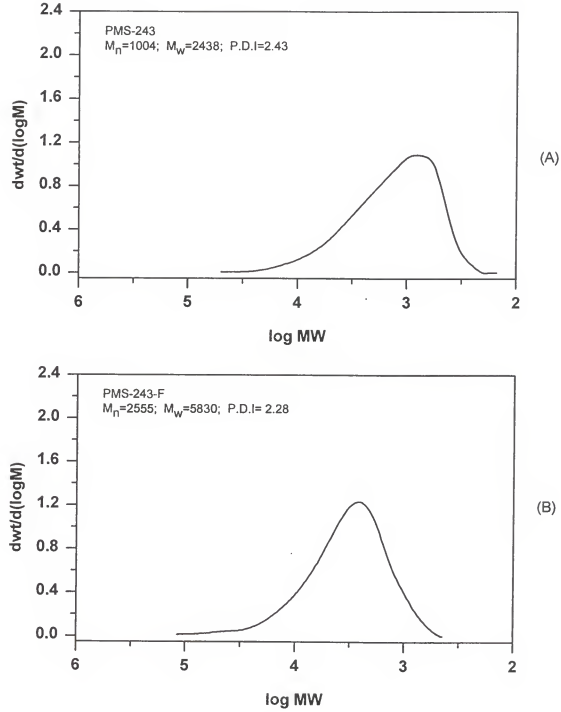

Figure I-2. GPC distributions for PMS-243 polymer: (A) before and (B) after fractional precipitation with acohols.

APPENDIX J
GPC MOLECULAR WEIGHT DISTRIBUTIONS FOR PMS POLYMERS
FRACTIONALLY-PRECIPITATED BY ADDITION OF ACETONE

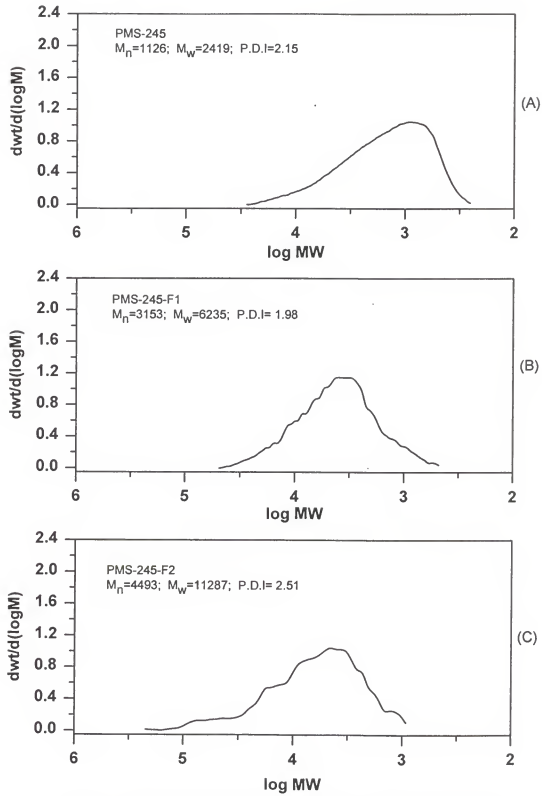

Figure J-1.GPC distributions for PMS-245 polymer: (A) before and, (B) and (C) after two fractional precipitations with acetone.

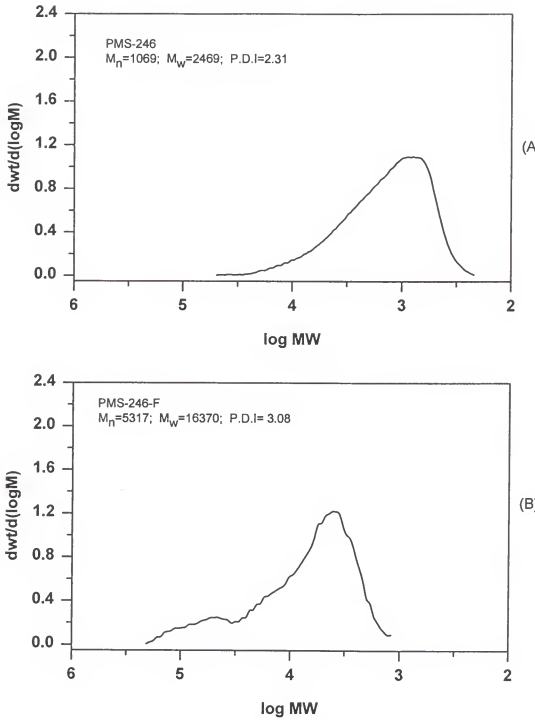

Figure J-2. GPC distributions for PMS-246 polymer: (A) before and (B) after fractional precipitation with acetone.

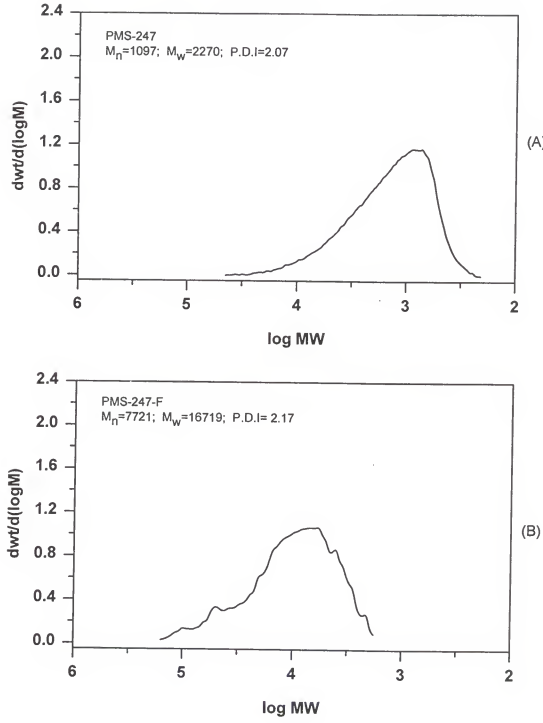

Figure J-3. GPC distributions for PMS-247 polymer: (A) before and (B) after fractional precipitation with acetone.

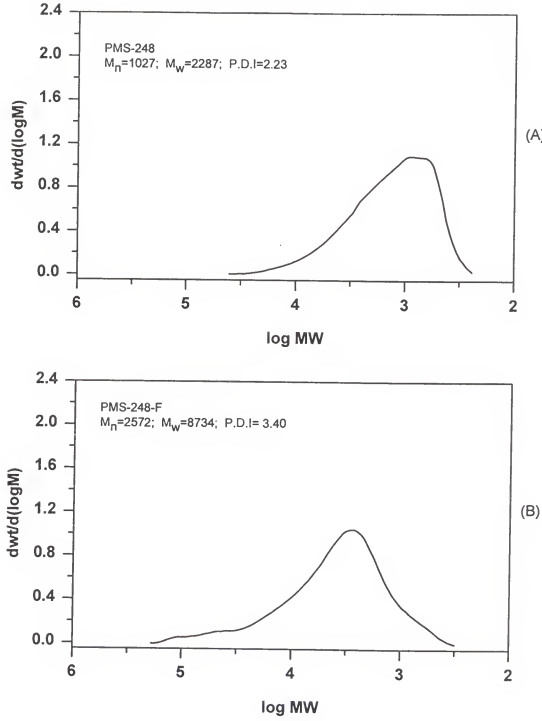

Figure J-4. GPC distributions for PMS-248 polymer: (A) before and (B) after fractional precipitation with acetone.

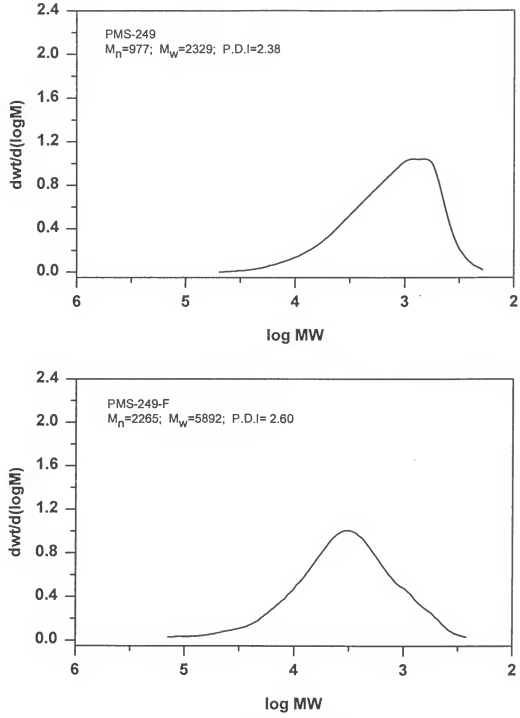

Figure J-5. GPC distributions for PMS-249 polymer: (A) before and (B) after fractional precipitation with acetone.

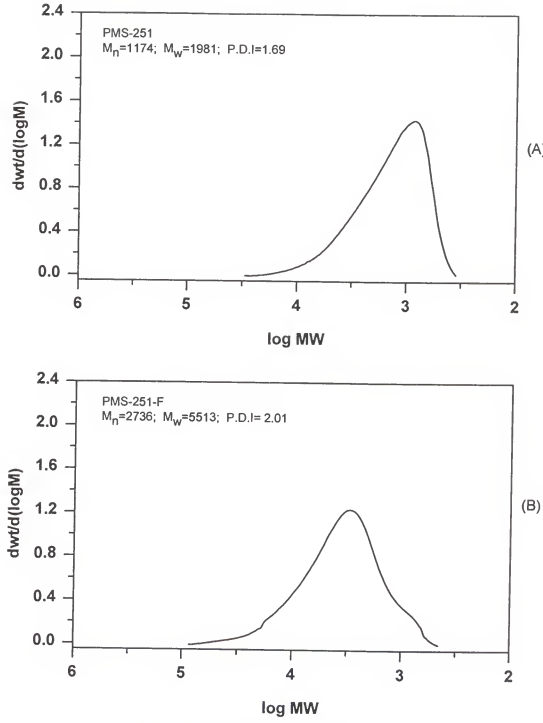

Figure J-6. GPC distributions for PMS-251 polymer: (A) before and (B) after fractional precipitation with acetone.

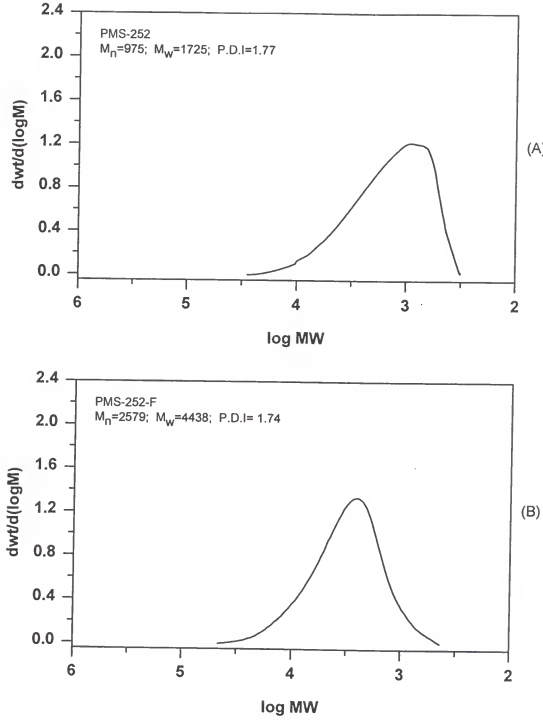

Figure J-7. GPC distribution of PMS-252 polymer: (A) before and (B) after fractional precipitation with acetone.

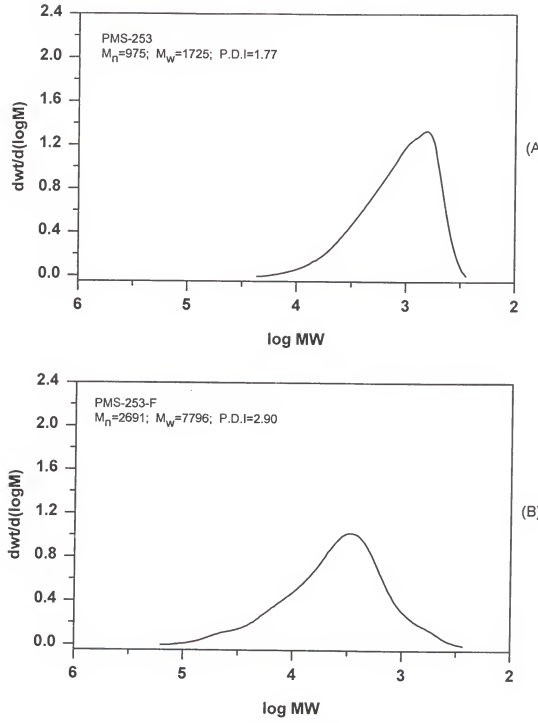

Figure J-8. GPC distributions for PMS-253 polymer: (A) before and (B) after fractional precipitation with acetone.

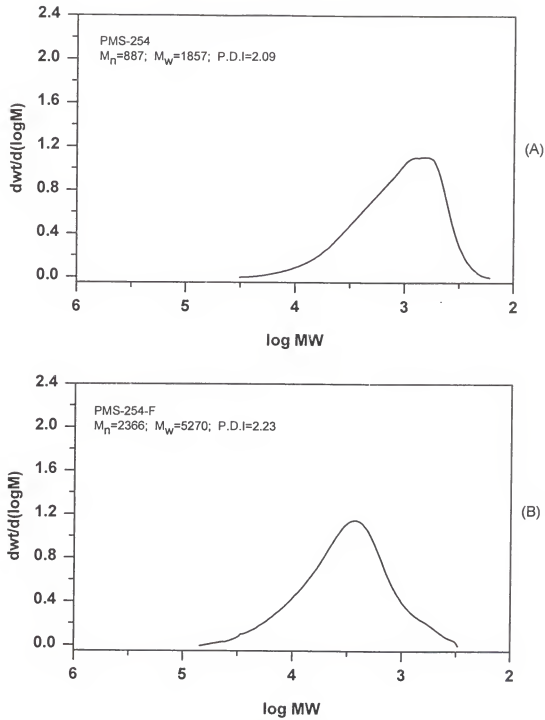

Figure J-9. GPC distributions for PMS-254 polymer before:(A) and (B) after fractional precipitation with acetone.

APPENDIX K
CALCULATIONS FOR EXCESS SILICON AND CARBON IN SIC FIBERS

1. Excess Si Calculations

Consider the composition of a 1150°C-pyrolyzed PMS-245 polymer. The elemental composition determined by Electron Microprobe Analysis (EMA) is 69.4 wt% Si, 26.0 wt% C, and 2.2 wt% O_2. Assuming that all O_2 is tied to Si as SiO_2 , we have 2.2 wt% O tied to 3.9 wt% Si (total of 7.1 wt% SiO_2). We, then, have 69.4 - 3.9 = 65.5 wt% Si for combination with C. Now, the stoichiometric composition of SiC is 70 wt% Si and 30 wt% C (i.e., 30 wt% C requires 70 wt% Si to form SiC). Therefore, 26 wt% C requires 61 wt% Si to form SiC. The excess Si in the pyrolyzed PMS polymer is 65.5 - 61.0 = 4.5 wt%.

2. Excess C calculations in PCS-based fibers

Consider the elemental composition of Nicalon™ SiC fiber: 55 wt% Si, 29 wt% C, and 15 wt% O [Tor92B]. Assuming that all O_2 is tied to Si as SiO_2, we have 15 wt% O_2 tied to 27 wt% Si as SiO_2 (total of 42 wt% SiO_2). We, then, have 55 - 27= 28 wt% Si available for combination with C. 28 wt% of Si requires 12 wt% of C to form stoichiometric SiC. The excess C in the Nicalon™ SiC fiber is then 29 - 12 = 17 wt%.

APPENDIX L
CHARACTERISTICS OF PMS POLYMERS SYNTHESIZED FROM MDCS MONOMER

Table L-1. Results of characterization of PMS polymers synthesized from methyldichlorosilane monomer

Batch Designation	Solvent(s)	Polymer Yield (%)	GPC MW distribution			Ceramic Yield (%)		XRD Results (1350°C/Ar)
			M_n	M_w	PDI	by pyrolysis	by TGA [b]	
PMS-206 [a]	Toluene, THF (95:5)	42.3	...	...	...	...	55	No Si peaks
PMS-260	Toluene, THF (95:5)	40.8	...	...	...	...	...	
PMS-262	Toluene, THF (95:5)	48.2	760	1156	1.52	...	45.0	
PMS-261	Toluene (100%)	42.4	642	816	1.27	...	40.1	
PMS-257	Toluene, 1,4-Dioxane (50:50)	39.4	1437	2878	2.00	51.5	46.7	Strong Si peaks
PMS-258	Toluene, 1,4-Dioxane (50:50)	39.6	1428	3054	2.14	41.6	55.0	Strong Si peaks
PMS-263	Toluene, 1,4-Dioxane (50:50)	43.8	1325	2594	1.96	...	47.5	

[a] Smaller batch size, prepared in 250 ml three-necked flask.
[b] TGA analysis carried out at 1200°C /Ar/10°C per min/0 h hold.

APPENDIX M
CHARACTERISTICS OF PMS POLYMERS SYNTHESIZED FROM MDCS AND MTCS MONOMER MIXTURE

Table M-1. Results of characterization of PMS polymers synthesized from MDCS:MTCS monomers (70:30 wt%)

Batch Designation	Solvent(s)	Polymer Yield (%)	GPC MW distribution			Ceramic Yield (%)		XRD Results (1350C/Ar)
			M_n	M_w	PDI	by pyrolysis	by TGA [b]	
PMS-208 [a]	Toluene, THF (95:5)	36.3	...	...	...	...	71.0	Strong Si peaks; Si cryst. size: 17.5 nm
PMS-209 [a]	Toluene, THF (95:5)	43.6	...	...	...	...	61.0	Weak Si peaks
PMS-216	Toluene, THF (95:5)	38.4	...	...	...	44.0	...	Strong Si; 17.5 nm
PMS-218	Toluene, THF (95:5)	32.4	...	...	...	41.0	...	Strong Si; 20.2 nm
PMS-219	Toluene, THF (95:5)	41.0	...	...	...	47.0	...	Strong Si; 23.8 nm
PMS-220	Toluene, THF (95:5)	32.9	...	...	...	47.0	...	Strong Si; 21.8 nm
PMS-221	Toluene, THF (95:5)	37.2	871	1566	1.80	48.0	51.3	Strong Si; 13.8 nm
PMS-222	Toluene, THF (95:5)	38.2	953	1725	1.81	45.0	53.3	Strong Si; 13.8 nm
PMS-223	Toluene, THF (95:5)	30.7	...	...	...	...	...	...
PMS-224	Toluene, THF (95:5)	31.1	...	...	...	...	...	...
PMS-225	Toluene, THF (95:5)	37.6	...	...	...	...	...	...

Table M-1. (Cont'd.)

Batch Designation	Solvent(s)	Polymer Yield (%)	GPC MW distribution			Ceramic Yield (%)		XRD Results (1350C/Ar)
			M_n	M_w	PDI	by pyrolysis	by TGA [b]	
PMS-226	Toluene, THF (95:5)	37.9	...	...	...	...	...	...
PMS-227	Toluene, THF (95:5)	40.7	...	...	...	...	...	...
PMS-228	Toluene, THF (95:5)	40.2	894	1674	1.87	...	52.1	...
PMS-229	Toluene, THF (95:5)	34.4	...	...	...	...	...	...
PMS-230	Toluene, THF (95:5)	27.6	...	...	...	...	...	...
PMS-231	Toluene, THF (95:5)	29.6	1352	2747	2.03	73.8	...	No Si peaks
PMS-232	Toluene, THF (95:5)	37.2	1001	1756	1.75	64.1	...	No Si peaks
PMS-233	Toluene, THF (95:5)	31.7	...	...	...	66.3	...	No Si peaks
PMS-234	Toluene, THF (95:5)	18.6	1120	2292	2.05	66.2	...	No Si peaks
PMS-235	Toluene, THF (95:5)	20.0	863	1531	1.77	...	...	...
PMS-236	Toluene, THF (95:5)	32.7	967	1149	1.23	...	...	...

Table M-1. (Cont'd.)

Batch Designation	Solvent(s)	Polymer Yield (%)	GPC MW distribution			Ceramic Yield (%)		XRD Results (1350C/Ar)
			M_n	M_w	PDI	by pyrolysis	by TGA [b]	
PMS-237	Toluene, THF (95:5)	20.7	945	1157	1.22	...	...	...
PMS-238	Toluene, THF (95:5)	22.3	888	1277	1.44	45.0	...	...
PMS-239	Toluene, THF (95:5)	11.7	857	1162	1.35	44.0	...	
PMS-240	Toluene, 1,4 Dioxane (60:40)	38.2	960	2395	2.49	...	...	...
PMS-241	Toluene, 1,4 Dioxane (40:60)	51.4	899	1865	2.07	...	...	...
PMS-242	Toluene, 1,4 Dioxane (50:50)	46.9	1653	3631	2.20	...	...	...
PMS-243	Toluene, 1,4 Dioxane (50:50)	54.7	1004	2438	2.43	...	...	...
PMS-244	Toluene, 1,4 Dioxane (50:50)	48.1	1055	2028	1.92	...	...	...
PMS-245	Toluene, 1,4 Dioxane (50:50)	50.4	1126	2419	2.15	...	...	...

Table M-1. (Cont'd.)

Batch Designation	Solvent(s)	Polymer Yield (%)	GPC MW distribution			Ceramic Yield (%)		XRD Results (1350C/Ar)
			M_n	M_w	PDI	by pyrolysis	by TGA [b]	
PMS-246	Toluene, 1,4 Dioxane (50:50)	42.0	1069	2469	2.31	...	...	...
PMS-247	Toluene, 1,4 Dioxane (50:50)	38.3	1097	2276	2.07	...	...	...
PMS-248	Toluene, 1,4 Dioxane (50:50)	46.4	1027	2287	2.33	...	...	
PMS-249	Toluene, 1,4 Dioxane (50:50)	45.7	977	2329	2.38	...	...	...
PMS-250	Toluene, 1,4 Dioxane (50:50)	49.6	1207	1919	1.59	...	51.3	...
PMS-251	Toluene, 1,4 Dioxane (50:50)	44.8	1174	1981	1.69	...	...	...
PMS-252	Toluene, 1,4 Dioxane (50:50)	47.9	1133	2118	1.87	...	51.1	...
PMS-253	Toluene, 1,4 Dioxane (50:50)	42.8	975	1725	1.77	...	...	...

Table M-1. (Cont'd.)

Batch Designation	Solvent(s)	Polymer Yield (%)	GPC MW distribution			Ceramic Yield (%)		XRD Results (1350C/Ar)
			M_n	M_w	PDI	by pyrolysis	by TGA [b]	
PMS-254	Toluene, 1,4 Dioxane (50:50)	42.0	887	1857	2.09	...	...	...
PMS-255	Toluene, 1,4 Dioxane (50:50)	48.8	971	2017	2.08	...	...	...
PMS-256	Toluene, 1,4 Dioxane (50:50)	45.3	953	1932	2.03	...	52.1	Strong Si; 15 nm
PMS-259	Toluene	15.2	815	1167	1.43	...	55.0	Strong Si; 15 nm

[a] Smaller batch size, prepared in 250 ml three necked flask.
[b] TGA analysis carried out at 1200°C/Ar/10°C per min/0 h hold.

APPENDIX N
CHEMICAL FORMULAS OF MONOMERS USED IN WURTZ-COUPLING POLYMERIZATION

Chemical formulas of monomers used in Wurtz-coupling polymerization

1. Dimethyldichlorosilane

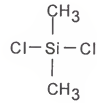

2. Methyldichlorosilane

3. Methyltrichlorosilane

4. Phenylmethyldichlorosilane

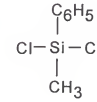

5. Hexylmethyldichlorosilane

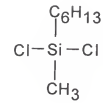

6. Hexyl-di-n-dichlorosilane

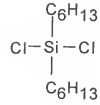

7. Dodecylmethyldichlorosilane

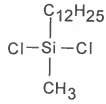

8. Dodecyl-di-n-dichlorosilane

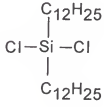

REFERENCES

[Abu92]. M.A. Abu-Eid, R.B. King, and A.M. Kotliar, "Synthesis of Polysilane Precursors and Their Pyrolysis to Silicon Carbides," Eur. Polym. J., 28 [3] 315-320 (1992).

[Ait85]. C. Aitken, J.F. Harrod, and E. Samuel, "Polymerization of Primary Silanes to Linear Polysilanes Catalyzed by Titanocene Derivatives," J. Organomet. Chem., 279 C11-C13 (1985).

[Ait87]. C. Aitken, J.F. Harrod, and U.S. Gill, "Structural Studies of Oligosilanes Produced by Catalytic Dehydrogenative Coupling of Primary Organosilanes," Can. J. Chem., 65 1804-1809 (1987).

[Ait89]. C. Aitken, J.-P. Barry, F. Gauvin, J.F. Harrod, A. Malek, and D. Rousseau, "A Survey of Catalytic Activity of η^5-Cyclopentadienyl Complexes of Groups 4-6 and Uranium and Thorium for the Dehydrocoupling of Phenylsilane," Organometallics, 8 1732-1736 (1989).

[And91]. R. Anderson, G.L. Larson, and C. Smith (Eds.), *Silicon Compounds: Register and Review* (5th ed.), Huls America, Piscataway, NJ (1991).

[AST88]. ASTM Designation D 446-85a, "Standard Specifications and Operating Instructions for Glass Capillary Kinematic Viscometers," Annual Book of ASTM Standards, Vol. 5.01, ASTM, Philadelphia, PA (1988).

[Att72]. D. Atton, S.A. Bone, and I.M.T. Davidson, "Chlorine-abstraction and Chlorine Migration Reaction of Silyl Radicals," J. Organomet. Chem, 39 C47 (1972).

[Ban82]. R.H. Baney, "High Yield Silicon Carbide Pre-ceramic Polymers," U.S. Pat. No. 4 310 482 (1982).

[Ban83]. R.H. Baney, J.H. Gaul, Jr., and T.K. Hilty, "Methylchloropolysilanes and Derivatives Prepared from the Redistribution of Methylchlorodisilanes," Organometallics, 2 [7] 859-863 (1983).

[Ban85]. R.H. Baney, "Method of Preparing Silicon Carbide," U.S. Pat. No. 4 534 948 (1985).

[Ben91]. R.E. Benfield, R.H. Cragg, R.G. Jones, and A.C. Swain, "Air-Stable Alkali Metal Colloids and the Blue Color in Wurtz Synthesis," Nature, 353 [26] 340-341 (1991).

[Ber92]. B.C. Berris, "Method of Producing Polysilane Compounds," U.S. Pat. No. 5 089 648 (1992).

[Bil83]. F. Billmeyer, *A Textbook of Polymer Science*, Wiley-Eastern Publications, New York, NY (1983).

[Bou91]. E. Bouillon, F. Langlais, R. Pailler, R. Naslain, F. Cruege, J.C. Sarthou, A. Delpuech, C. Laffon, P. Lagarde, M. Monthioux, A. Oberlin, "Conversion Mechanisms of a Polycarbosilane Precursor into an SiC-based Ceramic Material," J. Mater. Sci., 26 1333-1345 (1991).

[Bro85]. K.A. Brown-Wensley and R.A. Sinclair, "Polyhydridosilanes and Their Conversion to Pyropolymers," U.S. Pat. No. 4 537 942 (1985).

[Bro87]. K.A. Brown-Wensley, "Formation of Si-Si bonds from Si-H Bonds in the Presence of Hydrosilation Catalysts," Organometallics, 6 1590-1596 (1987).

[Buj90]. D.R. Bujalski, "Polysilane Pre-ceramic Polymers," U.S. Pat. No. 4 962 176 (1990).

[Bur49]. C. Burkhard, "Polydimethylsilanes," J. Am. Chem. Soc., 71 963 (1949).

[Bur90]. G.T. Burns, "Pre-ceramic Methylpolysilanes," U.S. Pat. No. 4 921 917 (1990).

[Cam89]. W.H. Campbell and T.K. Hilty, "Dimethylzirconocene-Catalyzed Polymerization of Alkylsilanes," Organometallics, 8 2615-2618 (1989).

[Car90]. D.J. Carlsson, J.D. Cooney, S. Gauthier, and D.J. Worsfold, "Pyrolysis of Silicon-Backbone Polymers to Silicon Carbide," J. Am. Ceram. Soc., 73 [2] 237-241 (1990).

[Cho93]. G.J. Choi, Ph.D Dissertation, University of Florida, 1993.

[Cla85]. T.J. Clark, R.M. Arons, J.B. Stamatoff, and J. Rabe, "Thermal Degradation of Nicalon SiC Fiber," Ceram. Eng. Sci. Proc., 6 [7-8], 576-578 (1985).

[Col64]. N. Colthup, L.H. Daly, and S.E. Wilberly, in *Introduction to Infrared and Raman Spectroscopy*, Academic Press, New York (1964).

[Cor91]. J.Y. Corey, X-H. Zhu, T.C. Bedard, and L.D. Lange, "Catalytic Dehydrogenative Coupling of Secondary Silanes with Cp_2MCl_2/nBuLi," Organometallics, 10 924-930 (1991).

[CRC92]. *Handbook of Physics and Chemistry*, CRC Publications, New York (1982).

[Dan93]. F. Danes, E. Saint-Aman, and L. Coudurier, "The Si-C-O System, Part I: Representation of Phase Equilibria," J. Mater. Sci., 28 489-495 (1993).

[Fen94]. Z.C. Feng, C.C. Tin, K.T. Yue, R. Hu, J. Williams, S.C. Liew, Y.G. Foo, S.K.L. Choo, W.E. Ng, and S.H. Tang, "Combined Structural and Optical Assessment of CVD-grown 3C-SiC/Si," in Mat. Res. Soc. Symp. Proc., *Diamond, SiC, and Nitride Wide Band Gap Semiconductors*, Vol. 339, Materials Research Society, Pittsburgh, PA (1994).

[Gau89]. S. Gauthier and D.J. Worsfold, "The Effect of Phase-Transfer Catalysts on Polysilane Formation," Macromolecules, 22 2213-2218 (1989).

[Gau90]. S. Gauthier and D.J. Worsfold, "Mechanistic Studies of Polysilane Polymerization," in *Silicon-Based Polymer Science--A Comprehensive Resource*, pp 299-308, Eds., J.M. Zeigler and F.W.G. Fearon, American Chemical Society, Washington, DC (1990).

[Gre72]. N.N. Greenwood, E.J.F. Ross, and B.P. Straughan, in *Index of Vibrational Spectra of Inorganic and Organometallic Compounds*, Vol. 1, CRC Press, Cleveland, OH (1972).

[Han97]. W. Han, S. Fan, Q. Li, W. Liang, B. Gu, and D. Yu, "Continuous Synthesis and Characterization of SiC Nanorods," Chem. Phys. Letters, 265 374-378 (1997).

[Har88]. J.F. Harrod, "Polymerization of Group 14 Hydrides by Dehydrogenative Coupling," in *Inorganic and Organometallic Polymers*, pp 89-100, Eds., M. Zeldin, K.J. Wynne, and H.R. Allcock, American Chemical Society, Washington, DC (1988).

[Has83A]. Y. Hasegawa and K. Okamura, "Synthesis of Continuous Silicon Carbide Fibre-Part 3, Pyrolysis of Polycarbosilane and Structure of Products," J. Mater. Sci., 18 3633-3648 (1983).

[Has83B]. Y. Hasegawa, M. Ilmura, and S. Yajima, "Synthesis of Continuous Silicon Carbide Fibre-Part 2, Conversion of Polycarbosilane Fibre into Silicon Carbide Fibres," J. Mater.Sci., 15 720-728 (1983).

[Has86]. Y. Hasegawa and K. Okamura, "Synthesis of Continuous Silicon Carbide Fibre-Part 4, The Structure of Polycarbosilane as the Precursor," J. Mater. Sci., 21 321-328 (1986).

[Has89]. Y. Hasegawa, "Synthesis of Continuous Silicon Carbide Fibre- Part 6, Pyrolysis Process of Cured Polycarbosilane Fibre and Structure of SiC Fibre," J. Mater. Sci., 24 1177-1190 (1989).

[Has92]. Y. Hasegawa, "Si-C Fibre Prepared from Polycarbosilane Cured Without Oxygen," J. Inorg. Organomet. Polym., 2 161-169 (1992).

[Has94]. Y. Hasegawa, "New Curing Method for Polycarbosilane with Unsaturated Hydrocrabons and Application to Thermally Stable SiC Fibre," Composites Sci. Technol., 51 161-166 (1994).

[Her70]. W.J. Herzberg, and J.E. Marian, "Relationship Between Contact Angle and Drop Size," J. of Colloid and Interface Sci., 33 [1] 161-163 (1970).

[Ich86]. H. Ichikawa, F. Machino, S. Mitsuno, T. Ishikawa, K. Okamura, and Y. Hasegawa, "Synthesis of Continuous Silicon Carbide Fibre- Part 5, Factors Affecting Stability of Polycarbosilane to Oxidation," J. Mater. Sci., 21 4352-4358 (1986).

[Ich90]. H. Ichikawa, F. Machino, H. Teranishi, and T. Ishikawa, "Oxidation Reaction of Polycarbosilane," in *Silicon-Based Polymer Science--A comprehensive Resource*, pp 619-637, Eds., J. M. Zeigler, and F.W.G. Fearon, American Chemical Society, Washington, DC (1990).

[Ish94]. T. Ishikawa, "Recent Developments of the SiC Fiber Nicalon and its Composites, Including Properties of the SiC Fiber Hi-Nicalon for Ultra-High Temperature," Composites Sci. Technol., 51 135-144 (1994).

[Jon94]. R.G. Jones, R.E. Benfield, R.H. Cragg, P.J. Evans, and A.C. Swain, "The Formation of Polysilanes from Homogeneous Reagents in Tetrahydrofuran Solution at Low Temperatures," Polymer, 35 [22] 4924-4925 (1994).

[Kim88]. H.K Kim and K. Matyjaszewski, "Preparation of Polysilanes in the Presence of Ultrasound," J. Am. Chem. Soc., 110 3321-3323 (1988).

[Kip21]. F.S. Kipping and J.E. Sands, "Organic Derivatives of Silicon, Part XXV, Saturated and Unsaturated Silicohydrocarbons $Si_4 Ph_8$," J. Chem. Soc., 119 830-835 (1921).

[Lip89]. J. Lipowitz, G. LeGrow, T. Lim, and N. Langley, "Silicon Carbide Fibers from Methylpolysilane Polymers," in *Ceramic Transactions-Volume 2, Silicon Carbide '87*, Eds., J.D. Cawley and C.E. Semler, The American Ceramic Society, Westerville, OH (1989).

[Lip91A]. J. Lipowitz, J.A. Rabe, and G.A. Zank, "Polycrystalline SiC Fibers from Organosilicon Polymers," Ceram. Eng. Sci. Proc., 12 [9-10] 1819-1831 (1991).

[Lip91B]. J. Lipowitz, "Structure and Properties of Ceramic Fibers Prepared from Organosilicon Polymers," J. Inorg. Organomet. Polym., 1 [3] 277-297 (1991).

[Lip94A]. J. Lipowitz, T. Barnard, D. Bujalski, J.A. Rabe, G.A. Zank, Y. Xu, and A. Zangvil, "Fine-Diameter Polycrystalline SiC Fibers," Composites Sci. Technol., 51 167-171 (1994).

[Lip94B]. J. Lipowitz, and J.A. Rabe, "Polycrystalline Silicon Carbide Fibers," U.S. Pat. No. 05 366 943 (1994).

[Lip95]. J. Lipowitz, J.A. Rabe, K.T. Nguyen, L.D. Orr, and R.R. Androl, "Structure and Properties of Polymer-derived Stoichiometric SiC Fiber," Ceram. Eng. Sci. Proc., 16 [4] 55-62 (1995).

[Mah84]. T. Mah, N.L. Hecht, D.E. McCullum, J.R. Hoenignman, H.M. Kim, A.P. Katz, and H.P. Lipsitt, "Thermal Stability of Nicalon Fibers," J. Mater. Sci., 19 [4] 1191-1201 (1984).

[Mar92]. J.E. Mark, H.R. Allcock, and R. West, "Polysilanes and Related Polymers," in *Inorganic Polymers*, pp186-236, Prentice Hall, Englewood Cliffs, New Jersey (1992).

[Mat88]. K. Matyjaszewski, Y.L. Chen, and H.K. Kim, "New Synthetic Routes to Polysilanes," in Inorganic and Organometallic Polymers, pp 78-88, Eds., M. Zeldin, K.J. Wynne, and H.R. Allcock, American Chemical Society, Washington, DC (1988).

[Mat91]. K. Matyjaszewski, M. Cypryk, H. Frey, J. Hrkach, H.K. Kim, M. Moeller, K. Ruehl, and M. White, "Synthesis and Characterization Polysilanes," J. Macromol. Sci., Chem., A28 [11 & 12] 1151-1176 (1991).

[Mat92]. R.B. Mathur, O.P. Bahl, and J. Mittal, "A New Approach to Thermal Stabilization of PAN Fibers," Carbon, 30 [4] 657-663 (1992).

[Mil88]. R.D. Miller, J.F. Rabolt, R. Sooriyakumaran, W. Fleming, G.N. Fickes, B.L. Farmer, and H. Kuzmany, "Soluble Polysilane Derivatives: Chemistry and Spectroscopy," in *Inorganic and Organometallic Polymers*, pp 43-60, Eds., M. Zeldin, K.J. Wynne, and H.R. Allcock, American Chemical Society, Washington, DC (1988).

[Mil89]. R.D. Miller and J. Michl, "Polysilane High Polymers," Chem. Rev., 89 1359-1410 (1989).

[Mil90]. R.D. Miller, "Radiation Sensitivity of Soluble Polysilane Derivatives," in *Silicon-Based Polymer Science - A Comprehensive Resource*, pp 413-458, Eds., J.M. Zeigler and F.W.G. Fearon, American Chemical Society, Washington, DC (1990).

[Mil91]. R.D. Miller, D. Thompson, R. Sooriyakumaran, and G.N. Fickes, "Synthesis of Soluble, Substituted Silane High Polymers by Wurtz Coupling Techniques," J. Polym. Sci., Part A: Polym. Chem., 29 813-824 (1991).

[Mil93]. R.D. Miller, E.J. Ginsburg, and D. Thompson, "Low Temperature Wurtz Type Polymerization of Substituted Dichlorosilanes," Polym. J., 25 [8] 807-823 (1993).

[Moc93]. D. Mocaer, R. Pailler, R. Naslain, C. Richard, J.P. Pillot, J. Dunogues, C. Gerardin, and F. Taulelle, "Si-C-N Ceramics with a High Microstructural Elaborated from the Pyrolysis of New Polycarbosilazane Precursors: Part I. The Organic/Inorganic Transition," J. Mater. Sci., 28 2615-2631 (1993).

[Mu91A]. Y. Mu and J.F. Harrod, "Synthesis of Poly(methylsilylene) by Catalytic Dehydrocoupling with Cp_2MMe_2 (M=Ti, Zr) Catalysts," in *Inorganic and Organometallic Oligomers and Polymers*, pp 23-36, Eds., J.F. Harrod and R.M. Laine, Kluwer Academic Publishers, Dordrecht (The Netherlands) (1991).

[Mu91B]. Y. Mu, C. Aitken, B. Cote, and J.F. Harrod, "Reactions of Silanes with bis(cyclopentadienyl) Dialkylzirconium Complexes," Can. J. Chem., 69 264-276 (1991).

[Oka87]. K. Okamura, "Ceramic Fibers from Polymer Precursors," Composites, 18 [2] 107-120 (1987).

[Pri94]. G.J. Price, A.M. Patel, and P.J. West, "Polymer Synthesis Using High Intensity Ultrasound," Macromol. Reports, A31 (Suppls. 6 & 7) 1037-1044 (1994).

[Qiu89A]. H.Qiu and Z. Du, "Organosilane Polymers: Formable Polymers Containing Methyl Silylene Units," J. Polym. Sci., Part A: Polym. Chem., 27 2849-2860 (1989).

[Qiu89B]. H. Qiu and Z. Du, "Organosilane Polymers: Formable Polymers Containing Reactive Side Groups," J. Polym. Sci., Part A: Polym. Chem., 27 2861-2869 (1989).

[Ree58]. T. Ree and H. Eyring, "Relaxation Theory of Transport Phenomena," in *Rheology: Theory and Applications*, Ed., Eirich, Vol. II, Academic Press, New York (1958).

[Rei90]. E. Reichmanis, A.E. Novembre, R.C. Tarascon, A. Shugard, and L.F. Thompson, "Organosilicon Polymers for Microlithographic Applications," in *Silicon-Based Polymer Science - A Comprehensive Resource*, pp 265-284, Eds., J.M. Zeigler and F.W.G. Fearon, American Chemical Society, Washington, DC (1990).

[Sac86]. M.D. Sacks, "Rheology of Suspensions," in *Science of Ceramic Processing*, pp 337-344, Eds., L.L. Hench and D.R. Ulrich, John Wiley & Sons, New York (1986).

[Sac95A]. M.D. Sacks, G.W. Scheiffele, M.Saleem. G.A. Staab, A.A. Morrone, and T.J. Williams, "Polymer-Derived Fibers with Near-Stoichiometric Composition and Low Oxygen Content," in Mat. Res. Soc. Symp. Proc., *Ceramic Matrix Composites*, Materials Research Society, Pittsburgh, PA (1995).

[Sac95B]. M.D. Sacks, A.A. Morrone, G.W. Scheiffele, and M.Saleem, "Characterization of Polymer-Derived SiC Fibers with Low Oxygen Content, Near-Stoichiometric Composition, and Improved Thermomechanical Stability," Ceram. Eng. Sci. Proc., 16 [4] 25-37 (1995).

[Sak91] T. Sakakura, H-J. Lautenschlager, M. Nakajima, and M. Tanaka, "Dehydrogenative Condensation of Hydrosilanes Catalyzed by an Organoneodymium Complex," Chem. Lett., 913-916 (1991).

[Sak93]. T. Sakakura, M. Tanaka, and T. Kobayashi, "Method for Producing Polysilanes," U.S. Pat. No. 5 252 766 (1993).

[Sal93]. M. Saleem, unpublished work.

[Sal96]. M. Saleem and M.D. Sacks, unpublished work.

[Sch84]. C.L. Schilling, Jr, and T.C. Williams, "Polymeric Routes to Silicon Carbide: Polycarbosilanes, Polysilahydrocarbons and Vinylic Polysilanes," Polym. Prepr., 25 1 (1984).

[Sch88]. C.L. Schilling, Jr, and B. Kanner, "Polysilane Precursors Containing Olefinic Groups for Silicon Carbide," U.S. Pat. No. 4 783 516 (1988).

[Sch91]. W.R. Schmidt, L.V. Interrante, R.H. Doremus, T.K. Trout, P.S. Marchetti, and G.E. Maciel, "Pyrolysis Chemistry of an Organometallic Precursor to Silicon Carbide," Chem. Mater., 3 257-267 (1991).

[Sey88]. D. Seyferth, G.H. Wiseman, Y-F. Yu, T.S. Targos, C.A.Sobon, T.G. Wood, and G.E. Koppetsch, "Applications of Methyldichlorosilane in the Preparation of Silicon-Containing Ceramics," in *Silicon Chemistry*, pp 415-424, Eds., J.Y. Corey, E.R. Corey, and P.P. Gaspar, Ellis Horwood Ltd., Chichester, U.K (1988).

[Sey90]. D. Seyferth, "Synthesis of Some Organosilicon Polymers and Their Pyrolytic Conversion to Ceramics," in *Silicon-Based Polymer Science - A Comprehensive Resource*, pp 565-591, Eds., J.M. Zeigler and F.W.G. Fearon, American Chemical Society, Washington, DC (1990).

[Sey92]. D. Seyferth, T.G. Wood, H.J. Tracy, and J.L. Robison, "Near-Stoichiometric Silicon Carbide from an Economical Polysilane Precursor," J. Am. Ceram. Soc., 75 [5] 1300-1302 (1992).

[Sey93]. D. Seyferth, H.J. Tracy, and J.L. Robison, "Preparation of Silicon Carbide Ceramics from the Modification of an Si-H Containing Polysilane," U.S. Pat. No. 5 204 380 (1993).

[Shi58]. K. Shina and M. Kumada, "Thermal Rearrangement of Hexamethyldisilane to Trimethyl(dimethylsilylmethyl) Silane," J. Org. Chem., 23 139 (1958).

[Sim84]. G. Simon and A.R. Bunsell, "Mechanical and Structural Characterization of the Nicalon Silicon Carbide Fiber," J. Mater. Sci., 19 [11] 3649-3657 (1984).

[Tak91]. M. Takeda, Y. Imai, H. Ichikawa, and T. Ishikawa, "Properties of the Low Oxygen Content SiC Fiber on High Temperature Heat-Treatment," Ceram. Eng. Sci. Proc., 12 [7-8] 1007-1018 (1991).

[Tak92]. M. Takeda, Y. Imai, H. Ichikawa, T. Ishikawa, N. Kasai, T. Suguchi, and K. Okamura, "Thermal Stability of the Low Oxygen Content Silicon Carbide Fibers Derived from Polycarbosilane," Ceram. Eng. Sci. Proc., 13 [7-8] 209-217 (1992).

[Tak94]. M. Takeda, J. Sakamoto, Y. Imai, H. Ichikawa, and T. Ishikawa, "Properties of Stoichiometric Silicon Carbide Fiber Derived from Polycarbosilane," Ceram. Eng. Sci. Proc., 15 133-141 (1994).

[Tak95]. M. Takeda, J. Sakamoto, A. Sacki, Y. Imai, and H. Ichikawa, "High Performance Silicon Carbide Fiber Hi-Nicalon for Ceramic Matrix Composites," Ceram. Eng. Sci. Proc., 16 37-42 (1995).

[Til91]. T.D. Tilley and H-G. Woo, "Catalytic Dehydrogenative Polymerization of Silanes to Polysilanes by Zirconocene and Hafnocene Catalysts - A New Polymerization Mechanism," in *Inorganic and Organometallic Oligomers and Polymers*, pp 3-12, Eds., J.F. Harrod and R.M. Laine, Kluwer Academic Publishers, Dordrecht, The Netherlands (1991).

[Til93]. T.D. Tilley, "High-Molecular Weight, Silicon-Containing Polymers and Methods for the Preparation and Use thereof," U.S. Pat. No. 5 229 481 (1993).

[Tor90]. W. Toreki, N.A. Creed, and C.D. Batich, "Silicon-Containing Vinyl Polymers as Precursors to Ceramic Materials," Polymer Preprints, 31 [2] 611-612 (1990).

[Tor92A]. W. Toreki, G.J. Choi, C.D. Batich, M.D. Sacks, and M. Saleem, "Polymer-Derived Silicon Carbide Fibers with Low Oxygen Content," Ceram. Eng. Sci. Proc., 13 [7-8] 198-208 (1992).

[Tor92B]. W. Toreki, C.D. Batich, M.D. Sacks, M. Saleem, and G.J. Choi, "Polymer-Derived Silicon Carbide Fibers with Improved Thermomechanical Stability," Mat. Res. Soc. Symp., 271 761-769 (1992).

[Tor94]. W. Toreki, C.D. Batich, M.D. Sacks, M. Saleem, G.J. Choi, and A.A. Morrone, "Polymer-Derived Silicon Carbide Fibers with Low Oxygen Content and Improved Thermomechanical Stability," Composites Sc. Technol., 51 145-159 (1994).

[Tre85]. P. Trefonas, III, R. West, and R.D. Miller, "Polysilane High Polymers: Mechanism of Photodegradation," J. Am. Chem. Soc., 107 2732-2742 (1985).

[Wes81]. R. West, L.D. David, P.I. Djurovich, K.L. Stearley, K.S.V. Srinivasan, and H. Yu, "Phenylmethylpolysilanes: Formable Silane Copolymers with Potential Semiconducting Properties," J. Am. Chem. Soc., 103 7352-7354 (1981).

[Wes86A]. R. West, "The Polysilane High Polymers," J. Organomet. Chem., 300 327-346 (1986).

[Wes86B]. R. West, X-H. Zhang, P.I. Djurovich, and H. Stuger, "Cross-linking of Polysilanes as Silicon Carbide Precursors," in *Science of Ceramic Processing*, pp 337-344, Eds., L.L. Hench and D.R. Ulrich, John Wiley & Sons, New York (1986).

[Wes88]. R. West and J. Maxka, "Polysilane High Polymers: An Overview," in *Inorganic and Organometallic Polymers*, pp 6-20, Eds., M. Zeldin, K.J. Wynne, and H.R. Allcock, American Chemical Society, Washington, DC (1988).

[Wey69]. D.R. Weyenberg, L.G. Mahone, and W.H. Atwell, "Redistribution Reactions in the Chemistry of Silicon," Ann. N.Y. Acad. Sci., 159 [1] 38-55 (1969).

[Wol88]. A.R. Wolff, I. Nozue, J. Maxka, and R. West, "^{29}SI NMR of Dimethyl and Phenylmethyl Containing Polysilanes," J. Polym. Sci., Part A: Polym. Chem., 26 [3] 701-712 (1988).

[Woo84]. T.G. Wood, "I: Phosphido-Bridged Diiron Hexacarbonyl Complexes and II: Polymeric Precursors to Silicon Carbide," Ph.D Dissertation, Massachusetts Institute of Technology, Cambridge, MA (1984).

[Wor88]. D.J. Worsfold, "Polysilylene Preparations," in *Inorganic and Organometallic Polymers*, pp 101-111, Eds., M. Zeldin, K.J. Wynne, and H.R. Allcock, American Chemical Society, Washington, DC (1988).

[Wu82]. S. Wu, *Polymer Interface and Adhesion*, Marcel Dekker, New York (1982)

[Wyn87]. K.J. Wynne and R.W. Rice, "Ceramics via Polymer Pyrolysis," Ann. Rev. Mater. Sci., 14 297-324 (1987).

[Xu93]. Y. Xu, A. Zangvil, J. Lipowitz, J.A. Rabe, and G.A. Zank, "Microstructure and Microchemistry of Polymer-Derived Crystalline SiC Fibers," J. Am. Ceram. Soc., 76 [12] 3034-3040 (1993).

[Yaj75]. S. Yajima, J. Hayashi, and M. Omori, "Continuous Silicon Carbide Fiber of High Tensile Strength," Chem. Lett, 931-934 (1975).

[Yaj78A]. S. Yajima, Y. Hasegawa, J. Hayashi, and M. Ilmura, "Synthesis of Continuous Silicon Carbide Fibers with High Tensile Strength and High Young's Modulus- Part 1, Synthesis of Polycarbosilane as Precursor," J. Mater. Sci., 13 2569-2576 (1978).

[Yaj78B]. S. Yajima, Y. Hasegawa, K. Okamura, and T. Matsuzawa, "Development of High Tensile Strength Silicon Carbide Fibre Using an Organosilicon Polymer Precursor," Nature, 273 [5663] 525-527 (1978).

[Zei86A]. J.M. Zeigler, "Mechanistic Studies of Polysilane Synthesis by Reductive Coupling of Dichlorosilanes," Polym. Prepr., 27 109-110 (1986).

[Zei86B]. J.M. Zeigler, "Methods for Synthesis of Polysilanes," U.S. Pat. No. 4 987 202 (1986).

[Zei87]. J.M. Zeigler, L.A. Harrah, and A.W. Johnson, "Synthesis, Photophysics, and Photochemistry of Organo and Silyl-substituted Polysilane Resist Materials," Polym. Prepr., 28 424-425 (1987).

[Zha91A]. Z-F. Zhang, F. Babonneau, R.M. Laine, Y. Mu, J.F. Harrod, and J.A. Rahn, "Poly(methylsilane) - A High Ceramics Yield Precursor for Silicon Carbide," J. Am. Ceram. Soc., 74 [3] 67-673 (1991).

[Zha91B]. Z-F. Zhang, Y. Mu, F. Babonneau, R.M. Laine, J.F. Harrod, and J.A. Rahn, "Polymethylsilane as a Precursor to High Purity Silicon Carbide" in *Inorganic and Organometallic Oligomers and Polymers*, pp 127-146, Eds., J.F. Harrod and R.M. Laine, Kluwer Academic Publishers, Dordrecht (The Netherlands) (1991).

[Zha94A]. Z-F. Zhang, C.S. Scotto, and R.M. Laine, "Processing of Silicon Carbide Fiber with Controlled Stoichiometry using Polymethylsilane, -$[MeSiH]_x$" in *Covalent Ceramics II: Non-Oxides* , Mater. Res. Soc. Symp. Proc., V 327, pp 207-213, Materials Research Society, Pittsburgh, PA (1994).

[Zha94B]. Z-F. Zhang, C.S. Scotto, and R.M. Laine, "Pure Silicon carbide Fibers from Polymethylsilane," Ceram. Eng. Sci. Proc., 15 152-160 (1994).

BIOGRAPHICAL SKETCH

The author was born in Kerala, India, on May 30th, 1965. He graduated with a Bachelor of Technology (B.Tech) degree in chemical engineering from Regional Engineering College, Trichy, India, in 1986. After working for 1 year at Tamil Nadu Petroproducts Ltd., Madras, India, as a deputy manager, he came to the U.S. in 1987 to pursue the Master of Science degree in chemical engineering at Tufts University, Medford, Massachusetts. After completing the M.S degree in the Fall of 1989, he moved to the University of Florida in Spring 1990 to pursue the Ph.D degree in materials science and engineering. He is presently employed as a technology development engineer at Ultra Clean Technology, a semiconductor equipment manufacturing company, in Menlo Park, California.

I certify that I have read this study and that in my opinion it conforms to acceptable standards of scholarly presentation and is fully adequate, in scope and quality, as a dissertation for the degree of Doctor of Philosophy.

Michael D. Sacks, Chair

Professor of Materials Science and Engineering

I certify that I have read this study and that in my opinion it conforms to acceptable standards of scholarly presentation and is fully adequate, in scope and quality, as a dissertation for the degree of Doctor of Philosophy.

Joseph H. Simmons

Professor of Materials Science and Engineering

I certify that I have read this study and that in my opinion it conforms to acceptable standards of scholarly presentation and is fully adequate, in scope and quality, as a dissertation for the degree of Doctor of Philosophy.

E. Dow Whitney

Professor of Materials Science and Engineering

I certify that I have read this study and that in my opinion it conforms to acceptable standards of scholarly presentation and is fully adequate, in scope and quality, as a dissertation for the degree of Doctor of Philosophy.

Christopher D. Batich

Professor of Materials Science and Engineering

I certify that I have read this study and that in my opinion it conforms to acceptable standards of scholarly presentation and is fully adequate, in scope and quality, as a dissertation for the degree of Doctor of Philosophy.

Daniel R. Talham

Associate Professor of Chemistry

This dissertation was submitted to the Graduate Faculty of the College of Engineering and to the Graduate School and was accepted as partial fulfillment of the requirements for the degree of Doctor of Philosophy.

August 1998

Winfred M. Phillips

Dean, College of Engineering

Karen A. Holbrook

Dean, Graduate School

LD
1780
1998
.5163